The enamel-dentine junction of the upper premolars of *Homo naledi* and other hominins: a morphometric study

William Philip Plummer

MSc dissertation

University of Kent

Supervisor: Dr Matthew Skinner

Dissertation for the degree of MSc by research.

Submitted for examination: 29th March 2021

Submitted with corrections: 18th May 2021

Submitted to the University of Kent academic repository: 25th May 2021

Acknowledgements

I would like to thank my supervisor, Dr Matthew Skinner, for his help and guidance throughout this project. I would also like to thank my fellow students in the Virtual Anthropology Laboratory at the University of Kent at Canterbury; in particular, Tom Davies and Simon Chapple for their many interesting discussions about tooth morphology and Christopher Dunmore for his discussions and advice about more general matters. I would also like to thank Dr Tracy Kivell for supervision and everyone in the APE lab for their help and advice in lab meetings. Thanks are also due to everyone in the Anthropology department for providing a stimulating and supportive atmosphere for study.

I suffered from serious illness during this study and I am extremely grateful to Matt Skinner for his personal support and advice. The academic and administrative staff in the School of Anthropology and Conservation and in the University of Kent more widely have been extremely helpful and supportive to me. I would like to give special thanks to Nicola Kerry-Yoxall and Professor Dimitrios Theodossopoulos. I would not have been able to complete this project without their wisdom, advice and support.

For CT scanning I would like to thank Jean-Jacques Hublin and the technical staff of the Department of Human Evolution, Max Planck Institute for Evolutionary Anthropology (MPI). I would especially like to thank David Plotzki at the MPI for scanning a clinical sample of modern human teeth specifically for this study. I would also like to give special thanks to Philip Gunz, who wrote the Mathematica worksheets upon which my geometric morphometric analysis depended very heavily.

I thank the curators of the following collections for access to the specimens in their care and for help with scanning: the Croatian Museum of Natural History; the Ditsong National Museum (Nat. Hist.), South Africa; the Geological Research and Development Centre, Bandung, Indonesia; the Kenya National Museum; the Max Planck Institute for Evolutionary Anthropology, Leipzig; the Senckenberg Museum, Frankfurt; the Staatlicher Museen, Berlin; the Staatlicher Museen, Stuttgart; Tel Aviv University, Israel; the University of the Witwatersrand, South Africa and the curators of the Scladena fossil hominin collection in Spain.

ABSTRACT.

Homo naledi is a hominin species first described in 2015 based on remains from the Dinaledi Chamber in the Rising Star cave system in South Africa. There has been much debate about the taxonomy and phylogenetic relationships of *H. naledi* because of its unique mix of primitive and advanced features. It has a primitive body size, chest, shoulders and hips and the brain size is small both absolutely and in relation to its body size. However, it does show more advanced features in the wrist, foot and thumb. The dentition also shows mixed features, being small, as in modern humans, but retaining certain primitive features in morphology.

In this study, geometric morphometric analysis was applied to the enamel-dentine junction (EDJ) of the upper premolars of *H. naledi* and a comparative sample of living and fossil hominins. The aims of the study were to determine whether this technique can distinguish between the upper premolars of different hominin taxa and of tooth position within taxa and, if so, to use the method to elucidate the taxonomic relationships of *Homo naledi*. Additionally, the study identified qualitative morphological features of the EDJ. Their frequency of expression between species and tooth position was analyzed and the differences between group mean frequencies of expression was summarised by multidimensional scaling.

The principal components of shape, derived from a Procrustes analysis, were able to differentiate well between hominin taxa and between tooth position within taxa. There is a morphological trend from *Paranthropus robustus* at one extreme to modern *Homo sapiens* at the other. This is also an allometric trend, as the size of the EDJ is correlated with the first principal component of shape. At the *Paranthropus* extreme, the EDJ is short and broad, especially in the bucco-lingual direction. The EDJ ridge has a square or rectangular outline with expansion of the talon in a disto-lingual direction. At the other end of the trend, the EDJ is taller and narrower, with a more triangular outline due to a flatter disto-lingual portion of the EDJ ridge. Third upper premolars differ from fourth upper premolars by having taller, more distally placed buccal dentine horns.

H. naledi has a unique morphology within the genus *Homo*. The EDJ is small but, has retained a more primitive morphology. It has a prominent distal accessory buccal dentine horn and a short main buccal dentine horn with prominent disto-lingual extension of the talon, leading to a relatively flat and broad EDJ profile. In addition, the size of the fourth upper premolar is greater than that of the third, as is seen in *Australopithecus* and *Paranthropus* and unlike other species of *Homo*, where the teeth are more equal in size or the third upper premolar is larger. This autapomorphy could suggest that *H. naledi* was adapted to a different dietary lifestyle than other members of the genus *Homo*.

Qualitative trait analysis identified and described some features at the EDJ for the first time in the hominin study sample. Third upper premolars of the genus *Homo* are associated with a notch and mesial 'bulge' in the mesial EDJ ridge together with a depression or concavity in the mesial surface of the EDJ (except for *H. naledi*

where there is a bulge but no notch); fourth upper premolars of all hominin species have a tendency to form a distinct distal accessory buccal dentine horn, except for *H. neanderthalensis*, where there is a distinctive distal buccal shoulder instead; *A. africanus* teeth are associated with prominent ridges on the buccal surface of the tooth together with extension of the buccal cingulum and lingual cingulum but *P. robustus* is more strongly associated with a shelf-like lingual cingulum; third upper premolars of *H. neanderthalensis* have a distinctive boss-shaped bulge in the buccal cingulum. *P. robustus* and, to a lesser extent *A. africanus*, show a tendency towards molarisation, with an oblique ridge, distal accessory lingual dentine horn and talon expansion. A transverse crest is almost universally present in the EDJs of all *Homo* species except for *H. sapiens* (both fossil and modern) and in *H. naledi*, where there is a distinctive bucco-mesial ridge in place of the transverse crest in 43% of third upper premolars. This contrasts with the outer enamel surface (OES), where transverse crests are rarely observed in *Homo* species.

TABLE OF CONTENTS

1 INTRODUCTION. 10
2 LITERATURE REVIEW 11
2.1 Teeth in the fossil record 11
2.1.1 The abundance of teeth in the fossil record 11
2.1.2 The primate dentition 11
2.2 The morphology of the enamel-dentine junction. 12
2.2.1 The development and morphogenesis of the EDJ and the OES 12
2.2.2 The strong genetic signal of the enamel-dentine junction (EDJ) 13
2.2.3 Methods of studying the EDJ 13
2.2.4 Relationships between the morphology of the EDJ and the OES 15
2.3 Qualitative morphometrics and geometric morphometrics 17
2.3.1 Qualitative morphometrics 17
2.3.2 Geometric morphometrics 18
2.3.3 Geometric morphometric studies of hominin upper premolars 20
2.4 Conclusions 21
3 SAMPLE. 22
4 Methods 25
4.1 Microtomography 25
4.2 Image filtering 25
4.3 Tissue segmentation 27
4.4 Landmark collection 27
4.5 Derivation of landmark sets 29
4.6 Data checking and relabelling of premolar position. 32
4.7 Organisation of the sample and naming and labelling conventions 33
4.8 Statistical and geometric morphometric analysis. 34
4.8.1 Premolar crown size. 34
4.8.2 Shape analysis. 36
4.9 Qualitative morphometric analysis. 37
5 RESULTS. 39
5.1 Intraspecific variation between third and fourth upper premolars 39
5.1.1 *Homo sapiens* 39
5.1.2 *Homo neanderthalensis* 48

5.1.3 *Australopithecus africanus* 53
5.1.4 *Paranthropus robustus* 62
5.1.5 *Homo naledi* 70
5.2 Intra- and interspecific comparison of premolar crown size 76
5.3 Comparison of premolar EDJ shape between species and tooth position. . 81
5.3.1 Multivariate Analysis of Variance (MANOVA) of the Shape Principal Components 83
5.3.2 Linear discriminant analysis (LDA) 84
5.3.3 Extended analysis: STS 61 and early to mid-Pleistocene Homo species…. 90
5.4 Influence of size on interspecific comparisons of EDJ morphology 93
5.4.1 Regression of size and shape 93
5.4.2 The first principal component of shape regressed on centroid size 94
5.4.3 The second principal component of shape regressed on centroid size…….. 95
5.4.4 Multivariate analysis in form space. 97
5.5 Differences between the EDJ of third upper premolars and the EDJ of fourth upper premolars which are common to all hominin species 102
5.6 Geometric morphological differences between species. 109
5.6.1 The first principal component of shape. 109
5.6.2 The second principal component of shape. 112
5.6.3 Mean shapes of hominin upper premolar EDJs by species and tooth position.. 113
5.6.4 A note on talon expansion 121
5.7 Qualitative morphometrics: Examination of the non-metric traits of the EDJ in hominin upper premolars 122
5.7.1 Qualitative morphometrics: Descriptions of the morphological features.. 122
5.7.2 Qualitative morphometrics: Frequencies of the expression of features by species and tooth position 130
5.7.3 Qualitative morphometrics: Multidimensional scaling of group mean percentages of the qualitative features. 134
5.7.4 Summary of the qualitative analysis. 136
5.8 Anomalies. 138
6 DISCUSSION 139
6.1 Geometric Morphometric trends in hominin upper premolars. 139
6.2 The discriminatory power of geometric morphometrics of the EDJ. 140

6.3 *Homo naledi* 142
6.4 Qualitative morphometrics 144
7 FURTHER WORK 147
8 CONCLUSION 148
9 REFERENCES. 149
10 APPENDIX 1: Table of specimens included in the sample 168
11 APPENDIX 2: Table of EDJ qualitative morphological features 179

LIST OF FIGURES

Figure 2.4.1 *Poor contrast between tissues (left) and good contrast (right).* _____ *22*

Figure 4.2.1 *The median filter and the mean of least variance (MLV) filter.*_____ *26*

Figure 4.2.2 *The effect of filtering on EDJ morphology.*_____ *26*

Figure 4.4.1 *Checking landmark positioning against the unfiltered image.* _____ *27*

Figure 4.4.2 *Estimation of the position of dentine horn tips in worn teeth.* _____ *28*

Figure 4.5.1 *Landmarking protocols.* _____ *30*

Figure 4.5.2 *Landmarks which are initially equally spaced along the EDJ and CEJ spline curves, are slid along the curves to reduce bending energy.*_____ *31*

Figure 4.8.1 *Some properties of the centroid size.*_____ *35*

Figure 4.8.2 *Centroid size compared with some other common measures of size.* _____ *36*

Figure 5.1.1 *Principal Component Plot of EDJ shape.* _____ *39*

Figure 5.1.2 *Summary of differences between third and fourth upper premolars in modern humans. 40*

Figure 5.1.3 *Modern human teeth plotted by first three principal components of shape.*_____ *42*

Figure 5.1.4 *Enamel-dentine junction of the EDJ of modern human tooth MPI 07 604*_____ *43*

Figure 5.1.5 *Enamel-dentine junction of MPI_T08_348* _____ *44*

Figure 5.1.6 *Enamel-dentine junction of MPI_T09_181*_____ *45*

Figure 5.1.7 *Principal Component Plot of EDJ shape for* Homo sapien*s (Qafzeh).* _____ *46*

Figure 5.1.8 *Differences in tooth morphology between third upper premolars and fourth upper premolars in* H. sapiens *(Qafzeh).* _____ *47*

Figure 5.1.9 *Principal components of shape for the EDJ of Neanderthal teeth.* _____ *48*

Figure 5.1.10 *Summary of EDJ shape differences between third and fourth upper premolars in* H. neanderthalensis. _____ *49*

Figure 5.1.11 *Disto-lingual EDJ shape and the boss shaped cingulum in the EDJ of* H. neanderthalensis. _____ *50*

Figure 5.1.12 *Neanderthal teeth, showing some possibly mis-identified teeth.*_____ *51*

Figure 5.1.13 *Comparison of 'suspect' teeth with third and fourth upper premolar teeth from Krapina Dental Person 1 (KDP 1)*_____ *52*

Figure 5.1.14 *Principal components of shape for the EDJ of* A. africanus *teeth.*_____ *53*

Figure 5.1.15 *Summary of differences between third and fourth upper premolars in* A. africanus*.* __ *54*

Figure 5.1.16 *Plot of* A. africanus *teeth against the first three principal components of shape with convex hulls for third upper premolars (Red) and fourth upper premolars (Blue).* _____ *56*

Figure 5.1.17 *The morphology of the EDJ and occlusal enamel surface of STS 47.*_____ *57*

Figure 5.1.18 *Comparison of the EDJ of suspect teeth (centre column) with the EDJ of teeth of known position.* _____ *58*

Figure 5.1.19 *Comparison of the EDJ of suspect teeth (centre column) with the EDJ of teeth of known position.* _____ *59*

Figure 5.1.20 *Comparison of the EDJ of suspect teeth (centre column) with the EDJ of teeth of known position.* _____ *60*

Figure 5.1.21 *Plot of* P. robustus *teeth on the first three principal components of EDJ shape.* _____ *62*

Figure 5.1.22 *Summary of differences in EDJ morphology between third and fourth upper premolars of* P. robustus. _____ *63*

Figure 5.1.23 *Plot of* P. robustus *teeth against the first and second principal components of shape with convex hulls for tooth type.*_____ *64*

Figure 5.1.24 *Comparison of the EDJ of SK 28 with* P. robustus *third and fourth upper premolars of known tooth position.* _____ *66*

Figure 5.1.25 *Comparison of the EDJ of SK 28 with* P. robustus *third and fourth upper premolars of known tooth position.* _____ *67*

Figure 5.1.26 *Comparison of the EDJ of SK 28 with* P. robustus *third and fourth upper premolars of known tooth position.* _____ *68*

Figure 5.1.27 *Plot of* H. naledi *teeth on the first two principal components of EDJ shape.* _____ *70*

Figure 5.1.28 *Summary of differences in EDJ morphology between third and fourth upper premolars of* H. naledi. _____ *72*

Figure 5.1.29 *All* H. naledi *EDJs in the study sample in occlusal view.*_____ *73*

Figure 5.1.30 *All H. naledi EDJs in the study sample in mesial view.*_____ *74*

Figure 5.1.31 *All* H. naledi *EDJs in the study sample in buccal view.*_____ *75*

Figure 5.2.1 *Box and whisker plot of centroid size by species and tooth type.*_____ *77*

Figure 5.2.2 *Group means for centroid size by species and by tooth type.*_____ *78*

Figure 5.2.3 *Difference in centroid tooth size (UP3 – UP4) for individual specimens within the sample that possess both tooth positions.* _____ *79*

Figure 5.3.1 *Plot of shape principal component scores.*_____ *82*

Figure 5.3.2 *Mean shape values predicted by the MANOVA model (Hollow circles) and the observed mean shape values (filled circles)..* _____ *84*

Figure 5.3.3 *Scatterplot of scores on the first and second linear discriminant functions for shape.* __ *86*

Figure 5.3.4 *Principal component scores for shape. The position of STS 61 in the principal component analysis (STS 61 is circled in red)* _____ *90*

Figure 5.3.5 *Principal component scores for shape. Position of early and mid-Pleistocene species of Homo among the study sample.* _____ *91*

Figure 5.3.6 *Upper fourth premolars from STS 61, STS 57 and Steinheim 1.* _____ *92*

Figure 5.4.1 *Linear regression of the first principal component of tooth shape against tooth centroid size.*_____ *94*

Figure 5.4.2 *Analysis of covariance (ANCOVA) of the first principal component of tooth shape against tooth centroid size with* H. naledi *as a factor.* _____ *95*

Figure 5.4.3 *Plot of scores on the first two principal components in form space.* _____ *97*

Figure 5.4.4 *Plot of scores on the first two discriminant functions/canonical variates of form.* _____ *98*

Figure 5.5.1 *Wireframe models showing the height of the buccal dentine horn relative to the height of the lingual dentine horn for each tooth position by species..* _____ *105*

Figure 5.5.2 *The position of the buccal dentine horn relative to the lingual dentine horn in hominin third and fourth upper premolars.* _____ *106*

Figure 5.5.3 *The mean shape of the CEJ and of the EDJ ridge in each species in this study, seen in occlusal view.* _____ *107*

Figure 5.5.4 *Features of the EDJ ridge: Accessory dentine horns and the mesial EDJ notch.* _____ *108*

Figure 5.6.1 *. Principal component analysis for shape [upper graph] and form (shape plus size) [lower graph].* _____ *110*

Figure 5.6.2 *Differences in morphology at the extremes of the first principal components of shape and of form.*_____ *111*

Figure 5.6.3 *Buccal dentine horn height in* H. naledi *compared with* P. robustus *and* A. africanus. _ *112*

Figure 5.6.4 *Trends in EDJ morphology in hominin third upper premolars.* _____ *114*

Figure 5.6.5 *Trends in EDJ morphology inhominin fourth upper premolars..*_____ *115*

Figure 5.6.6 *Trends in the form of the CEJ ridge and the EDJ ridge in occlusal view in hominin upper premolars*_____ *116*

Figure 5.6.7 *Comparison of the EDJ ridge of* H. naledi *in occlusal view with that of other hominins. 117*

Figure 5.6.8 *Bounding boxes for mean third upper premolar EDJ surfaces.* _____ *118*

Figure 5.6.9 *Bounding boxes for mean fourth upper premolar EDJ surfaces.*_____ *119*

Figure 5.6.10 *Trends in aspect ratio of bucco-lingual width to dentine horn height for third upper premolars.* _____ *120*

Figure 5.6.11 *Trends in aspect ratio of bucco-lingual width to dentine horn height for fourth upper premolars.* _____ *120*

Figure 5.6.12 *Talon expansion..* _____ *121*

Figure 5.7.1 *Qualitative features of the EDJ ridge.*_____ *123*

Figure 5.7.2 *Degrees of expression of the mesial and distal ridges of the buccal surface of the EDJ.* *124*

Figure 5.7.3 *Extension of the cingulum and other features of the buccal and lingual cingulum.*____ *125*

Figure 5.7.4 *Shield-boss shaped cingulum bulge.*_____ *125*

Figure 5.7.5 *Features of the transverse crest including the distinction between a central transverse crest and a mesial transverse crest.* _____ *126*

Figure 5.7.6 *Ridges of the occlusal surface of the EDJ (Excluding transverse crests).*_____ *128*

Figure 5.7.7 *Features of premolars which suggest a degree of molarisation.* _____ *129*

Figure 5.7.8 *Multidimensional scaling of the Mahalanobis D^2 distances between group means.*___ *135*

Figure 5.8.1 *anomalies of the buccal dentine horn.*_____ *138*

Figure 5.8.2 *The Krapina 48 upper left third premolar, showing a cuspule in the mesio-buccal cingulum.* _____ *138*

LIST OF TABLES.

Table 2.4.1 *Summary description of sample by species, site and tooth position. 23*

Table 2.4.2 *Number of subjects by species and tooth position 24*

Table 4.7.1 *Labels for species and tooth position..... 33*

Table 4.7.2 *Colour coding for species 33*

Table 5.2.1 *Mean centroid size by tooth type and species. 76*

Table 5.2.2 *t - tests for size differences between UP4s for* H. naledi *and other hominin species. 80*

Table 5.2.3 *t - tests for size differences between UP3s for* H. naledi *and other hominin species. 80*

Table 5.3.1 *Predicted classification under the linear discriminant model. 87*

Table 5.3.2 *Predicted classification under the 'leave one out' cross validated linear discriminant model. 88*

Table 5.3.3 *lists the teeth which are misclassified under the "leave one out" cross validation analysis. 89*

Table 5.4.1 *Correlation and covariance between size and the first five principal components of shape. 93*

Table 5.4.2 *Tooth classification under the linear discriminant analysis including centroid size. 99*

Table 5.4.3 *Tooth classification under the 'leave one out' cross-validated analysis including centroid size. 100*

Table 5.4.4 *List of teeth misclassified by the linear discriminant analysis (LDA) and by the 'leave one out' cross-validated analysis. 101*

Table 5.7.1 *Counts and percentages of qualitative features of the EDJ ridge 130*

Table 5.7.2 *Counts and percentages of qualitative features of the buccal and lingual surfaces of the EDJ. 131*

Table 5.7.3 *Counts and percentages of the transverse crest of the EDJ. 132*

Table 5.7.4 *Counts and percentages of the most prominent ridges on the occlusal surface the EDJ.. 133*

Table 5.7.5 *Counts and percentages of features suggesting molarisation of premolars. 134*

Table 5.7.6 *Summary of associations between morphological characteristics and tooth category ... 136*

1 INTRODUCTION.

Homo naledi was discovered by cave explorers in 2013 in the Dinaledi Chamber of the Rising Star cave system in the 'Cradle of Humankind' world heritage site in South Africa (Berger and Hawkes, 2017; Berger *et al.*, 2015). More fossils were later recovered from a second chamber in the cave, the Lesedi Chamber (Hawkes *et al.,* 2017). The Dinaledi chamber was dated at ca. 335 - 236 ka (Dirks *et al.*, 2017). This late date, overlapping with the earliest modern humans, is surprising, given the many primitive features of *H. naledi.* The fossils show similarities with *Homo habilis, Homo rudolfensis, Homo erectus* and *Homo heidelbergensis* (Berger *et al.* 2015). Dembo *et al*. (2016) used Bayesian phylogenetic analyses on craniodental data in *H. naledi* and 19 hominin species from Africa, Europe, and Asia. They concluded that *H. naledi* belongs in the genus *Homo* but is sufficiently different from other known species to be regarded as a new species. Irish *et al.* (2018) did a qualitative morphometric analysis based on 78 nonmetric dental traits. They found that the permanent post-canine dentition has small teeth that retain the principal molar cusps, as in modern humans, but seemingly lack accessory crown traits common in other African hominin groups. They, too, concluded, based on this dental evidence, that *H. naledi* is a distinct new species of *Homo*.

Nevertheless, debate has continued about the taxonomy and phylogenetic relationships of *H. naledi* because of its unique mix of primitive and advanced features. The body size, body form, arms, fingers, chest and pelvis all appear primitive (Feuerriegel *et al.*, 2017; Kivell *et al.*, 2015; Williams *et al.*, 2017; VanSickle *et al.*, 2018). Brain size is small, both absolutely and in proportion to body size (Garvin *et al.*, 2017). The thigh and leg show mixed features (Marchi *et al.* 2017). On the other hand, certain features in the morphology of the foot, wrist and thumb appear modern (Harcourt-Smith *et al.*, 2015; Kivell *et al.*, 2015). Recent morphometric studies of the lower (mandibular) premolar enamel-dentine junction (EDJ) demonstrate that this method is capable of distinguishing between hominin taxa (Pan *et al.*, 2016, Davies *et al.*, 2019) including *H. naledi* (Davies *et al.*, 2020). However, there is more morphological variation in hominin lower premolars, especially in the third lower premolar, than there is in in upper premolars. The purpose of this study is to extend this work to examine the upper (maxillary) premolars, focusing on *H. naledi* but also reporting variation in upper premolar EDJ morphology among hominins for the first time. Specifically, its aims are:

1) To determine whether geometric morphometric analysis of maxillary premolars based on landmarks on the enamel-dentine junction (EDJ) ridge and the cementum-enamel junction (CEJ) can distinguish between hominin taxa and between tooth position within taxa
2) To apply this method to *H. naledi*, in order to assess its taxonomic validity based on upper premolar morphology and to elucidate its relationship with other species of the genus *Homo*.
3) To identify morphological features of the hominin EDJ which have the potential to distinguish between taxa and tooth position in a qualitative morphometric analysis.

2 LITERATURE REVIEW

2.1 Teeth in the fossil record

2.1.1 The abundance of teeth in the fossil record

Enamel is the hardest and most durable tissue in the vertebrate body and comprises only 1 – 2% by weight of organic material (Berkovitz *et al.,* 2018). Therefore, it is less prone than other tissues to the processes of *post-mortem* decomposition. Dentine is also a dense and durable tissue. As a result, teeth are well represented in the fossil record of primates, including hominins[1]. Martin (1990, p.39) estimated that "more than 65% of primate fossil species recognized at present by palaeontologists are based on extremely fragmentary remains, consisting at most of isolated partial jaws and often only of a few teeth". Similarly, Le Gros Clark (1970, p.17) wrote that "a great deal more is known of the teeth of extinct mammals than of any other part of the body, and for this reason the comparative anatomy and evolution of the dentition have been studied in very considerable detail".

It is often possible to identify a species by the morphology of its teeth alone. In some cases, the discovery of just a single tooth can extend the known temporal or geographic range of a species. Or alternatively, a single tooth, if it is distinctive enough, may provide evidence of a previously unknown species. For example, in 1935 G. H. R von Koenigswald found a single large primate tooth in a Hong Kong pharmacy, which was the first indication of the existence of *Gigantopithecus blacki* (Simons, 1970) and *Gigantopithecus* is today predominantly known from dentognathic remains (Zhang *et al.*, 2016).

2.1.2 The primate dentition

Tooth morphology varies greatly within mammals and has made major contributions to the description and classification of mammalian species and to an understanding of their phylogenetic relationships. Hillson (2005), Ungar (2010) and Berkovitz and Shellis (2018) have reviewed the variations in tooth morphology found in mammals and Swindler (2002) reviews the diversity of tooth morphology within the living primates. Szaley and Delson (1979) and Hartwig (2002) have reviewed the fossil primates, including detailed discussions of their dental morphologies.

Primates tend to be generalists and have teeth which have not deviated a great deal from the primitive mammalian dentition. The baseline dental formula for mammals is $\frac{3.1.4.3}{3.1.4.3}$. Primates have only two incisors and have a tendency to reduce and lose the premolars. The New World Monkeys (Platyrrhini) retain three premolars but the

[1] In this thesis, the term 'hominin' is used to refer to the subtribe Hominina – the clade which contains modern humans and all fossil species which are closer to modern humans than they are to living chimpanzees and bonobos (the subtribe Panina).

Catarrhini (Cercopithecoidea (old world monkeys) and Hominoidea (apes and humans)) have only retained the third and fourth premolars. There is also a tendency for premolars to become more complicated in structure in primates, especially in the distal part of the tooth row, often with a degree of molarisation. The upper molars show a tendency to develop a quadritubercular form by the addition of a hypocone. The lower molars also have a tendency to develop a quadritubercular quadrilateral form by loss of the paraconid, in all Primates except the tarsiers, and by the protoconid moving into line with the metaconid. The talonid broadens and rises to become roughly equal in height with the trigonid to form a relatively flat occlusal surface. Other characteristic features of the primate dentition are the bilophodont molars of the Catarrhine monkeys (with two prominent transverse ridges on each molar) and the 'Dryopithecine' or Y shaped pattern of fissures in the lower molars of the Hominoidea. Hominins are rather uniform in their dental arcade with variation being restricted to the size and shape of the crowns at each tooth position.

2.2 The morphology of the enamel-dentine junction.

2.2.1 The development and morphogenesis of the EDJ and the outer enamel surface (OES).

The morphology of the EDJ derives from folding of the inner enamel epithelium of the enamel organ due to differential rates of cell division under the controlling influence of enamel knots, groups of non-proliferating cells derived from the inner enamel epithelium (Berkovitz *et al*, 2018). The primary enamel knot determines overall crown size and shape and is removed by apoptosis[2] at the end of the cap stage of development. In the early bell stage, the secondary enamel knots control the morphological development of the main tooth cusps (Jernvall and Jung, 2000). This process is controlled by a complex interactive web of excitatory and inhibitory factors, including genes, proteins and transcription factors (Jernvall and Thesleff, 2000; Thesleff, 2014).

Only after the form of the future EDJ has been created by folding of the inner enamel epithelium, does enamel production begin. The description here of enamel production and deposition follows the review by Berkovitz *et al*. (2018). Ameloblasts (enamel producing cells from the inner enamel epithelium) migrate out perpendicularly from a basement membrane which will eventually form the EDJ. As they do so, enamel is formed in their wake . This process starts at the dentine horns with a wave of amelogenesis spreading down over the rest of the surface and forming the cervix upon completion. Although enamel deposition starts at the tips of the dentine horns, it also ceases there first, so continued growth in the 'basins' of

[2] Apoptosis is programmed cell death. After the enamel knot has performed its developmental function, the cells of which it consists die and the cell remains are removed by the immune system - but without provoking an inflammatory response.

the tooth surface tends to smooth and round the contours of the final OES. One should therefore expect that the major features of the OES resemble the form of the underlying EDJ but that they will differ in some respects and that some details may be obscured. Recently Häkkinen *et al.* (2019) proposed a computational model of enamel matrix secretion that maps the dentine topography to the enamel surface topography and which attempts to explain the similarities and differences between them.

2.2.2 The strong genetic signal of the enamel-dentine junction (EDJ)

Unlike most tissues of the body, including the skeleton, teeth are not re-modelled during the life of an individual. The morphology of the EDJ and the enamel cap is formed prior to the eruption of the tooth and is not affected by environmental factors unless there is severe disruption during tooth development due to trauma, disease or malnutrition (Berkovitz *et al.*, 2018; Hillson, 2014). Hence, the morphology of the tooth strongly reflects the genotype of the individual, whereas skeletal morphology reflects both the genotype and the uses to which the bone has been put during life that result in remodelling.

However, this lack of re-modelling also means that the outer enamel surface (OES) of the tooth is subject to being worn away through use, with the rate and pattern of wear being determined by the properties of the food which is eaten and the mechanism of chewing (In humans, there may also be behavioural or deliberate modification of the teeth (Scott *et al.,* 2018)). The pattern of wear, including the examination of micro-abrasions on the tooth surface, can be informative about the diet and lifestyle of an extinct species (Ungar *et al.,* 2008). On the other hand, tooth wear can alter, obscure or obliterate morphological features of the OES making taxonomic comparisons difficult (Burnett *et al.,* 2013). The EDJ, protected by the overlying enamel cap, is not affected by wear until it has reached an advanced stage. Hence, its morphology is not altered and it is potentially a more reliable taxonomic indicator than the OES. However, the enamel cap also makes the EDJ relatively inaccessible, buried deep within the hard substance of the tooth.

2.2.3 Methods of studying the EDJ

Many of the early researchers of the EDJ were stimulated to investigate it because they believed that it retained primitive features and phylogenetic signals which are obscured to some extent by the overlying enamel. As Korenhof (1978, p. 157) wrote:

> "[The inner enamel surface] represented more conservative conditions than the outer surface, often displaying details which are unknown from the outer anatomy of man but are known in earlier hominoid dentitions, especially in the Dryopithecinae. This could be expected on embryological grounds because the inner enamel surface […] is identical to the original contact surface of ameloblasts and odontoblasts before both types of cell start producing the matrices of their specific tissues. Owing to the thickness of the enamel and its uneven distribution over the tooth, the external surface

grows to a larger, rounder form reflecting the dentine surface only imperfectly."

Early studies of the EDJ (Butler, 1956; Kraus and Jordan, 1965) looked at the embryological form of the folded *inner enamel epithelium* of the enamel organ at the early bell stage of development – the precursor of the EDJ before enamel and dentine deposition begins. Other studies (Kraus, 1952; Corruccinni, 1987, 1998) dissolved the enamel away from the dentine surface of humans and other living primates by using acids (after recording the morphology of the outer enamel surface as a cast). Sakai *et al.* (1965, 1967a,b, 1969, 1971, 1973a,b) also examined the EDJ in modern Japanese populations by dissolving away the enamel surface with acids.

Korenhof (1960, 1978, 1982) made use of a fortuitous discovery, originally by G. H. R. von Koenigswald, of many isolated enamel crowns (the dentine having decomposed) washed out of medieval graves on the Island of Java. Thin sections of teeth have also been used but not often in fossil specimens because they destroy the specimen and the grinding and polishing process leads to tissue loss, which may remove important features such as dentine horns.

Nager (1960) decalcified 96 human teeth to compare the shapes of the OES and the EDJ of the same tooth. Based on his observations he defined three types of structures. A ''primary-definitive'' feature consists of structures that are present on both the EDJ and on the unworn OES. A ''primary-temporary'' feature consists of structures that are present on the EDJ but cannot be observed on the unworn OES. A ''secondary'' trait consists of structures not seen on the EDJ, but which are evident on the OES.

Modern studies of the enamel-dentine junction began with the invention of computerised tomography (CT), particularly of micro-computed tomography (µCT), in which x-rays are projected at an object and the intensity of the transmitted x-ray radiation is measured as the object is rotated through 360 degrees. Specialised software then analyses this data and produces images of the object as a stack of high-resolution 'slices', usually representing about 10 – 60 microns thickness per slice (Kono, 2004; Olejniczak *et al*., 2004; Olejniczak and Grine, 2005, 2006; Olejniczak, 2006; Olejniczak *et al*., 2007; Skinner, 2008; Skinner *et al.,* 2008b). Many of these early studies primarily examined enamel thickness in cross sections of a tooth or the morphology of the EDJ in planar slices, rather than three dimensional reconstructions of the dentine surface.

Macchiarelli *et al*. (2008) review some of the early studies using this technique and give an account of its scientific and technical background. Using specialised software, it is possible to take two dimensional slices through the image stacks in any desired direction (and hence, for example, standardise measurements of enamel thickness in relation to landmarks on the EDJ). Also, the image stacks can be segmented into different materials and used to create three dimensional images of the EDJ and other surfaces, suitable for numerical measurement and statistical analysis (Weber and Bookstein, 2011).

2.2.4 Relationships between the morphology of the EDJ and the OES

The relationship between individual morphological features of the EDJ and that of the OES has been investigated in several studies. Nager (1960) classified OES features according to their relationship to the underlying EDJ. Skinner *et al.* (2008b) found that dental traits in hominoid lower molars originate at the EDJ, where they may show variations in morphology which are not reflected at the OES. They concluded that different developmental processes, evident at the EDJ, may show similar morphology at the OES and caution should therefore be exercised when using these OES characters to make taxonomic inferences. Skinner *et al.* (2009b) investigated protostylid expression in robust and gracile australopiths and found taxon-specific patterns of morphology in the EDJ which were not evident at the OES. Ortiz *et al.* (2012, p.586), studied Carabelli's trait in *Pan* and *Homo sapiens*, highlighting the "wealth of morphological data that can be obtained at the EDJ for understanding tooth development and for characterizing tooth crown variation in worn fossil teeth". Ortiz *et al.* (2017) investigated cusp 5 of upper molars and cusps 6 and 7 of lower molars in a range of hominoids, finding evidence of homoplasy. For each of the characters investigated a range of different developmental processes, identified at the EDJ, gave rise to a similar appearance at the OES. The trigonid crest in the EDJ and OES has been investigated in the lower molars of Neanderthals (Bailey *et al.,* 2011) and in the Sima de los Huesos hominins (de Pinillos *et al.*, 2017) and strong concordance was found in the expression of this feature at both surfaces. In summary, although the strength of correlation between the EDJ and the OES may differ from one feature to another, it seems that individual features do tend to be expressed both at the EDJ and at the OES, but that in most cases the EDJ provides more detailed morphological and phylogenetic information, especially where the enamel is thick.

Looking at the relationship between the morphology of the EDJ and the OES as a whole, Skinner *et al.* (2010) investigated the relative contributions of enamel-dentine junction shape and enamel deposition to primate molar crown complexity and found that both of these factors do contribute to overall crown complexity. Guy *et al.* (2015) examined the relationship between the EDJ and the OES in a sample of 76 primate upper second molars. For each tooth they divided the EDJ and the OES into the same large number of small triangular patches and then estimated the correlation at the corresponding patches on each surface for elevation, orientation and curvature. They found a strong correlation for elevation and moderate to strong correlations for orientation in all their specimens. They found a moderately strong correlation for curvature. All these correlations tended to be less strong with increasing enamel thickness. They concluded that the EDJ carries "the majority of the occlusal morphology" of the tooth. Morita (2014; 2016) examined an archaeological sample of modern human permanent upper first molars (UM1) and deciduous upper second molars (um2) by landmarking the main cusps and ridges on both the EDJ and the OES. They showed that shape was strongly correlated between these two surfaces and concluded that enamel formation does not alter the basic morphology of the EDJ ridges and dentine horns. However, the pattern of change

between the OES and the EDJ was different between the two tooth types and the strength of correlation was stronger in the deciduous tooth. These differences may be due to thinner enamel or to differences in the timing, location or duration of enamel deposition, and suggest that, even though basic tooth morphology is set by the EDJ, enamel deposition does play some role in creating the final morphology of the OES. Taking these studies overall, it seems that the EDJ determines the main features of tooth morphology, including the main cusps and ridges. Broad differences in the timing, location and duration of enamel deposition in different teeth may contribute to the final morphology of the OES and add some complexity to the surface morphology of the tooth. However, there is little evidence that the localised control of enamel deposition contributes significantly or consistently to the characteristics of the OES.

2.3 Qualitative morphometrics and geometric morphometrics

2.3.1 Qualitative morphometrics

Certain features of crown and root morphology vary in their frequency of expression in modern human populations. The identification, description and analyses of these features has been of great interest to dental anthropologists since Georg von Carabelli (1842) first described the mesio-lingual accessory cusp which bears his name. The history and current state of qualitative dental morphology are comprehensively reviewed by Scott *et al.* (2018). In modern human populations there is no universally accepted set of dental traits for morphological analysis but the Arizona State University Dental Anthropology System (ASUDAS) (Turner *et al.*, 1991; Scott and Irish, 2017) is widely used. This set of features has been successful in differentiating modern human populations from each other and in elucidating their evolutionary relationships (Scott *et al.*, 2018). However, it is not necessarily applicable to fossil *Homo* populations or to other hominins. Features which show variability in modern human populations may be non-variable in past populations – either universally present or always absent. Other traits, which do not distinguish between modern populations, or do not appear in modern populations, may be important in differentiating fossil hominin populations from each other.

Bernard Wood and a series of collaborators (Wood and Abbott, 1983; Wood *et al.*, 1983; Wood and Uytterschaut, 1987; Wood and Engleman, 1988; Bailey and Wood, 2007) extended the methods of qualitative morphometrics to the post-canine dentition of Plio-Pleistocene hominin populations. They identified traits such as additional cusps on the maxillary and mandibular molars and an extended lower fourth premolar talonid, which distinguish between Plio-Pleistocene hominin populations. Starting with a putative last common ancestor, Bailey and Wood (2007) postulate an increase in crown size and morphological complexity in *Paranthropus* and a decrease in crown size and complexity in the genus *Homo.* In the genus *Australopithecus* they identify an early tendency for increasing complexification of molar morphology compared with species of the genus *Homo.*

Bailey (2000, 2002a, 2002b), Bailey *et al.* (2011) and Bailey and Hublin (2013) have used ASUDAS and other dental features to study Neanderthal and modern human populations in order to elucidate the dental characteristics of Neanderthals and modern humans and to explore the evolutionary relationship between them. This work is the foundation which recently led to the identification of a possible mixed Neanderthal and modern human ancestry in the dental remains of a hominin from La Cotte de St. Brelade in Jersey (Compton *et al.,* 2021). Martinón -Torres *et al.* (2007, 2013) applied qualitative morphometrics to study Pleistocene species of *Homo*, including the hominin population from Dmanisi, Georgia (Martinón -Torres *et al.*, 2008) and the hominins from Sima de los Huesos in Spain (Martinón -Torres *et al.*, 2012). Qualitative morphometric studies have also been carried out on *Homo floresiensis* (Kaifu *et al.*, 2015) and *H. naledi* (Irish *et al.* 2018). The method has also

been applied, in combination with other methods, to elucidate the complex relationships of hominins in East Asia (Bailey and Liu, 2010; Liu *et al.,* 2013; Xing *et al.* 2014, 2015, 2016, 2018, 2019, 2021).

Qualitative morphometric studies tend to look at the dentition as a whole or, at least, the parts of the dentition which are available for study. Much attention has been focussed on the incisors, which have distinctive patterns of curvature and of shovelling, and on the molars, which have rich, complex cusp patterns and other features. The lower premolars have also been studied, especially the honing complex of the third lower premolar and some distinctive features in the shape and transverse crest of the lower fourth premolar. The upper premolars have been relatively less studied. The ASUDAS features of the upper premolars are mesial or distal accessory (occlusal) ridges on the buccal cusp, and mesial or distal accessory cusps (on the mesial or distal occlusal margin) in either the third or fourth upper premolar. Also included is the Uto-Aztecan premolar, premolar odontomes and premolar root number (1 or 2 roots on UP3). (Scott and Irish, 2017). To this, Bailey has added a buccal median ridge (Bailey and Hublin, 2013; Irish *et al.*, 2018). Kaifu (2015) added the presence of a transverse crest on the third or fourth upper premolar, the presence of grooves on the buccal surface of the third upper premolar and P^4 lingual crown development (the mesiodistal width of the lingual part of the tooth is equal to or greater than the mesio distal width of the buccal part of the tooth). Martinón-Torres and her collaborators (for example, Martinón-Torres *et al.* 2008, 2012) emphasize the presence of a transverse crest and/or a bifurcated essential ridge on either the buccal or lingual cusp in the third or fourth upper premolar as relatively primitive features of the genus *Homo* which have been lost in modern humans. Although most recent qualitative morphometric studies do include images of the EDJ surface and comparisons of the EDJ surface with the OES as part of a comparative morphometric analysis there are no systematic studies of the relationship of the EDJ to the OES in upper premolars of fossil hominins or any attempts to identify qualitative morphometric features which are specific to the EDJ of upper premolars.

2.3.2 Geometric morphometrics

Measuring the shape of the dentition is an important technique of dental anthropology. The ratio between the length and breadth of a tooth or the relative sizes of teeth in different positions along the tooth row are aspects of shape. Indeed, any ratio of lengths giving a dimensionless quantity can be regarded mathematically as a measure of shape. Simple measurements of tooth dimensions and cusp lengths analysed by traditional multivariate methods are capable of distinguishing between hominoid taxa and of measuring the degree of variation within taxa. For example, Pilbrow (2007) showed that molar metrics are successful in differentiating between the genera, species and subspecies of great apes and suggested that the degree of variation between taxa in living hominoids might help to assess the degree of variation between the equivalent taxa in fossil hominoids.

A similar approach is to analyse absolute and relative cusp areas in post-canine teeth by traditional multivariate analysis. For example, Bernard Wood and various collaborators examined the absolute and relative cusp areas of Plio-Pleistocene hominid mandibular molars (Wood and Abbott, 1983; Wood *et al.*, 1983), mandibular premolars (Wood and Uytterschaut, 1987) and maxillary postcanine teeth (Wood and Engleman, 1988) and were able to identify patterns of variation between various hominid groups. Their main finding in upper premolars was that 'East African Robustus' upper premolars have a relatively larger buccal cusp than other Plio-Pleistocene hominids, including 'South African Robustus'. Moggi-Cecci and Boccone (2007) applied similar methods to a comparison of absolute and relative cusp size in the maxillary molars of *Paranthropus* and *Australopithecus.* Grine *et al.* (2009) used a multivariate analysis of postcanine cusp areas to explore the affinities of early *Homo* specimens from South Africa. Grine *et al.* (2013) used the same techniques on mandibular postcanine teeth to question whether one or two species of *Australopithecus* may be present in the Member 4 deposits at Sterkfontein.

Geometric morphometrics based on landmark data developed in the 1980s and started to become established in biology in the 1990s (Kendall, 1989; Rohlf and Marcus, 1993; Bookstein, 1997; Adams, Rohlf and Slice, 2004). Reviews of the current field of geometric morphometrics are given by Bookstein (2018) and by Dryden and Mardia (2016).

Two-dimensional geometric morphometrics have been used to study the occlusal outline and cusp patterns of the OES of hominin teeth, photographed in occlusal view. Gómez-Robles *et. al* (2007, 2008, 2011, 2012, 2015) used this technique in a series of studies of the post-canine dentition of Pleistocene populations of the genus *Homo* with special reference to the population at Sima de los Huesos. Their findings in relation to upper premolars are discussed in Section 2.3.3.

It has been shown that it is possible to reliably classify specimens of teeth into established taxa, and even populations within taxa, by using the morphology of the EDJ. Smith *et al.* (2006) examined plane cross sections of modern human molars and found that both EDJ shape and enamel thickness vary with tooth position (metameric variation), sex and population of origin. Sexual dimorphism is difficult to study in fossil hominins because the sex is nearly always unknown. In modern humans, male canine and post-canine teeth tend to be larger in the dimensions of the EDJ but female teeth have relatively more enamel (Feeney, 2009; Feeney *et al.*, 2010; García-Campos *et al*., 2018; Sorenti *et al.*, 2019). The ratio of dentine volume to enamel volume is higher in males than in females and this ratio can differentiate between male and female teeth (Saunders *et al.*, 2007; García-Campos *et al*., 2018). García-Campos *et al.* (2020) have shown that the Sima de los Huesos population of hominins shows similar sex differences to modern humans in the ratio of the dentine volume to enamel volume of their canine teeth.

Olejniczak *et al*. (2007) examined homologous planar cross sections of upper molars from a wide range of living and fossil anthropoid species. A discriminant function analysis of EDJ shape in planar cross section was able to successfully classify the

living taxa, suggesting that it may also be a reliable taxonomic indicator in fossil taxa. Skinner *et al.* (2009a) examined the EDJ of first and second lower molars of the living species and subspecies of *Pan* (chimpanzees and bonobos). They created images of the EDJ surface which they landmarked and then classified using geometric morphometric analysis. Discriminant function analysis distinguished between the species and subspecies with a high degree of reliability[3]. This is an important study because it shows that geometric morphometric analysis of the EDJ can pick up variation between living taxa at the subspecies level. If the variation between fossil species is as great as in living hominids, then the morphology of the EDJ should be able to distinguish between them. Skinner *et al.* (2007) have investigated taxonomic reliability in fossil species directly by studying the lower molars of *Paranthropus robustus* and *Australopithecus africanus* specimens from South Africa using the geometric morphometric analysis of landmarked EDJ surfaces. They found that EDJ morphology could distinguish between the two species and that it could also distinguish between first, second and third lower molars within each species.

Braga *et al.* (2019) have shown that it is possible to discriminate between Early Pleistocene hominin mandibular molars (*P. robustus, A. africanus and Homo sp*.) using diffeomorphic surface matching (DSM) of the EDJ. In this technique a smooth transformation is calculated between pairs of surfaces, optimised by minimising an energy function. Essentially, this calculates the simplest and most direct transformation which will deform one of the surfaces into the other. All such deformations are reversible. The 'distance' between the two surfaces is the average degree of deformation required to deform each surface into the other (the distance being the same for each deformation and its reverse). Using these distances, it is possible to categorise the EDJ surfaces into clusters, which can be visualized by multidimensional scaling. This seems to discriminate between taxa at least as well as traditional geometric morphometric approaches but has the advantage that it is not necessary to landmark the surfaces. The correspondence between features on the two surfaces is accounted for automatically during the process of calculating the best deformation. This also means that DSM uses information from the whole surface, not just information from the chosen landmarks, and is therefore potentially capable of automatically including what have traditionally been labelled as 'discrete' features or characteristics in the analysis of surfaces.

2.3.3 Geometric morphometric studies of hominin upper premolars

Geometric morphometrics of the OES was used to analyse hominin upper premolars by Gomez-Robles *et al.* (2011). They placed landmarks on the margin of the OES in occlusal view and on the cusps and fossae of the occlusal surface. The technique was able to discriminate reasonably well between taxa within the genus *Homo*. The same

[3] This study landmarked the cusps and ridges of the EDJ and the CEJ. The same team (Skinner et al, 2009c), instead of using the CEJ, added extra landmarks to the occlusal basins of the EDJ and found small increases in the accuracy of classification as the number of landmarks is increased.

technique has subsequently been used in other studies of upper premolars (for example: Xing *et al.*, 2016; Xing *et al.*, 2019)

Braga *et al.* (2010) used micro-computed tomography (μMCT) of the EDJ to examine metameric and antimeric variation in the dentition of a specimen of *A. africanus* (Sts 52). Détroit, *et al.* (2019) carried out a procrustes analysis of the landmarked EDJ ridge in a comparative study of the upper premolars of the recently described *Homo luzonensis.* Diffeomorphic surface matching has been applied recently to a geometric morphometric analysis of the EDJ of East Asian hominin premolars (Pan *et al.,* 2020). However, upper premolar EDJ morphology within and between hominin taxa remains largely unexplored.

2.4 Conclusions

The morphology of the EDJ carries a strong genetic signal, unaltered by stresses upon the tooth during its lifetime and immune to tooth wear until it has reached an advanced stage. In morphology, the EDJ corresponds closely to the morphology of the unworn OES and where the morphology of the EDJ and the OES differ, it seems that the EDJ carries a stronger phylogenetic signal than the OES. Early studies of the EDJ were limited due to its relative inaccessibility but micro-CT techniques have now made it possible to visualise the EDJ in hominins and to conduct morphological and statistical studies upon it. These studies have shown that the morphology of the EDJ can reliably discriminate between both existing and fossil hominin taxa, certainly down to the species level and possibly down to subspecies level. The morphology of the EDJ is also capable of identifying sexual dimorphism and metameric variation within species.

Previous comparative studies of the EDJ of hominin upper premolars, although limited in number and scope, have shown that it is possible to differentiate hominin taxa from each other and to explore their taxonomic relationships. In this study, the power of three-dimensional landmark based geometric morphometrics to discriminate between taxa will be tested and will be used specifically to explore the taxonomy and relationships of *H. naledi*.

3 SAMPLE.

The sample of *H. naledi* upper premolars in this study is from the Rising Star chamber at Dinaledi in South Africa. Teeth from the Lesedi chamber at Dinaledi (Hawkes *et al.* 2017) were inspected but the enamel surfaces were too worn for any teeth from the second chamber to be included in the study. An *Australopithecus africanus* sample was obtained from the sites of Makapansgat and Sterkfontein in South Africa and a *Paranthropus robustus* sample was obtained from Swartkrans in South Africa. *Homo* species are represented by early Neanderthals (*Homo neanderthalensis*) from the sites of Krapina in Croatia and Scladina in Belgium. Later Neanderthals are included from the sites of Le Moustier in France and El Sidron in Spain. In the analysis, all Neanderthals were analysed as a single group. There is a small sample of fossil *Homo sapiens* from the site of Qafzeh in Israel.

A modern human (*Homo sapiens)* comparative sample of upper premolars was taken from a clinical collection of extracted teeth held by the Max Planck Institute for Evolutionary Anthropology in Leipzig, Germany. Teeth were identified in this collection that did not appear to show major damage or disease to the enamel surface or to the cervix of the tooth and these were then micro-CT scanned. These are drawn from a Western European population

Because the intention of this study is to compare the morphology of the whole of the EDJ between species, teeth were only included if the EDJ was substantially complete and intact. Teeth which were broken or incomplete were excluded. Worn teeth, in which the dentine was exposed, were excluded unless the tips of the dentine horns could be reconstructed with a high degree of certainty. Teeth in which the EDJ or the CEJ were incomplete were also excluded.

Unfortunately, some teeth which could potentially have been included in the sample had to be excluded because poor contrast made segmentation of the tooth impossible (Fig. 2.4.1).

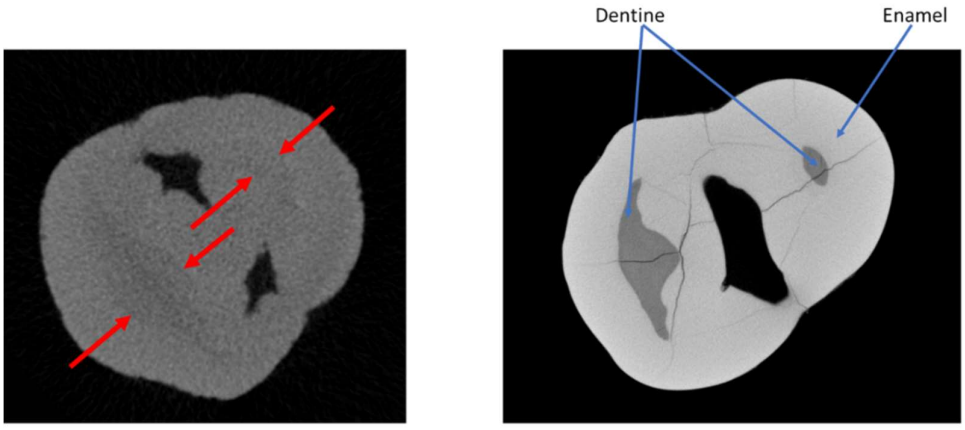

Poor Contrast. Arrows indicate boundary of EDJ. *Homo erectus.* Sangiran SMF_S7_31

Good contrast. Modern Human MPI_07_114

Figure 2.4.1 Poor contrast between tissues (left) and good contrast (right).

A summary of the sample for this study is given in Table 2.4.1. Full details of the sample are tabulated in Appendix 1.

Table 2.4.1 Summary description of sample by species, site and tooth position.

Species/Site/Tooth position	Number	Age
Australopithecus africanus	18	
Makapansgat, South Africa	4	2.85 - 2.58 Ma
P3	2	
P4	2	
Sterkfontein, South Africa	14	2.6 - 2.0 Ma
P3	8	
P4	6	
Homo erectus	5	
Sangiran, Java	3	1.6 Ma
P3	2	
P4	1	
Koobi Fora, Kenya	2	1.63 Ma
P3	1	
P4	1	
Homo heidelbergensis	1	
Steinheim, Germany	1	243 -191 ka (OIS 7)
P4	1	
Homo naledi	14	
Rising Star, South Africa	14	335 - 236 ka
P3	7	
P4	6	
Homo neanderthalensis	27	
El Sidron, Spain	4	49 – 39 ka
P3	1	
P4	3	
Krapina, Croatia	20	130 ka (OIS 5e)
P3	11	
P4	9	
Le Moustier, France	2	40 ka
P3	1	
P4	1	
Scladina, Belgium	1	100 ka
P4	1	
Homo rhodesiensis	2	
Thomas Quarry, Morocco	2	470 - 360 ka
P3	1	
P4	1	
Homo sapiens	43	
Anatomical Collection MPI,	43	Modern
P3	25	
P4	18	
Homo sapiens (Qafzeh)	8	
Qafzeh, Israel	8	100 - 80 ka
P3	4	
P4	4	
Paranthropus robustus	7	
Swartkrans, South Africa	7	2.25 - 1.8 Ma
P3	4	
P4	3	

There are 109 subjects in the sample. When grouped by species and tooth position, the sample groups are not equal in size (Table 2.4.2). The largest group contains 22 observations and the smallest group contains only three observations.

Table 2.4.2 Number of subjects by species and tooth position

	Aafr	Hnal	Hnean	Prob	Hsap(Q)	Hsap	Total
UP3	9	7	8	5	3	22	54
UP4	9	6	16	4	4	16	55
Total	18	13	24	9	7	38	109

(**Key:** Aafr = *A. africanus*, Hnal = *Homo naledi*, Hnean = *Homo neanderthalensis*, Prob = *P. robustus*, Hsap(Q) = Fossil *Homo sapiens* (Qafzeh), Hsap = *H. sapiens*).

The main study and the statistical analysis only included populations for which there were at least three teeth in each tooth position in the sample, but a few isolated specimens of *Homo* species were included in the qualitative morphometric analysis and in a supplementary quantitative morphometric analysis. (Reported in Section 5.3.3). These are *Homo erectus* from Kenya (KNM ER 3733) and from Sangiran in Java, *Homo rhodesiensis* from Thomas Quarry in Morocco and *Homo heidelbergensis* from Steinheim in Germany.

Where antimeres were present (the same tooth position on both sides of the jaw for the same individual) only the better-preserved tooth of the pair was included in the study. Unerupted teeth were virtually 'dissected' from the surrounding jaw and were only included in this study if enamel crown formation was complete, as indicated by the growth of dentine beyond the cementum-enamel junction (CEJ).

4 Methods

4.1 Microtomography

Microtomographic scans of the premolar sample were obtained using either a SkyScan 1173 at 100-130 kv and 90-130 microA, a BIR ACTIS 225/300 scanner at 130 kV and 100-120 microA, or a Diondo d3 at 100-140kv and 100-140 microA. The range of resolutions in the image stacks was voxel size 13 – 35 microns. Images with resolutions less than voxel size 28 microns were re-sampled to 28 microns. This voxel size gives a sharp definition of the features of enamel-dentine (EDJ) morphology. Smaller voxel sizes demand exponential increases in computer processing time and can cause problems in the visualisation and real time manipulation of surface images. Most of the images were in 8 bit greyscale (256 intensity levels of grey). A few images were 16 bit greyscale initially and these were re-sampled to 8 bit images, both for consistency with the other 8 bit images and to reduce image processing time.

4.2 Image filtering

The image stacks for each premolar were filtered using a three-dimensional median filter, followed by a mean of least variance (MLV) filter (Fig. 4.2.1), both with a kernel size of either one or three, implemented using MIA open-source software (Wollny et al., 2013). This process facilitates the segmentation of enamel from dentine by improving the homogeneity of the greyscale values for the enamel and dentine, and by sharpening the boundaries at the interface between tissue types (Schulze and Pearce, 1994). The kernel size was decided by visually assessing the level of contrast between enamel and dentine; a kernel size of three was used on those scans with low contrast. The effect of filtering on the morphology of the EDJ has previously been shown to be minimal (Skinner, 2008). Filtering reduces noise and gives a smoother, sharper image of the EDJ, as illustrated in Figure 4.2.2.

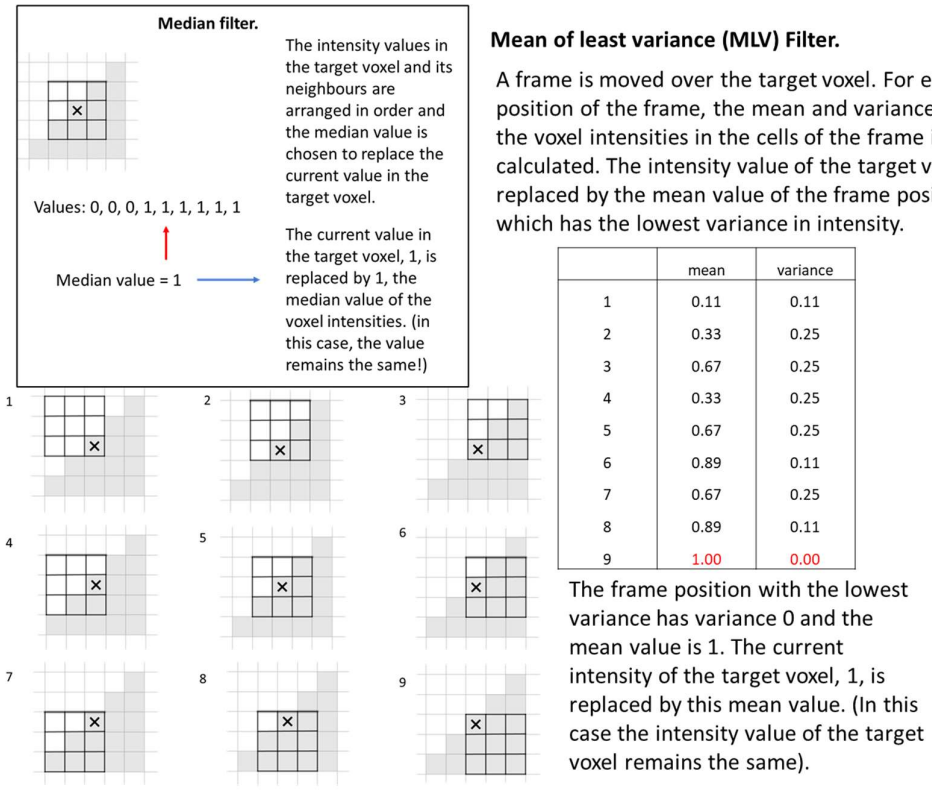

Figure 4.2.1 The median filter and the mean of least variance (MLV) filter.

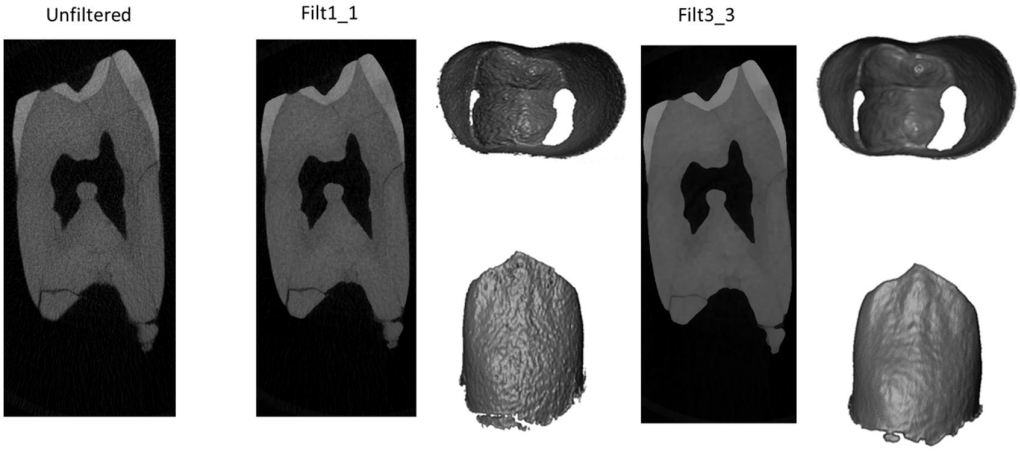

KRP D38 URP3 Median and Mean of Least Variance Filtering

Figure 4.2.2 The effect of filtering on EDJ morphology. The unfiltered image is at the left. The kernel size 1 filtered image is in the centre and the kernel size 3 filtered image on the right. For this tooth, the kernel size 3 filtered image gives a smooth, sharply defined surface image for the EDJ, preserving the details of its morphology.

4.3 Tissue segmentation

The filtered image stacks were processed using Avizo 6.3 (www. thermofisher.com) in order to produce surface models of the EDJ. Enamel and dentine were segmented using the LabelField facility in Avizo 6.3. Segmentation partitions the entire collection of pixels in three dimensions into regions of relatively homogeneous greyscale intensity. These regions represent the different tissues of the tooth. Where there is good contrast in the images the histogram of greyscale intensity across the entire pixel population of the image stack falls into a distribution with three distinct modes (for enamel, dentine and pulp) and the segmentation is relatively straightforward. In some cases, poor contrast between the voxel greyscale intensity in different tissues made segmentation through this method more difficult. In this case, the initial segmentation was carried out using custom made algorithms developed at the Max Planck Institute for Evolutionary Anthropology (MPI). These include an edge detection algorithm followed by a watershed algorithm. For the watershed, seeds are placed manually onto the image stacks and these are then expanded by the accumulation of adjacent voxels until an edge is reached or the boundaries of two seeded regions meet. The segmentation was then refined and corrected by eye. The EDJ was defined as the boundary at which the segmented enamel and dentine regions meet. A triangle-based surface model of the EDJ was then produced in Stanford .PLY format, using the unconstrained smoothing parameter in Avizo.

4.4 Landmark collection

3D landmarks were collected in Avizo 6.3 in three distinct sets; 'EDJ main', 'EDJ ridge' and 'CEJ ridge'. The placement of landmarks was checked by examining the landmark placement against oblique slices through the original unfiltered image stack. This is necessary because filtering can sometimes alter the greyscale intensity of a voxel to such an extent that it can be segmented into the wrong tissue. For example, where the enamel is very thin, filtering may lead to voxels in the enamel being wrongly segmented into dentine, causing potential inaccuracies in landmarking the CEJ. (Fig. 4.4.1)

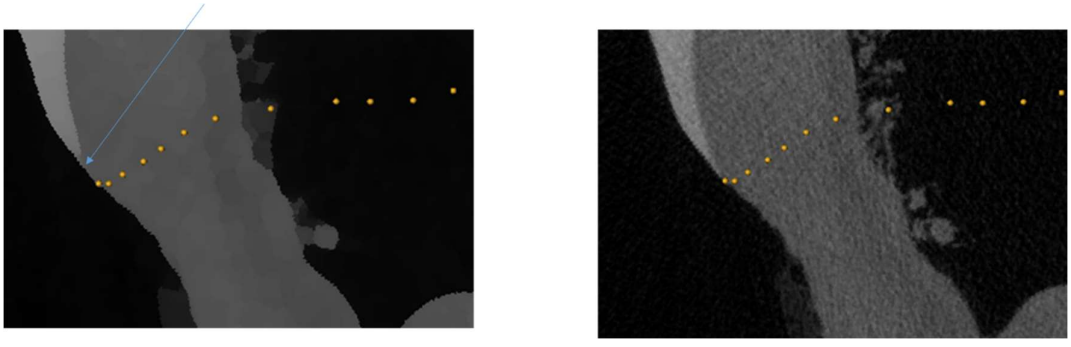

Figure 4.4.1 Checking landmark positioning against unfiltered image. In the filtered image (left) the margin of the enamel has been displaced (blue arrow) by the mislabelling of voxels in the segmentation. The unfiltered image (right) allows the correct placement of landmarks.

In hominin upper premolars there is a buccal dentine horn and a lingual dentine horn and continuous mesial and distal ridges join these horns so, when combined, the ridges form a continuous closed curve. The EDJ main landmark set consists of two landmarks, the first placed on the tip of the buccal dentine horn, and the second placed on the tip of the lingual dental horn. The EDJ ridge landmarks were placed on the continuous curve of the EDJ ridge starting at the tip of the buccal dentine horn and initially moving mesially along the mesial EDJ ridge to the lingual dentine horn, then along the distal EDJ ridge back to the starting place at the buccal dentine horn. In order to capture the details of the EDJ ridge, Landmarks were placed more closely to each other at points of high curvature along the ridge and less closely where the ridge was relatively straight.

CEJ ridge landmarks were placed on a surface rendering of the morphology of the tooth or, when the tooth is *in situ* in the jaw and access to the CEJ is restricted by adjacent teeth, on a surface reconstruction of the tooth using the segmented voxels in the LabelField. The placing of landmarks was checked using oblique slices through the unfiltered image stacks (Fig. 4.4.1). The first landmark was placed on the CEJ at the midpoint of the buccal face of the tooth, then landmarks were placed mesially around the CEJ.

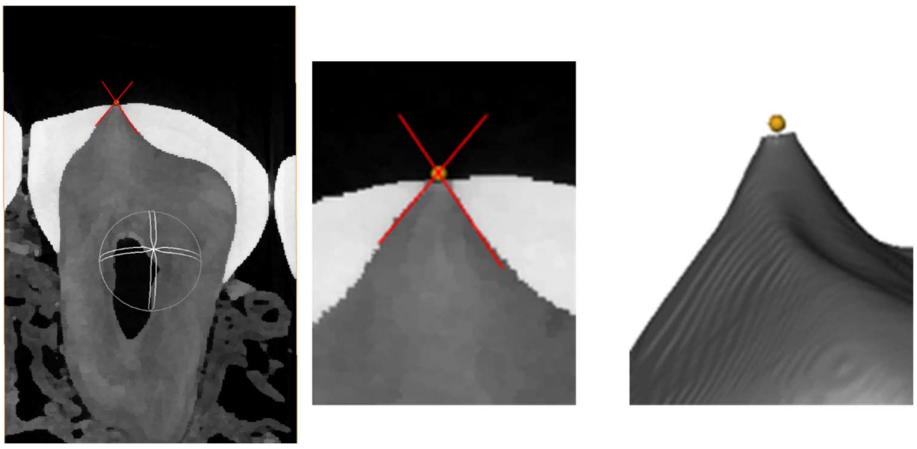

Figure 4.4.2 Estimation of the position of dentine horn tips in worn teeth. Tangents are drawn on the EDJ junction and projected until they meet outside surface of the tooth. The tangents must not be applied at the very outer surface of the tooth as wear distorts the enamel anatomy for a short depth below the tooth surface. This shows one cross section but two orthogonal cross sections are used

In some specimens, dental wear had removed the tips of dentine horns. Provided the wear was minimal, the position of the tip was estimated by extrapolation of the

slope of the EDJ close to the tip in orientated oblique slices in at least two nearly orthogonal planes (Fig. 4.4.2). Any teeth with more than minimal wear of the dentine horns were excluded from the analysis.

4.5 Derivation of landmark sets

The landmarks collected from the segmentations are not the landmarks used in the statistical or morphological analysis. Instead, for each tooth, equal numbers of morphologically homologous landmarks and semilandmarks were derived using a software routine written by Philipp Gunz (Gunz *et al.,* 2005; Gunz and Mitteroecker, 2013) implemented in Mathematica 8.0 (www.wolfram.com). A three-dimensional cubic spline function was used to fit a smooth curve to the landmarks of the EDJ ridge and CEJ ridge. This is the reason that the original landmarks were placed more closely around areas of high curvature. Because of this landmarking protocol, the spline curve more accurately reflects the morphology of the EDJ ridge and CEJ ridge and does not, by interpolation between the landmarks, smooth out highly curved regions such as the dentine horns. For the EDJ ridge set, the EDJ main landmarks were projected on to the curve, dividing the curve into mesial and distal portions. A fixed number of equally spaced landmarks were placed along the curve; the EDJ has 20 landmarks in the mesial portion and 25 in the distal. For the CEJ ridge 30 landmarks were used (Fig. 4.5.1).

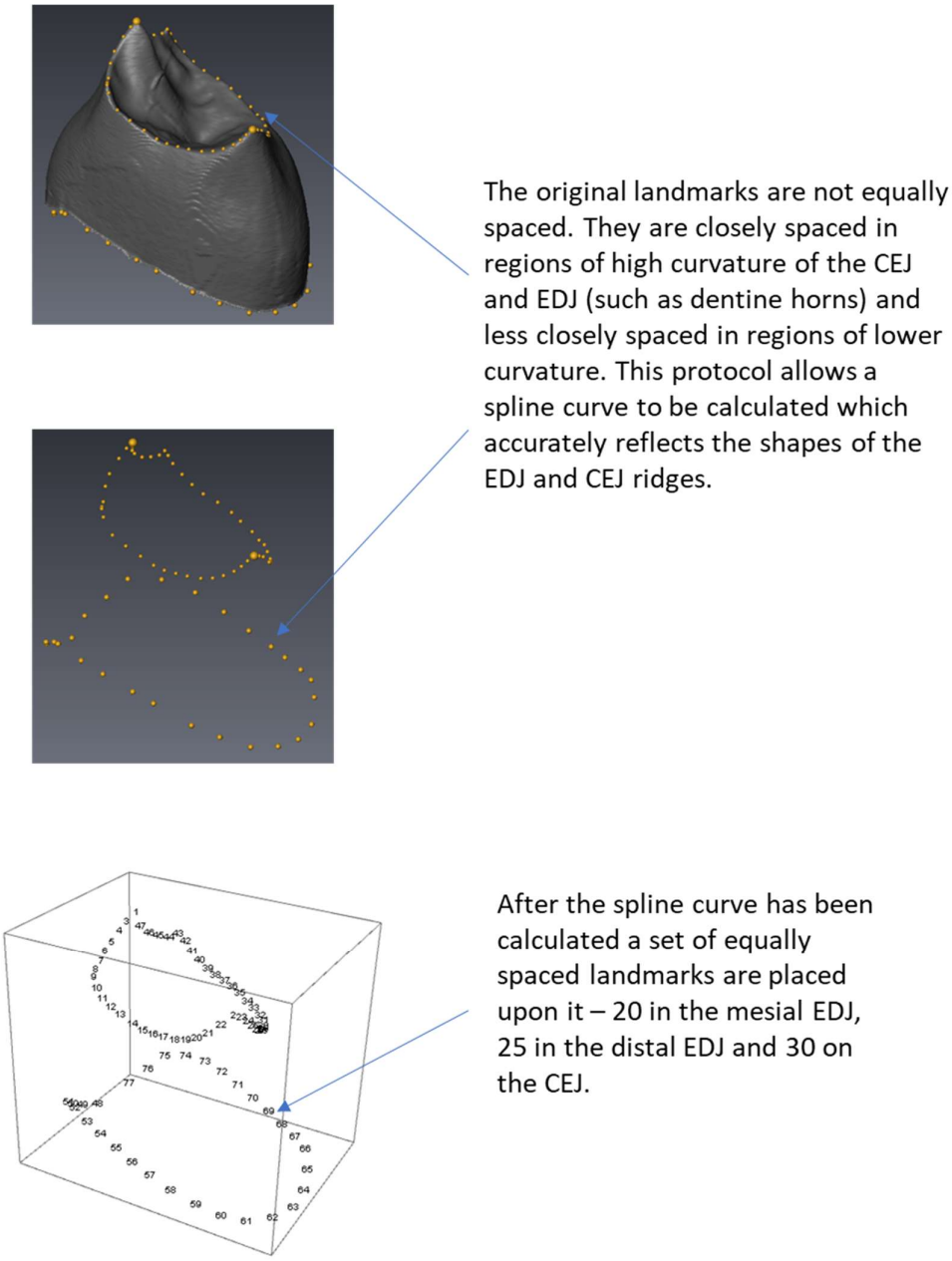

Figure 4.5.1 Landmarking protocols.

The EDJ main landmarks were fixed whilst those in the EDJ ridge and the CEJ ridge were treated as semi-landmarks. The semi-landmarks were slid along tangents to the spline curve and then projected back onto the curve. (Fig. 4.5.2). This reduces the bending energy of the transformation from the mean Procrustes curve shape to the curve shape of the individual specimen (Gunz *et al.,* 2005; Gunz and Mitteroecker, 2013). The reason for doing this is that when the ridge shape of the individual tooth is obtained from the Procrustes mean ridge shape through a continuous transformation the most direct and simplest transformation is the one with the least bending energy. This process of finding the best arrangement of semi-

landmarks is likened by Gunz *et al.* (2005) to that of using the least squares principal to find the best straight line through a cloud of points in linear regression.

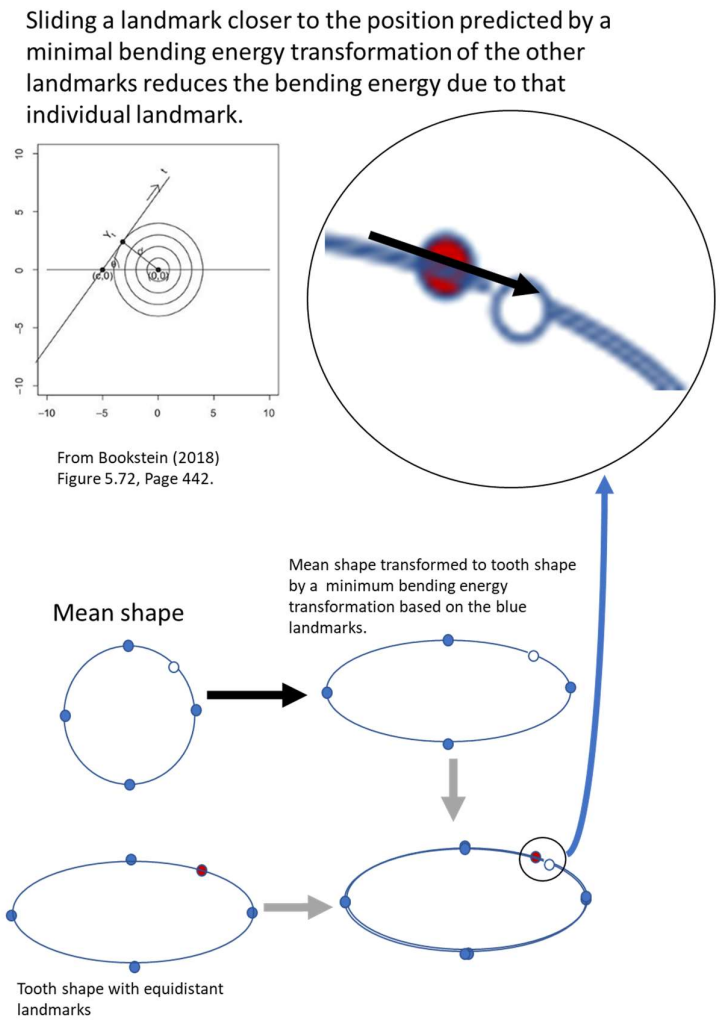

Figure 4.5.2 Landmarks which are initially equally spaced along the EDJ and CEJ spline curves, are slid along the curves to reduce bending energy.

The sliding operation was performed twice, after which the landmarks were considered to be morphologically homologous. They were converted into shape coordinates in Procrustes space, using generalized Procrustes analysis which removes scale, location, and orientation information from the coordinates (Dryden and Mardia, 2016). The data produced by this procedure consists of a single set of points in three-dimensional space representing the mean shape of all the teeth in the sample and, for each specimen in the sample, a set of three values for each landmark representing the co-ordinates of the three dimensional vector displacement of this landmark from the position of the equivalent landmark in the mean Procrustes shape. In addition, each tooth has a centroid size, representing the scaling factor applied to the tooth in order to standardize its size in the generalised Procrustes analysis.

4.6 Data checking and relabelling of premolar position.

For each species in this study, individually, the data were examined by doing a principal components analysis and plotting the principal component scores for the first two or three principal components. In all the plots, the first two principal components captured most of the total variation (50 - 70%) in the sample. The third principal component was added to some plots to aid visualisation but generally contributed little to the total variance explained (generally, less than 10%). These plots allowed the main patterns and relationships in the data to be visualised and the detection of any suspicious data points or outliers. It also raised some unexpected issues and problems. It appears that for several of the species in the sample, based on the statistical analysis of EDJ morphology, some third upper premolars may have been misclassified as fourth upper premolars and *vice versa*. This is not surprising because individual teeth are often found in isolation and the morphology of third and fourth upper premolars is similar within each species, especially where there has been a significant amount of wear on the external enamel surface. It is difficult for even skilled and experienced researchers to make a definitive diagnosis of some teeth. It seems reasonable that the morphology of the EDJ in isolated teeth is a better indicator of tooth position in some cases than the external morphology of the tooth.

The possible misidentification of tooth position was explored by comparing the EDJs of teeth of known position (because they are *in situ* in a jaw) with the EDJs of the suspect teeth. In some cases, two linear discriminant analyses were carried out with the suspect tooth allocated to each of the two possible tooth positions and the tooth was assigned to the group that produced the greatest between-group separation in the linear discriminant analysis. The policy adopted for this study was to allocate each tooth to the tooth position to which it was statistically the closest, based on EDJ morphology. This does not take account of other aspects of tooth morphology, nor of the context in which the tooth was found. The main analysis in this study was carried out on the relabelled teeth.

4.7 Organisation of the sample and naming and labelling conventions

The sample was grouped for analysis by the factors of 'tooth position' and 'species' into twelve groups.

Table 4.7.1 Labels for species and tooth position.

Factor Labels	Group
Aafr	*Australopithecus africanus*
Nal	*Homo naledi*
Nean	*Homo neanderthalensis*
Qaf	Fossil *Homo sapiens* (Qafzeh)
Prob	*Paranthropus robustus*
Sap	*Modern Homo sapiens*
UP3	Third upper premolar
UP4	Fourth upper premolar

For convenience, one factor is labelled 'Species' although some of the distinct populations included in it may not be separate at the species level. In particular, the Qafzeh hominins are included here as a separate category, even though they belong to the species *H. sapiens*.

The factor labels are used throughout the tables, diagrams and graphs in the results section. They are combined to create group labels in crossed two factor analyses. For example, Nean_UP4 refers to *H. neanderthalensis* fourth upper premolars. In addition, a colour coding convention is used: when comparing tooth type, third upper premolars (UP3) are coloured red and fourth upper premolars (UP4) are coloured blue.

Table 4.7.2 Colour coding for species

Aafr	*Australopithecus africanus*	Brown
Nal	*Homo naledi*	Green
Nean	*Homo neanderthalensis*	Black
Qaf	Archaic *Homo sapiens* (Qafzeh)	Red
Prob	*Paranthropus robustus*	Orange (occasionally Purple)
Sap	Modern *Homo sapiens*	Blue

4.8 Statistical and geometric morphometric analysis.

4.8.1 Premolar crown size.

This study uses the standard measure of size used in geometric morphometric studies, which is the centroid size. Although this has the dimension of length, it is quite a subtle concept and does not relate easily to any of the dimensions of a landmark configuration. Perhaps the simplest way of describing it is to say that

$$S = \sqrt{k} \times s(r)$$

Where S is the centroid size, k is the number of landmarks in a configuration and s(r) is the standard deviation of the radial distance of the landmark from the centroid of the configuration. For configurations with equal numbers of landmarks, it measures the dispersion of the landmarks around the centroid. Some of the properties of the centroid size are illustrated in Figure 4.8.1. Figure 4.8.2 compares centroid size with some other common measures of size. A box and whisker plot was constructed for the 12 groups in the analysis (two tooth positions for each of the six species) and the group means were also plotted on an interaction plot.

A two-way factorial analysis of variance (ANOVA) was carried out to examine any differences between the mean centroid size of the teeth using the factors of tooth position crossed with species. The null hypothesis for this test is that all the groups have the same mean centroid size and the alternative hypothesis is that at least one of the groups has a different mean centroid size from the others. Initially the ANOVA included an interaction term between the two factors (tooth position and species). If the interaction term were not significant, a main effects two factor ANOVA would be carried out. If the interaction term is significant, the mean tooth size of *H. naledi* would then be tested against the mean size of each of the other species separately for the P3s and for the P4s (with Bonferroni correction for multiple testing).

The centroid size is defined as

$$S(X) = \sqrt{\sum_{i=1}^{i=k} \|(X)_i - (\bar{X})\|^2}$$

Where $(X)_i$ is the ith row of the shape matrix (the position of the *i*th landmark of *k* landmarks) and $(\bar{X})$ is the centroid. Essentially, the centroid size is the square root of the sum of all the squared distances between each landmark and the centroid.

Sometimes, especially if the number of landmarks on each specimen is different, a normalised version of the centroid size is used: $\frac{S(X)}{\sqrt{k}}$

Dryden and Mardia (2016)

The centroid size depends upon the number and positioning of the landmarks which make up the pre-shape. Note that, mathematically, 'shape' is not defined as the shape of the boxes in the examples below. The shape is defined by the number and configuration of the **landmarks**.

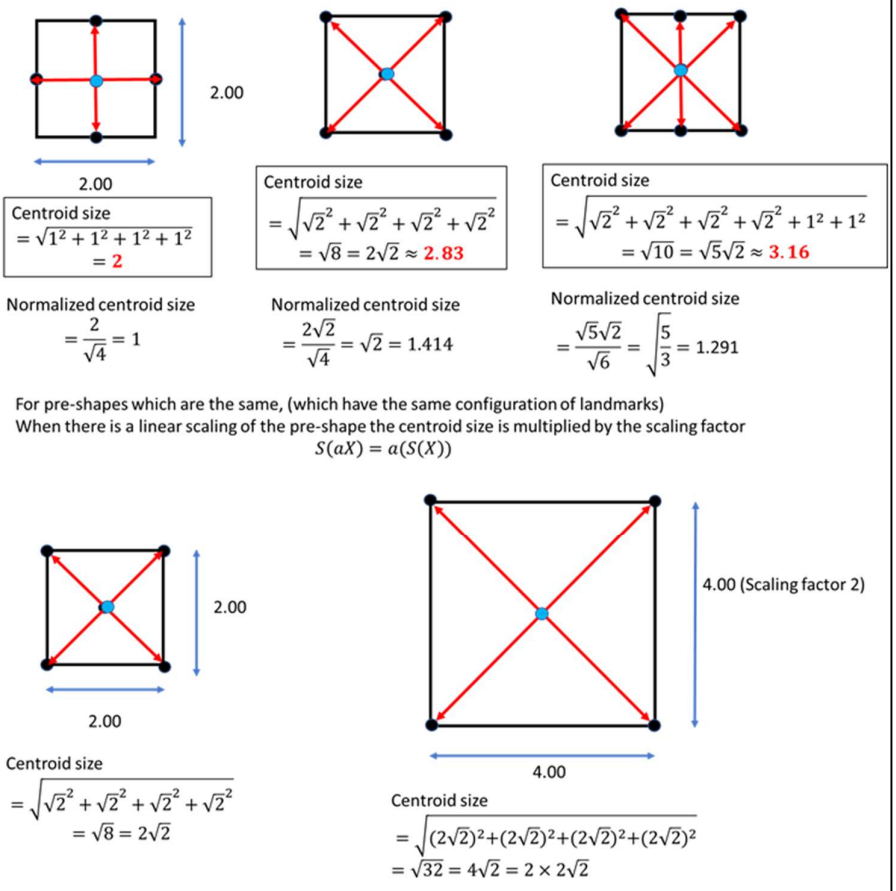

For pre-shapes which are the same, (which have the same configuration of landmarks)
When there is a linear scaling of the pre-shape the centroid size is multiplied by the scaling factor

$$S(aX) = a(S(X))$$

Figure 4.8.1 Some properties of the centroid size.

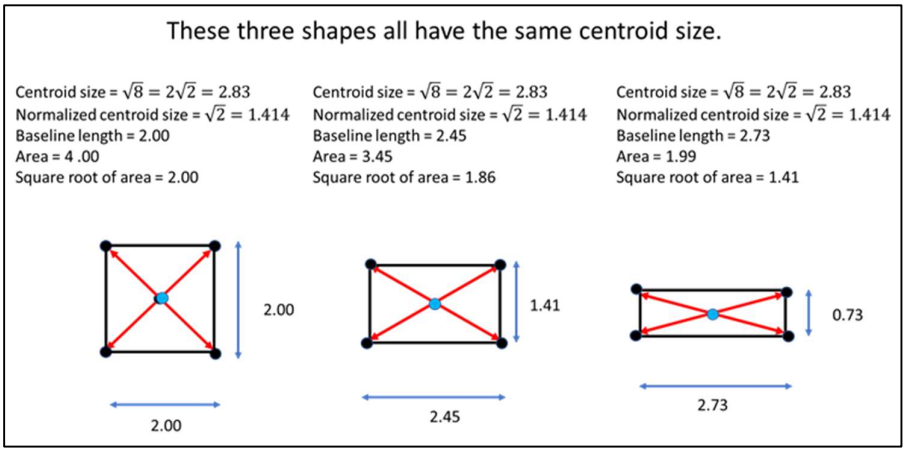

Figure 4.8.2 Centroid size compared with some other common measures of size.

4.8.2 Shape analysis.

4.8.2.1 Statistics

The statistical analysis was based on a generalized Procrustes analysis of enamel-dentine junction (EDJ) shape data grouped by species and by tooth position. The analysis was based on a tangent space approximation to the non-Euclidean Procrustes shape space. Data reduction was carried out by principal components analysis (PCA), from 231 variables to the first five principal components (80% of total variance) for a multivariate analysis of variance (MANOVA) and 16 principal components (95% of total variance) for a linear discriminant function (LDA) analysis. So, for the LDA the p/n ratio (Bookstein, 2019) is 16/109 = 0.15. This is well below 1, suggesting that it is unlikely for there to be any problems in the analysis due to high dimensionality.

The smaller number of principal components was used in the MANOVA in order to test for variation which is morphologically significant. That is, the intention was to detect any major differences in the overall shape of the EDJ between groups rather than to detect small differences in the details of ridge shape. The null hypothesis for the MANOVA is that there is no difference in mean shape between any of the groups in the sample. The alternative hypothesis is that the mean shape is different in at least one of the groups.

The larger number of components was used in the LDA because the results would be validated by a 'leave one out' cross validation which would detect any over-fitting of the model to the data. That is, any differences in group assignation due to over-fitting of the model to small, morphologically non-significant, details in ridge shape should be detected and corrected by the cross validation.

The principal component scores for the first three principal components were plotted with convex hulls constructed around each of the groups in the sample. This allows any separation between groups to be visualised and allows the detection of any major patterns or trends in the data. The first two or three linear discriminant functions (also known as 'canonical variates') were plotted with convex hulls.

4.8.2.2 Morphology

The mean shapes of each of the groups in the sample were compared by plotting wire frame graphs of the mean shape for each group (as centred and orientated by the Procrustes analysis). Comparison of these wire frame graphs was also used to understand the main morphological trends associated with the first two principal components of shape.

4.8.2.3 Size and shape together: allometry and form analysis

The correlation between tooth size and each of the first five principal component scores for shape were calculated to assess any possible allometric relationships. Linear regression was carried out for each of the first two principal components of shape as the response variable against centroid size as the predictor variable and the scatter plot and linear regression line were plotted. Analysis of covariance was carried out for any groups which did not seem to lie on the trend of the linear regression line.

To analyse size and shape together (form), the natural logarithm of centroid size was added as a variable to the shape data in tangent space (Mitteroecker and Gunz, 2009; Bookstein, 2018). The natural logarithm of centroid size is used because it is on the same scale as the variables of the shape tangent space , assuming that there is isotropic variation of landmark positions around an average configuration. The rest of the form analysis followed the same methods as the shape analysis, as described above. The difference between these two analyses is not in the methods but in the data. The data for the form analysis incorporates an extra variable giving information on size, so size and shape are analysed together, whereas the shape analysis only includes the shape data.

4.9 Qualitative morphometric analysis.

Qualitative features of the upper premolar EDJ were identified whose frequencies of expression might have the potential to discriminate between species and tooth positions. Since these qualitative features were neither identified nor specified in advance, their descriptions appear in the qualitative morphometrics section of the results (Section 5.8).

Potential features were identified by a careful examination of every EDJ surface in the sample, to find features which occur in some but not in all teeth. This investigation was informed in part by known features of the OES which have previously been used in qualitative morphometric analysis (ASUDAS (Scott and Irish, 2017); Bailey, 2000, 2002a, 2002b; Bailey and Hublin, 2013; Bailey and Wood, 2007;

Bailey *et al.*, 2011; Kaifu *et al.*, 2015, Irish *et al.,* 2018.; Martinón -Torres *et al.*, 2007, 2008, 2012, 2013; Wood and Engleman, 1988) but mostly by the systematic inspection of the different parts of the EDJ surface, including but not limited to the EDJ ridge, the buccal, lingual, mesial, distal and occlusal surfaces.

For the complete set of features in this study, multidimensional scaling (MDS) based on the Mahalanobis D^2 distances between group mean percentages of feature expression was used to visualise and summarise the differences in qualitative morphology between species and tooth positions. Studies in dental anthropology often use the mean measure of divergence (MMD) for this kind of analysis (Harris and Sjøvold, 2004; Irish, 2010) but for this study I prefer the Mahalanobis D^2 distance, which, unlike the MMD, automatically compensates for correlations between the frequencies of expression of features within the data set[4].

[4] Krzanowski (1988) suggests using the Mahalanobis D^2 distance for binary data in "a purely descriptive fashion" (p. 316) because binary data is unlikely to meet the multivariate normality and equal variance-covariance structure assumptions necessary for inferential analysis.

5 RESULTS.

5.1 Intraspecific variation between third and fourth upper premolars

For each species in this study the differences in morphology between third and fourth upper premolars are first described according to the final allocation of each tooth to its tooth position. This is followed, in each species, by a detailed discussion of how potentially mislabelled or misidentified teeth were identified and re-labelled.

5.1.1 Homo sapiens

5.1.1.1 Recent/contemporary *H. sapiens*

A plot of the first three principal components of shape shows good separation between third and fourth modern human upper premolars (Fig. 5.1.1).

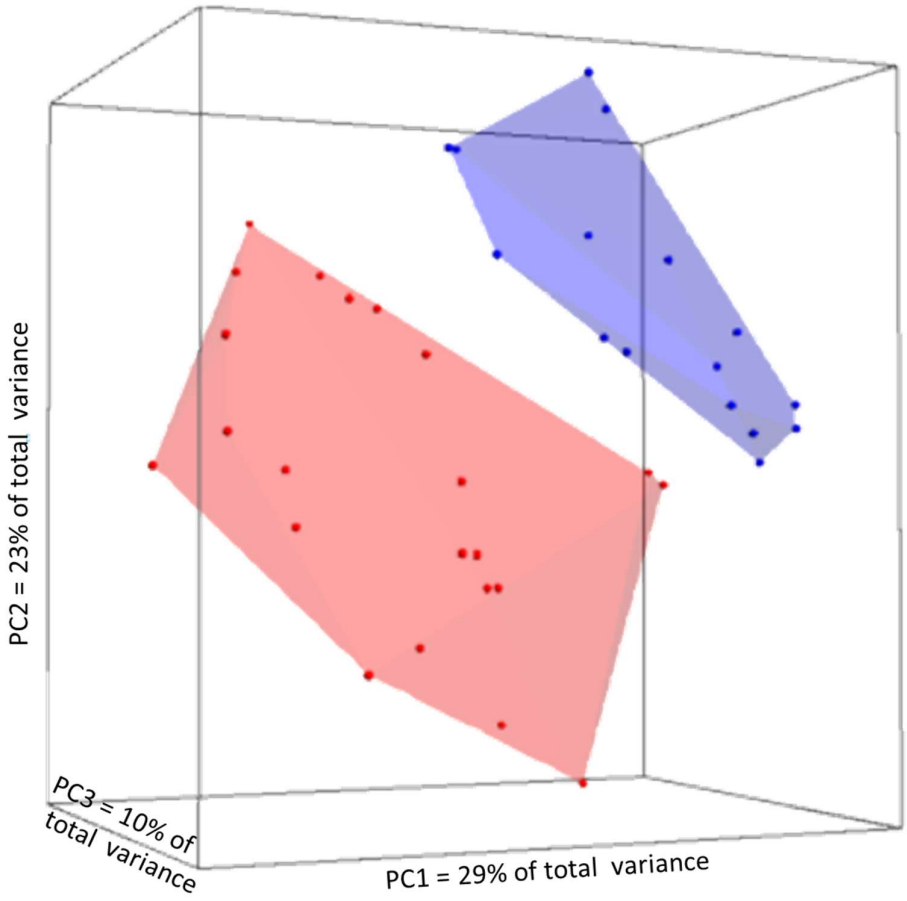

Figure 5.1.1 Principal Component Plot of EDJ shape. Blue = fourth upper premolars. Red = third upper premolars.

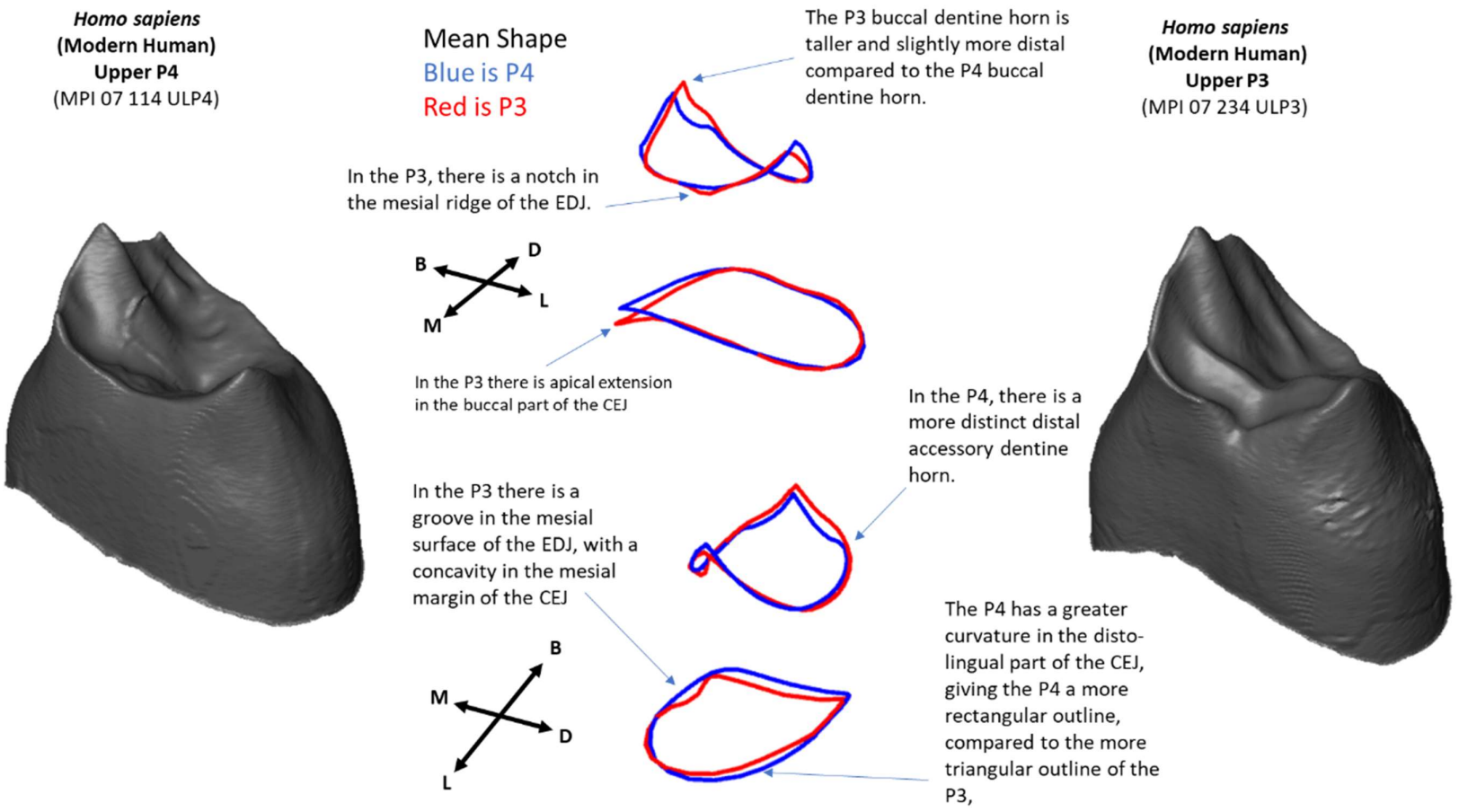

Figure 5.1.2 Summary of differences between third and fourth upper premolars in modern humans.

A detailed examination of wire frame models for the mean shape of third and fourth upper premolars and inspection of the EDJ surfaces revealed the following features (Fig. 5.1.2). In third upper premolars the buccal dentine horn is relatively taller than in fourth upper premolars. In third upper premolars the distal displacement of the buccal dentine horn is greater than in fourth upper premolars and the buccal dentine horn occupies a more central position on the buccal ridge of the EDJ. In the third upper premolar there is greater apical extension of the CEJ in the buccal cusp than in fourth upper premolars, where apical extension is absent or slight. When combined with the greater height of the buccal dentine horn this means that in the EDJ the buccal surface of the EDJ is significantly longer than the lingual surface. In the fourth upper premolar, the distal accessory dentine horn, when present, is more widely separated from the (main) buccal dentine horn and is more prominent than in the third upper premolar.

In the third upper premolar there is frequently a 'notch' in the mesial ridge of the EDJ, approximately where the buccal two thirds of the ridge meet the lingual one third. This is often associated with a mesial 'bulge' in the buccal third of the mesial EDJ ridge. In the third upper premolar there is a concavity or 'developmental groove' in the mesial surface of the EDJ and this is reflected in a corresponding concavity in the shape of the CEJ. In addition to this the CEJ is often also concave in the occlusal direction in its middle part, most prominently on the mesial surface but also on the distal surface. In the fourth upper premolar there is disto-lingual extension of the disto-lingual part of the EDJ ridge – and to a lesser extent the CEJ ridge – giving a more quadrilateral outline compared to the triangular or wedge-shaped outline of the third upper premolar.

<u>Modern Humans: Investigation of possible abnormal or misidentified teeth.</u>

The first three principal components of shape for the modern human teeth in this sample were plotted on a scatterplot and convex hulls added for the third upper premolar teeth and the fourth upper premolar teeth. Figure 5.1.3 shows the principal component analysis of the sample of modern human teeth *before* the removal of abnormal teeth and the re-allocation of tooth position for the apparently mis-identified teeth.

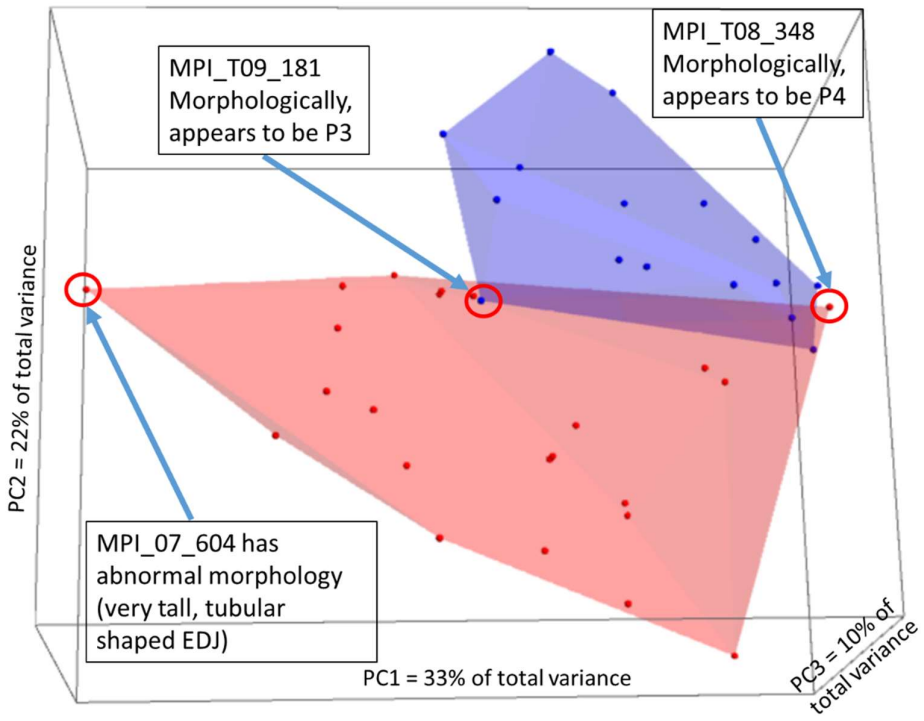

Figure 5.1.3 Modern human teeth plotted by first three principal components of shape. The plot shows teeth which are abnormal or which may be misidentified. (Red = third upper premolars, Blue = fourth upper premolars).

The initial plot showed one possible outlier, MPI_07_604. Inspection of this tooth (Fig. 5.1.4) showed an unusually tall and vertically straight sided EDJ, which differed significantly in shape from all other teeth in the sample, so it was removed from the sample.

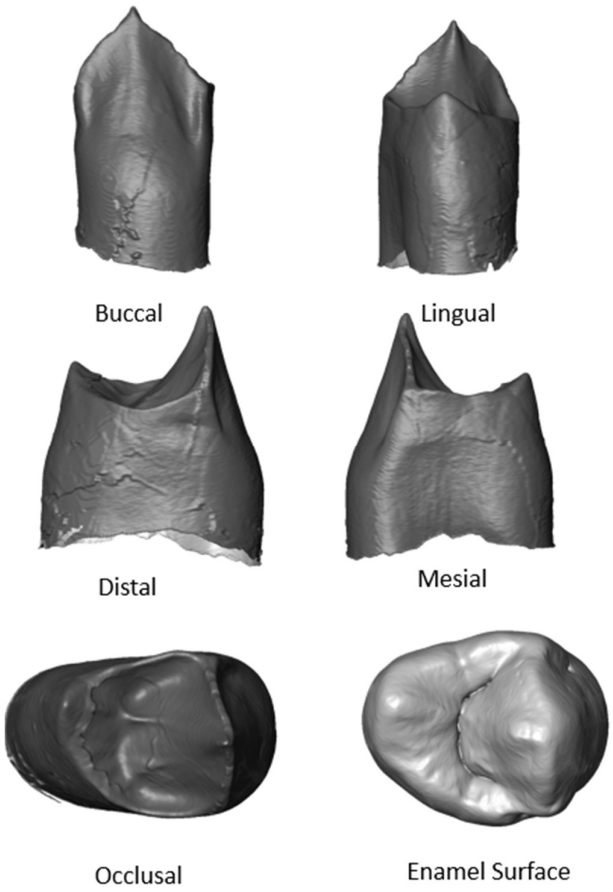

Figure 5.1.4 Enamel-dentine junction of the EDJ of modern human tooth MPI 07 604, showing its abnormally tall, straight sided shape, especially in the body of the tooth.

The plot also suggested that tooth MPI_T08_348 was mis-labelled as a third upper pre-molar. It falls close to the convex hull of the fourth upper premolars. In addition, tooth MPI_T09_181 lies within the convex hull of the third upper premolars but is labelled as a fourth upper premolar. (Two other fourth upper premolars lie within the convex hull of the third premolars but this is only because the convex hull of the third upper premolars is extended by the labelling of MPI_T08_348 as a third upper premolar). The EDJ of MPI_T08_348 (Fig. 5.1.4) was re-examined and it shows the characteristic features of a fourth upper premolar, which are well known from human dental anatomy (as, for example, described in Scheid and Weiss, 2017). The buccal dentine horn is only slightly taller than the lingual dentine horn and only slightly distally displaced relative to the lingual dentine horn. There is no depression or notch in the mesial ridge of the EDJ and the broad outline of the tooth is quadrilateral rather than triangular.

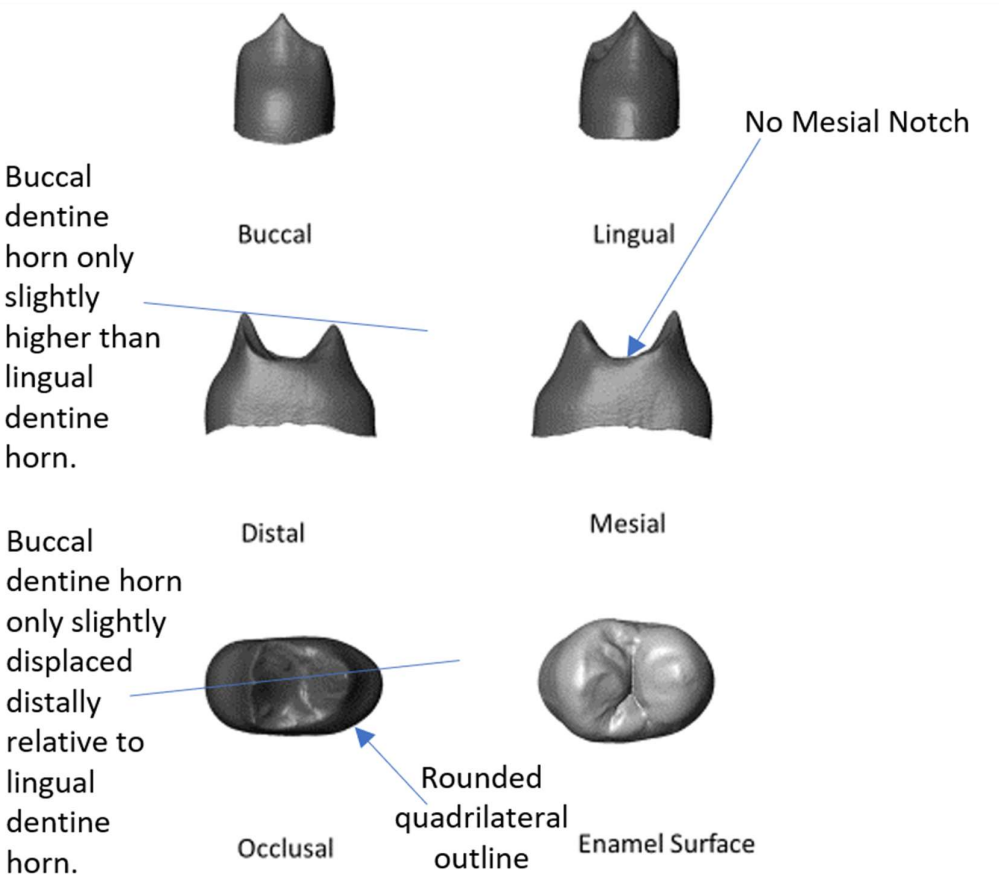

Figure 5.1.5 Enamel-dentine junction of MPI_T08_348, annotated to show the characteristic features of fourth upper premolar anatomy.

By contrast, the EDJ of MPI_T09_181 (Fig. 5.1.5) shows the characteristic features of a third upper premolar. There is a notch in the mesial ridge of the EDJ and a mesial ('developmental') depression or 'groove' on the mesial surface of the EDJ. The buccal dentine horn is significantly taller than the lingual dentine horn and is significantly displaced distally relative to the lingual dentine horn. The broad outline of the tooth is triangular rather than quadrilateral. In summary, there is strong evidence that MPI_T08_348 and MPI_T09_181 have been mis-labelled and both teeth were re-allocated; MPI_T08_348 as a fourth upper premolar and MPI_T09_181 as a third upper premolar.

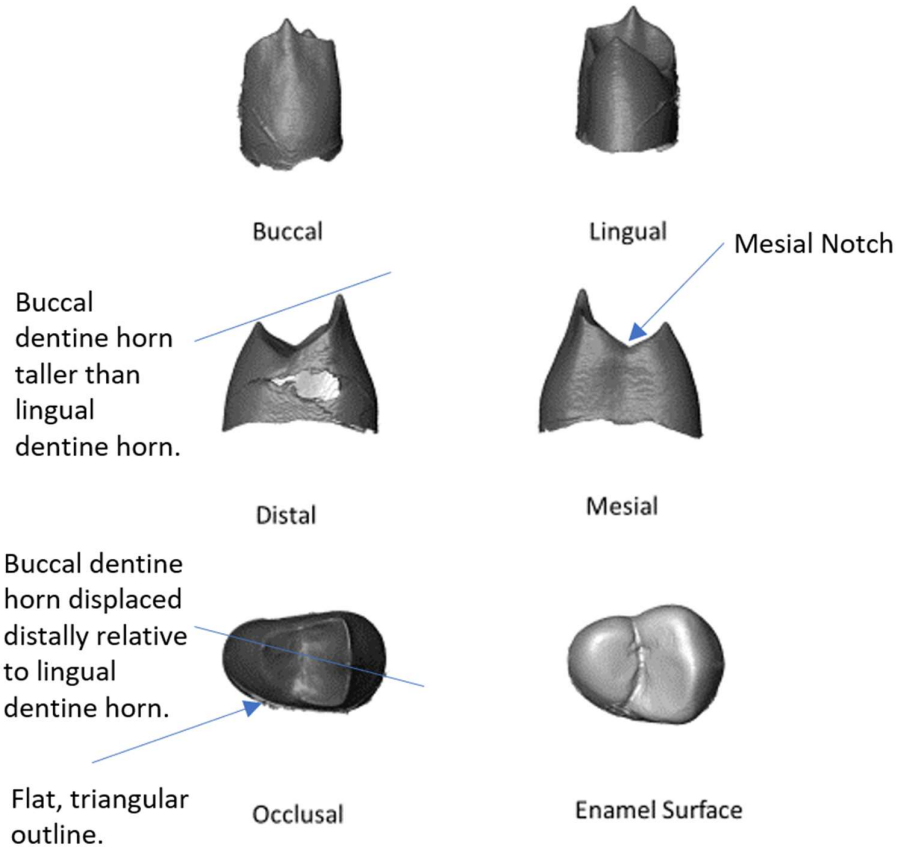

Figure 5.1.6 Enamel-dentine junction of MPI_T09_181, annotated to show the characteristic features of third upper premolar anatomy.

5.1.1.2 Archaic *Homo sapiens* (Qafzeh).

A plot of the first three principal components of shape shows good separation between the third and fourth Qafzeh hominin upper premolars (Fig. 5.1.6). All of the teeth in this sample are *in* situ in the maxilla (several of them unerrupted) so the tooth position is certain. The Qafzeh 11 tooth in this sample might possibly be an 'outlier' but is retained in the analysis because, since it is *in situ* in a maxilla, it can be identified with a high degree of confidence as a *H. sapiens* (Qafzeh) fourth upper premolar. (The segmentation of this tooth in Avizo was checked carefully and seems to be correct).

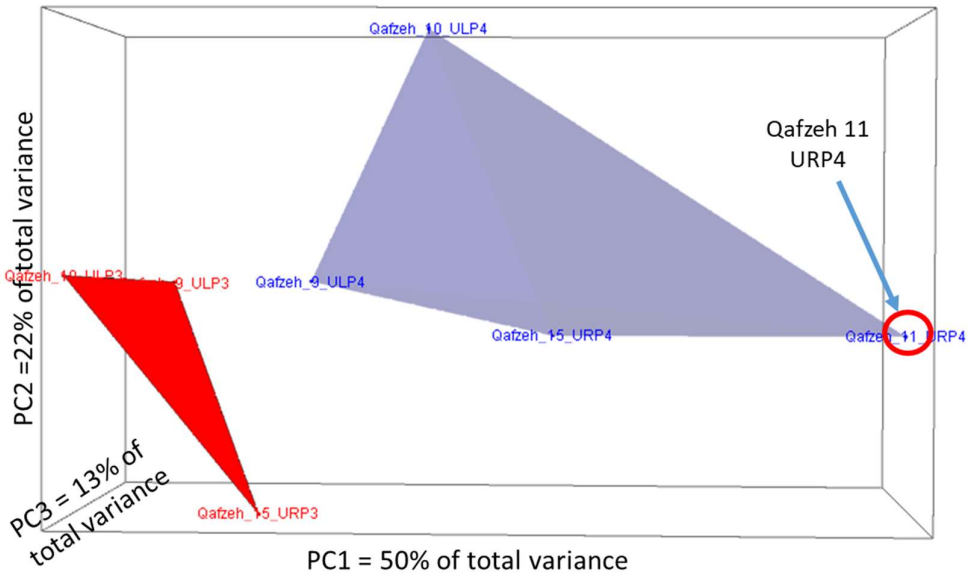

Figure 5.1.7 Principal Component Plot of EDJ shape for *Homo sapiens* (Qafzeh). Blue = fourth upper premolars (UP4). Red = third upper premolars (UP3).

In this sample, the differences in morphology between third upper premolars and fourth upper premolars are essentially the same as the differences in morphology for these tooth positions in modern humans. These are summarised in Figure 5.1.7.

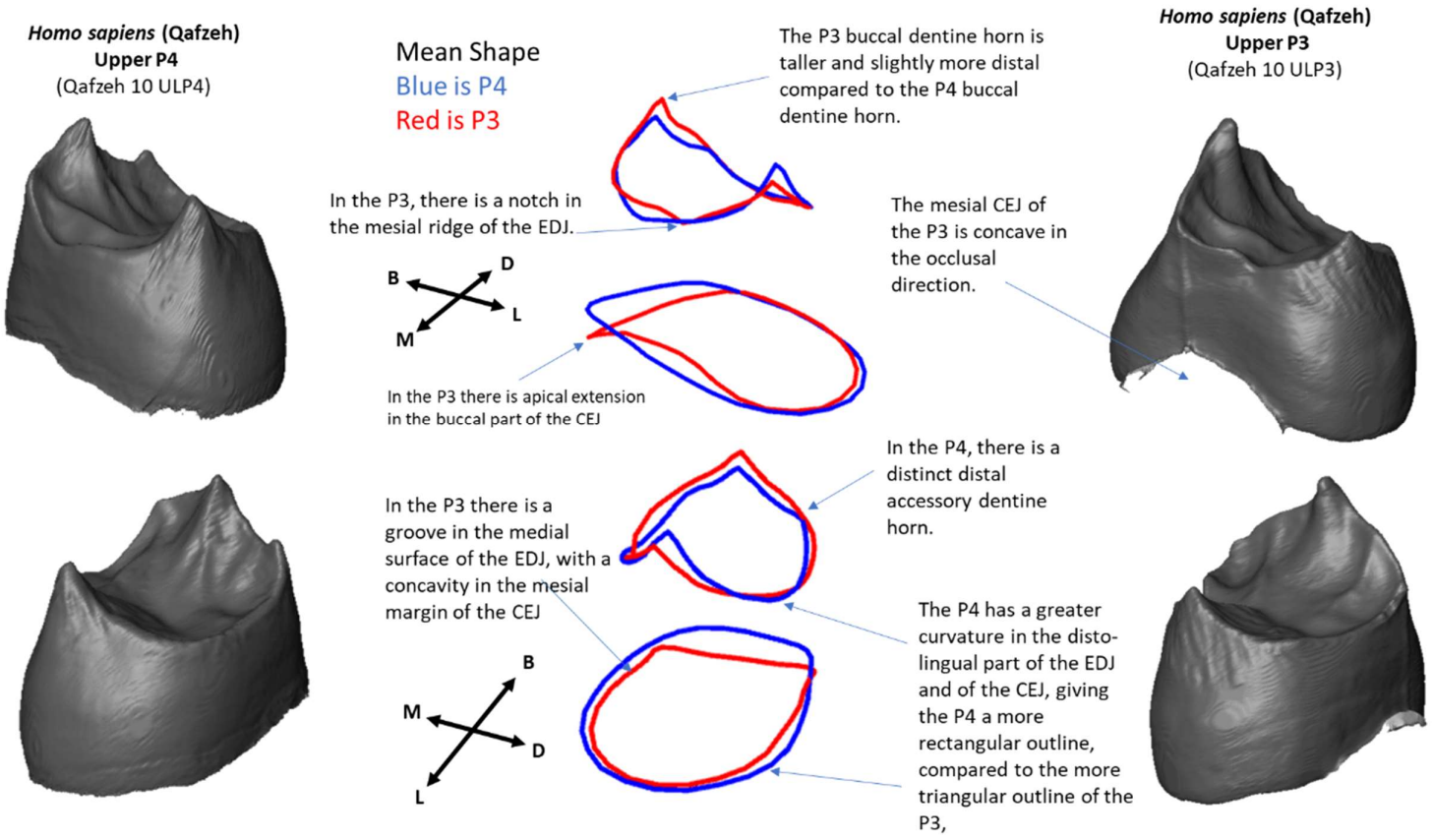

Figure 5.1.8 Differences in tooth morphology between third upper premolars and fourth upper premolars in *H. sapiens* (Qafzeh).

5.1.2 Homo neanderthalensis

A plot of the first three principal components of shape shows good separation between third and fourth upper premolars, both for the Krapina Neanderthals and for the later Neanderthals (Fig. 5.1.8). A detailed examination of wire frame models for the mean shape of third and fourth upper premolars and inspection of the EDJ surfaces revealed that the differences in morphology between the third and fourth upper premolars of *H. neanderthalensis* are essentially the same as are seen in *H. sapiens* (summarised in Figure 5.1.9) - except for two features. Firstly, instead of having a prominent distal accessory buccal dentine horn in the fourth upper premolar, there is a distal buccal 'shoulder' in the Neanderthal fourth upper premolar. This is a rounded prominence on the distal part of the buccal ridge of the EDJ separated from the buccal dentine horn by a slight depression. The second feature is the presence of a distinctive shield boss shaped bulge in the buccal cingulum of the third upper premolar (Fig. 5.1.10). This may be present in the fourth upper premolar but is much less prominent.

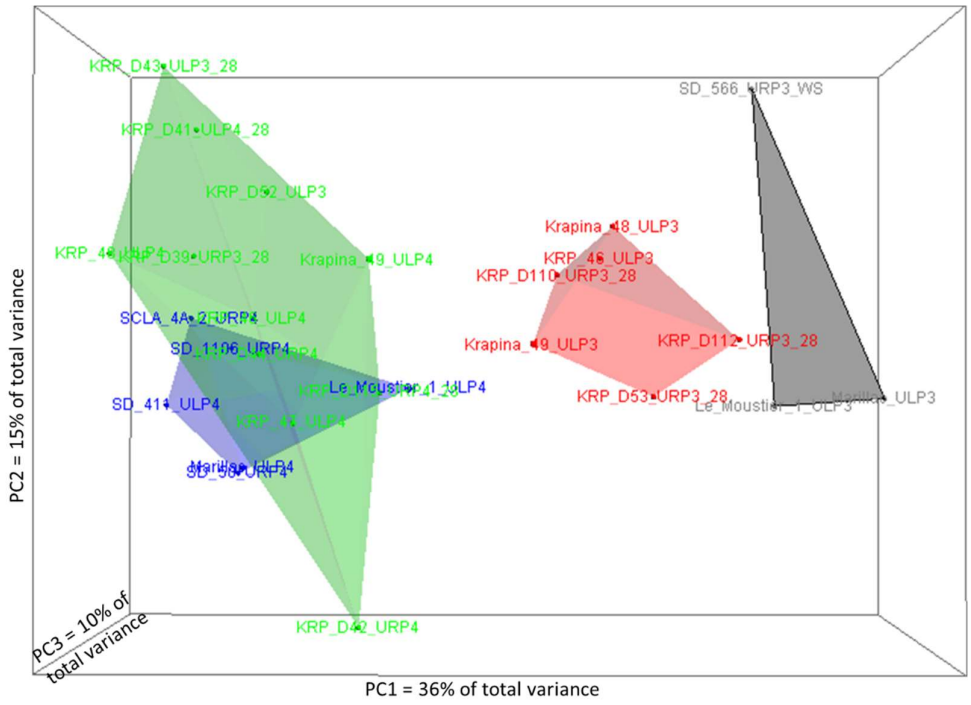

Figure 5.1.9 Principal components of shape for the EDJ of Neanderthal teeth. Green = Krapina UP4, Red = Krapina UP3, Blue = Late Neanderthal UP4, Black = Late Neanderthal UP3.

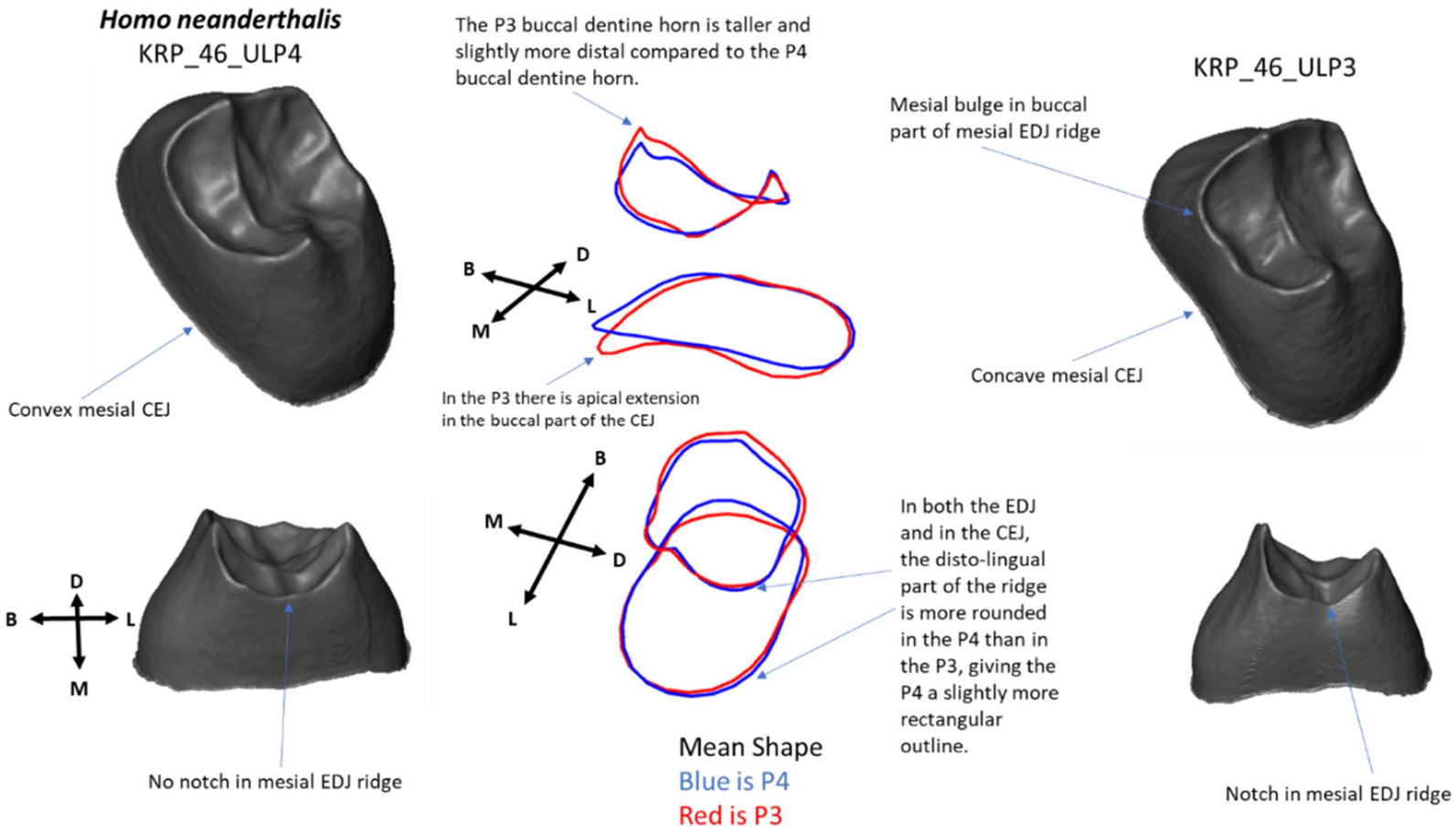

Figure 5.1.10 Summary of EDJ shape differences between third and fourth upper premolars in *H. neanderthalis*.

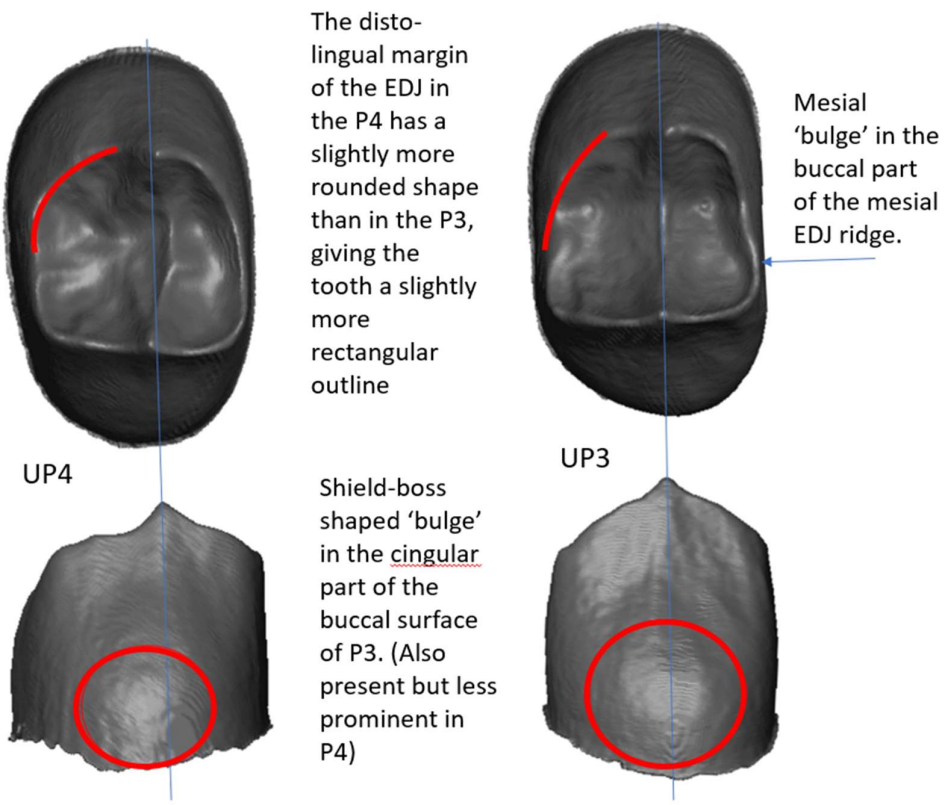

Figure 5.1.11 Disto-lingual EDJ shape and the boss shaped cingulum in the EDJ of *H. neanderthalensis*. Fourth upper premolar on the left and third upper premolar on the right.

<u>*H. neanderthalensis* – Investigation of possible abnormal or misidentified teeth</u>

The Neanderthal teeth in this sample were plotted against the first three components of shape with convex hulls for each tooth type (Fig. 5.1.11.) In this plot, the Krapina Neanderthals were plotted separately from the non-Krapina Neanderthals as the Krapina Neanderthals represent an earlier Neanderthal population. The plot shows good separation between third upper premolars and fourth upper premolars, except that the Krapina third upper premolars are split into two distinct groups. Three teeth, KRP D39, KRP D43 and KRP D52, which are all classified as Krapina third upper premolars (Radovčić *et al.* 1988) appear to group with the Krapina fourth upper premolars.

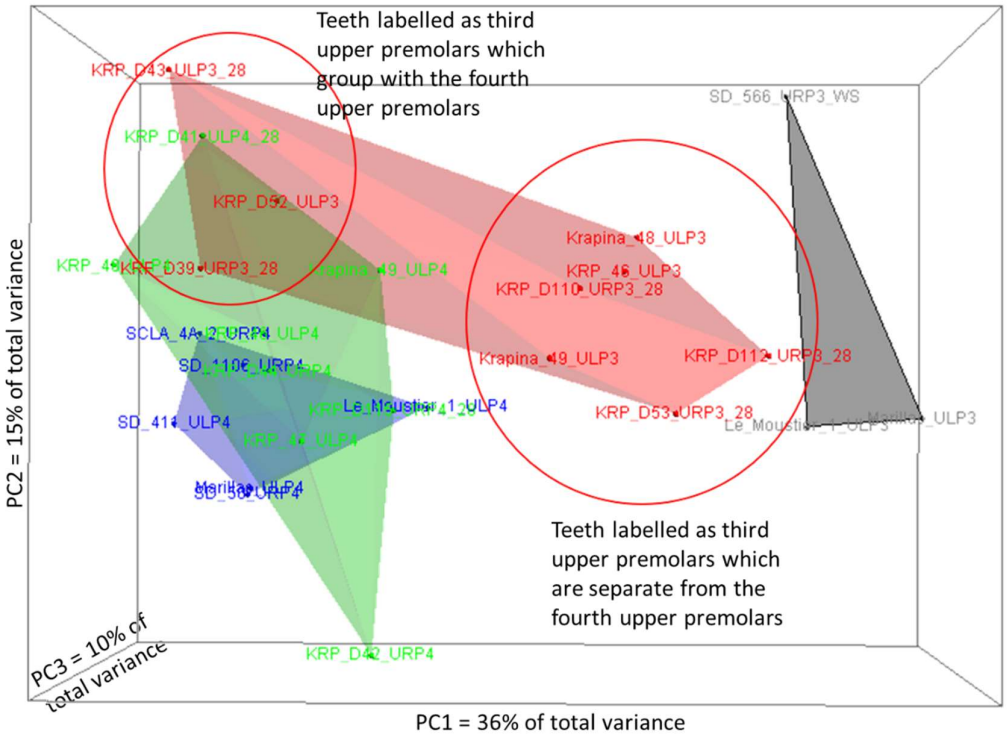

Figure 5.1.12 Principal components of shape for Neanderthal teeth, showing some possibly mis-identified teeth. (Green = Krapina fourth upper premolars, Red = Krapina third upper premolars, Blue = non-Krapina Fourth upper premolars, Black = non-Krapina third upper premolars.)

When the EDJs of these teeth are compared with teeth of more certain attribution, all three of them show the characteristic features of upper fourth premolars in the Krapina population. The buccal dentine horn is only slightly taller than the lingual dentine horn, there is no notch in the mesial ridge of the EDJ and there is a rounded 'quadrilateral' outline rather than a flatter 'triangular' outline in the disto-lingual part of the tooth. This is illustrated in Figure 5.1.12, using teeth from Krapina Dental Person one (KDP 1, Wolpoff, 1979) as a comparison sample for the three teeth of interest. As a result of these investigations, the three teeth, KRP D39, KRP D43 and KRP D52, were all re-labelled as fourth upper premolars for the statistical and morphological analysis in this study.

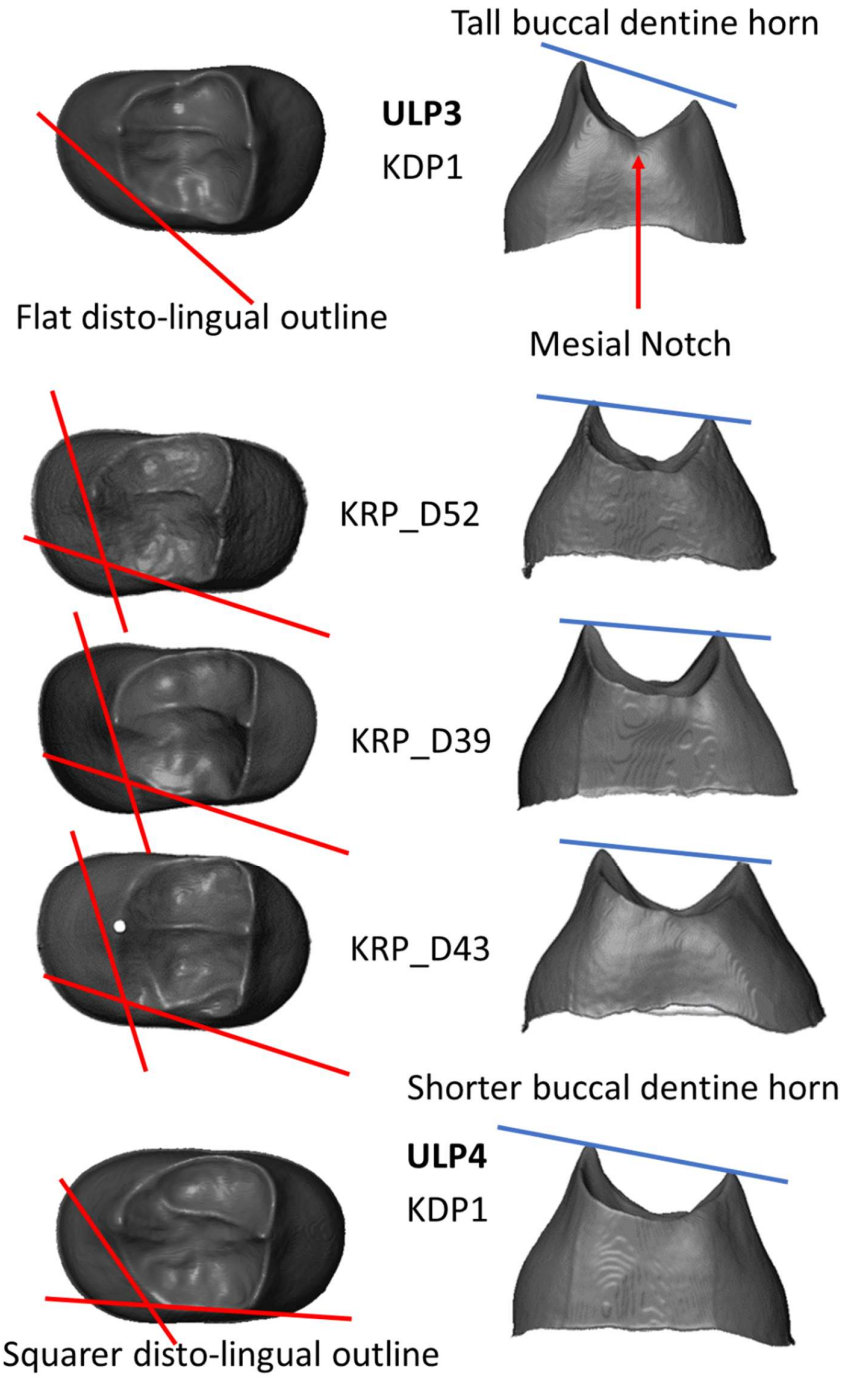

Figure 5.1.13 Comparison of 'suspect' teeth with third and fourth upper premolar teeth from Krapina Dental Person 1 (KDP 1), in which tooth position is well established. The annotations show the main features which distinguish third upper premolars from fourth upper premolars in the Krapina hominin population.

5.1.3 Australopithecus africanus

A plot of the first three principal components of shape for the *A. africanus* EDJ shows good separation between the third and fourth upper premolars (Fig. 5.1.13). A detailed examination of wire frame models for the mean shape of third and fourth upper premolars and inspection of the EDJ surfaces revealed the differences in EDJ morphology between third and fourth upper premolars (Summarised in Figure 5.1.14). The relative height of the buccal and lingual dentine horns is more equal in *A. africanus* than in species of *Homo* but in the third upper premolar the buccal dentine horn is still taller and more distally displaced, relative to the lingual dentine horn, than in the fourth upper premolar.

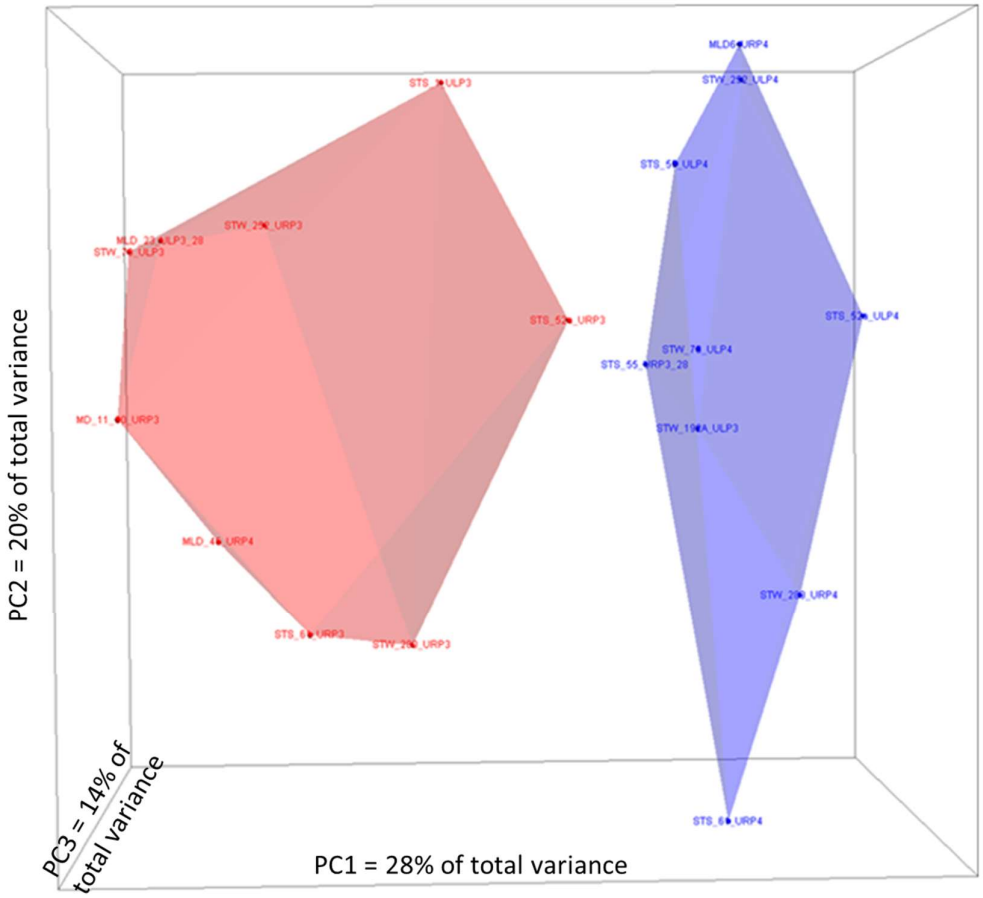

Figure 5.1.14 Principal components of shape for the EDJ of *A. africanus* teeth. Red = third upper premolar, Blue = fourth upper premolar.

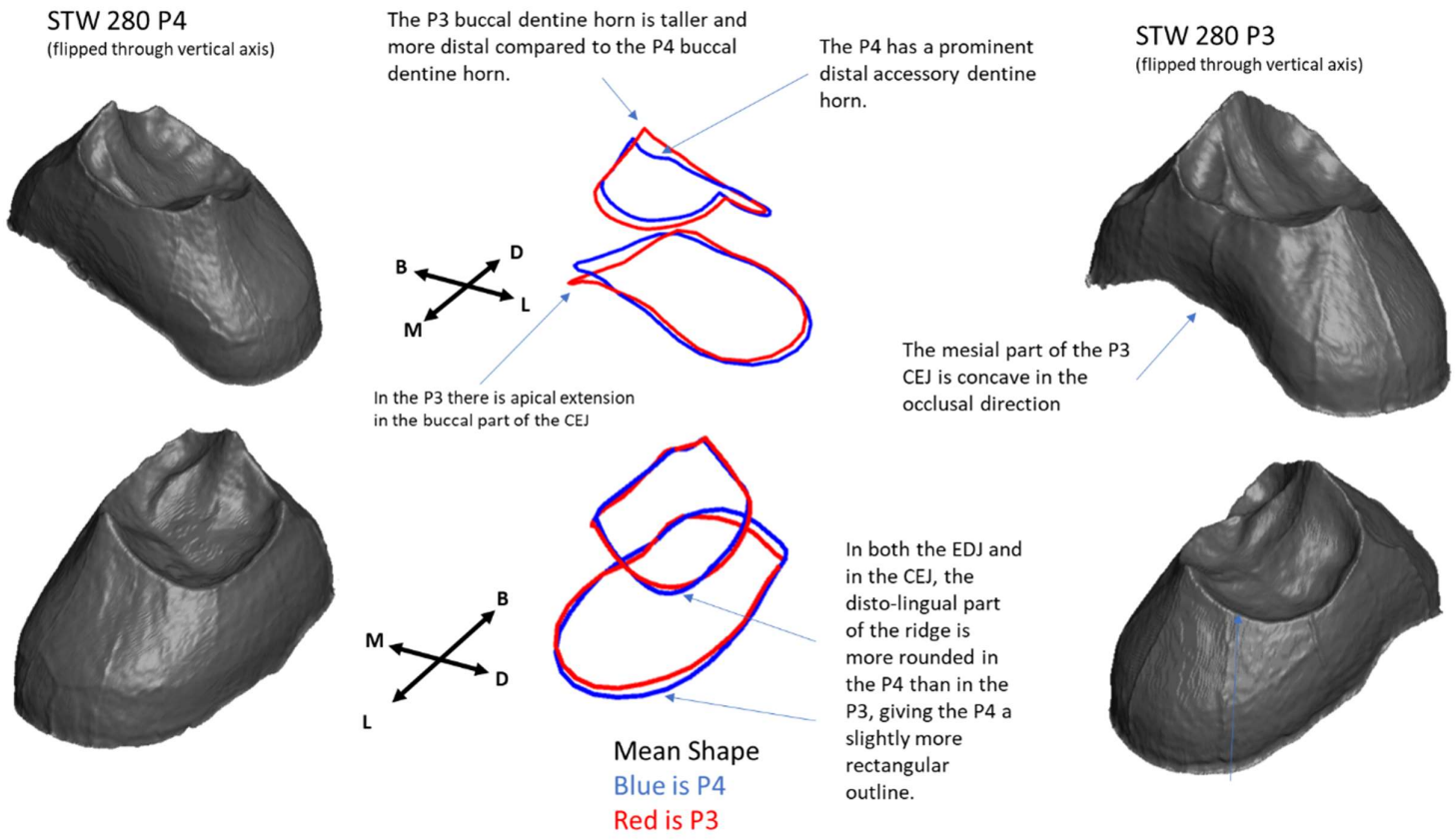

Figure 5.1.15 Summary of differences between third and fourth upper premolars in *A. africanus*.

There is not a mesial notch in the mesial EDJ ridge in *A. africanus* third upper premolars and any mesial bulge is not prominent. The outline of the EDJ ridge in occlusal view tends to be quadrilateral in outline in the third upper premolar but there is still a disto-lingual expansion of the EDJ which makes the fourth upper premolar squarer in this part of the EDJ.

A. africanus: Investigation of possible abnormal or misidentified teeth

The *A. africanus* teeth in this sample were plotted against the first three principal components of shape (Fig.5.1.15). Inspection of the plot shows that STS 47 is an outlier and on inspection (Fig. 5.1.16) the EDJ shows a very unusual morphology, unlike any other hominin upper premolar, with a circular EDJ ridge of relatively small diameter. Because of this atypical appearance the tooth was excluded from the sample

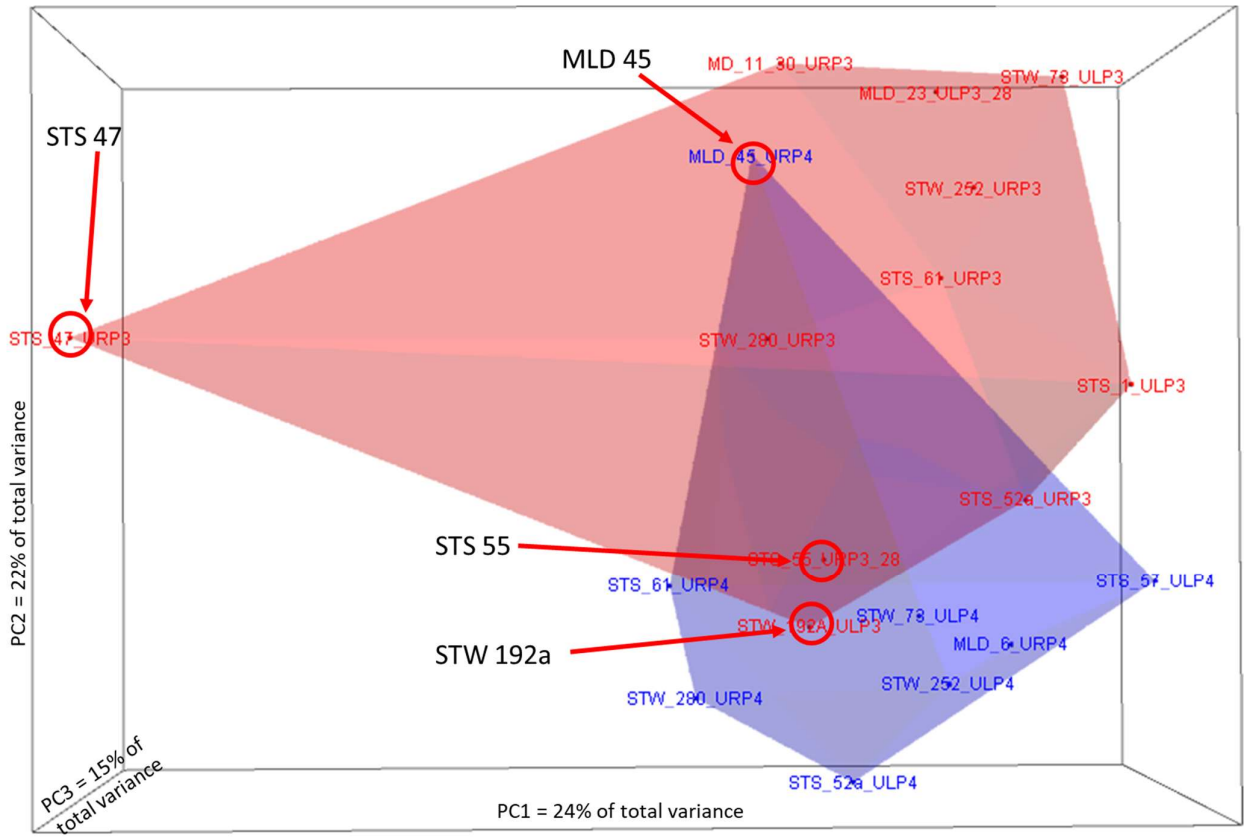

Figure 5.1.16 Plot of *A. africanus* teeth against the first three principal components of shape with convex hulls for third upper premolars (Red) and fourth upper premolars (Blue). STS 47 appears to be an outlier. MLD 45 is labelled as a fourth upper premolar but groups with the third upper premolars. STS 55 and STW 192a are labelled as third upper premolars but appear to group with the fourth upper premolars.

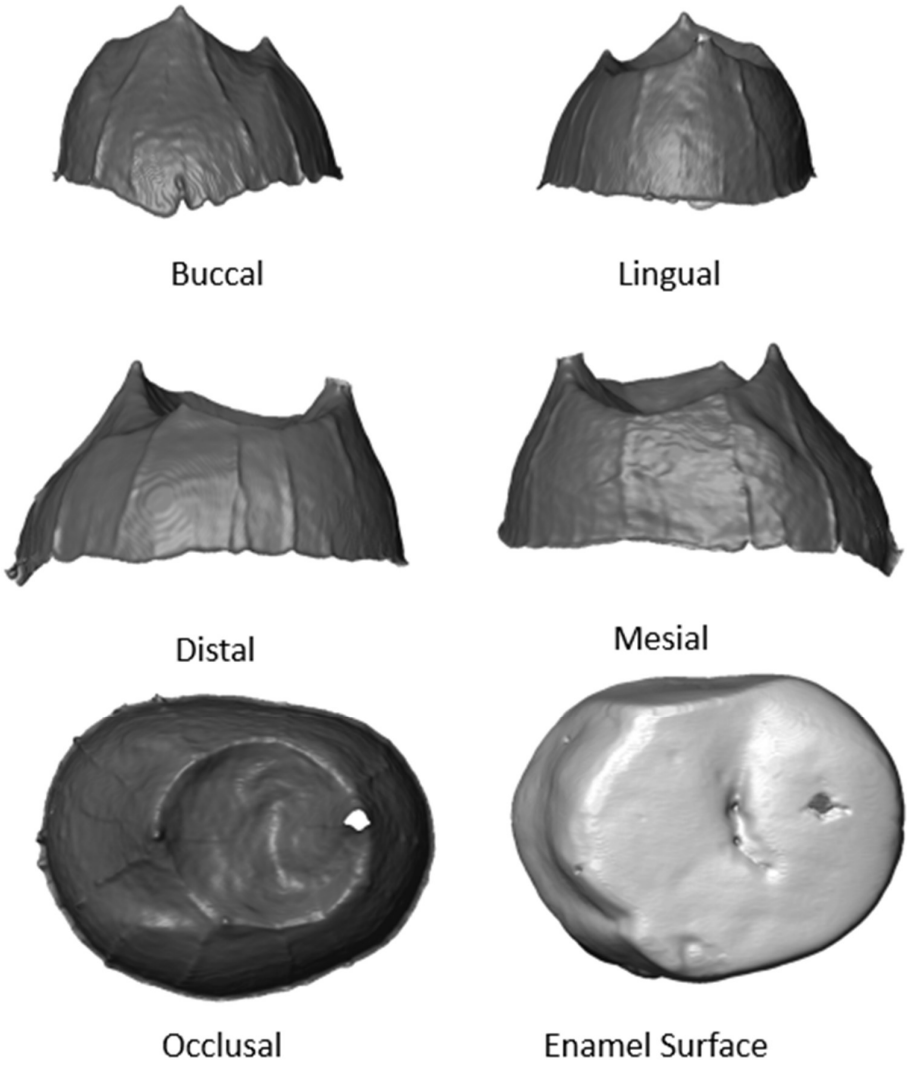

Figure 5.1.17 The morphology of the EDJ and occlusal enamel surface of STS 47.

STW 192a and STS 55 are identified as third upper premolars but group with the fourth upper premolars. Conversely, MLD 45 is identified as a fourth upper premolar but groups with the third upper premolars. The EDJs of these teeth were examined in detail and were compared with teeth of known position in the maxillae STW 252 and STW 280. (Figs. 5.1.17, 5.1.18, 5.1.19)

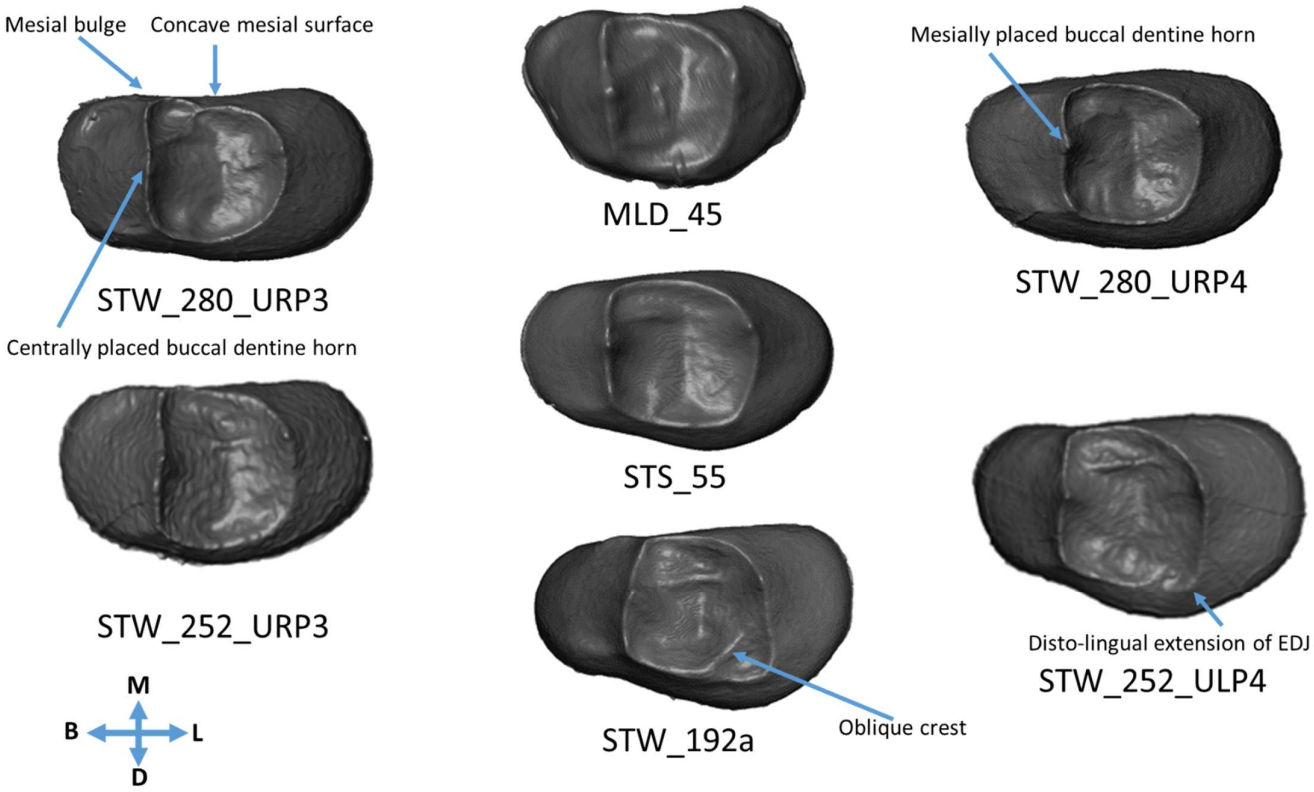

Figure 5.1.18 Comparison of the EDJ of suspect teeth (centre column) with the EDJ of teeth of known position (*In situ* in the jaw – third upper premolars in the left hand column, fourth upper premolars in the right hand column). Occlusal view. Left sided teeth flipped to aid comparison.

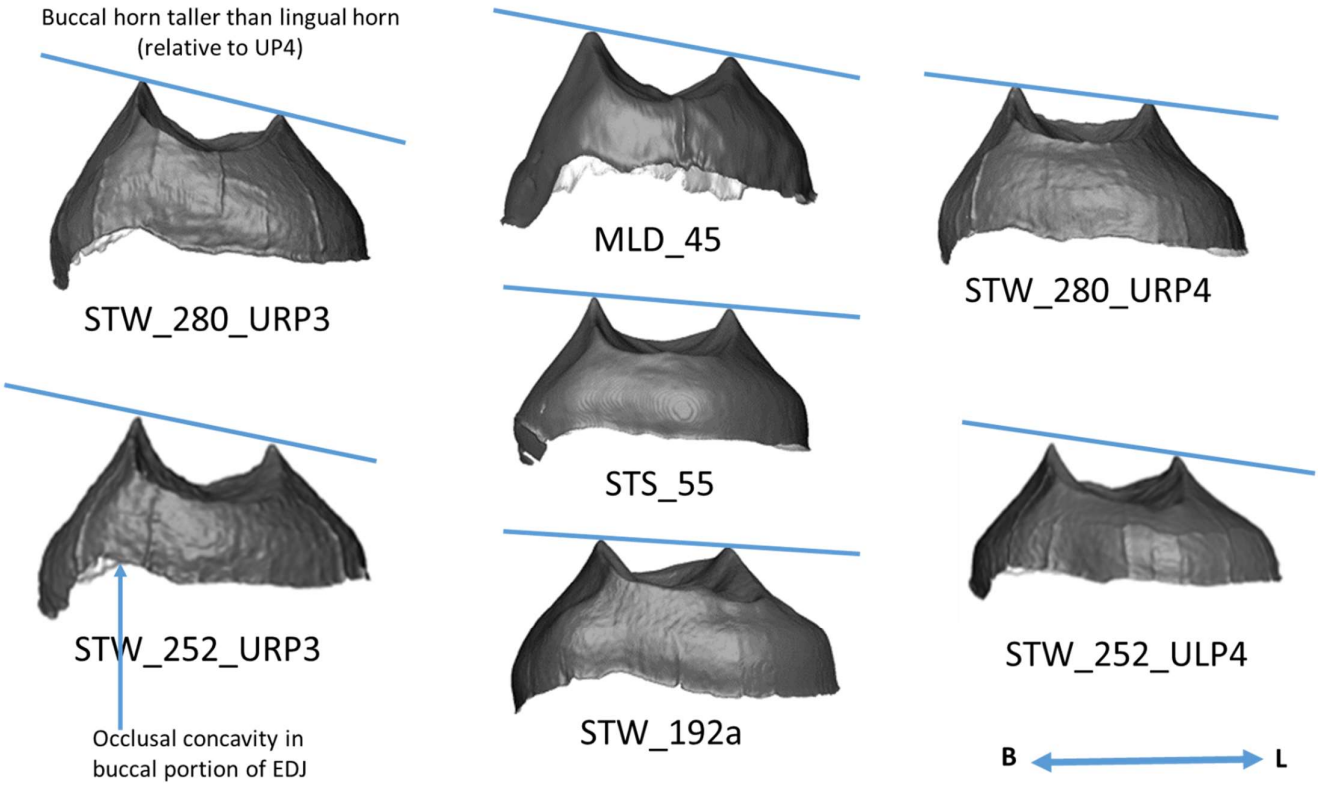

Figure 5.1.19 Comparison of the EDJ of suspect teeth (centre column) with the EDJ of teeth of known position (*In situ* in the jaw – third upper premolars in the left hand column, fourth upper premolars in the right hand column). Occlusal view. Left sided teeth flipped to aid comparison.

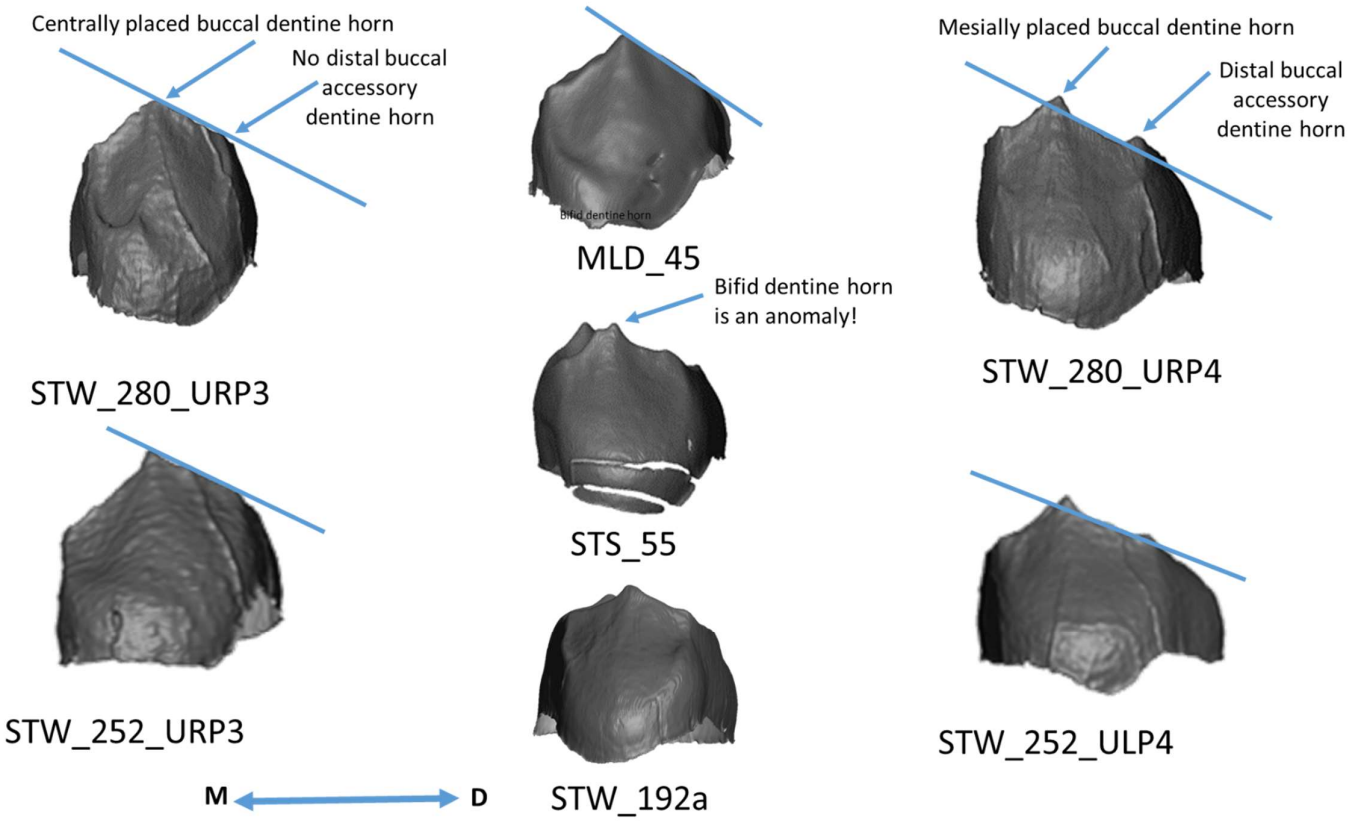

Figure 5.1.20 Comparison of the EDJ of suspect teeth (centre column) with the EDJ of teeth of known position (*In situ* in the jaw – third upper premolars in the left hand column, fourth upper premolars in the right hand column). Occlusal view. Left sided teeth flipped to aid comparison.

The EDJ of STS 192a shows typical features of an *Australopithecus* upper fourth premolar. The buccal dentine horn is only slightly taller than the lingual dentine horn and is only slightly distally displaced compared with the lingual dentine horn. By contrast, in *Australopithecus* third upper premolars the buccal dentine horn is significantly taller and distally displaced when compared to the lingual dentine horn. In addition, there is talon expansion in STW 192a, with a small accessory distal buccal dentine horn, as is typical of *Australopithecus* fourth upper premolars. There is also incipient molarisation in STS 192a with a disto-lingual extension of the EDJ (in the position of the hypocone in *Australopithecus* upper molars) and a partial oblique ridge.

The EDJ of MLD 45 shows the typical features of an *Australopithecus* third upper premolar. The buccal dentine horn is taller than the lingual dentine horn and is displaced distally compared with the lingual dentine horn, occupying a central position in the buccal EDJ ridge. There is no talon extension and no accessory distal buccal dentine horn. There is a mesial convexity in the buccal part of the mesial EDJ ridge and the mesial CEJ ridge is concave in shape.

The EDJ of STS 55 shows typical features of an *Australopithecus* upper fourth premolar. The buccal dentine horn is only slightly taller than the lingual dentine horn and is only slightly distally displaced compared with the lingual dentine horn. In addition, there is talon expansion in STS 55, with a small accessory distal buccal dentine horn, as is typical of *Australopithecus* fourth upper premolars. The disto-lingual EDJ ridge is rounded in outline, giving the ridge an overall quadrilateral shape, in contrast to *Australopithecus* third upper premolars, which have a flatter outline in this region, giving a slightly more triangular appearance. As a result of these investigations, STS 55 and STS 192a were re-labelled as fourth upper premolars and MLD 45 was re-labelled as a third upper premolar.

5.1.4 Paranthropus robustus

A plot of the first three principal components of shape for the *P. robustus* EDJ shows good separation between the third and fourth upper premolars (Fig. 5.1.20). In the third upper premolar the buccal dentine horn is taller and more distally placed, relative to the lingual dentine horn, than in the fourth upper premolar (Fig. 5.1.21). There is no notch or bulge in the mesial EDJ ridge in either third or fourth upper premolars. In the fourth upper premolar there is a large and distinct distal accessory buccal horn which is separated from the main buccal dentine horn by an extension of the talon. In the third upper premolar there may be a small distal buccal accessory horn which is not separated from the main buccal dentine horn by a concavity in the buccal EDJ ridge.

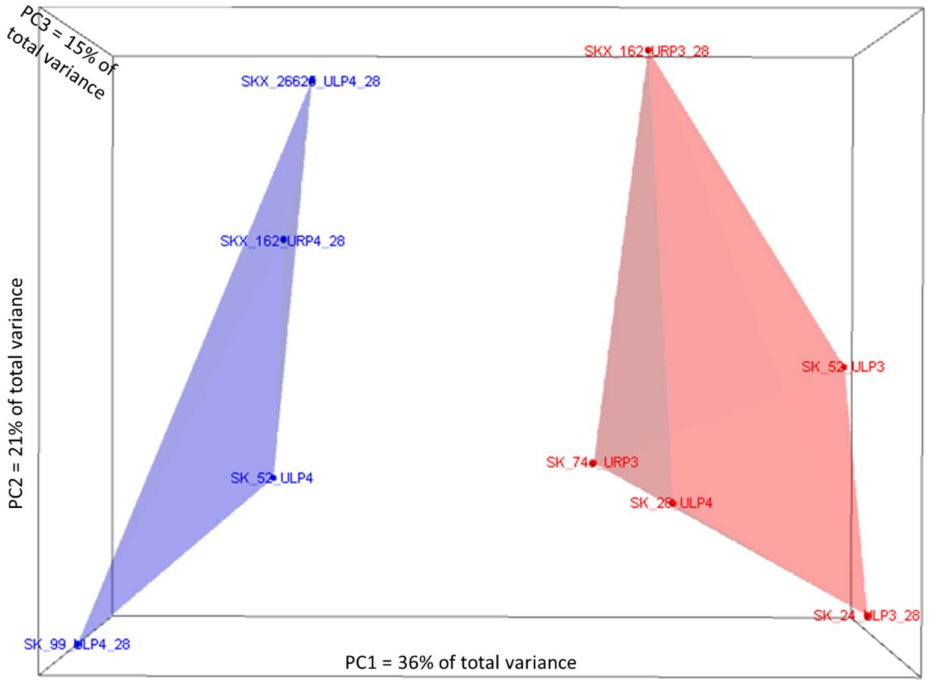

Figure 5.1.21 Plot of *P. robustus* teeth on the first three principal components of EDJ shape. Red = third upper premolar, blue = fourth upper premolar.

In the occlusal view in both the EDJ ridge and in the CEJ the outline of the EDJ is roughly quadrilateral. In the disto-lingual part of the EDJ ridge in both tooth positions there is a prominent lingual extension. In the fourth upper premolar, this extension culminates in a distal lingual accessory dentine horn. This is partially separated from the rest of the occlusal surface of the EDJ by an oblique ridge.

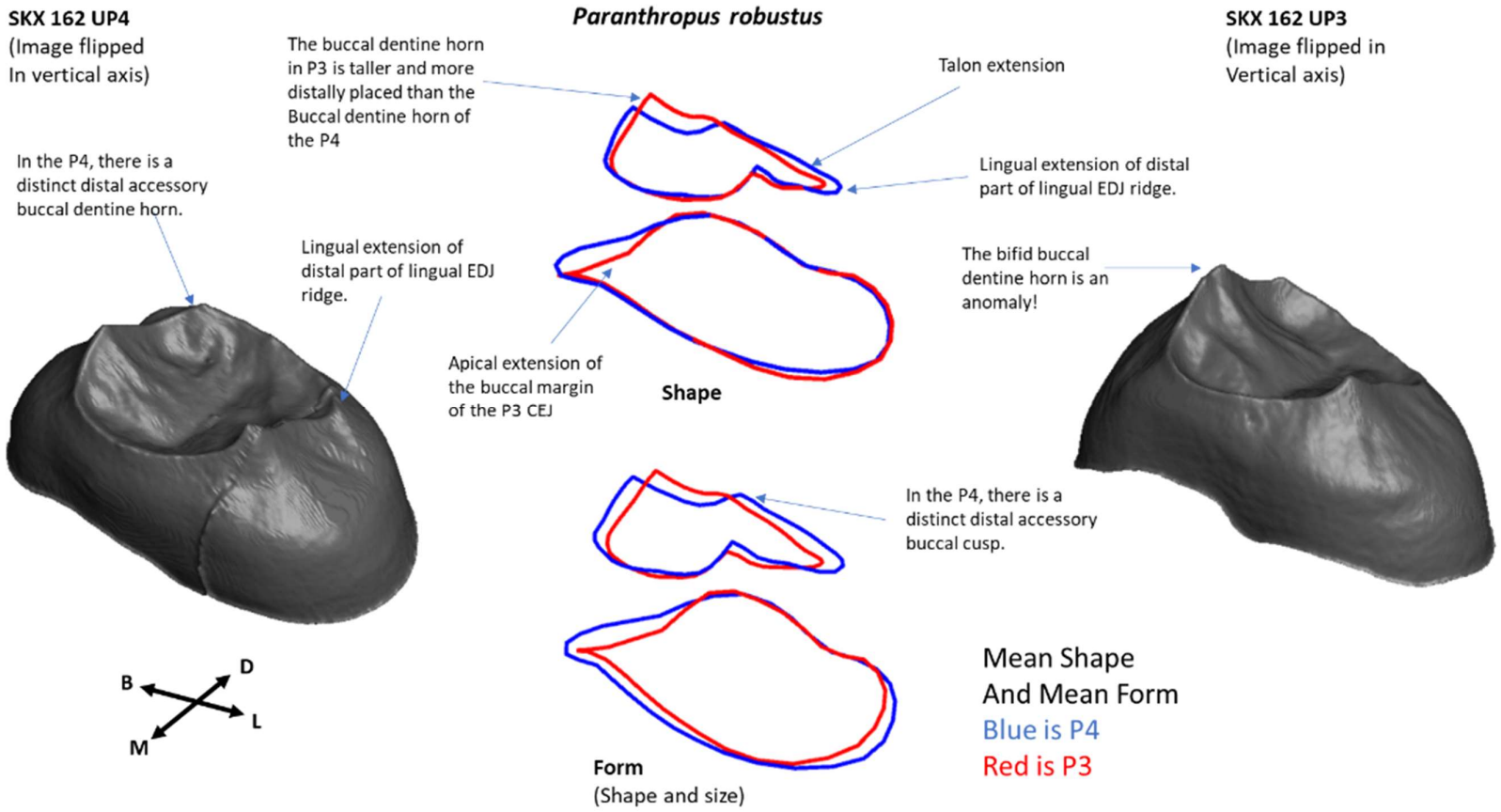

Figure 5.1.22 Summary of differences in EDJ morphology between third and fourth upper premolars of *P. robustus*.

P. robustus: Investigation of possible abnormal or misidentified teeth

The *P. robustus* teeth in this sample were plotted against the first three principal components of shape (Fig. 5.1.22). This plot shows that the fourth upper premolar SK 28 groups with the third upper premolars. Inspection of the tooth was carried out and its EDJ was compared with teeth of certain tooth position – such as teeth from the maxillae SK 52 and SKX 162 (Figs. 5.1.23, 5.1.24, 5.1.25).

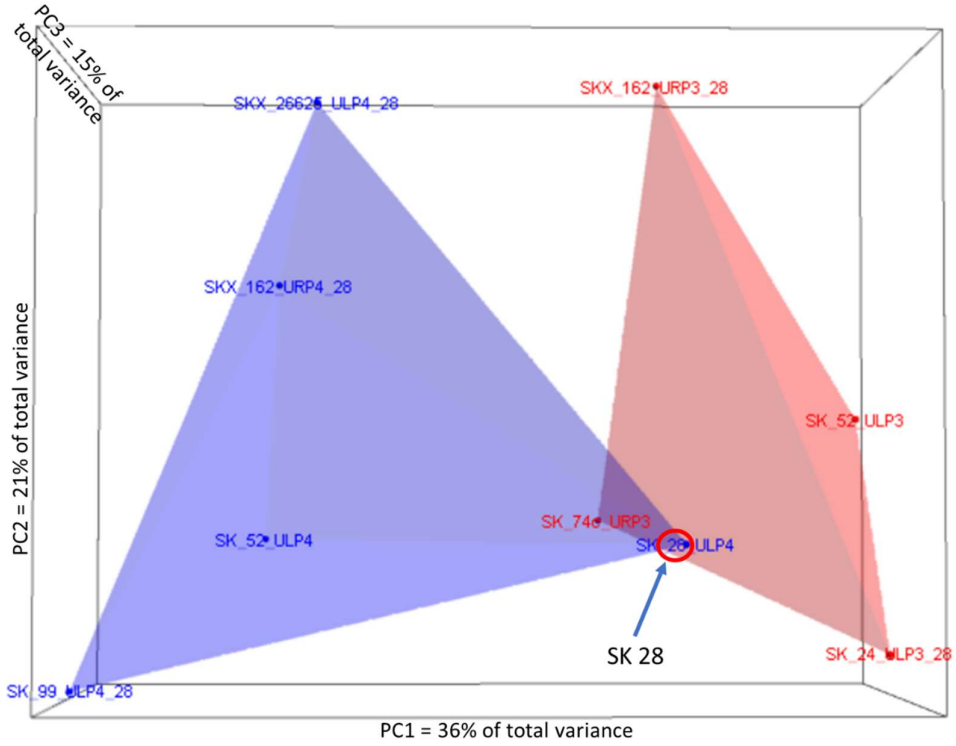

Figure 5.1.23 Plot of *P. robustus* teeth against the first three principal components of shape with convex hulls for tooth type. Red = third upper premolars, Blue = fourth upper premolars.

In overall morphology, SK 28 more closely resembles other *P. robustus* third upper premolars, rather than fourth upper premolars. In particular, the root structure is similar to SK 24 in that the "mesial buccal root is connected to the lingual root by a thin plate so that only the actual apices are separate" (Robinson, 1956, p. 62). Robinson (1956) presumably identified this tooth as a fourth upper premolar based on two features. Firstly, the tooth has a large oval mesial contact facet, which Robinson seems to have regarded as a diagnostic feature of fourth upper premolars:

> "When a wear facet is developed on the mesial face of P^4 it has the shape of that of the distal face of P^3 – a round or oval facet. This is one of the means of separating P^3 and P^4 when isolated, because a wear facet on the mesial face of P^3 in this form is a narrow elongate facet arranged at an angle of approximately 45 degrees buccalward"
>
> (Robinson, 1956, p.61)

The second feature is a “distinct buccal cuspule” (Robinson, 1956, p. 61) on the distal part of the buccal cusp. Whilst this is clearly visible on the outer enamel surface, examination of the EDJ shows that there is not a distinct distal accessory buccal dentine horn, separated by a talon expansion from the primary buccal dentine horn, as is typically seen in *P. robustus* fourth upper premolars, but rather there is a small dentine horn on the buccal ridge of the EDJ, as is often seen in *P. robustus* third upper premolars (Fig. 5.1.25).

On the lingual part of the talon, fourth upper premolars have a distinctive lingual extension of the distal EDJ ridge. This is in the position of the hypocone in upper molar teeth and (along with the distinct distal buccal dentine horn and talon extension) may represent incipient molarisation of the fourth upper premolar. Third upper premolars – and SK 28 - do have a small lingual convexity in this area of the EDJ ridge but this is far less pronounced and angular than in fourth upper premolars.

In third upper premolars, and in SK 28, the buccal dentine horn is taller than the lingual dentine horn and is displaced distally relative to the lingual dentine horn, occupying a more central position in the buccal ridge of the EDJ. By contrast, in fourth upper premolars, the buccal dentine horn is only slightly taller and only slightly distally displaced compared with the lingual dentine horn. It lies in the mesial half of the buccal ridge of the EDJ due to talon extension.

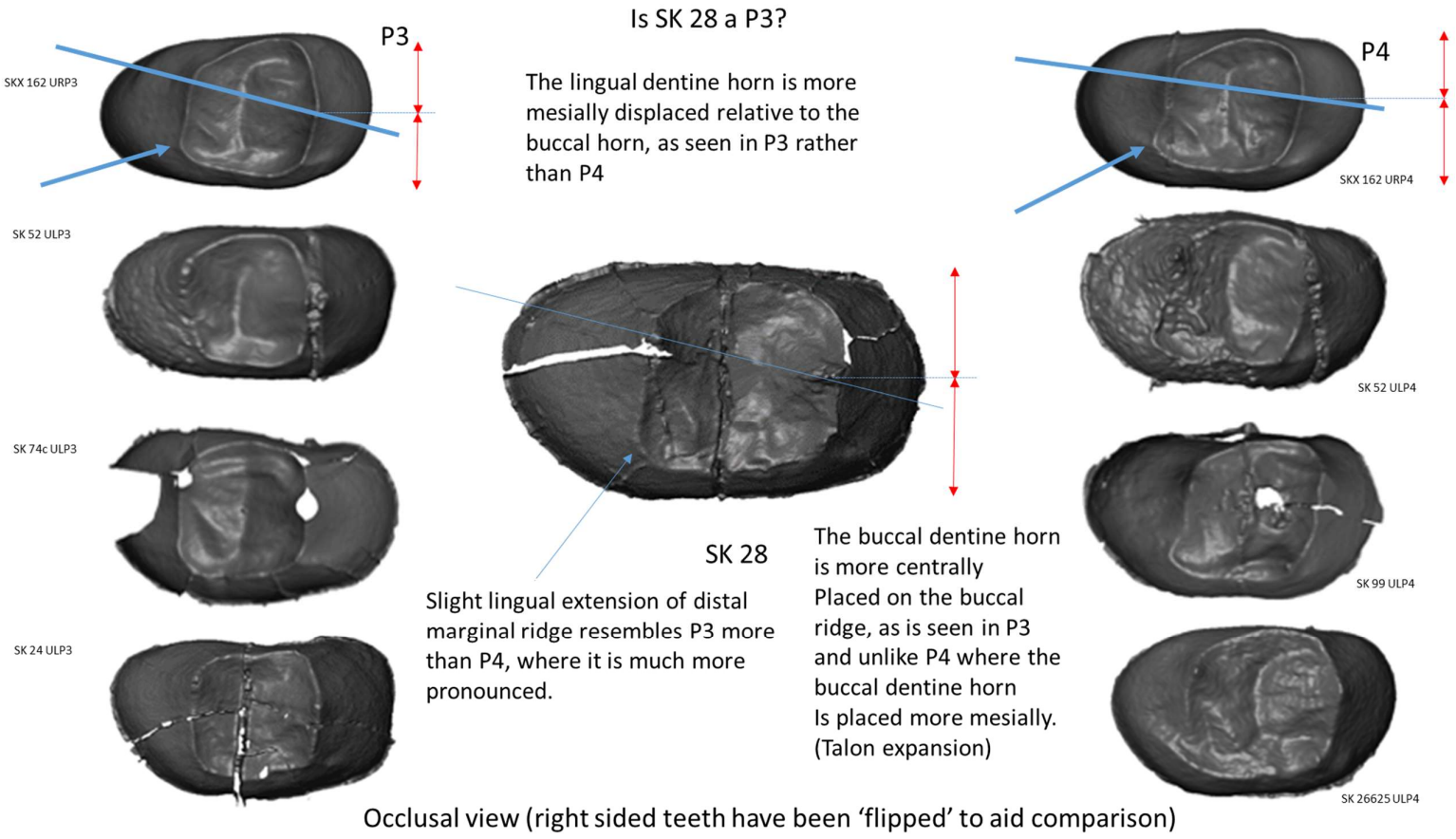

Figure 5.1.24 Comparison of the EDJ of SK 28 with *P. robustus* third and fourth upper premolars of known tooth position.

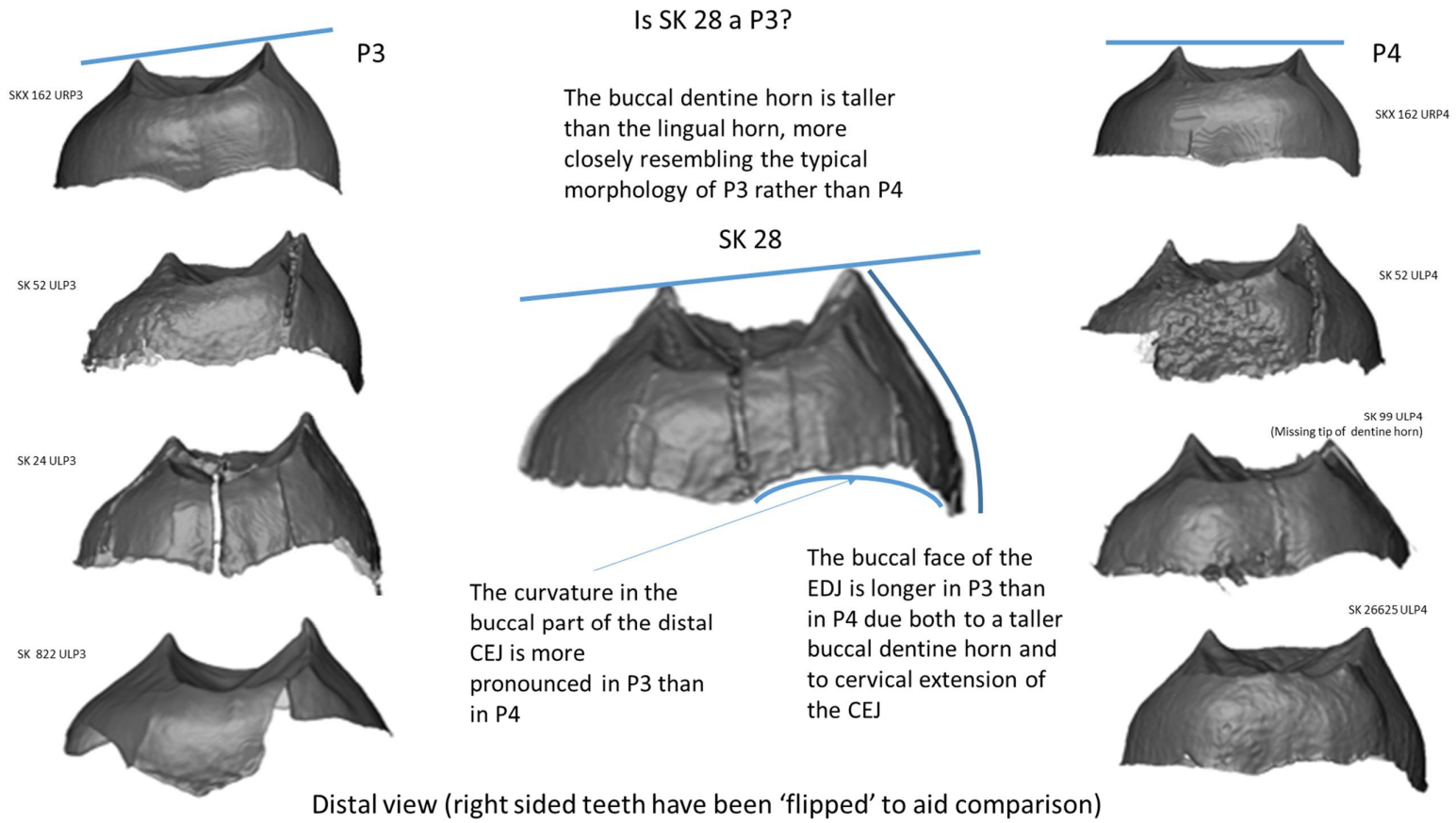

Figure 5.1.25 Comparison of the EDJ of SK 28 with *P. robustus* third and fourth upper premolars of known tooth position.

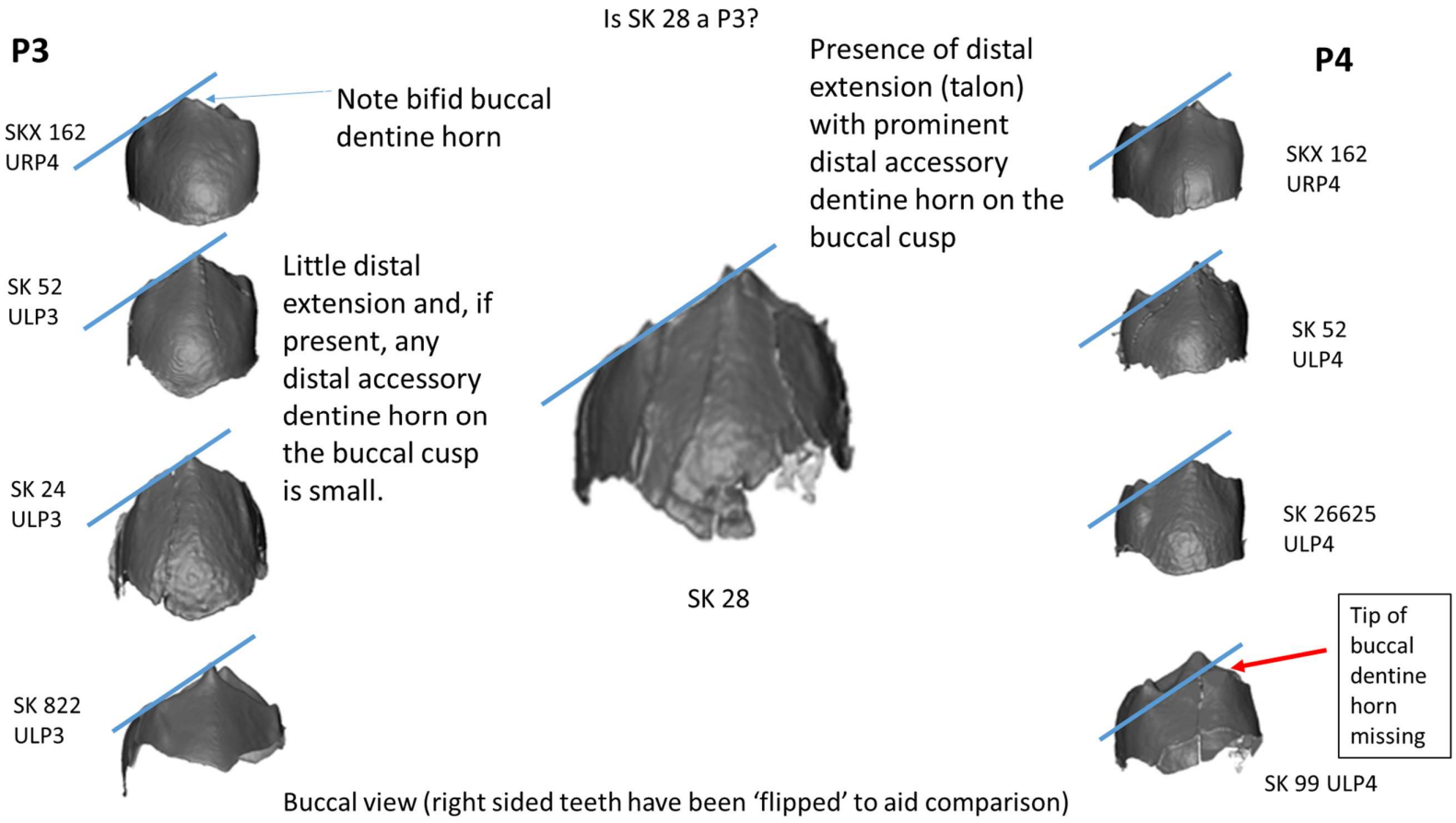

Figure 5.1.26 Comparison of the EDJ of SK 28 with *P. robustus* third and fourth upper premolars of known tooth position.

In third upper premolars, and in SK 28, the buccal surface of the EDJ is expanded in the apical – occlusal direction due both to the taller buccal dentine horn and due to an apical extension of the cemento-enamel junction (CEJ). In distal view there is a concavity in the occlusal direction of the buccal part of the CEJ of third upper premolars – and in SK 28. In contrast, the CEJ of the fourth upper premolar has a much less pronounced or absent occlusal curvature in this region of the CEJ.

Taking all this evidence from the EDJ into consideration, which was not available to Robinson, there seems to be a good case for re-labelling SK 28 as a third upper premolar.

5.1.5 Homo naledi

The *H. naledi* teeth in this study have not yet, at the time of writing, been formally described. The allocation of teeth to tooth position has been done partly by analysing the morphology of the EDJ using statistical techniques, including principal component analysis and discriminant function analysis but also by examination of crown and root morphology, on archaeological associations between teeth and on other factors such as contact facets and tooth wear based on Lucas Delezene *et al.*'s, description of the Rising Star dental material (in preparation). Principal component analysis of the *H. naledi* teeth, based on this provisional labelling of tooth positions, does show good separation between third and fourth upper premolars (Fig. 5.1.26).

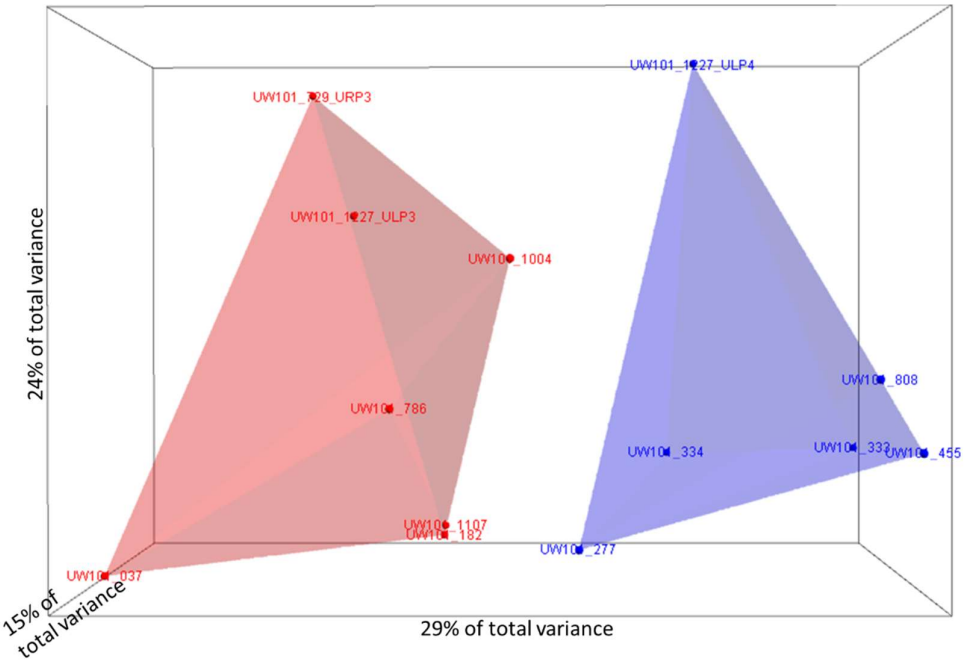

Figure 5.1.27 Plot of *H. naledi* teeth on the first two principal components of EDJ shape. Red = third upper premolars, Blue = fourth upper premolars.

A detailed examination of wire frame models for the mean shape of third and fourth upper premolars and inspection of the EDJ surfaces (Fig. 5.1.27) reveals a number of distinctive features. In *H. naledi* the height of the buccal and lingual dentine horns is similar in both the third and fourth upper premolars but in the third upper premolar the buccal dentine horn is slightly taller and slightly more distally displaced than in the fourth upper premolar. In the fourth upper premolar there is a large and distinct distal accessory buccal horn which is separated from the main buccal dentine horn by an extension of the talon. In the third upper premolar there is a small distal buccal accessory dentine horn, which is more prominent than in other species..

The CEJ of both upper premolars is markedly concave in the occlusal direction in the buccal part of both the mesial and the distal CEJ and this concavity is deeper in the third upper premolar. In the occlusal view in both the EDJ ridge and in the CEJ the outline of the EDJ is roughly quadrilateral. However, there is a slightly greater expansion of the disto-lingual part of the EDJ ridge in the fourth upper premolar, leading to a slightly squarer outline of the EDJ ridge in the fourth upper premolar.

Because these teeth have not yet been formally described, I have included pictures of the EDJs of all *H. naledi* teeth in this sample, grouped by tooth position, in occlusal view (Fig. 5.1.28), mesial view (Fig. 5.1.29) and buccal view (Fig. 5.1.30). Left sided teeth have been flipped in the vertical axis to aid comparison.

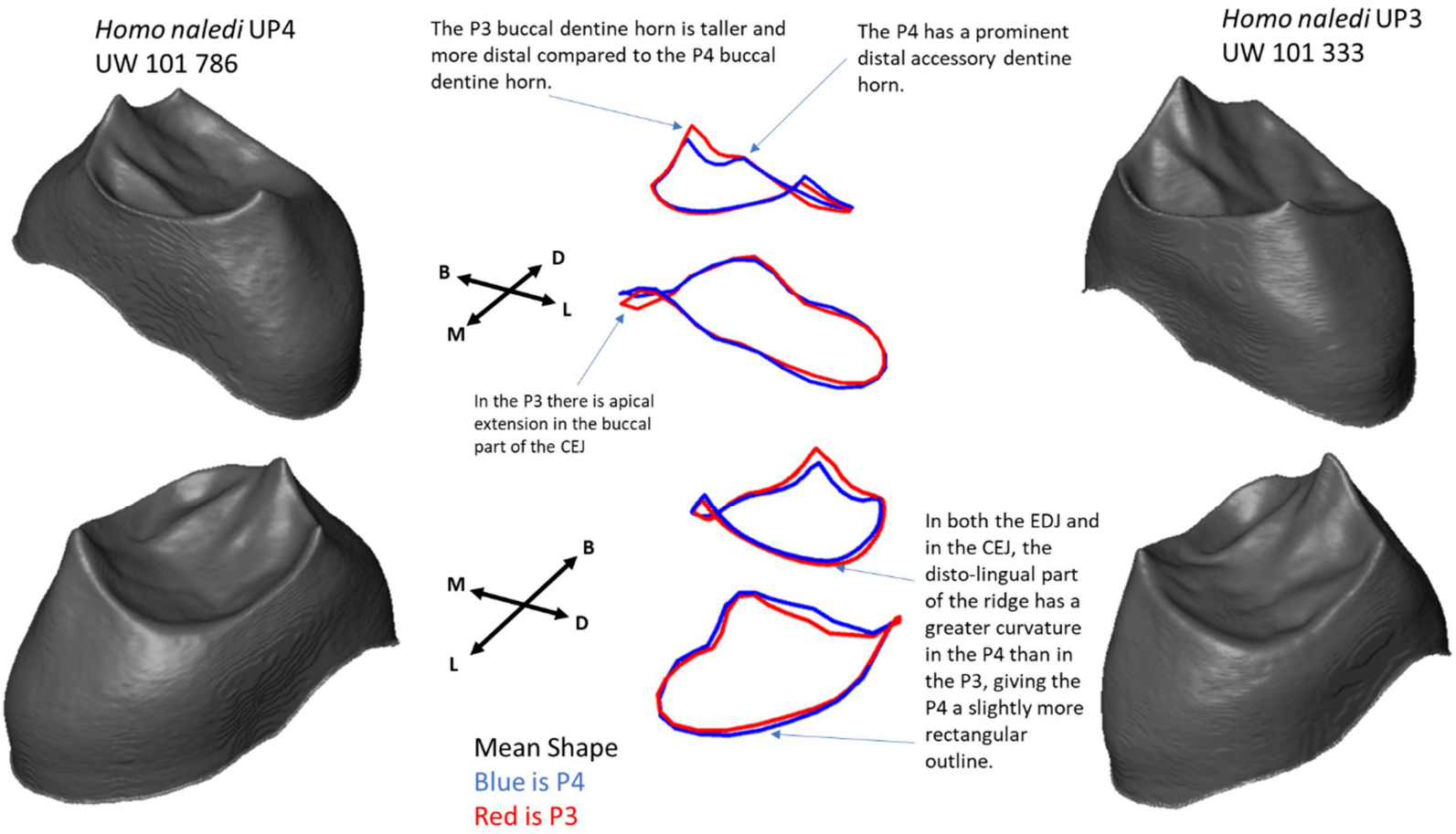

Figure 5.1.28 Summary of differences in EDJ morphology between third and fourth upper premolars of *H. naledi*.

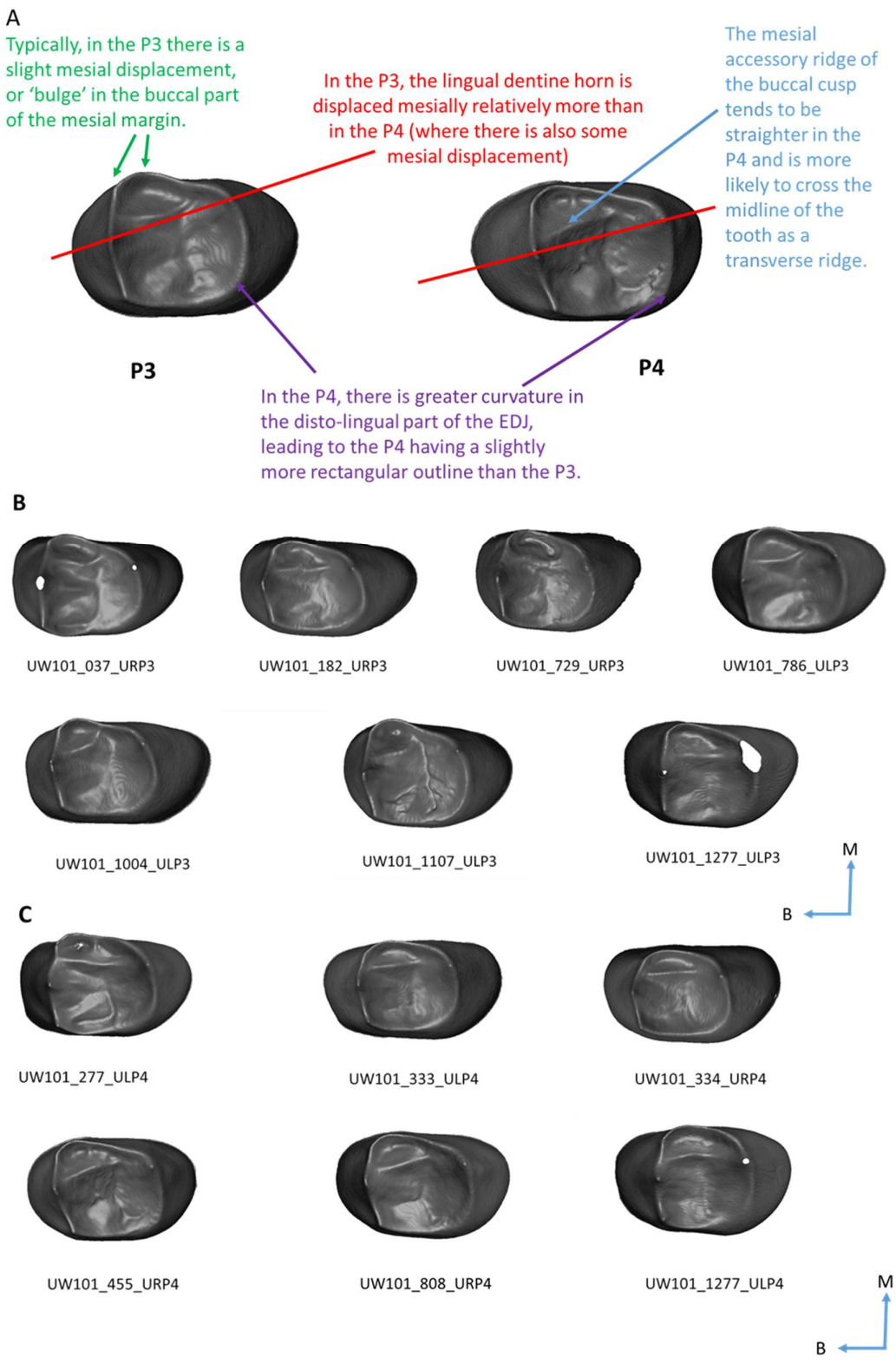

Figure 5.1.29 All *H. naledi* EDJs in the study sample in occlusal view. Left sided EDJs are 'flipped' to aid comparison. **A**: Comparison of the EDJ of a third upper premolar (UW101 786) with the EDJ of a fourth upper premolar (UW101 455). **B**: Third upper premolars. **C**: Fourth upper premolars.

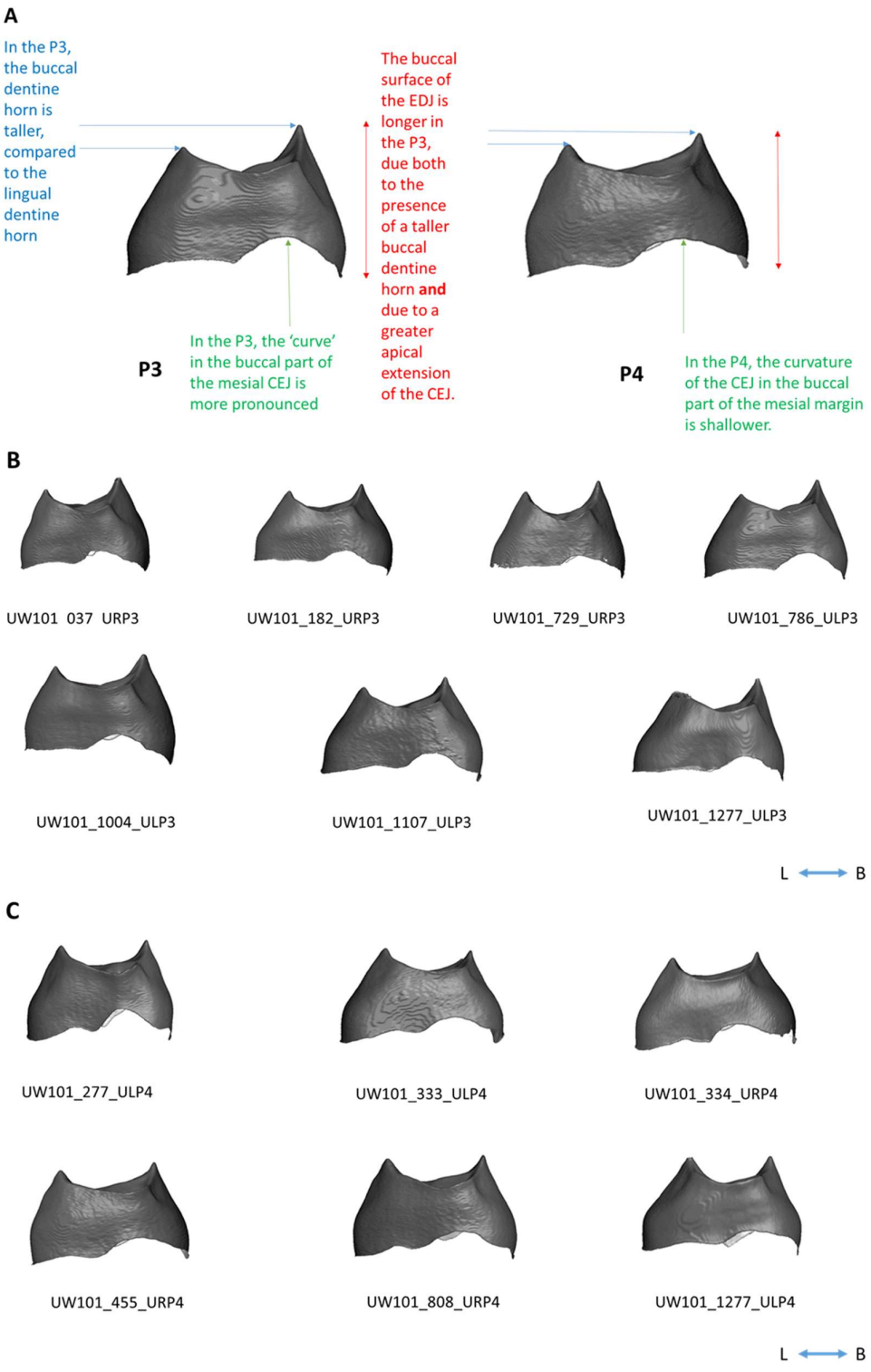

Figure 5.1.30 All *H. naledi* EDJs in the study sample in mesial view. Left sided EDJs are 'flipped' to aid comparison. **A**: Comparison of the EDJ of a third upper premolar (UW101 786) with the EDJ of a fourth upper premolar (UW101 455). **B**: Third upper premolars. **C**: Fourth upper premolars.

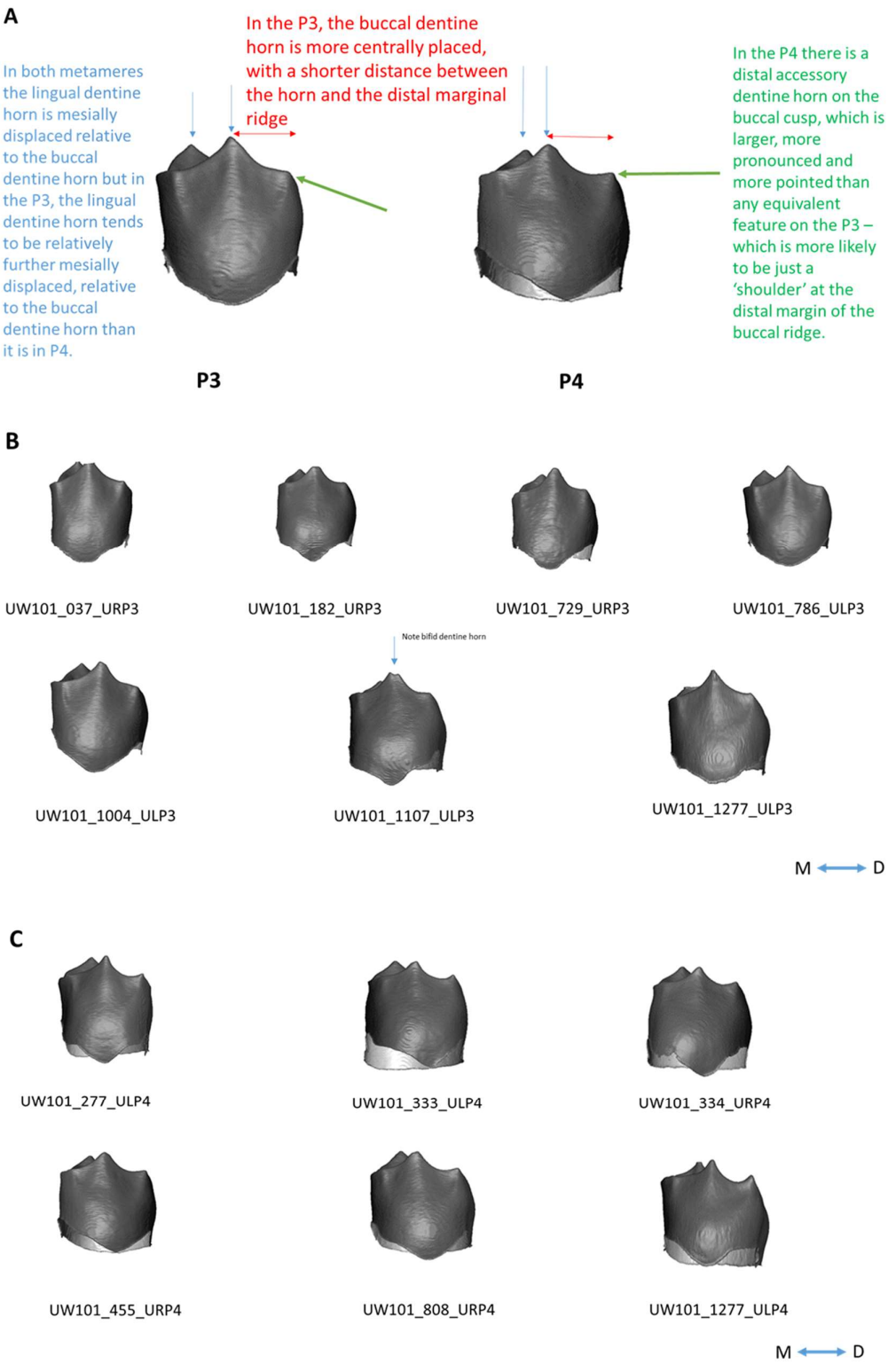

Figure 5.1.31 All *H. naledi* EDJs in the study sample in buccal view. Left sided EDJs are 'flipped' to aid comparison. **A**: Comparison of the EDJ of a third upper premolar (UW101 786) with the EDJ of a fourth upper premolar (UW101 455). **B**: Third upper premolars. **C**: Fourth upper premolars.

5.2 Intra- and interspecific comparison of premolar crown size

Patterns of relative UP3 and UP4 size within species

To test for patterns in premolar crown size a two-factor analysis of variance was conducted with factors for tooth type and for species and the outcome variable is centroid size. The assumptions for this analysis are that within each group, the outcome variable has a Normal distribution and the variance of the outcome variable is equal in all groups. Figure 5.2.1 shows a box and whisker plot of centroid size grouped by species and by tooth type. The distributions appear to be symmetrical about the median value in each group and to have similar variances. There is no reason from this plot to doubt the assumptions of Normal distributions with equal variances in each group.

The two-factor analysis of variance shows a statistically significant term for interaction between the factors of species and tooth type ($p = 0.018$). This means that the difference in size between the third and fourth upper premolar is not constant between species. Inspection of the box and whisker plot Figure 5.2.1 (showing medians), the interaction plot Figure 5.2.2 (showing means) and the table of group means (Table 5.2.1) shows that *P. robustus*, *A. africanus* and *H. naledi* have larger fourth upper premolars than third upper premolars, *Homo* species other than *H. naledi* have smaller fourth upper premolars than third upper premolars.

Table 5.2.1 Mean centroid size by tooth type and species.

	Aafr	Nal	Nean	Prob	Qaf	Sap	Total
UP3	40.44	34.08	38.65	44.30	36.35	33.59	36.90
UP4	41.35	35.31	37.43	47.07	34.52	32.19	36.59
Total	40.90	34.65	37.85	45.53	35.31	33.00	

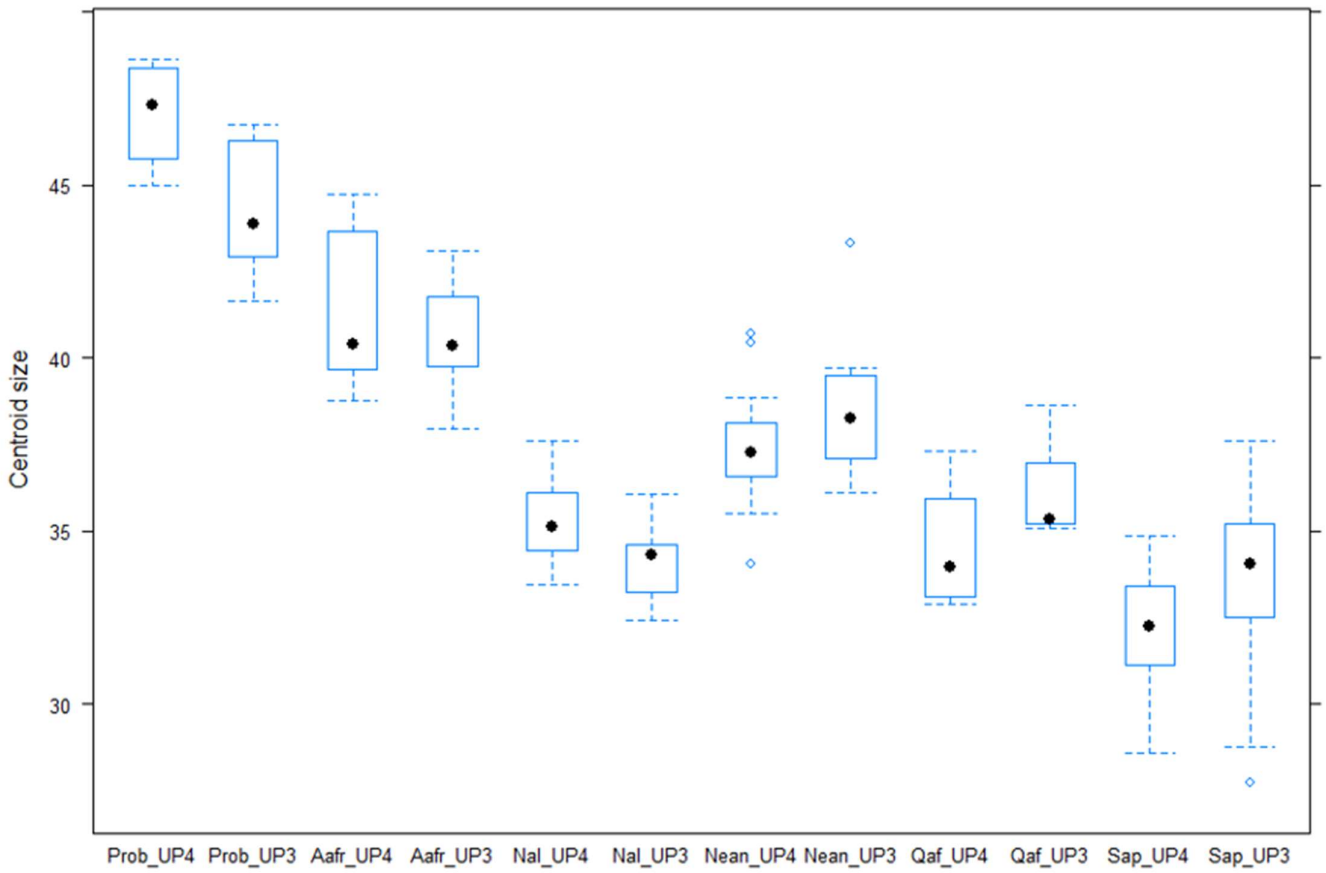

Figure 5.2.1 Box and whisker plot of centroid size by species and tooth type.

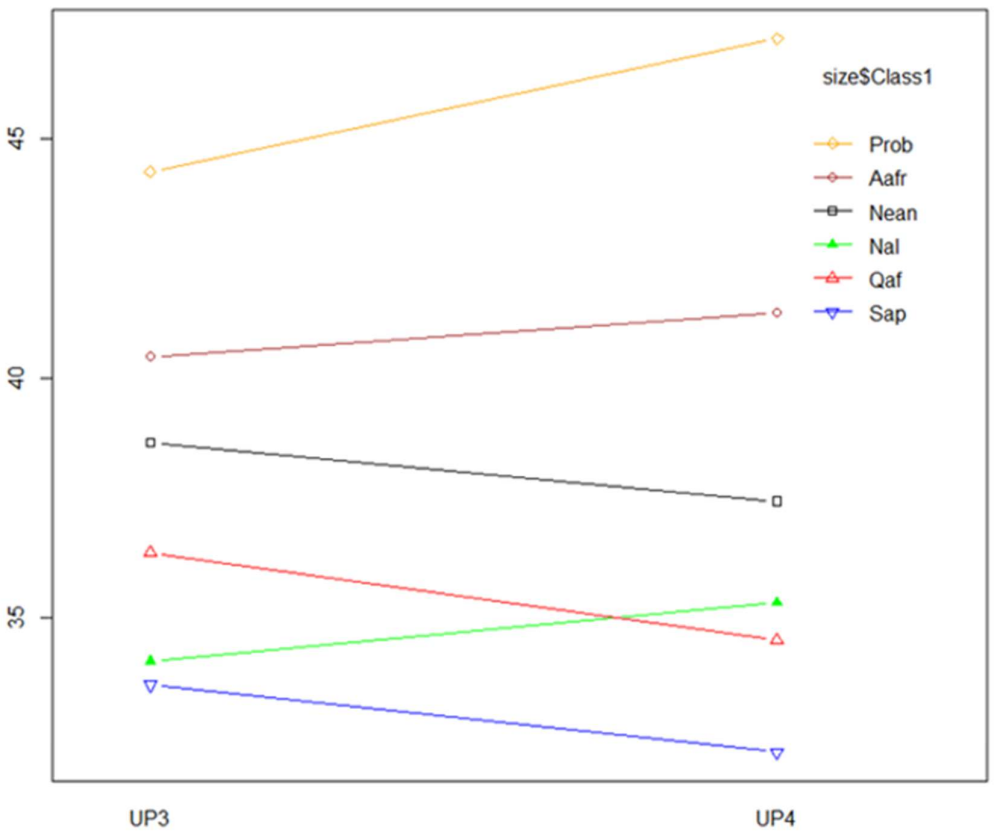

Figure 5.2.2 Group means for centroid size by species and by tooth type.

The analysis of mean centroid size in this study shows a pattern in which the difference between the size of the third and the fourth upper premolars varies between species, with *A. africanus* and *P. robustus* having larger fourth upper premolars than third upper premolars and the opposite pattern being seen in species of *Homo* (other than *H. naledi*). To examine whether this pattern also applies to individuals, the difference in centroid size between the third upper premolar and the fourth upper premolar was calculated for all specimens in the sample for which both tooth types were present in the same individual (Fig. 5.2.3). Individuals from the *Australopithecus* and *Paranthropus* populations tend to have a larger fourth upper premolar than third upper premolar. In *Homo* species the opposite is the case, with individuals tending to have a larger third upper premolar than fourth upper premolar. The *H. naledi* maxilla (UW101_1277) has a larger fourth than third upper premolar.

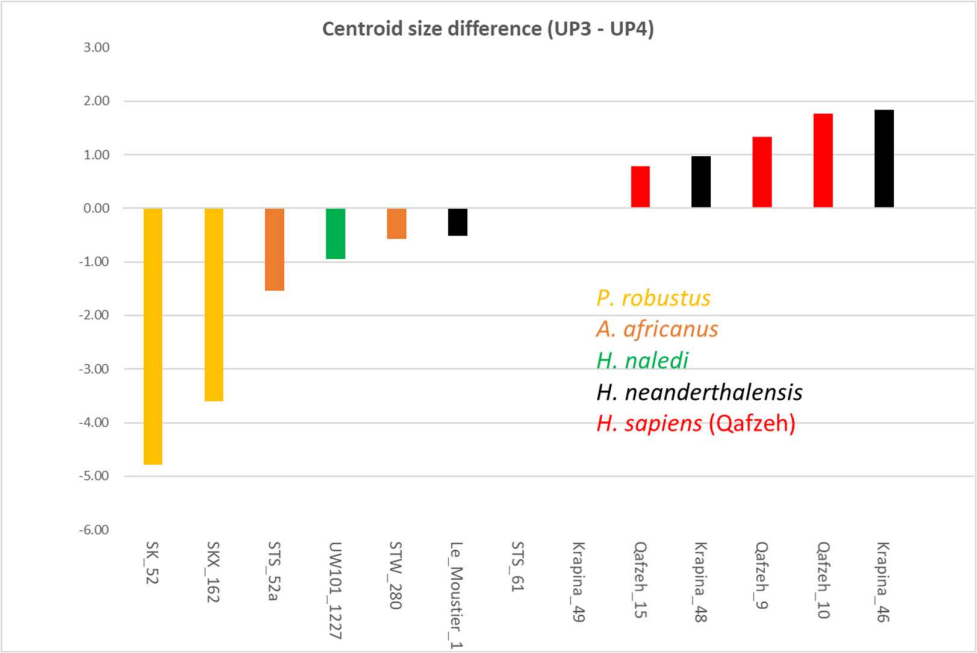

Figure 5.2.3 Difference in centroid tooth size (UP3 – UP4) for individual specimens within the sample that possess both tooth positions.

Differences in premolar size between species

Analysis of variance (ANOVA) for centroid size by species was carried out separately for each tooth type. Both for upper third premolars and for upper fourth premolars, the analysis shows strong evidence of differences between the species' group mean centroid sizes ($p < 0.0001$ in both analyses). *P. robustus* has the largest teeth, followed by *A. africanus*. Species of *Homo* have smaller teeth, with a decrease in size from the *H. neanderthalensis* to fossil *H. sapiens* (the Qafzeh hominins) and a further decrease in size to modern humans. The centroid size of the teeth of *H. naledi* was similar in size to the Qafzeh hominins.

Since this study focusses on a comparison between *H. naledi* and other hominin species, Bonferroni corrected t-tests were conducted for the difference in size between *H. naledi* and each other species according to tooth type (Tables 5.2.2, 5.2.3). For the fourth upper premolar, there is no statistical evidence for a size difference between the centroid size of *H. naledi* and that of fossil *H. sapiens* (Qafzeh) and there is some evidence of a size difference between *H. naledi* and *H. neanderthalensis*. There is strong evidence that the centroid size of *H. naledi* is smaller than that of *Australopithecus* and *Paranthropus* and larger than that of *H. sapiens.* For the third upper premolar, there is no statistical evidence that the centroid size in *H. naledi* differs from that of modern *H. sapiens* or fossil *H. sapiens* (Qafzeh). There is strong evidence that the centroid size of the third upper premolar is smaller in *H. naledi* than in *H. neanderthalensis* and very strong evidence that it is smaller in size than in *Australopithecus* and *Paranthropus*.

Table 5.2.2 t - tests for size differences between UP4s for *H. naledi* and other hominin species.

Species	Size	Difference	95% confidence interval	p – value.	Adjusted Sig. level[5]
Prob	47.1	- 11.8	(- 14.24, - 9.29)	< 0.0001	< 0.0005
Aafr	41.4	- 6.1	(- 8.07, -4 .03)	< 0.0001	< 0.0005
Nean	37.4	- 2.1	(- 3.71, - 0.53)	0.014	< 0.05
Qaf	34.5	0.8	(- 2.16, 3.72)	0.526	0.526
Nal	35.3	-	-	-	
Sap	32.2	3.1	(1.52, 4.72)	0.001	< 0.005

Table 5.2.3 t - tests for size differences between UP3s for *H. naledi* and other hominin species.

Species	Size	Difference	95% confidence interval	p – value.	Adjusted Sig. level
Prob	44.3	- 10.2	(- 12.89, - 7.54)	< 0.0001	< 0.0005
Aafr	40.4	- 6.3	(- 7.94, - 4.78)	< 0.0001	< 0.0005
Nean	38.6	- 4.5	(- 6.60, - 2.53)	0.0004	< 0.01
Qaf	36.4	- 2.3	(- 6.42, 1.88)	0.172	0.172
Nal	34.1		-	-	
Sap	33.6	0.5	(-0.99, 1.97)	0.496	0.496

[5] A Bonferroni correction was applied to calculate the significance level. This correction is sequential. (The full correction is applied to the first test, with the smallest p-value. For each subsequent test, the number of comparisons in the test is reduced by one).

5.3 Comparison of premolar EDJ shape between species and tooth position.

Figure 5.3.1 presents the results of a principal component analysis of the combined P3 and P4 sample. The first principal component accounts for 57% of the total variance. The second principal component represents only 9% of the total variance and the third represents 6% of the total variance. The first five principal components account for 80% of the total variance and the first 16 principal components account for 95% of the total variance. There is a clear separation between the convex hulls of the groups, both between species and between tooth type within species, except for the third upper premolars in species of *Homo* (other than *H. naledi*), where there is some overlap between modern humans, the Qafzeh hominins and Neanderthals. The *H. naledi* sample lies between the *Australopithecus/Paranthropus* groups on one side, and the other *Homo* species on the other side, being closest in shape to *A. africanus*.

The species are well separated by the first principal component with *P. robustus* at one extreme of the first principal component and modern humans at the other extreme. The second principal component seems to capture those shape difference between third upper premolars and fourth upper premolars which are not already explained by the first principal component. Within each species there is excellent separation between third upper premolars and fourth upper premolars with the fourth upper premolars having higher scores on the second principal component of shape, and slightly higher scores (towards the *Paranthropus* end of the scale) on the first principal component. *H. naledi* has higher scores on the second principal component of shape than other species. The third upper premolars of *H. naledi* seem similar in shape to the fourth upper premolars of other hominin species and the fourth upper premolars of *H. naledi* have more extreme scores on the second principal component than any other species.

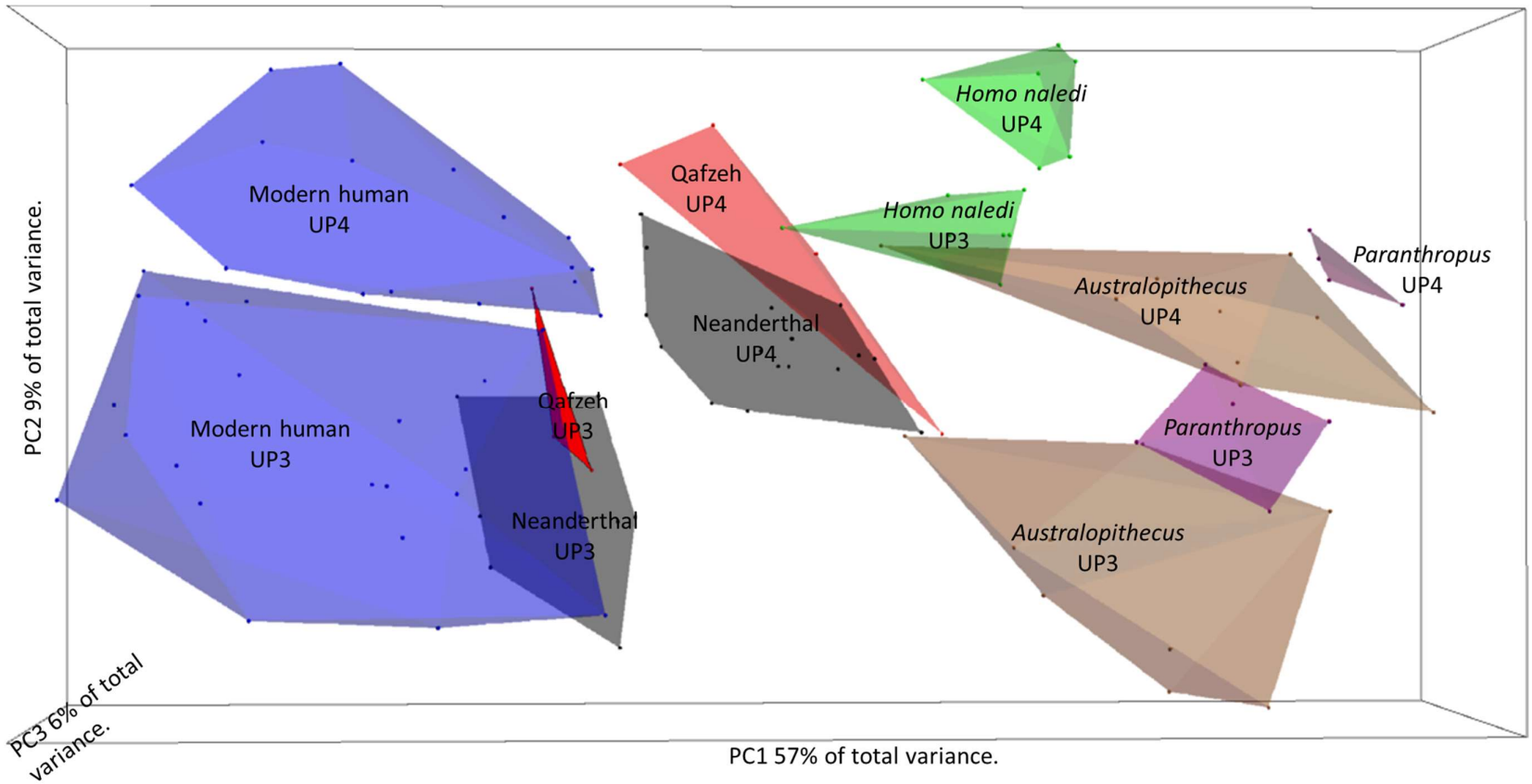

Figure 5.3.1 Plot of shape principal component scores. Groups are indicated by convex hulls. Blue = Modern Humans, Red = Qafzeh hominins, Black = Neanderthals, Green = *H. naledi*, Brown = *A. africanus*, Purple = *P. robustus*.

5.3.1 Multivariate Analysis of Variance (MANOVA) of the Shape Principal Components

Tests for the assumptions of multivariate Normality (Dornik-Hansen) and of equal variance-covariance structures within each study group (Scatter plots, Box's M test) showed no evidence to doubt these assumptions for the first four principal components of shape[6]. In the two-way factorial MANOVA with an interaction term using the first five principal components of shape, the test for interaction (Pillai test p-value 0.103, Wilk's test p-value 0.101) does not provide any evidence to reject the null hypothesis of no interaction between the factor levels for tooth type and species. The interaction term was therefore dropped from the model and a main effects model was used instead. In the main-effects MANOVA both factors – 'species' and 'tooth type' show strong evidence (p-value < 0.001 on all Wilks and Pillai tests) to reject the null hypothesis that the mean shape within each group is equal. This indicates that the mean EDJ shape does differ between species and that, within each species, the mean shape for third upper premolars is different to the mean shape of fourth upper premolars. Given that there is no interaction term, this statistical model suggests that the difference in shape between third upper premolars and fourth upper premolars is similar for all species. The predicted group mean shapes and observed group mean shapes for the first two principal components are shown in Figure 5.3.2. The model predicts that, within each species, the fourth upper premolar has a higher score than the third upper premolar on the second principal component and a slightly higher score than the third upper premolar on the first principal component. The residuals on this plot are reasonably small.

[6] There was some doubt about the homogeneity of variance-covariance structure when the fifth principal component of shape was included. Although not reported here, I performed MANOVA for the first four principal components in addition to the test for the first five principal components which is reported here as originally planned in the experimental protocol. The results were, in all important respects, the same.

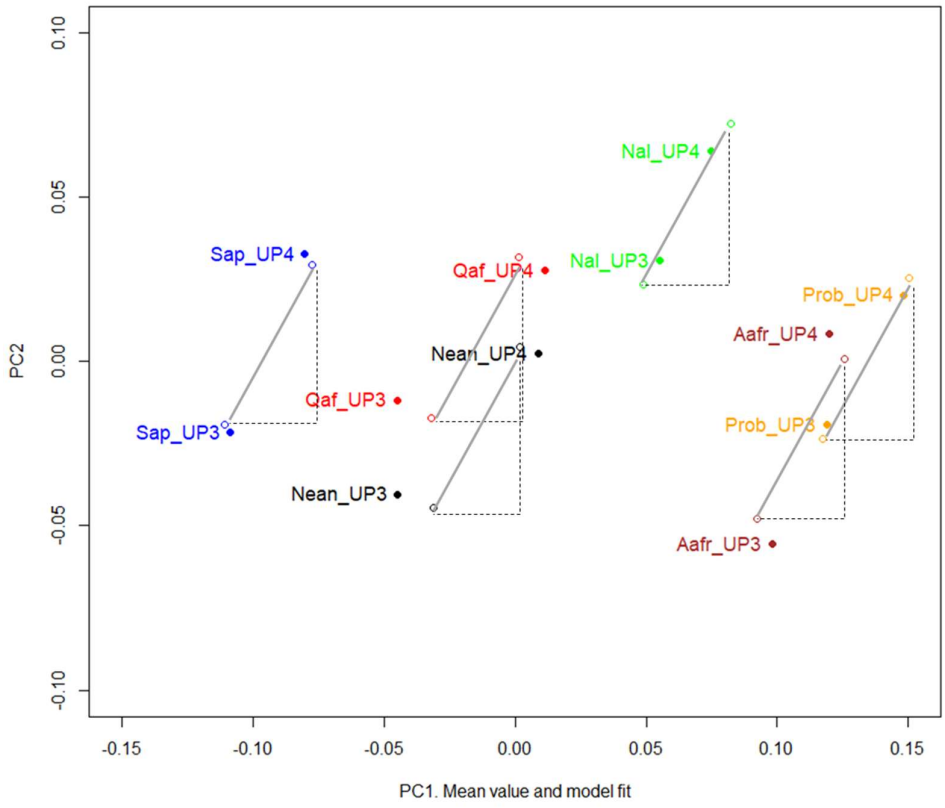

Figure 5.3.2 Mean shape values predicted by the MANOVA model (Hollow circles) and the observed mean shape values (filled circles). (Orange = *P. robustus,* Brown = *A. africanus*, Black = *H. neanderthalensis*, Red = *H. sapiens* (Qafzeh), Green = *H. naledi*, Blue = *H. sapiens* (Modern Human)).

5.3.2 Linear discriminant analysis (LDA)

A linear discriminant analysis was performed using the first 16 principal components as the outcome variables and twelve groups (two tooth types by six species) as the grouping variable. Eleven linear discriminant functions were calculated because the maximum number of discriminant functions, *r*, is the minimum of the number of outcome variables, *p*, and one less than the number of groups, *g*:

$$r = \min(p, g - 1)$$

The percentage of 'difference explained' between the groups (the ratio of the between group variance to the within group variance) was 58% for the first discriminant function, 16% (cumulative 74%) for the second discriminant function and 11% (cumulative 85%) for the third discriminant function.

Figure 5.3.3 shows the scatter plot, with convex hulls, of the linear discriminant function scores of the first linear discriminant function against the second linear discriminant functions. The first and second discriminant functions show good separation of tooth type within species. The species are also well separated from each other, although there is some overlap between the Qafzeh hominin and Neanderthal fourth upper premolars and between modern human, Neanderthal and Qafzeh hominin third upper premolars. *P. robustus* third upper premolars overlap slightly with *A. africanus* fourth upper premolars. Table 5.3.1 shows the allocated group under the linear discriminant function model with equal priors. Table 5.3.2 shows the same model with "leave one out" cross validation.

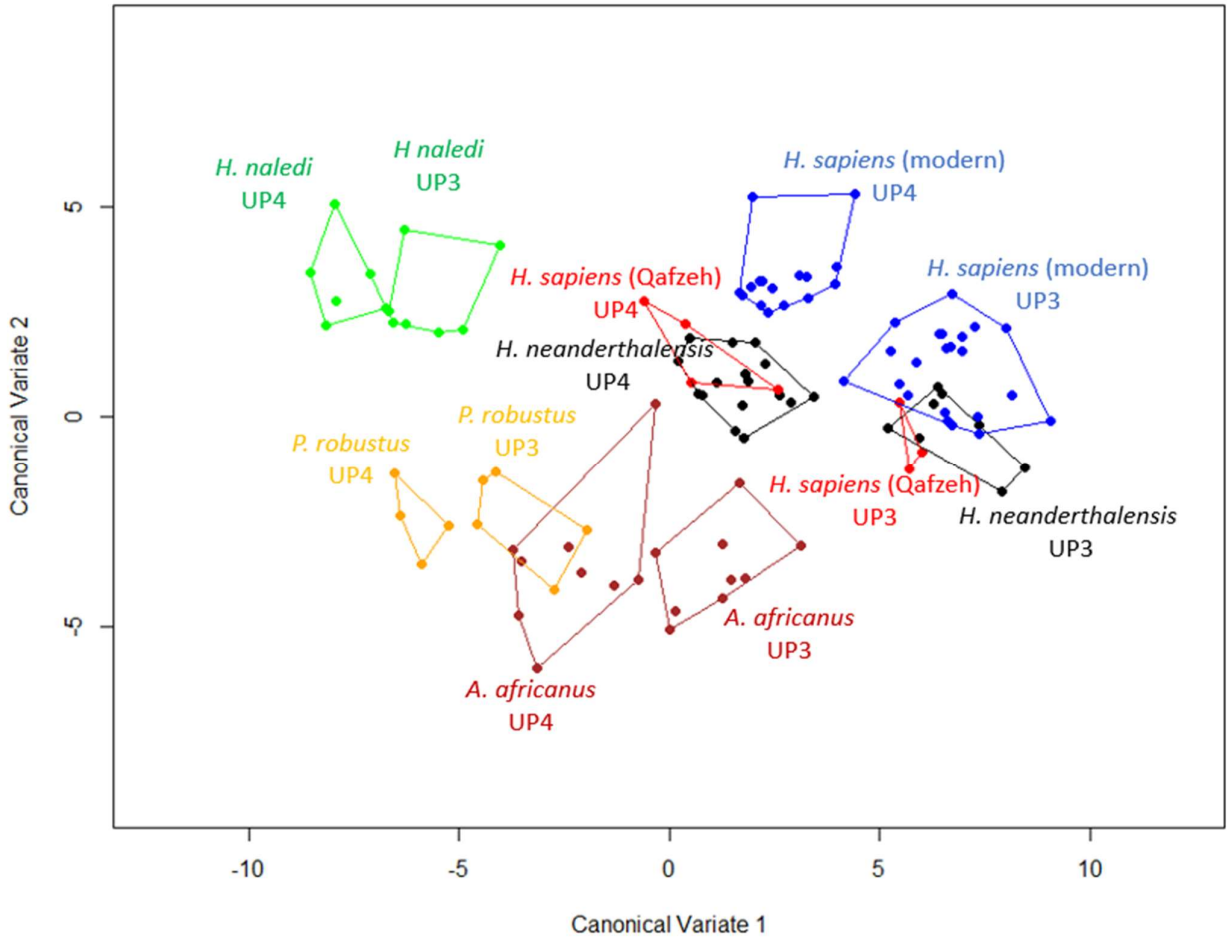

Figure 5.3.3 Scatterplot of scores on the first and second linear discriminant functions for shape.

Table 5.3.1 Predicted classification under the linear discriminant model for EDJ shape.

Row Labels	Aafr_UP3	Aafr_UP4	Nal_UP3	Nal_UP4	Nean_UP3	Nean_UP4	Prob_UP3	Prob_UP4	Qaf_UP3	Qaf_UP4	Sap_UP3	Sap_UP4	Grand Total
Aafr_UP3	9												9
Aafr_UP4		8								1			9
Nal_UP3			7										7
Nal_UP4				6									6
Nean_UP3					8								8
Nean_UP4						16							16
Prob_UP3							5						5
Prob_UP4								4					4
Qaf_UP3									3				3
Qaf_UP4										4			4
Sap_UP3									1		21		22
Sap_UP4												16	16
Grand Total	9	8	7	6	8	16	5	4	4	5	21	16	109

Table 5.3.2 Predicted classification under the 'leave one out' cross validated linear discriminant model for EDJ shape.

	Aafr_UP3	Aafr_UP4	Nal_UP3	Nal_UP4	Nean_UP3	Nean_UP4	Prob_UP3	Prob_UP4	Qaf_UP3	Qaf_UP4	Sap_UP3	Sap_UP4	Grand Total
Aafr_UP3	8	1											9
Aafr_UP4		7					1			1			9
Nal_UP3			7										7
Nal_UP4				6									6
Nean_UP3					7				1				8
Nean_UP4						14				1		1	16
Prob_UP3			1				4						5
Prob_UP4								4					4
Qaf_UP3					1				0		1	1	3
Qaf_UP4						3				1			4
Sap_UP3					1				2		19		22
Sap_UP4										1		15	16
Grand Total	8	8	8	6	9	17	5	4	3	4	20	17	109

The overall misclassification rate under the linear discriminant function model fitted to this data set is 2/109 = 1.8 %. The overall misclassification rate in the 'leave one out' cross validated model is 17/109 = 16% but 12 (11%) of these involve the Qafzeh hominins, where there is quite a large within species variation in morphology and some overlap with both Neanderthals and with modern humans. Six of the seven Qafzeh teeth were misclassified (four as Neanderthal, two as modern human). One australopith, two Neanderthal and three modern human teeth were misclassified as Qafzeh hominins.

Apart from this, one Neanderthal fourth upper premolar was misclassified as a modern human fourth upper premolar and one modern human third upper premolar was misclassified as a Neanderthal third upper premolar. One *A. africanus* fourth upper premolar was misclassified as a *P. robustus* third upper premolar and one *A. africanus* third upper premolar was misclassified as a fourth upper premolar. Finally, one *P. robustus* third upper premolar was misclassified as a *H. naledi* third upper premolar.

In summary, the 'leave one out' cross validated linear discriminant functions discriminate very well between *A. africanus*, *P. robustus*, *H. naledi* and the other *Homo* species taken as a whole. There is some misclassification between modern humans, Neanderthals and the Qafzeh hominins. The Qafzeh hominins are particularly vulnerable to misclassification under the leave one out cross validation procedure because the sample size is small, there is quite a large within species variation in tooth morphology and the sample overlaps with both Neanderthals and modern humans.

Table 5.3.3 lists the teeth which are misclassified under the "leave one out" cross validation analysis of EDJ shape.

Tooth	Class	CV Predicted Class
KRP_D42_URP4	Nean_UP4	Sap_UP4
Le_Moustier_1_ULP3	Nean_UP3	Qaf_UP3
MPI_T08_062	Sap_UP4	Qaf_UP4
MPI_T08_074	Sap_UP3	Qaf_UP3
MPI_T08_092	Sap_UP3	Qaf_UP3
MPI_T09_181	Sap_UP3	Nean_UP3
Qafzeh_10_ULP3	Qaf_UP3	Sap_UP3
Qafzeh_10_ULP4	Qaf_UP4	Nean_UP4
Qafzeh_11_URP4	Qaf_UP4	Nean_UP4
Qafzeh_15_URP3	Qaf_UP3	Nean_UP3
Qafzeh_9_ULP3	Qaf_UP3	Sap_UP4
Qafzeh_9_ULP4	Qaf_UP4	Nean_UP4
SD_50_URP4	Nean_UP4	Qaf_UP4
SKX_162_URP3	Prob_UP3	Nal_UP3
STS_52a_URP3	Aafr_UP3	Aafr_UP4
STS_61_URP4	Aafr_UP4	Qaf_UP4
STW_192A_ULP3	Aafr_UP4	Prob_UP3

5.3.3 Extended analysis: STS 61 and early to mid-Pleistocene Homo species.

On inspection of the principal component plot and of the linear discriminant function plots for shape and form of the EDJs of the teeth in this sample, it was noticed that the upper premolars of specimen STS 61 seem to form an outlier for the sample of *A. africanus* teeth, to which this specimen has been assigned (the premolars are *in situ* in a fragment of maxilla). The fourth upper premolar lies much closer to *H. neanderthalensis* and to archaic *H. sapiens* than it does to other australopiths (Fig. 5.3.4). In the 'leave one out' cross-validated discriminant analysis of both shape and of form, the third upper premolar is classified as *A. africanus* but the fourth premolar is classified as a *H. neanderthalensis* fourth upper premolar.

It therefore seems possible that this specimen has been mis-classified as *A. africanus* and may, in fact, be an early species of *Homo.*

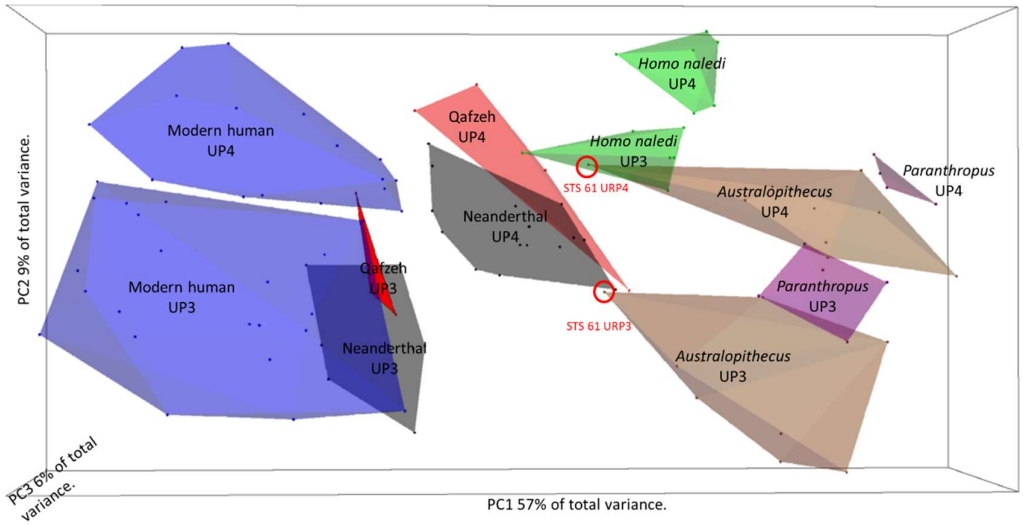

Figure 5.3.4 Principal component scores for shape. The position of STS 61 in the principal component analysis (STS 61 is circled in red)

Some isolated specimens of early Pleistocene *Homo* (*Homo erectus* KNM-ER 3733) and mid-Pleistocene *Homo* (*Homo heidelbergensis* from Steinheim and *Homo rhodesiensis* from Thomas Quarry 3 in Morocco) were added to the analysis and STS 61 was removed from the australopith group and included as an isolated specimen. The resulting principal component plot (Fig. 5.3.5) shows, as was expected, that these species of *Homo* lie between *Paranthropus* and *Australopithecus* on one side and more recent species of *Homo* on the other side. The *H. erectus* specimen lies closer to the australopiths.

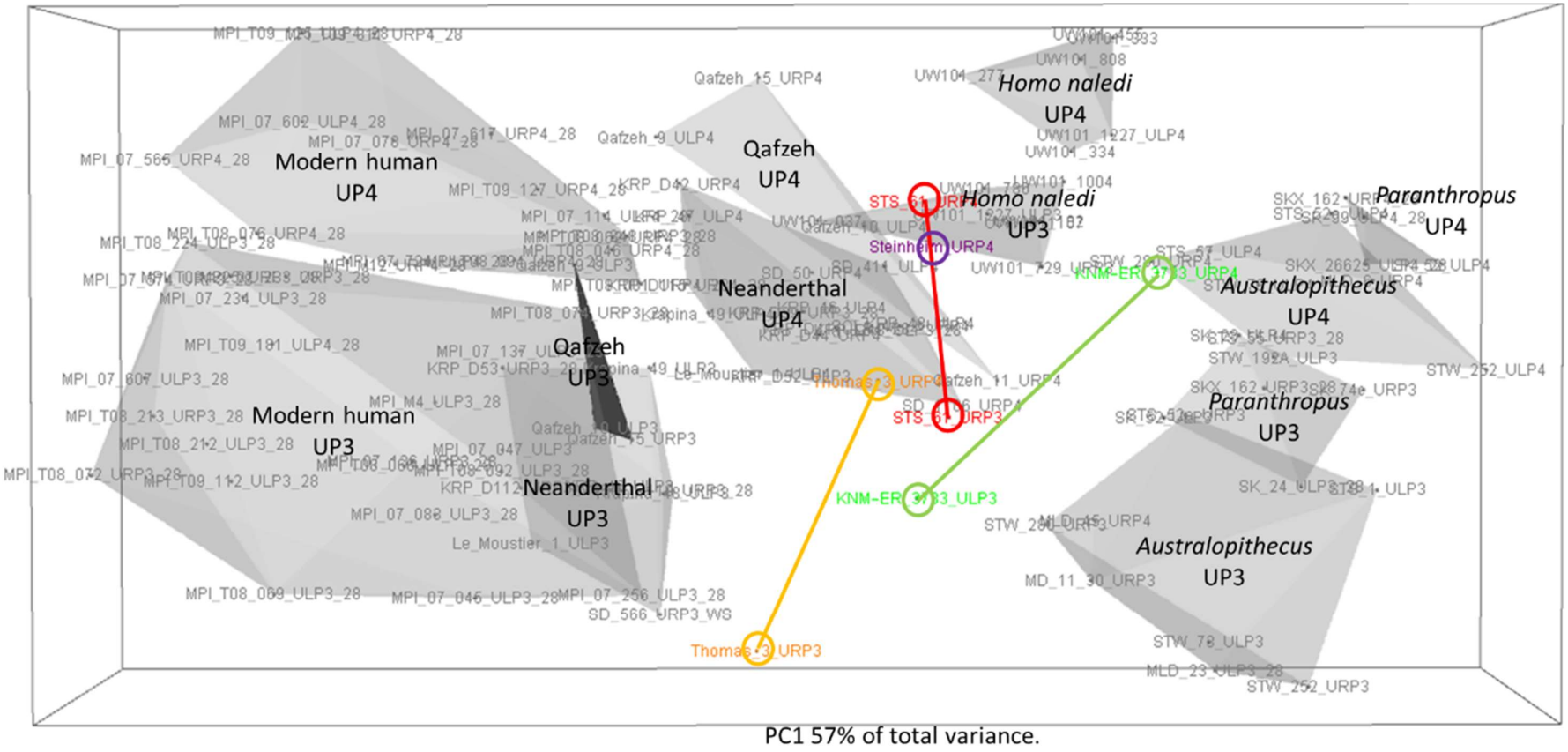

Figure 5.3.5 Principal component scores for shape. Position of early and mid-Pleistocene species of *Homo* among the study sample. Green = *H. erectus*, Orange = *H. rhodesiensis*, Purple = *H. heidelbergensis*, Red = STS 61. Note that when STS 61 is removed from *Australopithecus*, its convex hull is much smaller than when STS 61 is included.

In this plot, STS 61 occupies a similar position to other early to mid-Pleistocene species of *Homo* and, in particular, the fourth upper premolar of STS 61 lies close to the fourth upper premolar of *H. heidelbergensis* from Steinheim (Fig. 5.3.6).

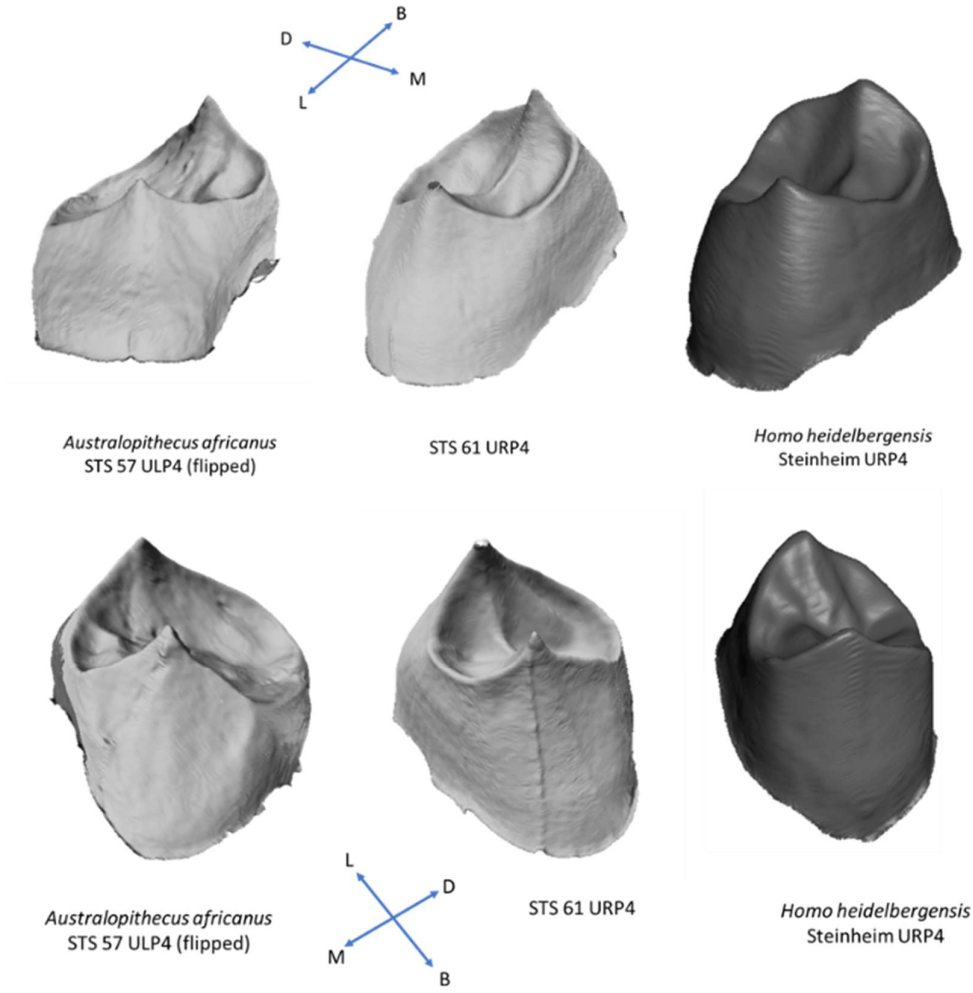

Figure 5.3.6 Upper fourth premolars from STS 61, STS 57 and Steinheim 1.

5.4 Influence of size on interspecific comparisons of EDJ morphology

5.4.1 Regression of size and shape

Firstly, the relationships between shape and size are explored by tabulating the correlation and covariance matrices for the size variable and the principal components of the Procrustes tangent shape space (Table 5.4.1). As expected, the variance of the size variable is very much larger than the variance of any of the shape principal components. This is because the shape variables are combinations of small deviations of landmarks away from the mean shape in Procrustes space, whereas the size variable includes the dimensions of the whole shape. Principal components are all orthogonal to each other so the correlations and covariances between them are all zero (the off-diagonal entries of the tables for the principal components). There is a moderately strong correlation (0.661) between size and the first principal component of shape space and a weak correlation (0.216) between size and the second principal component.

Table 5.4.1 Correlation and covariance between size and the first five principal components of shape.

Correlation

	Size	PC1	PC2	PC3	PC4	PC5
Size	1.0000	0.6611	0.2155	0.0836	-0.1825	-0.0575
PC1	0.6611	1.0000	0.0000	0.0000	0.0000	0.0000
PC2	0.2155	0.0000	1.0000	0.0000	0.0000	0.0000
PC3	0.0836	0.0000	0.0000	1.0000	0.0000	0.0000
PC4	-0.1825	0.0000	0.0000	0.0000	1.0000	0.0000
PC5	-0.0575	0.0000	0.0000	0.0000	0.0000	1.0000

Covariance

	Size	PC1	PC2	PC3	PC4	PC5
Size	19.1246	0.2652	0.0350	0.0109	-0.0229	-0.0055
PC1	0.2652	0.0084	0.0000	0.0000	0.0000	0.0000
PC2	0.0350	0.0000	0.0014	0.0000	0.0000	0.0000
PC3	0.0109	0.0000	0.0000	0.0009	0.0000	0.0000
PC4	-0.0229	0.0000	0.0000	0.0000	0.0008	0.0000
PC5	-0.0055	0.0000	0.0000	0.0000	0.0000	0.0005

Following the example of Dryden and Mardia (2016, Example 9.8, p.212), instead of conducting a multivariate regression with the shape principal components as outcome variables and centroid size as the explanatory variable, a multiple regression was carried out with the principal components as the explanatory variables and centroid size as the dependent variable. The first principal component of shape was a strong predictor of size ($p < 0.0001$). The second principal component was also statistically significant ($p < 0.002$), as was the fourth principal component ($p = 0.008$). When size was regressed against single variables, the first principal component of shape was still highly significant ($p < 0.0001$) but the second principal component was less so ($p = 0.024$) and the fourth principal component was not significant at the 0.05 significance level PC4, ($p = 0.058$).

Having identified from this analysis that centroid size is covariant with the first and second principal components of shape, these relationships are explored further by univariate regressions of these principal components against size, switching centroid size from the dependant variable in the regression to the explanatory variable because, biologically, it makes more sense that size would determine shape than that shape would determine size.

5.4.2 The first principal component of shape regressed on centroid size

When the first principal component of shape is regressed on centroid size, there is a clear linear relationship ($p < 0.0001$) between the two variables indicating that there is allometry in hominin upper premolar teeth (Fig. 5.4.1). The extremes of the first principal component of tooth shape are *Paranthropus*, which have large teeth and modern humans, with small teeth. Essentially, *Paranthropus* EDJs are relatively lower and broader in comparison to modern humans, where the EDJ tends to be taller and narrower. All hominin species except for *H. naledi* seem to lie close to the regression line but, as a species, *H. naledi* appears to be an outlier.

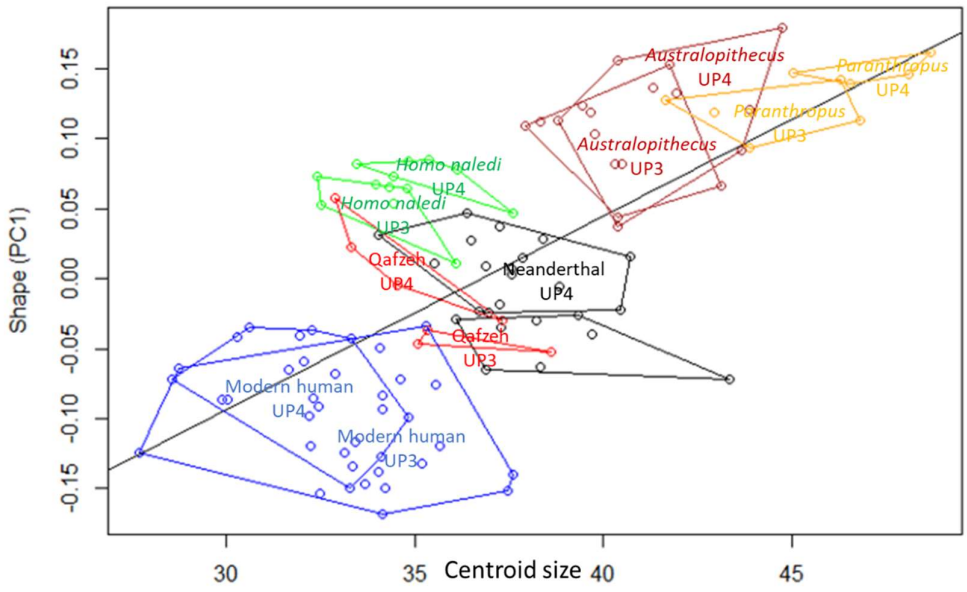

Figure 5.4.1 Linear regression of the first principal component of tooth shape against tooth centroid size. (Orange = *P. robustus,* Brown = *A. africanus*, Black = *H. neanderthalensis*, Red = *H. sapiens* (Qafzeh), Green = *H. naledi*, Blue = *H. sapiens* (Modern Human)).

To test the relationship of *H. naledi* to the other species an analysis of covariance was carried out with a dummy variable for *H. naledi*. There was no evidence of an interaction between the factor 'Naledi' and centroid size (p for the interaction term = 0.098) so a main effects model was used. The linear relationship between the first principal component of shape and centroid size was preserved (Regression coefficient 0.015, $p < 0.0001$, $R^2 = 0.575$) and there was strong evidence that, when this linear relationship is taken into account, *H. naledi* differs from all of the other species (difference in PC1 score = 0.109, $p < 0.0001$). In short, there is strong evidence that all the other species lie close to the main regression line but *H. naledi* does not. Figure 5.4.2 shows that the tooth size for *H. naledi* lies close to the tooth size for other species of *Homo* but that the first principal component of tooth shape in *H. naledi* lies closer to that of the *Australopithecus*.

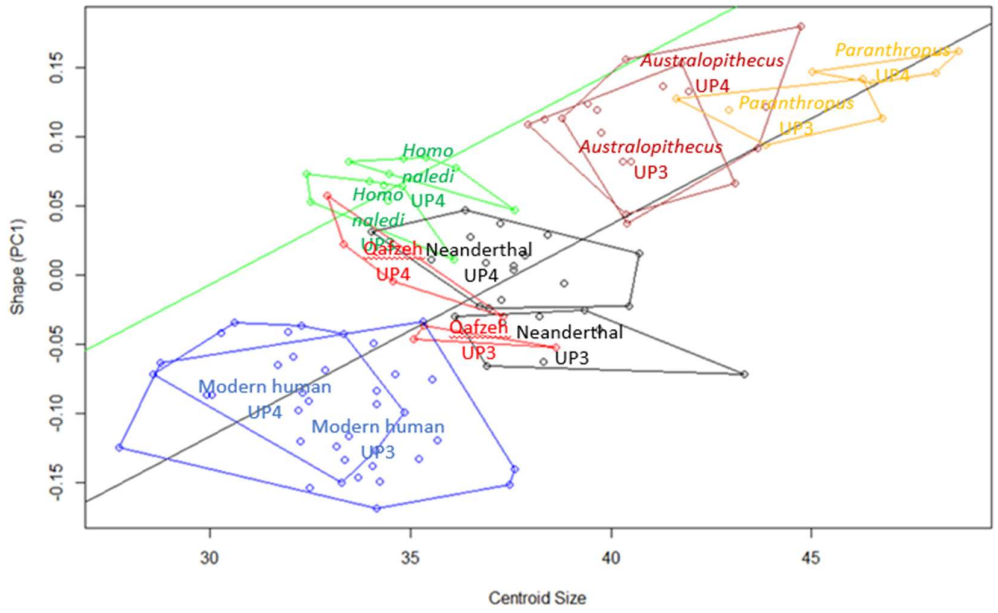

Figure 5.4.2 Analysis of covariance (ANCOVA) of the first principal component of tooth shape against tooth centroid size with Naledi as a factor.

5.4.3 The second principal component of shape regressed on centroid size.

When the second principal component of shape is regressed on centroid size, there is some evidence of a linear relationship ($p = 0.024$). *H. naledi* may have a disproportionate influence on the slope of the regression line, since it has small teeth but the EDJ shape resembles that of species with much larger teeth. Statistically, this is known as having a high 'leverage'. In order to test the influence of *H. naledi*, a dummy variable is included in the regression model (analysis of covariance with *H. naledi* as a factor). The factor for *H. naledi* is highly significant (difference in PC2 score = - 0.05, $p < 0.0001$) but centroid size is no longer a significant predictor of the second principal component of shape (Regression coefficient = 0.0012, $p = 0.113$, $R^2 = 0.214$) showing that *H. naledi* does have a high influence on the regression model.

In summary, when the influence of *H. naledi* is accounted for, there does not seem to be a significant relationship between tooth size and the second principal component of tooth shape. There is strong evidence that the second principal

component of shape in *H. naledi* differs from that of other hominin species. The second principal component of shape seems to capture the essence of what distinguishes hominin third upper premolars from hominin fourth upper premolars. *H. naledi* upper premolars of both types lie on the extreme 'fourth upper premolar' end of this principal component.

5.4.4 Multivariate analysis in form space.

The natural logarithm of centroid size is added as a variable to the shape data in tangent space (the displacements of each landmark from the Procrustes mean shape in three-dimensional Euclidean space). Principal components analysis of this enlarged data set was carried out. The first principal component accounts for 65% of the total variance, the second accounts for 13% so together they account for nearly 80% of the total variance. The first 11 principal components account for 95% of the total variance. However, for consistency with the previous analysis of Shape space, in which 16 principal components were retained, I retained the first 16 principal components for the linear discriminant analysis in form space, accounting for 97% of total variance.

Plots of the principal component scores for the first and second principal components of shape are shown in Figure 5.4.3. The first principal component is dominated by the centroid size with larger teeth at the left end of the plot and smaller teeth to the right. The correlation of centroid size with the first principal component is 0.96 and with the second principal component is 0.28. The correlations between centroid size and the other principal components are less than 0.05. The second principal component seems to contrast the shape of *H. naledi* teeth with the shape of all other hominins but especially with Neanderthal teeth.

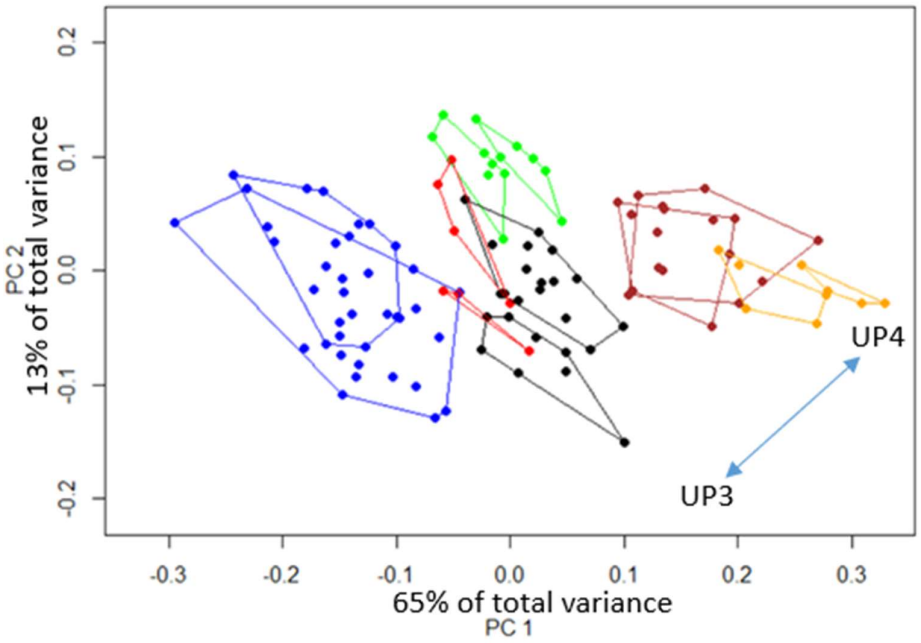

Figure 5.4.3 Plot of scores on the first two principal components in form space. (Orange = *P. robustus,* Brown = *A. africanus*, Black = *H. neanderthalensis*, Red = *H. sapiens* (Qafzeh), Green = *H. naledi*, Blue = *H. sapiens* (Modern Human)).

A linear discriminant analysis was carried out on the reduced data consisting of the first 16 principal components. A plot of the first two discriminant function scores (Figure 5.4.4) shows excellent separation between the groups of tooth type by species. There is a linear trend for the hominin species other than *H. naledi* from *P. robustus* at the upper left of the plot to Modern Humans at the lower right of the plot. *H. naledi* is isolated in the lower left corner of the plot. Table 5.4.2 shows the

allocated group under the linear discriminant analysis model with equal priors. Table 5.4.3 shows the same model with “leave one out” cross validation.

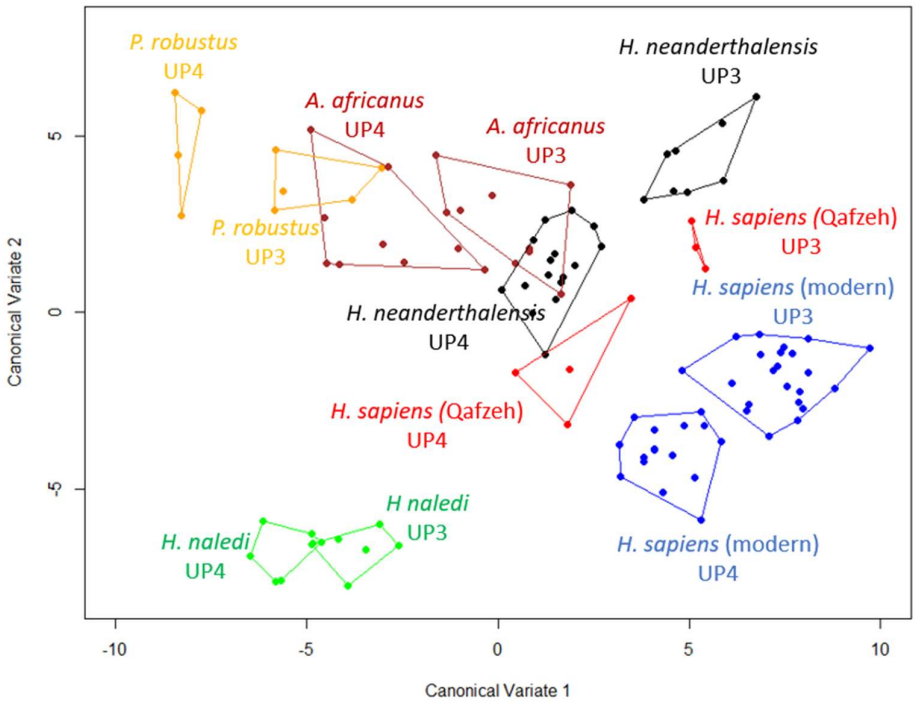

Figure 5.4.4 Plot of scores on the first two discriminant functions/canonical variates of form.

Table 5.4.2 Tooth classification under the linear discriminant analysis of form (including centroid size).

True group	Classified Aafr UP3	Aafr UP4	Nal UP3	Nal UP4	Nean UP3	Nean UP4	Prob UP3	Prob UP4	Qaf UP3	Qaf UP4	Sap UP3	Sap UP4	Total
Aafr UP3	9	0	0	0	0	0	0	0	0	0	0	0	9
Aafr UP4	0	8	0	0	0	1	0	0	0	0	0	0	9
Nal UP3	0	0	7	0	0	0	0	0	0	0	0	0	7
Nal UP4	0	0	0	6	0	0	0	0	0	0	0	0	6
Nean UP3	0	0	0	0	8	0	0	0	0	0	0	0	8
Nean UP4	0	0	0	0	0	15	0	0	0	1	0	0	16
Prob UP3	0	0	0	0	0	0	5	0	0	0	0	0	5
Prob UP4	0	0	0	0	0	0	0	4	0	0	0	0	4
Qaf UP3	0	0	0	0	0	0	0	0	3	0	0	0	3
Qaf UP4	0	0	0	0	0	0	0	0	0	4	0	0	4
Sap UP3	0	0	0	0	0	0	0	0	0	0	22	0	22
Sap UP4	0	0	0	0	0	0	0	0	0	0	0	16	16
Total	9	8	7	6	8	16	5	4	3	5	22	16	109

Table 5.4.3 Tooth classification under the 'leave one out' cross-validated analysis of form (including centroid size).

	LOO Classified												
True group	Aafr UP3	Aafr UP4	Nal UP3	Nal UP4	Nean UP3	Nean UP4	Prob UP3	Prob UP4	Qaf UP3	Qaf UP4	Sap UP3	Sap UP4	Total
Aafr UP3	8	1	0	0	0	0	0	0	0	0	0	0	9
Aafr UP4	1	7	0	0	0	1	0	0	0	0	0	0	9
Nal UP3	0	0	7	0	0	0	0	0	0	0	0	0	7
Nal UP4	0	0	2	4	0	0	0	0	0	0	0	0	6
Nean UP3	0	0	0	0	8	0	0	0	0	0	0	0	8
Nean UP4	0	0	0	0	0	15	0	0	0	1	0	0	16
Prob UP3	0	1	0	0	0	0	4	0	0	0	0	0	5
Prob UP4	0	0	0	0	0	0	0	4	0	0	0	0	4
Qaf UP3	0	0	0	0	1	1	0	0	1	0	0	0	3
Qaf UP4	0	0	0	0	0	2	0	0	0	2	0	0	4
Sap UP3	0	0	0	0	0	0	0	0	1	0	20	1	22
Sap UP4	0	0	0	0	0	0	0	0	0	0	0	16	16
Total	9	9	9	4	9	19	4	4	2	3	20	17	109

The overall misclassification rate under the linear discriminant function model fitted to this data set is 2/109 = 1.8 %. The overall misclassification rate in the cross validated model is 13/109 = 12% but 6 (6 %) of these involve the Qafzeh hominins, where there is quite a large within species variation in morphology and some overlap with both Neanderthals and with modern humans. In the cross-validated analysis, four of the Qafzeh hominin teeth were misclassified as Neanderthal teeth and one modern human tooth and one Neanderthal tooth were misclassified as teeth from Qafzeh hominins. Apart from this, one *P. robustus* third upper premolar was misclassified as an *A. africanus* fourth upper premolar and one *A. africanus* fourth upper premolar was misclassified as a Neanderthal fourth upper premolar. The other misclassifications are of tooth types within species. Two *H. naledi* fourth upper premolars were misclassified as third upper premolars. One modern human third upper premolar was misclassified as a fourth upper premolar and for *A. africanus* one of each tooth type was misclassified as the other.

In summary, as with the *shape* linear discriminant analysis, the *form* linear discriminant analysis assigns teeth to the correct classification in the great majority of cases. In the 'leave one out' cross-validation, half of the misclassifications involve the Qafzeh hominins, probably due to the small sample, large variation of shape within the species and some overlap with modern humans and with Neanderthals. Apart from this there is little misclassification between species and only slight misclassification between tooth types within species. In terms of misclassification rates, the cross-validated *form* analysis (12% misclassifications, 6% involving the Qafzeh hominins) performs slightly better than the *shape* analysis (16% misclassifications, 11% involving the Qafzeh hominins). Table 5.4.4 lists the teeth which are misclassified under the linear discriminant analysis of form and by the "leave one out" cross validation analysis.

Table 5.4.4 List of teeth misclassified by the linear discriminant analysis (LDA) of form and by the 'leave one out' cross-validated analysis.

Tooth	Original	LDA	Leave one out cross validation.
MPI_07_137	Sap_UP3		Sap_UP4
MPI_T08_074	Sap_UP3		Qaf_UP3
Qafzeh_11_URP4	Qaf_UP4		Nean_UP4
Qafzeh_15_URP3	Qaf_UP3		Nean_UP3
Qafzeh_9_ULP3	Qaf_UP3		Nean_UP4
Qafzeh_9_ULP4	Qaf_UP4		Nean_UP4
SCLA_4A_2_URP4	Nean_UP4	Qaf_UP4	Qaf_UP4
SK_24	Prob_UP3		Aafr_UP4
STS_52a_URP3	Aafr_UP3		Aafr_UP4
STS_57	Aafr_UP4		Aafr_UP3
STS_61	Aafr_UP4	Nean_UP4	Nean_UP4
UW101_1277	Nal_UP4		Nal_UP3
UW101_334	Nal_UP4		Nal_UP3

5.5 Differences between the EDJ of third upper premolars and the EDJ of fourth upper premolars which are common to all hominin species

Having discussed the morphological differences in the EDJs between third and fourth upper premolars in each species individually in Section 5.1, some differences are common to all hominin species and these are summarised here. (The figures for this section each require a full page to be read clearly and are placed at the end of the section). Note that this section refers to the wire-frame models of mean EDJ shapes and does not refer to the frequency of expression of certain features, which is examined later in the section on qualitative morphometrics (Section 5.7). Some of the points made here are illustrated by using the EDJ surfaces of individual teeth because some features can be more easily seen on surface models than in the wire-frame model.

1) The height and position of the buccal dentine horn.

In all the species in this study the third upper premolar has a buccal dentine horn which is taller and more distally placed than the fourth upper premolar. This is the most consistent and most obvious difference between the EDJs of third and fourth upper premolars (Figs. 5.5.1 and 5.5.2). In most hominin species the buccal dentine horn of the third upper premolar is slightly distal to the mid-point of the buccal EDJ ridge.

2) Apical extension of the buccal EDJ in third upper premolars.

In the third upper premolars of all species in this study there is apical extension of the buccal surface of the EDJ, seen as an apical convexity of the buccal CEJ (Fig. 5.5.1). This may also be present, but to a smaller extent, in the fourth upper premolar. The combined effect of (1) and (2) is for the buccal surface of the EDJ to be longer in hominin third upper premolars than in fourth upper premolars. In the mesial or distal view, the third upper premolar has a more pronounced wedge-shaped outline than the fourth upper premolar.

3) Occlusally directed concavity in the CEJ, most prominent in third upper premolars.

When viewed mesially, and to a slightly lesser extent in the distal view, there is an occlusally directed concavity in the CEJ (Fig. 5.5.1). The buccal apical extension (2) does contribute partly to this but this concavity is also a feature in its own right. In *Homo* species other than *H. naledi* the concavity is centrally placed in the mesial or distal CEJ ridge. In other species it occupies the buccal part (about one third) of the mesial CEJ and, to a slightly lesser extent, the buccal part of the of the distal CEJ. Whatever its position, this concavity is more pronounced in third upper premolars than in fourth upper premolars.

4) Groove or depression in the mesial surface of the EDJ of the third upper premolar.

In all of the species in this study there is a groove or depression in the mesial surface of the EDJ in the third upper premolar (This is present in *P. robustus* but its expression is minimal). This is most clearly seen as a concavity in the mesial CEJ in the occlusal view (Fig. 5.5.3).

5) The outline of the EDJ ridge in occlusal view is more triangular in third upper premolars and more quadrilateral in fourth upper premolars.

In species of *Homo* other than *H. naledi*, the EDJ ridge in occlusal view has a more triangular outline in third upper premolars, whilst in fourth upper premolars it has a more quadrilateral outline (Fig. 5.5.3). In the australopiths and in *H. naledi*, the EDJ ridge of the third upper premolar tends to be quadrilateral in outline but the fourth upper premolar has a pronounced disto-lingual expansion. In short, the fourth upper premolar has a greater curvature than the third upper premolar, which tends to have a 'flatter' outline in this part of the EDJ ridge.

6) A distal accessory buccal dentine horn (or shoulder) in fourth upper premolars.

In the fourth upper premolars of all species in this study there is a distal accessory buccal dentine horn (although in *H. neanderthalensis* this is somewhat blunted, to form a 'shoulder' rather than a distinct horn). This is a prominent structure which is separated from the main buccal dentine horn by a small depression in the buccal EDJ marginal ridge (Fig. 5.5.4). The third upper premolars of *H. naledi* and of *P. robustus* do also have a distal accessory buccal dentine horn but the accessory dentine horn in the fourth upper premolar is significantly larger, more prominent and more widely separated from the main buccal dentine horn than in the third upper premolar. Third upper premolars in other species do not characteristically have distinct distal accessory buccal dentine horns. All hominin species may have small, mesial or distal accessory dentine horns on the buccal EDJ ridge which do not significantly influence the overall shape of the ridge.

In *P. robustus*, uniquely in this sample, there is also a distal accessory *lingual* dentine horn in the fourth upper premolar, which may represent incipient molarisation in this tooth (being in the position of a molar hypocone).

Some differences between third and fourth upper premolars are common to some but not to all species:

7) In all taxa except Paranthropus the third upper premolar, in occlusal view, has a mesial bulge in the buccal part of the mesial EDJ ridge.

In this study, all species except *P. robustus* show a mesial bulge in the buccal third of the mesial EDJ ridge in the third upper premolar (Figs.5.5.2 and 5.5.3). This is not seen in the fourth upper premolar. This feature is most pronounced in species of *Homo*. In *Australopithecus*, this feature is too subtle to be seen in most individual teeth but can be seen when the wireframe models for mean shape are compared.

8) A notch in the mesial EDJ ridge.

In species of *Homo* other than *H. naledi* there is a distinctive notch or groove in the mesial EDJ ridge of the third upper premolar, roughly where the buccal two thirds of the ridge meet the lingual third (Fig. 5.5.4). This is not present in all teeth from each species but is present frequently enough to appear as a consistent feature in the mean shape of the EDJ. This feature does not appear in fourth upper premolars. In *H. naledi* there is a depression in this part of the EDJ ridge of the third upper premolar but not a distinct notch.

Features (7) and (8) often occur together, giving the mesial EDJ ridge of third upper premolars a distinctive morphology in species of *Homo*.

Summary

Overall, the morphology of the EDJ in third upper hominin premolars tends towards an emphasis on the buccal cusp, with a taller, more centrally placed buccal dentine horn and buccal apical extension. The disto-lingual part of the tooth in the occlusal view tends to be flatter in outline, leading to a more triangular outline overall and to a smaller lingual part of the tooth. There are also features of the third upper premolar, especially in species of *Homo* which may relate to its mesial contact with the canine tooth, including a depression in the mesial CEJ ridge, a notch in the mesial EDJ ridge and a mesial bulge in the buccal part of the EDJ ridge.

In the EDJ of fourth upper premolars, the cusps are more equal in height and there is more emphasis on the talon, with a greater relative distance between the buccal dentine horn and the distal margin of the tooth, the development of a distinct distal buccal accessory dentine horn and expansion of the occlusal surface of the EDJ in a disto-lingual direction, leading to a more quadrilateral outline in occlusal view. In relation to the tooth row as a whole, there is, superimposed on the basic bicuspid morphology of upper premolars, a subtle tendency for hominin third upper premolars to be slightly more canine like in morphology and for fourth upper premolars to be slightly more like upper molars in morphology[7].

[7] As would be predicted by morphogenetic field theory (Townsend *et al.*, 2009)

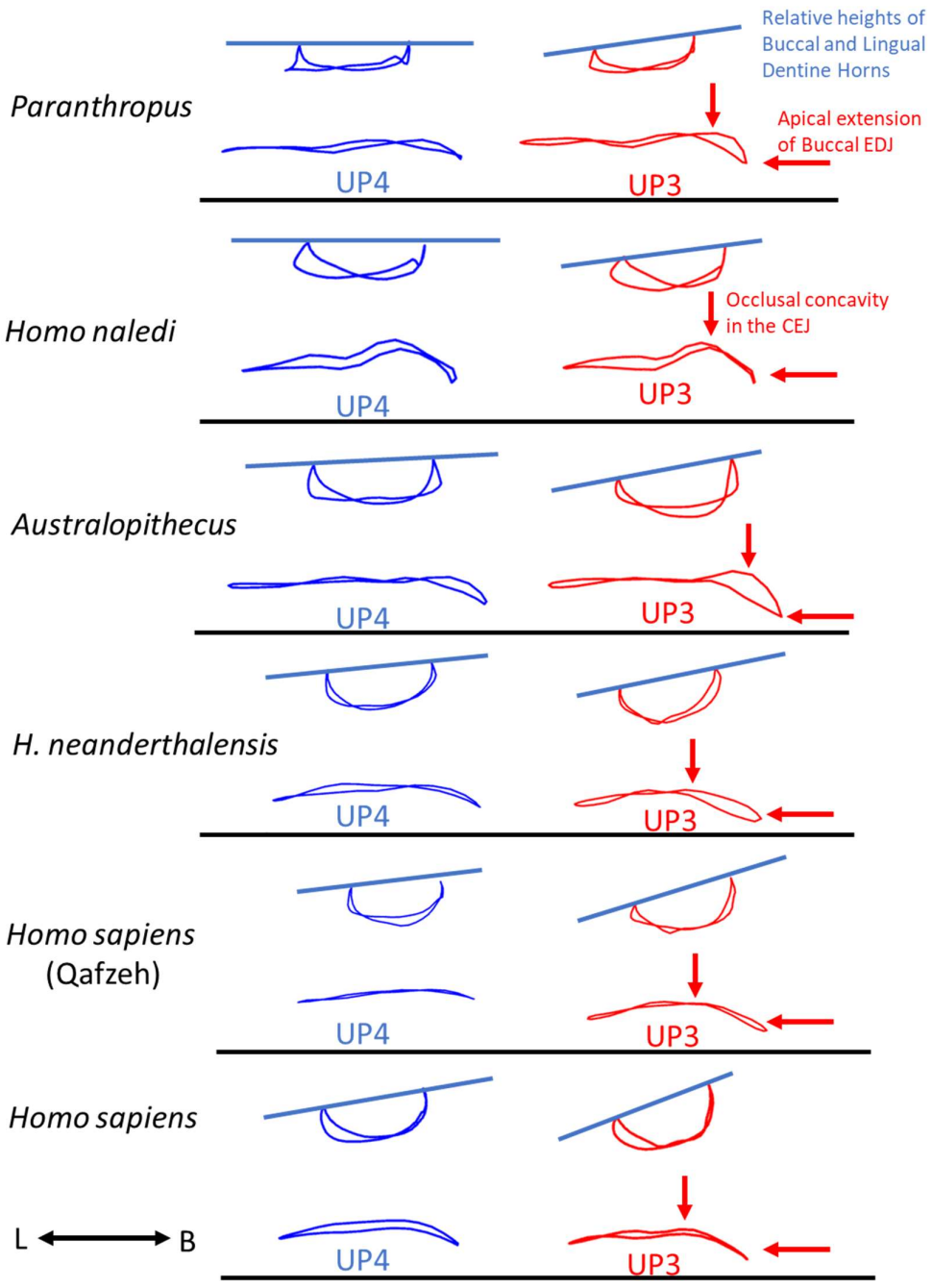

Figure 5.5.1 Wireframe models showing the height of the buccal dentine horn relative to the height of the lingual dentine horn for each tooth position by species. In each species, the buccal dentine horn is taller in the UP3 than in the UP4. It also shows the apical extension of the buccal CEJ in hominin third upper premolars.

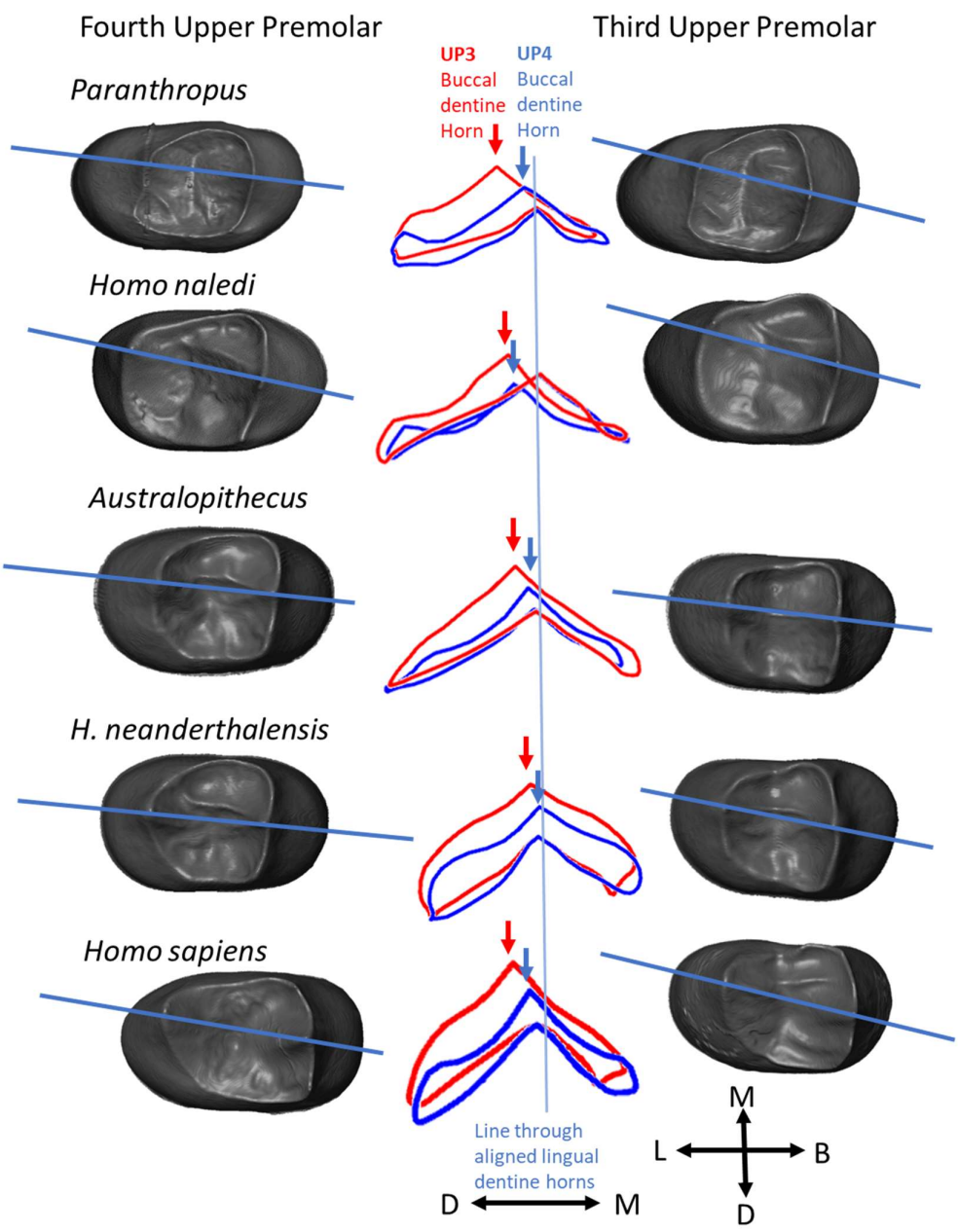

Figure 5.5.2 The position of the buccal dentine horn relative to the lingual dentine horn in hominin third and fourth upper premolars. In the third upper upper premolar the distal displacement of the buccal dentine horn is greater than in the fourth upper premolar. The wireframe models are a buccal view of the EDJ ridge (Blue = fourth upper premolar, Red = third upper premolar).

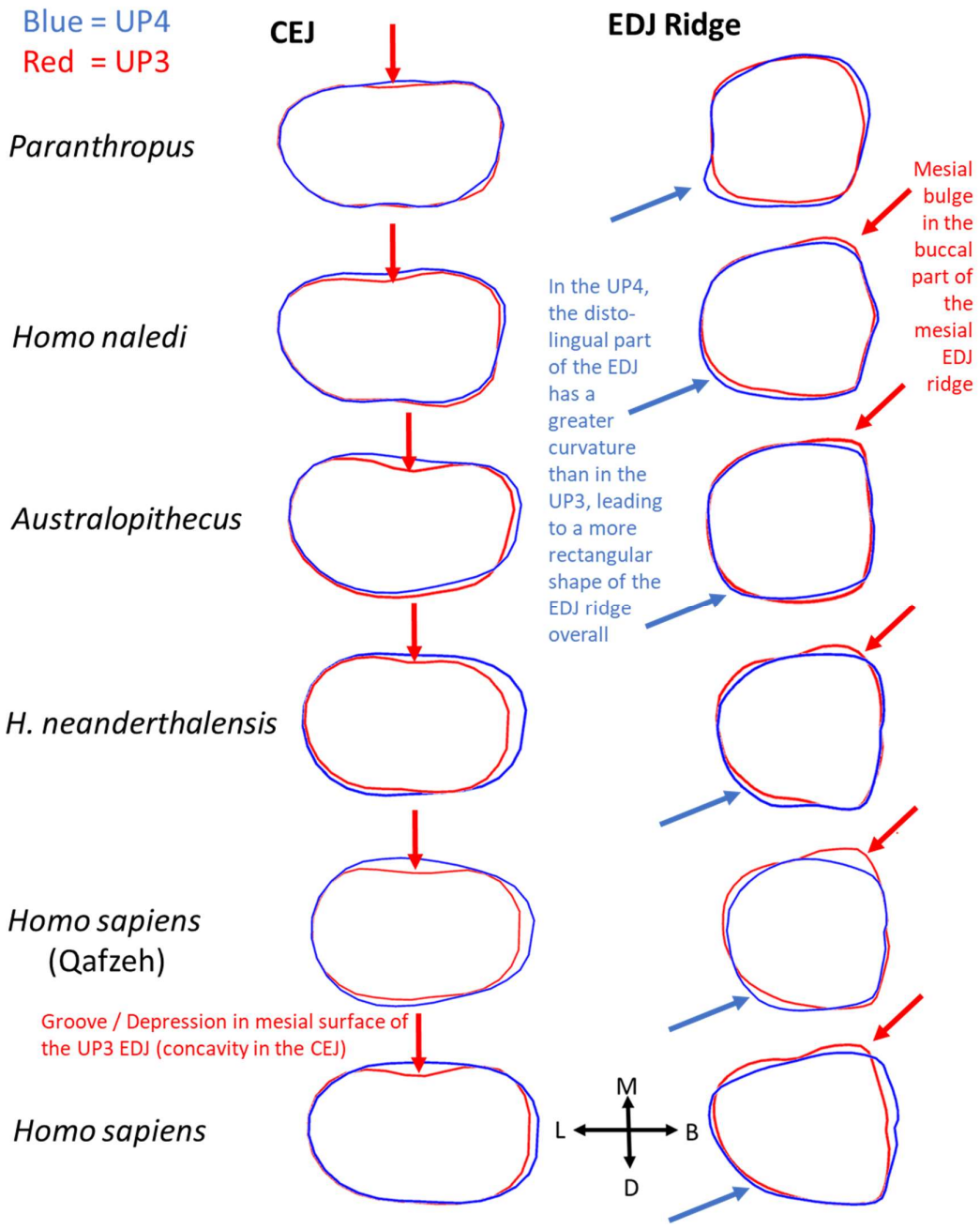

Figure 5.5.3 The mean shape of the CEJ and of the EDJ ridge in each species in this study, seen in occlusal view. Blue = fourth upper premolars, Red = third upper premolars.

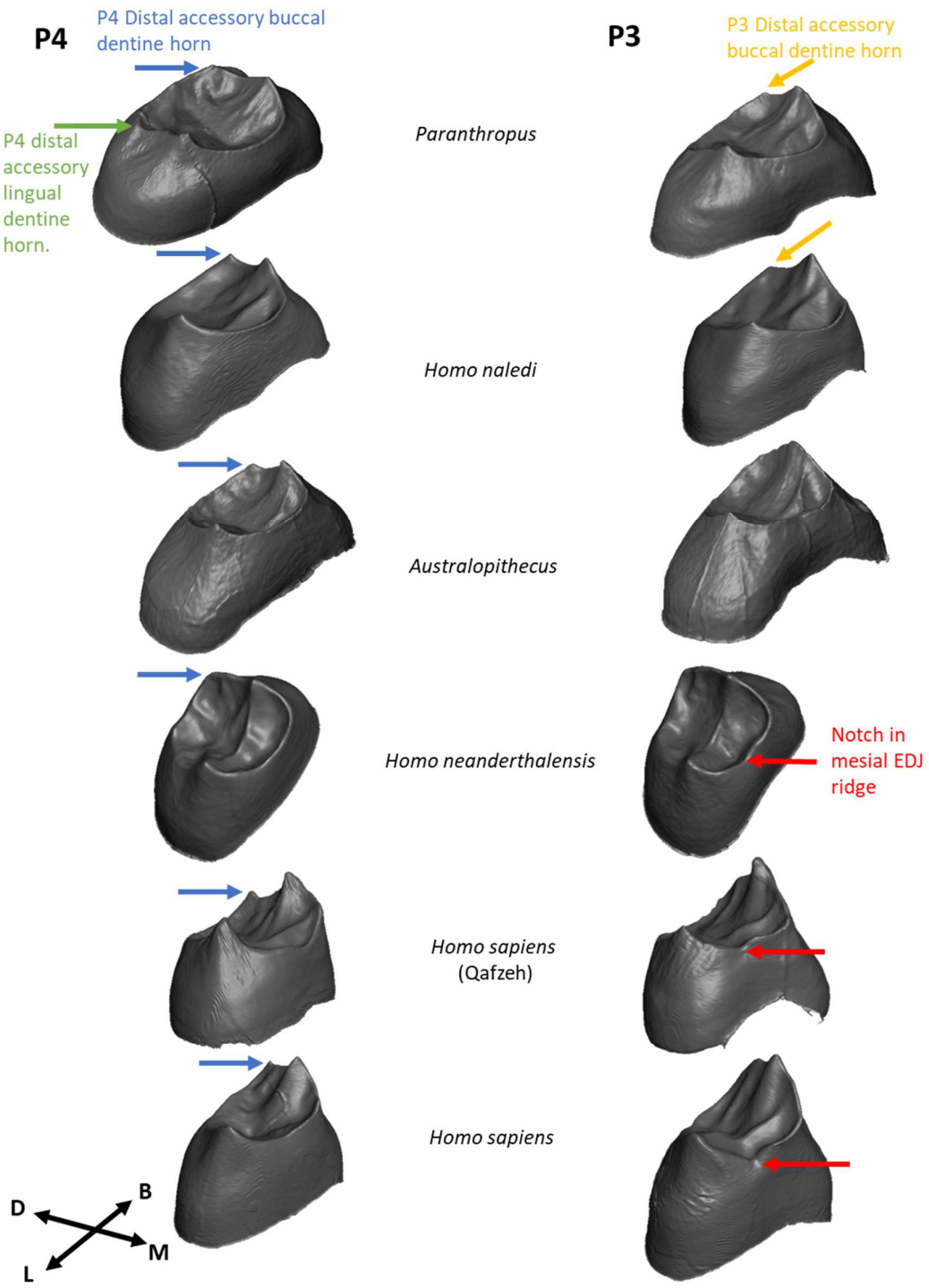

Figure 5.5.4 Features of the EDJ ridge: Accessory dentine horns and the mesial EDJ notch. Note: coloured arrows correspond to text of the same colour.

5.6 Geometric morphological differences between species.

In this section the morphological shape variation of the EDJ that distinguishes between hominin taxa is explored.

5.6.1 The first principal component of shape.

In the principal component analysis of shape (Fig. 5.6.1, top) there is a reasonably good separation of species, with *H. sapiens* at one extreme of the first principal component and *A. africanus* and *P. robustus* at the other extreme.

There is also an allometric trend - a significant correlation between shape and size - so the principal component analysis of form shows a similar pattern overall to that of shape, with small *H. sapiens* teeth at one extreme of the first principal component and large *P. robustus* teeth at the other (Fig. 5.6.1, bottom). The main difference between the first principal component of shape and the first principal component of form is that *H. naledi*, due to the small size of its teeth, is shifted along the first principal component of form in the direction of *H. sapiens.*

In order to understand the morphological features that distinguish between different hominin species, the mean shapes of the EDJs of species at the extremes of the first principal component of shape, *H. sapiens* and *P. robustus*, were compared (Fig. 5.6.2, upper half). There appear to be two main aspects of shape which differentiate between *H. sapiens* and *P. robustus*. Firstly, the EDJ of both the third and fourth upper premolars of *H. sapiens* is taller and narrower than that of the equivalent tooth in *P. robustus*. There is a greater distance between the EDJ ridge and the CEJ in *H. sapiens* and the width of the EDJ, both bucco-lingually and mesio-distally is less than that of *Paranthropus.*

Secondly, in both third and fourth upper premolars, but especially in the fourth upper premolar, there seems to be a greater development of the talon in *P. robustus* than in *H. sapiens*. There is a tendency to form a distal buccal dentine horn or shoulder in the buccal EDJ ridge of *Paranthropus*, the distal margin of the tooth is more platform-like, and in the fourth upper premolar tends towards having an elevated distal ridge. Most prominently, in the occlusal view (Figs.5.6.2, 5.6.6) there is expansion in the disto-lingual direction of the EDJ ridge, leading to a squarer, more quadrilateral outline of the EDJ in *Paranthropus*, compared with the more wedge-shaped or triangular outline in *H. sapiens.*

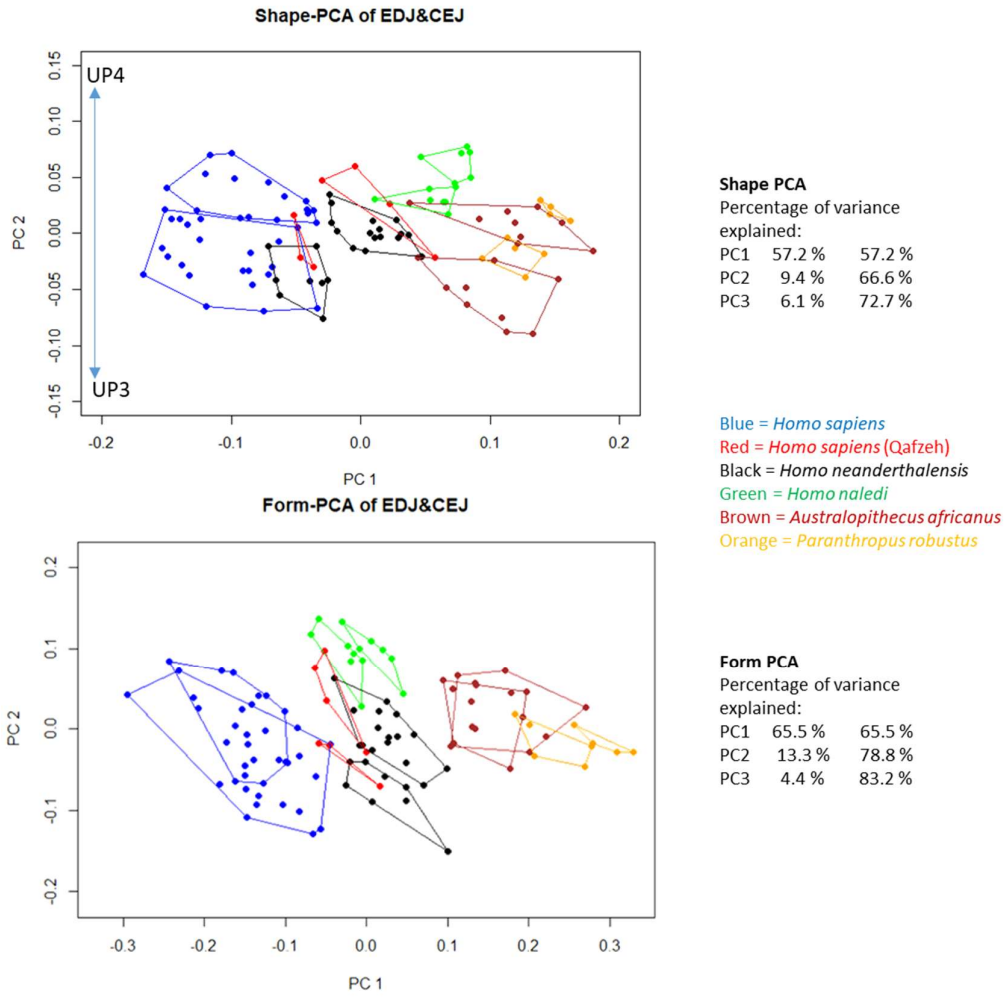

Figure 5.6.1 . Principal component analysis for shape [upper graph] and form (shape plus size) [lower graph]. (Orange = *Paranthropus,* Brown = *A.*, Black =*H. neanderthalensis*, Red = *H. sapiens* (Qafzeh), Green = *H. naledi*, Blue = *H. sapiens* (Modern Human)).

When differences in form (shape scaled by centroid size) are examined (Fig. 5.6.2, lower half) the height of the EDJ is roughly the same in *H. sapiens* and in *P. robustus.* Differences in the shapes of the tooth, as expressed by the aspect ratio of the height of the EDJ to its breadth, are not changed but they are expressed differently. Instead of the *H. sapiens* EDJ *appearing* to be 'taller and slightly narrower' than *Paranthropus* it now *appears* to be the same height as *P. robustus* but to be significantly narrower. The scaling of the EDJ by centroid size has not altered the differences in shape between *H. sapiens* and *P. robustus* but the same shape differences appear slightly differently because of the scaling. Because shape is not altered when it is scaled by centroid size, the features of talon extension in *P. robustus* are the same when examining form than they are when looking at shape (but perhaps a little easier to see (Figs. 5.6.2, 5.6.6)).

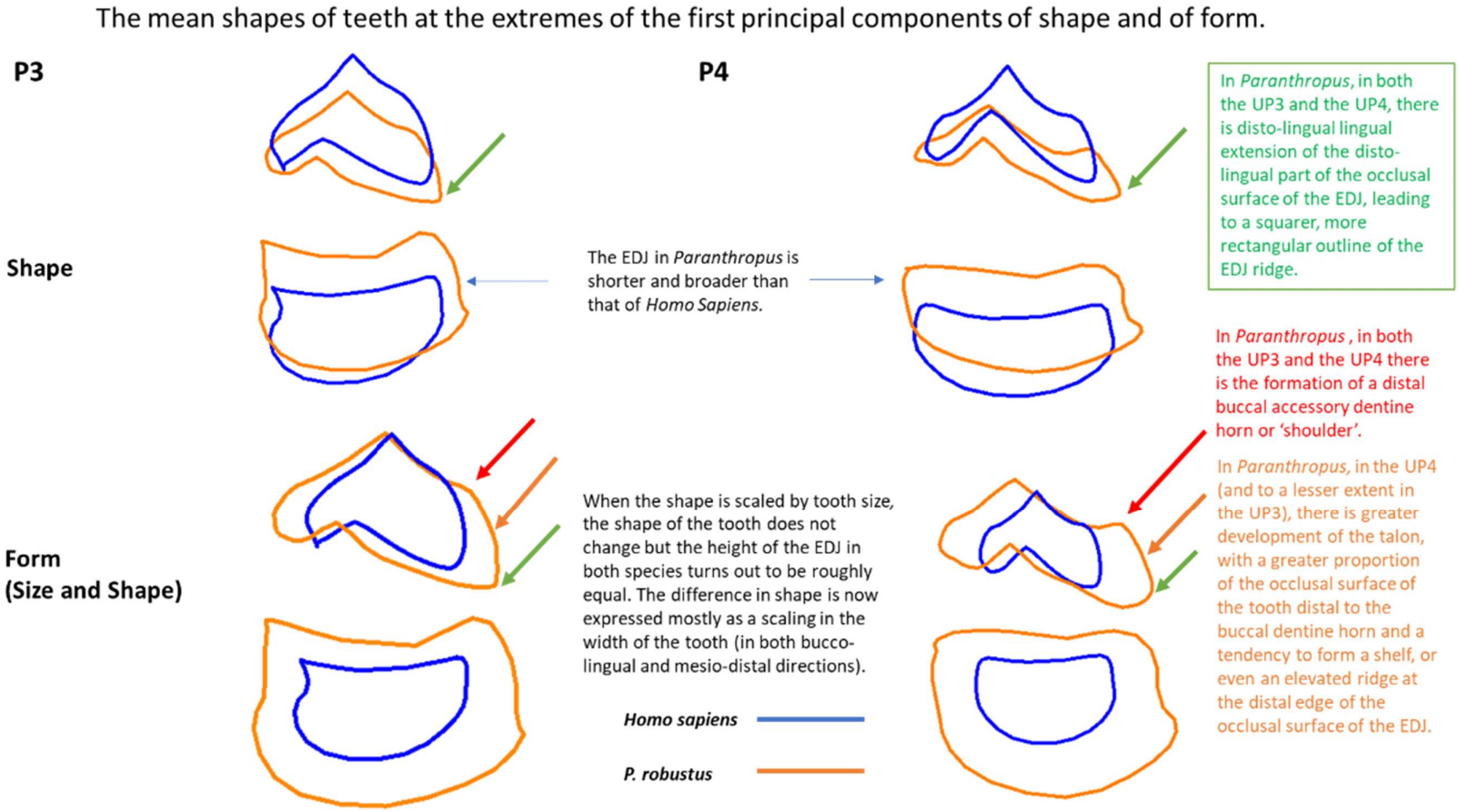

Figure 5.6.2 Differences in morphology at the extremes of the first principal components of shape and of form.

5.6.2 The second principal component of shape.

H. naledi has an extreme score on the second principal component of shape (Fig. 5.6.1). This principal component seems to capture the differences in shape between third upper premolars and fourth upper premolars within each species and *H. naledi* lies at the extreme 'fourth upper premolar' end of the spectrum. Perhaps the most distinctive difference between third and fourth upper premolar mean shapes for each species is the height of the buccal dentine horn relative to the lingual dentine horn. *H. naledi* does, indeed, have a buccal dentine horn which is lower in height than any other species, compared with the height of the lingual dentine horn, both in the third and the fourth upper premolar. Figure 5.6.3 illustrates the trend in buccal dentine horn height in *H. naledi*, *P. robustus* and *A. africanus*. This matches the trend in second principal component scores for these three species.

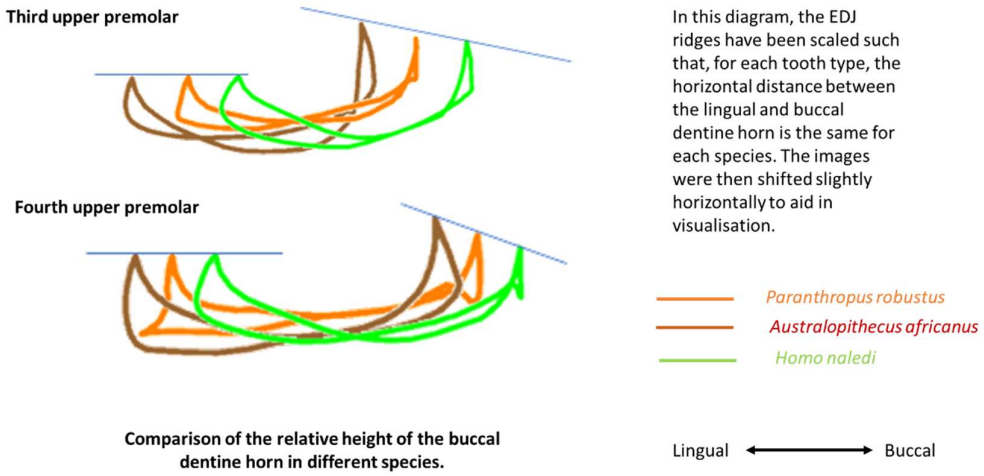

Figure 5.6.3 Buccal dentine horn height in *H. naledi* compared with *P. robustus* and *A. africanus*.

The impression that the profile of the *H. naledi* EDJ ridge is 'flatter' than in other species is also contributed to by the relatively tall and prominent distal accessory buccal dentine horn in *H. naledi.* The difference in height between the main buccal dentine horn and the accessory buccal dentine horn is small in both the third and the fourth upper premolars, giving the EDJ ridge in *H. naledi* a broad shape with a flat profile.

5.6.3 Mean shapes of hominin upper premolar EDJs by species and tooth position.

Examination of the form of the EDJ (Figs. 5.6.4, 5.6.5) in different hominin species reveals that, in most species, other than *H. naledi*, the EDJ of upper premolars is roughly the same height as in other species. The various species form a morphological trend, with *H. sapiens* at one extreme and *P.* robustus at the other extreme. As a result of this similarity in height, differences in morphology are strongly related to differences in tooth size. In large teeth the width of the EDJ is expanded in both the bucco-lingual and the mesio-distal directions (Fig. 5.6.6). This expansion is greater in the bucco-lingual direction than in the mesio-distal direction. The magnitude of the scaling transformation appears to be similar for both the EDJ and for the CEJ in the mesio-distal direction but in the bucco-lingual direction the scaling is slightly greater in the CEJ than in the EDJ. This is probably due, at least in part, to a greater development in larger teeth of the buccal and lingual cingulum.

In smaller teeth, the height of the EDJ remains the same but the tooth is 'compressed' in width. This compression also gives rise to the appearance of taller, sharper, cusps and other features on the EDJ surface, even where these features are of similar height to the same features on the EDJ surface of larger, broader and less laterally compressed teeth.

In *H. naledi* the EDJ **shape** in both the third and fourth upper premolar is like that of *P. robustus* and *A. africanus* (Figs. 5.6.4, 5.6.5, upper parts). Like *P. robustus* it has a large accessory buccal dentine horn, a raised distal EDJ ridge and, in the occlusal view (Fig. 5.6.6), disto-lingual extension of the EDJ ridge. When looking at the **form** of the *H. naledi* EDJ, however (Figs. 5.6.4, 5.6.5, lower parts), it does not fall into sequence with the other teeth in this sample. Whereas the EDJ in most other species is roughly similar in height, the EDJ of *H. naledi* is shorter.

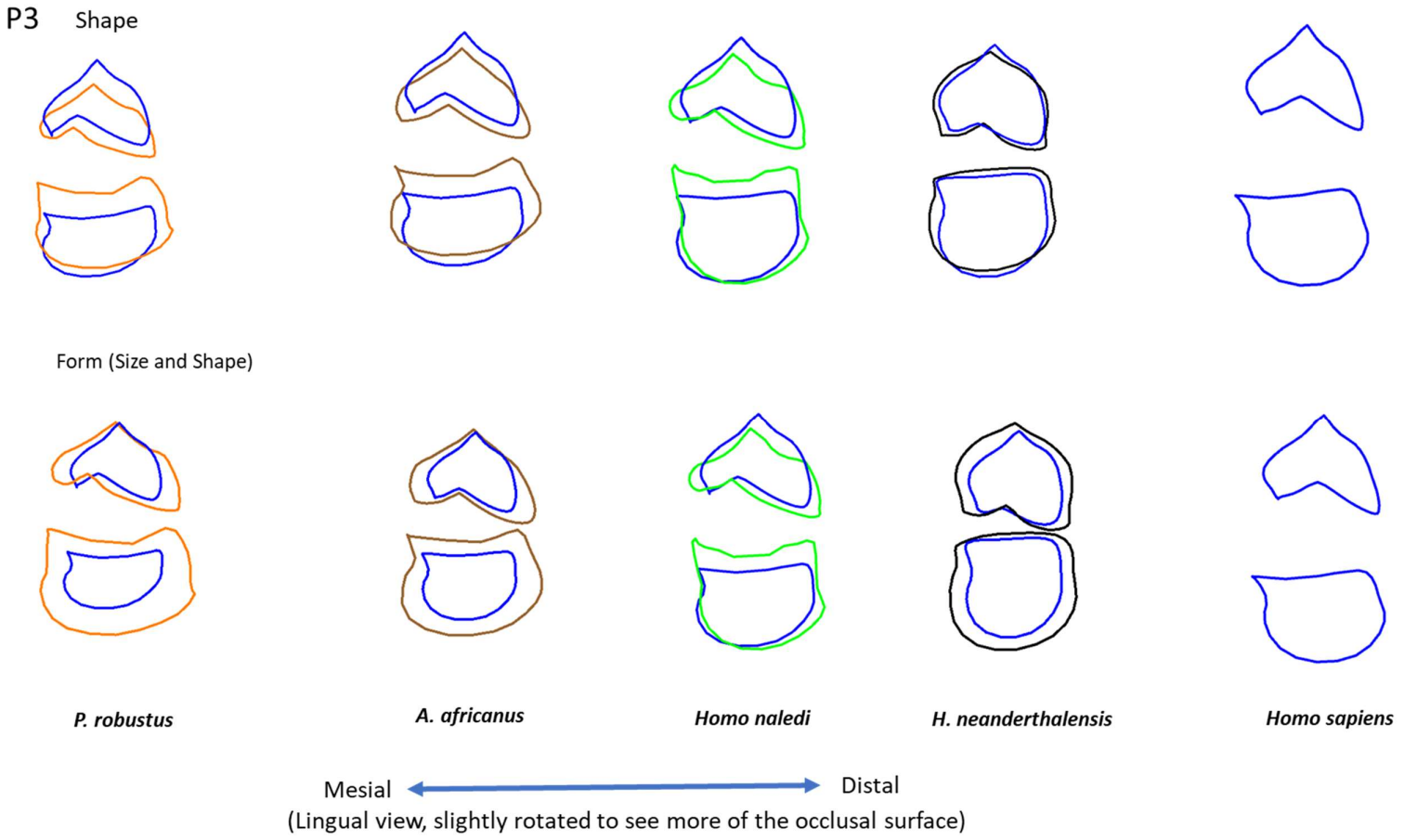

Figure 5.6.4 Trends in EDJ morphology in hominin third upper premolars. *H. sapiens* is used here as a reference surface to establish the relative size and orientation of the EDJ surfaces in other species.

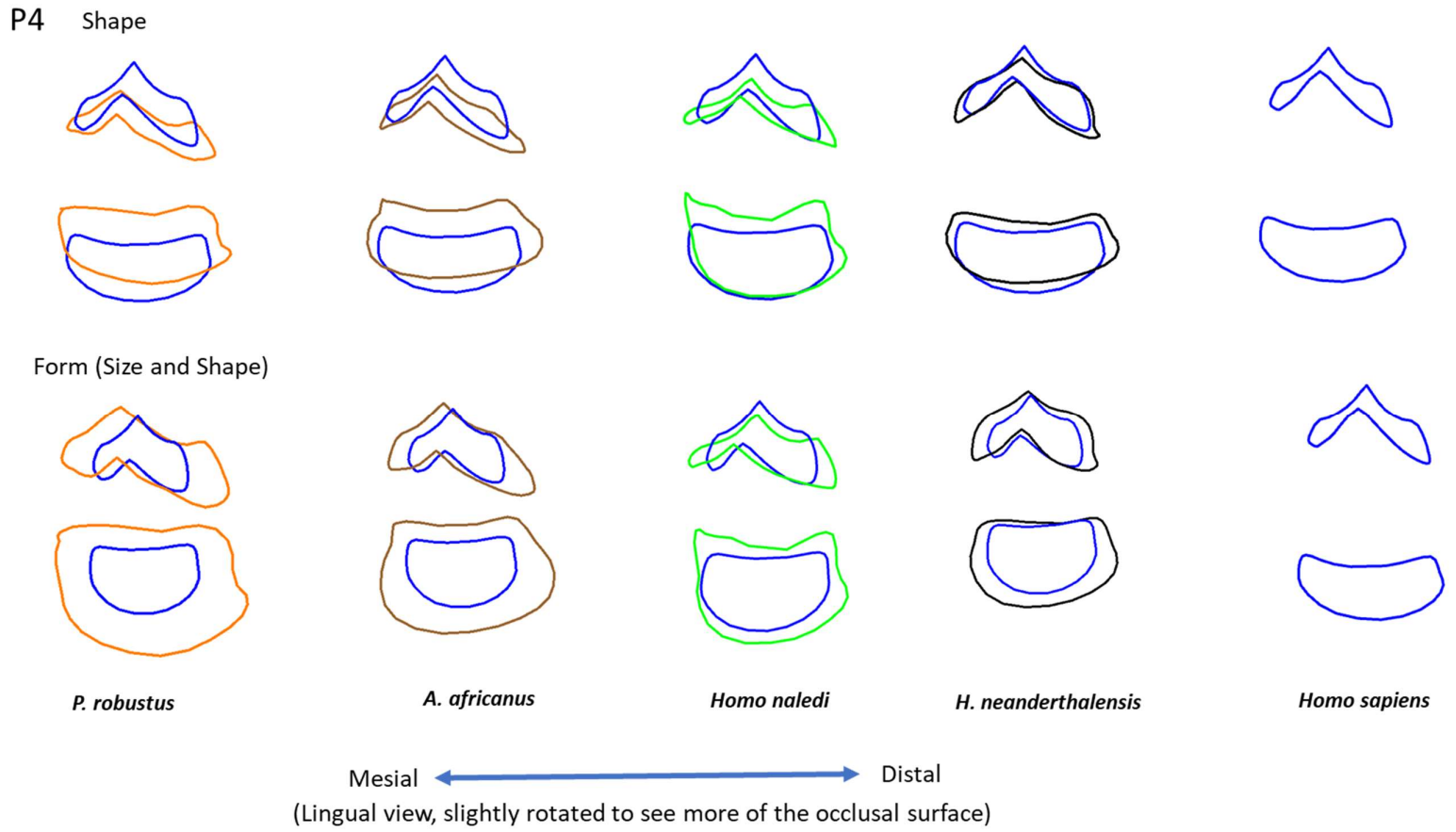

Figure 5.6.5 Trends in EDJ morphology inhominin fourth upper premolars. *H. sapiens* is used here as a reference surface to establish the relative size and orientation of the EDJ surfaces in other species.

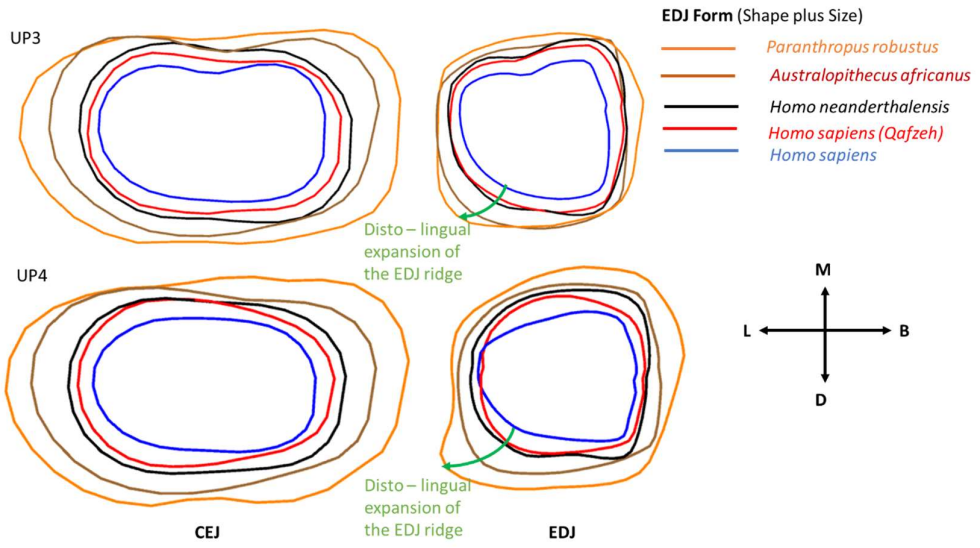

Figure 5.6.6 Trends in the form of the CEJ ridge and the EDJ ridge in occlusal view in hominin upper premolars (excluding *H. naledi*).

Looking in detail at the EDJ ridge in occlusal view (Fig. 5.6.7), the **shape** of the ridge in *H. naledi* in both third and fourth upper premolars is roughly square or quadrilateral in outline, like *P. robustus* and to *A. africanus.* However, when looking at the **form** of the EDJ ridge *H. naledi* is smaller in size than Paranthropus or *Australopithecus* and is similar in size to the other species of *Homo*, especially *H. neanderthalensis* and archaic *H. sapiens* (Qafzeh).

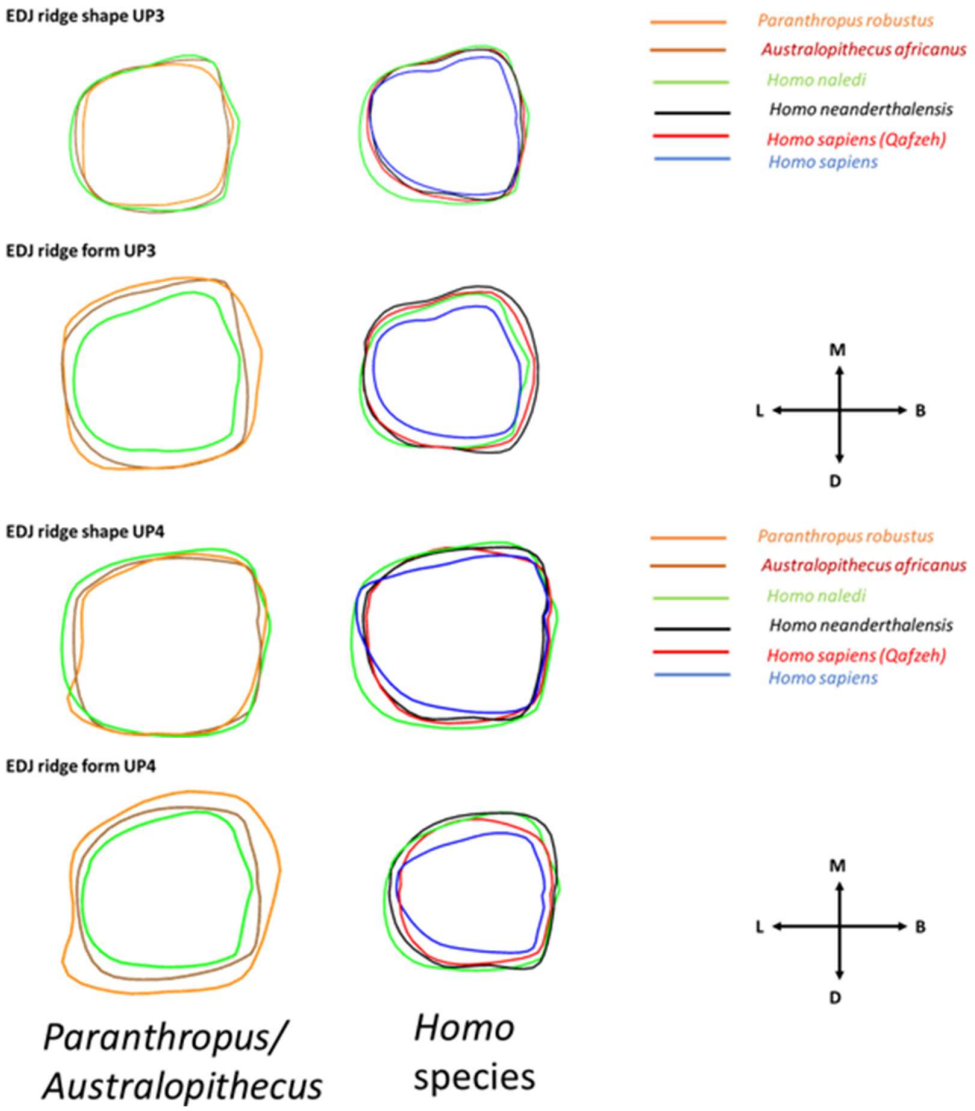

Figure 5.6.7 Comparison of the shape and form of the EDJ ridge of *H. naledi* in occlusal view with that of other hominins.

In order to quantify the trend in shape across the hominin species in this sample, bounding boxes were created for the mean EDJ surface of each species in distal view (Figs. 5.6.8, 5.6.9) and the aspect ratio (base divided by height) for each species was plotted on a graph (Figs 5.6.10, 5.6.11)). Figures 5.6.8 and 5.6.9 show the form of the EDJ but the aspect ratio is the same for both form and shape. Bounding boxes were created for both the tip of the lingual dentine horn, capturing the shape of the main body of the EDJ, and for the buccal dentine horn, capturing the shape of the maximum dimensions of the EDJ. The trend for both cusps was similar.

These graphs show a strong trend in aspect ratio. Using the lingual dentine horn as a reference landmark for height, at one extreme the (bucco-lingual) width of the *P. robustus* EDJ is roughly twice the height of the EDJ in both the third and fourth upper premolars. At the other extreme, the width of the *H. sapiens* (modern human) EDJ is just 1.2 times the height in the third upper premolar and 1.3 times the height in the fourth upper premolar.

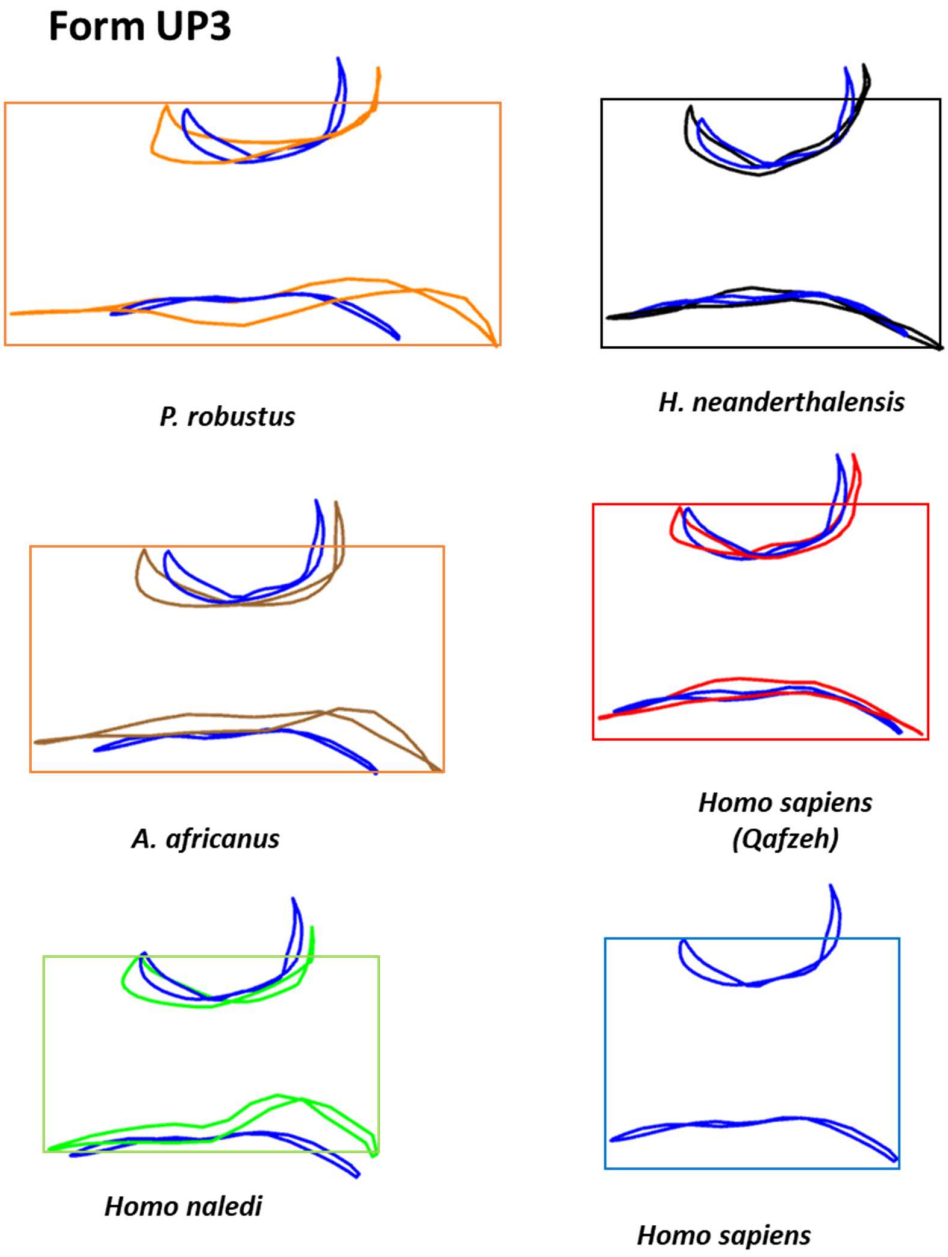

Figure 5.6.8 Bounding boxes for mean third upper premolar EDJ surfaces. The bounding boxes shown are for the limits of the CEJ and the tip of the lingual dentine horn for each species and tooth type.

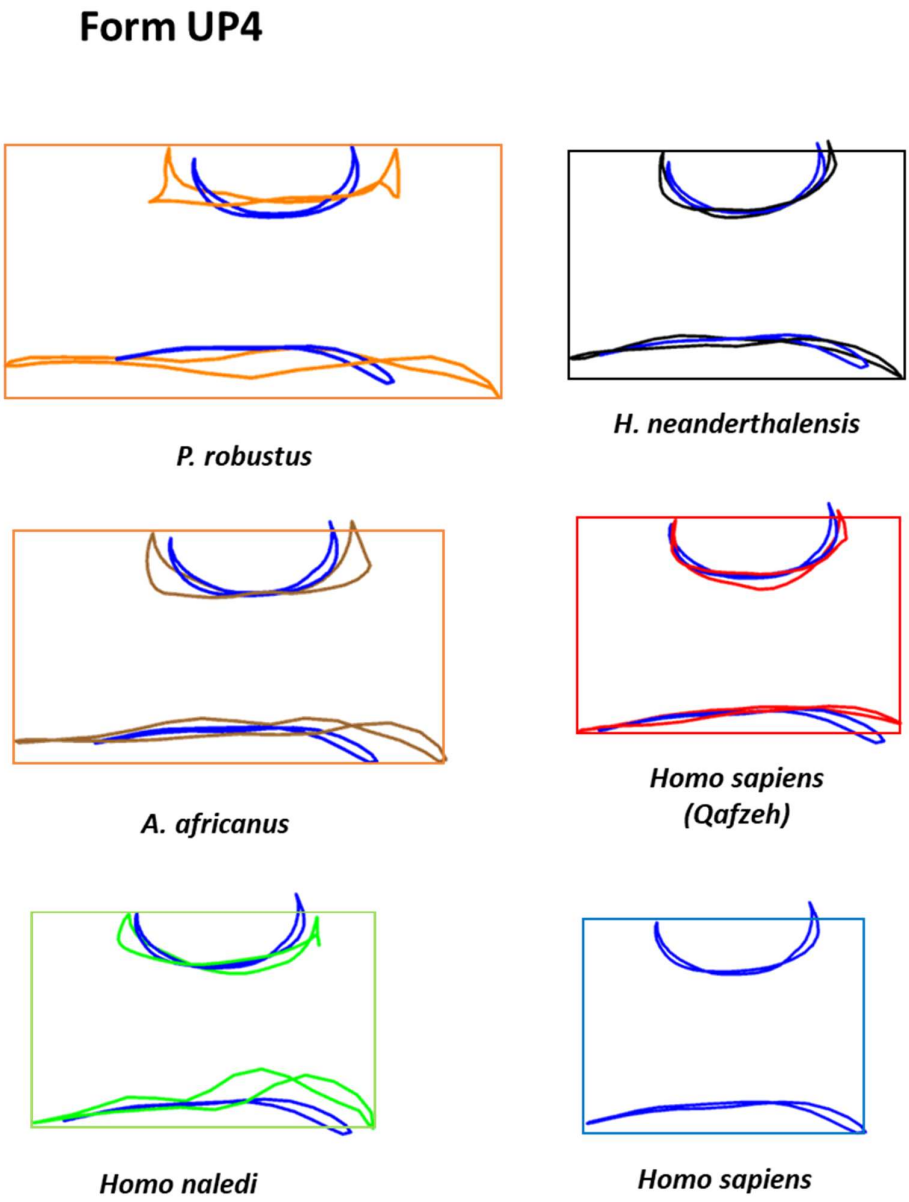

Figure 5.6.9 Bounding boxes for mean fourth upper premolar EDJ surfaces. The bounding boxes shown are for the limits of the CEJ and the tip of the lingual dentine horn for each species and tooth type.

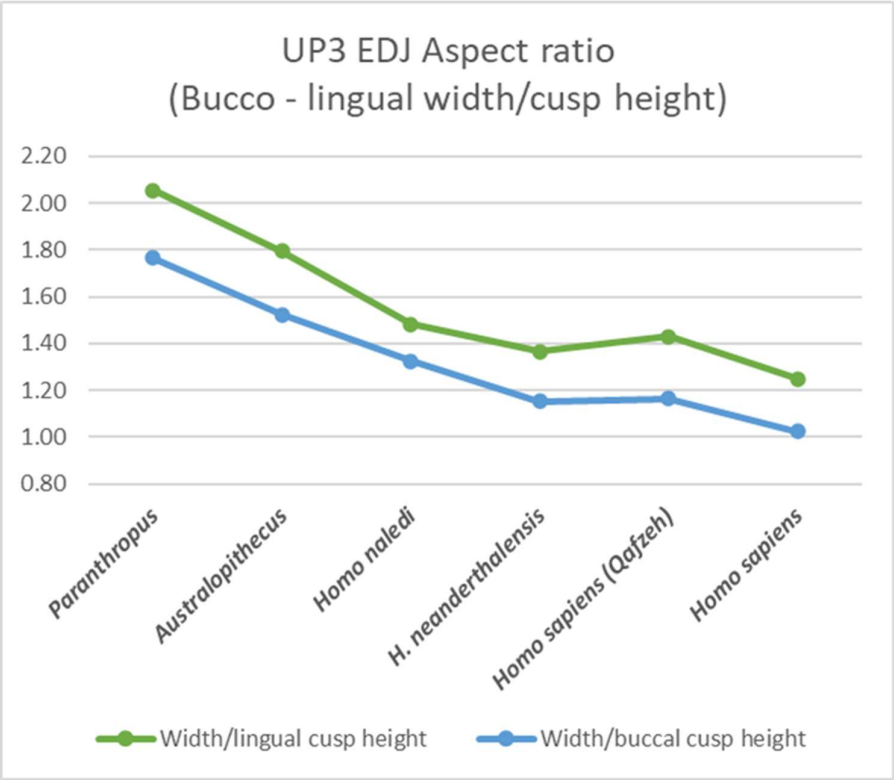

Figure 5.6.10 Trends in aspect ratio of bucco-lingual width to dentine horn height for third upper premolars.

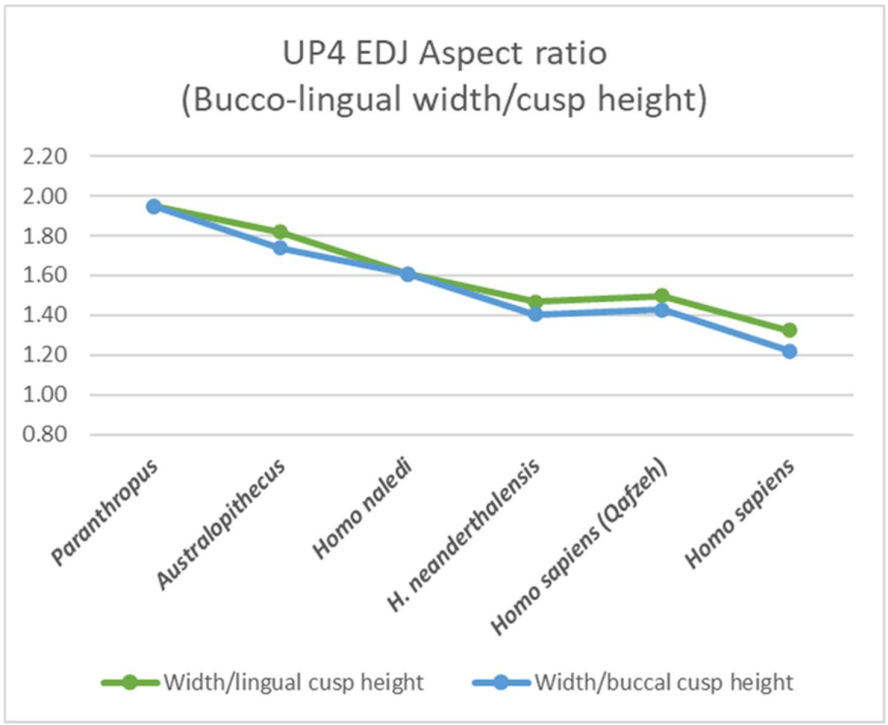

Figure 5.6.11 Trends in aspect ratio of bucco-lingual width to dentine horn height for fourth upper premolars.

5.6.4 A note on talon expansion

There is a trend of talon expansion along the first principal component of shape. As one travels from the *Homo* end of the principal component to the *Paranthropus* end there is a tendency to form a distal buccal dentine horn or shoulder in the buccal EDJ ridge and for this to become more and more widely separated from the main buccal dentine horn, there is expansion in the disto-lingual direction of the EDJ ridge, leading to a squarer, more quadrilateral outline of the EDJ and the talon becomes a proportionately larger, more distinctive, shelf like feature of the occlusal surface of the EDJ (Fig. 5.6.12). It is notable that *within each species* there is talon expansion in the fourth upper premolar relative to the third upper premolar and this may explain why the fourth upper premolar in each species is consistently placed closer than the third upper premolar to the *Paranthropus* end of the first principal component of shape.

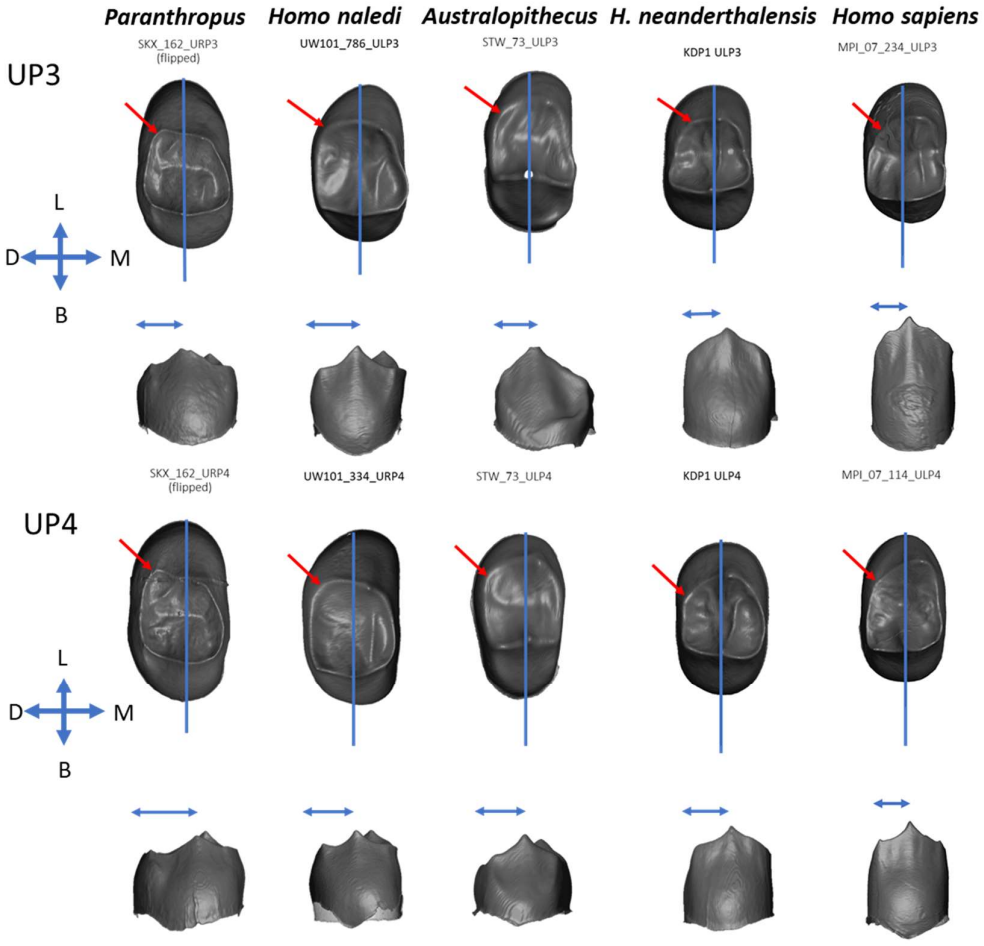

Figure 5.6.12 Talon expansion. The talon becomes proportionately larger and more distinctive along a morphological trend from *Homo* to *Paranthropus.* The talon is also extended in the fourth upper premolar of each species, when compared with the third upper premolar. The blue arrows indicate the distance between the main buccal dentine horn and the distal margin of the EDJ. The red arrows indicate extension of the EDJ ridge in a disto-lingual direction.

5.7 Qualitative morphometrics: Examination of the non-metric traits of the EDJ in hominin upper premolars

5.7.1 Qualitative morphometrics: Descriptions of the morphological features.

In addition to the main study, which focusses on quantitative morphometrics, a qualitative morphometric analysis was carried out to identify possible morphometric features, also referred to as non-metric traits, of interest in upper premolar EDJs and to count the frequencies of each of these features across the sample (note that due to time constraints no interobserver tests were carried out and the assessor was not blinded as to the identity of each tooth). The results are tabulated in Appendix 2.

Some qualitative features of the EDJ have already been discussed in the quantitative morphometric analysis. A feature may appear in the mean shape of the EDJ ridge if it occurs frequently enough or is prominent enough in some individuals for it to affect the mean shape. The difference in approach here is to count the frequency of expression of these traits in different subpopulations of the sample.

Mesial and distal accessory buccal dentine horns

These are thorn shaped elevations of the buccal EDJ ridge which may lie mesial or distal to the main buccal dentine horn (Fig. 5.7.1). The distal accessory buccal dentine horn may be large and widely separated from the main buccal dentine horn by a depression in the buccal EDJ ridge but the feature is scored as present or absent, regardless of its distinctiveness or size.

Distal shoulder of the buccal EDJ ridge

This is an elevation of the distal part of the buccal EDJ ridge, separated from the main buccal dentine horn by a slight depression of the buccal EDJ ridge (Fig 5.7.1).

Notch in mesial in EDJ ridge

This is a distinct notch in the mesial EDJ ridge, often near the junction of the buccal two thirds of the ridge with the lingual one third (Fig. 5.7.1).

Mesial bulge in mesial EDJ ridge

This is a mesial convexity in the buccal part of the mesial EDJ ridge in the plane of the occlusal surface of the EDJ (Fig. 5.7.1).

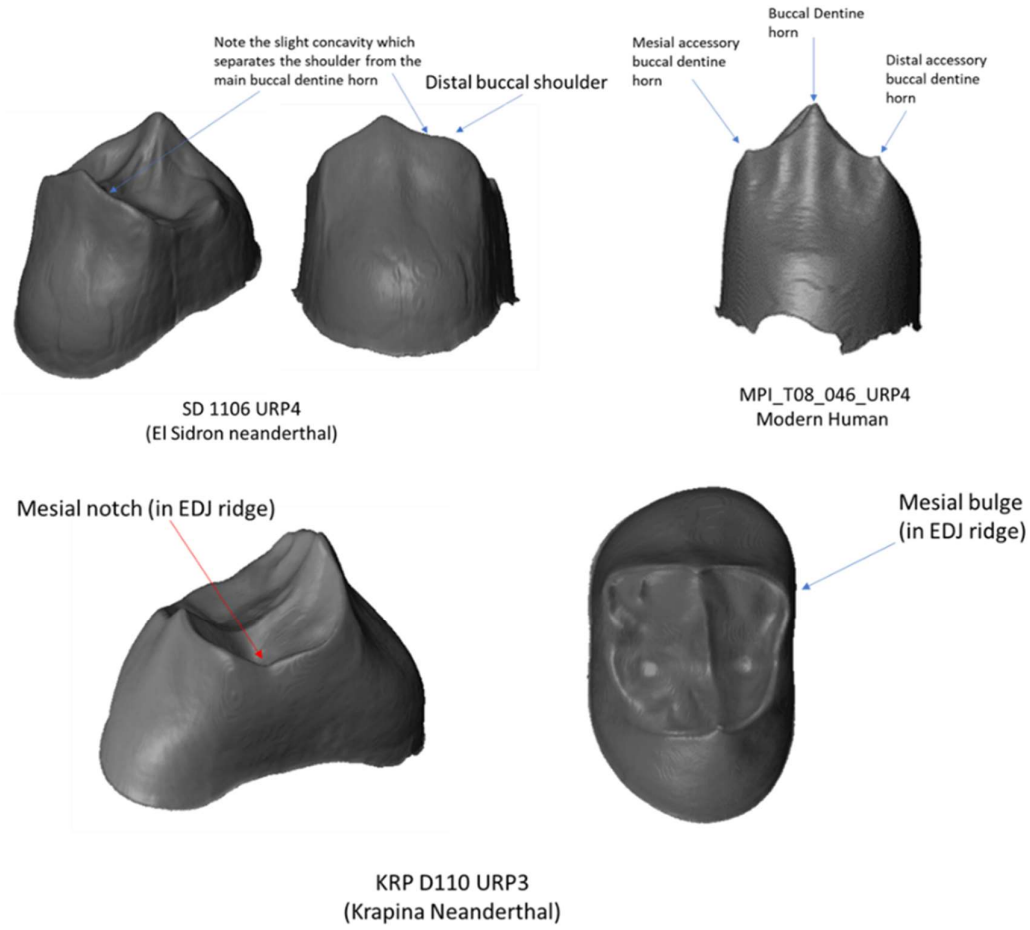

Figure 5.7.1 Qualitative features of the EDJ ridge.

Buccal surface ridges.

The buccal cusps of all the teeth in this sample show a tripartite structure. There is a central (essential) buccal dentine horn, often associated with an essential ridge on the buccal surface of the EDJ. There are also mesial and distal ridges on margins of the buccal surface of the tooth, separated from the essential crest by grooves or depressions. In some teeth, these crests and grooves are very subtle but in other teeth they are clear to see. Although the size and prominence of these ridges lies on a continuum, I have scored the presence of buccal ridges as ‘minimal’, ‘moderate’ or ‘prominent’, following Figure 5.7.2 as a reference.

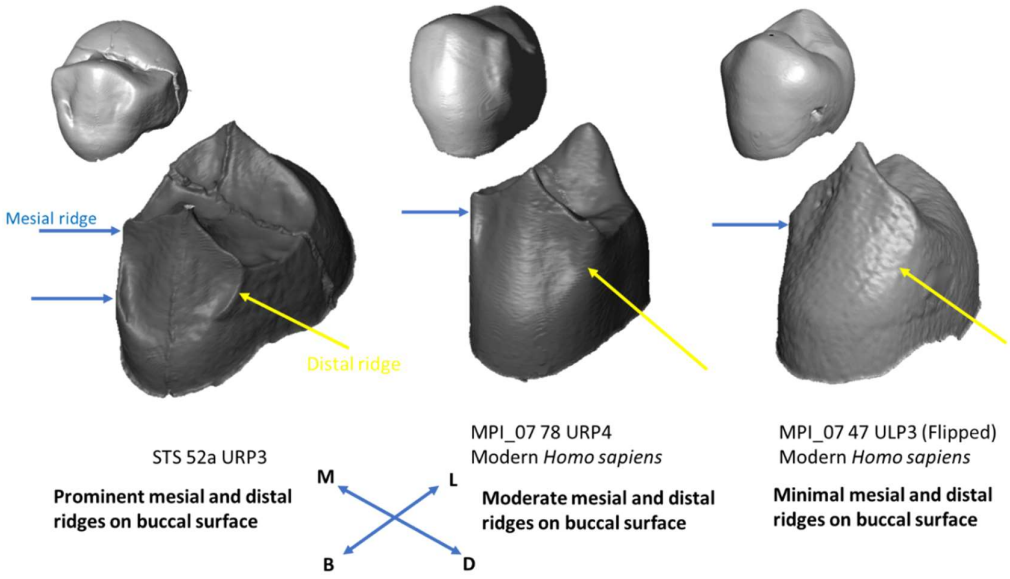

Figure 5.7.2 Degrees of expression of the mesial and distal ridges of the buccal surface of the EDJ.

Buccal and lingual cingulum

In addition to variations in the mesial and buccal ridges of the buccal surface of the tooth, there are differing degrees to which the cingulum is developed. In some *Australopithecus* teeth, for example, there is a shelf like buccal cingulum and this is often associated with very prominent mesial and buccal ridges, which extend onto the cingulum and meet there (Fig. 5.7.3). This is not found in all *Australopithecus* teeth. Some have a well-developed essential ridge, giving a much less shelf like appearance to the cingulum. I have only scored the buccal cingulum as 'present' if the buccal cingulum has a distinct shelf like appearance and not if there is a prominent essential ridge. Similarly, the lingual cingulum may also be extended into a shelf-like structure (Fig. 5.7.3).

Boss-like buccal cingulum

The buccal surface of *H. neanderthalensis* and some other fossil hominin third upper premolars has a distinctive shield-boss like bulge in the area of the buccal cingulum of the EDJ and this is also visible as a bulge or transverse ridge on the buccal enamel surface of the tooth (Fig. 5.7.4).

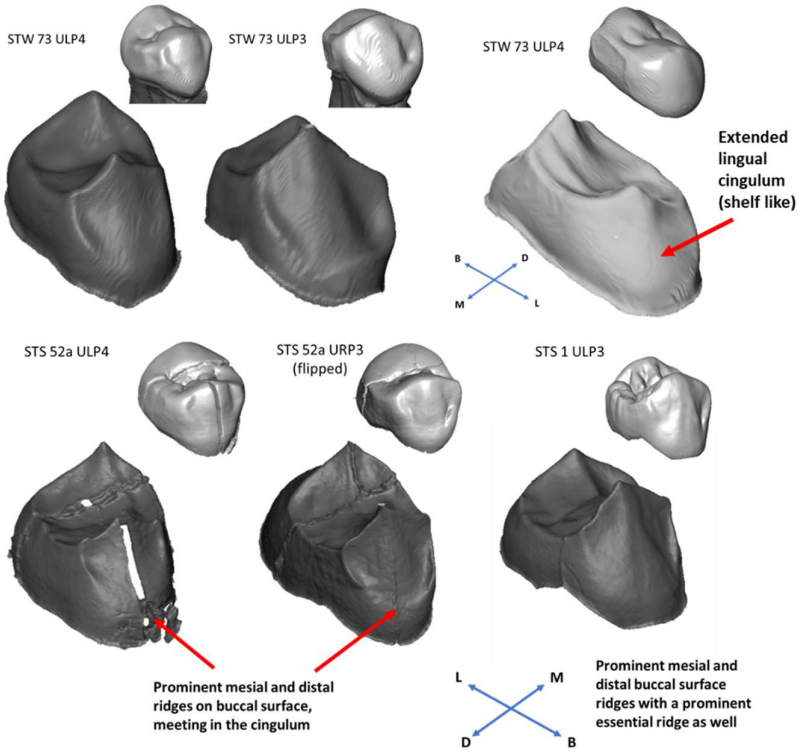

Figure 5.7.3 Extension of the cingulum and other features of the buccal and lingual cingulum.

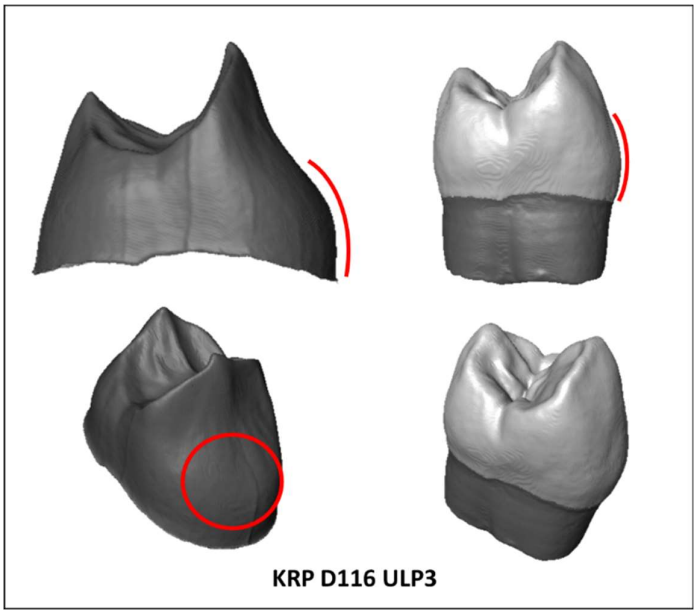

Figure 5.7.4 Shield-boss shaped cingulum bulge.

Transverse crest (Central and Mesial)

Some teeth have a transverse crest (Fig. 5.7.5). Here, I define a transverse crest as any continuous crest or ridge which crosses the midline of the occlusal surface of the EDJ. It may be lower in height in the mid-part of the EDJ but is not interrupted by any notch or groove. In many teeth there is a marked discrepancy between the appearance of a transverse crest at the EDJ and at the outer enamel surface (OES). At the EDJ the crest is continuous but in the OES the crest is interrupted by a groove, dividing it into two distinct ridges. The divided transverse crest and the essential ridge of the same cusp may give the appearance at the OES of a bifurcated essential ridge.

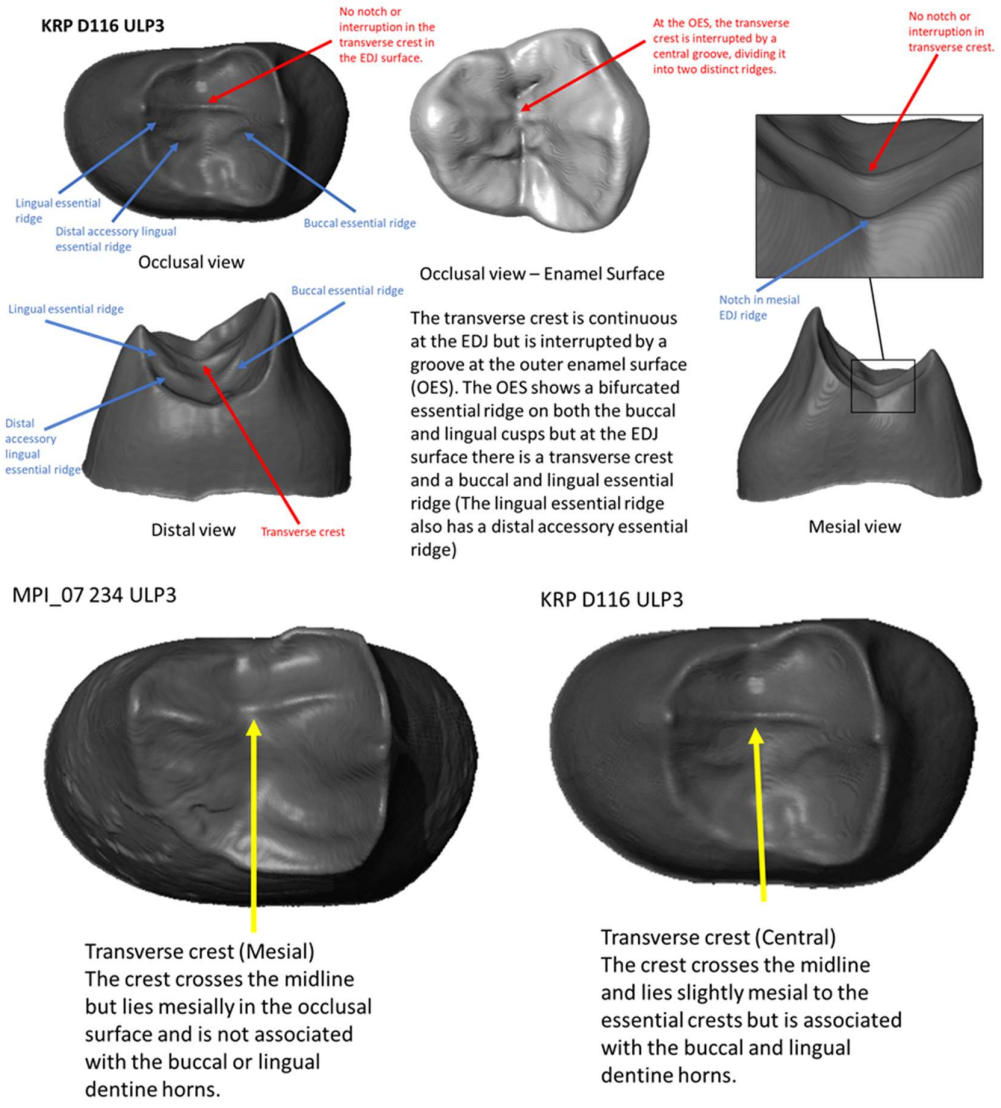

Figure 5.7.5 Features of the transverse crest including the distinction between a central transverse crest and a mesial transverse crest.

In addition, there seem to be two distinct types of transverse crest (Fig. 5.7.5). One type is situated centrally and is associated with the lingual and buccal dentine horns

(either joined to the horns or pointing towards them). The other type of transverse crest is situated mesially and is not associated with the dentine horns. For scoring, I have labelled a feature as a mesial transverse crest if it is situated mesially and is not associated with at least one of the dentine horns – that is, it may join or point towards one of the dentine horns but not to both.

Bucco-mesial ridge

The bucco-mesial ridge is a ridge which originates in the mesial part of the buccal EDJ ridge travelling in a lingual direction initially but which then curves mesially to meet the mesial EDJ ridge (Fig. 5.7.6).

Buccal and lingual essential ridges

Essential ridges are prominent occlusal ridges which are attached to, or which point towards, the buccal or lingual dentine horn. They do not cross the mid-line of the EDJ occlusal surface (Fig. 5.7.6).

Distal and mesial buccal accessory ridges.

Buccal accessory ridges are occlusal ridges which originate on the buccal EDJ ridge either mesial or distal to the main buccal dentine horn and travel towards the midline of the occlusal surface but do not cross it(Fig. 5.7.6). They are not attached to or associated with the main buccal dentine horn but may be associated with a distal or mesial accessory buccal dentine horn. They correspond to the ASUDAS (Scott and Irish, 2017) 'premolar accessory ridges' at the OES.

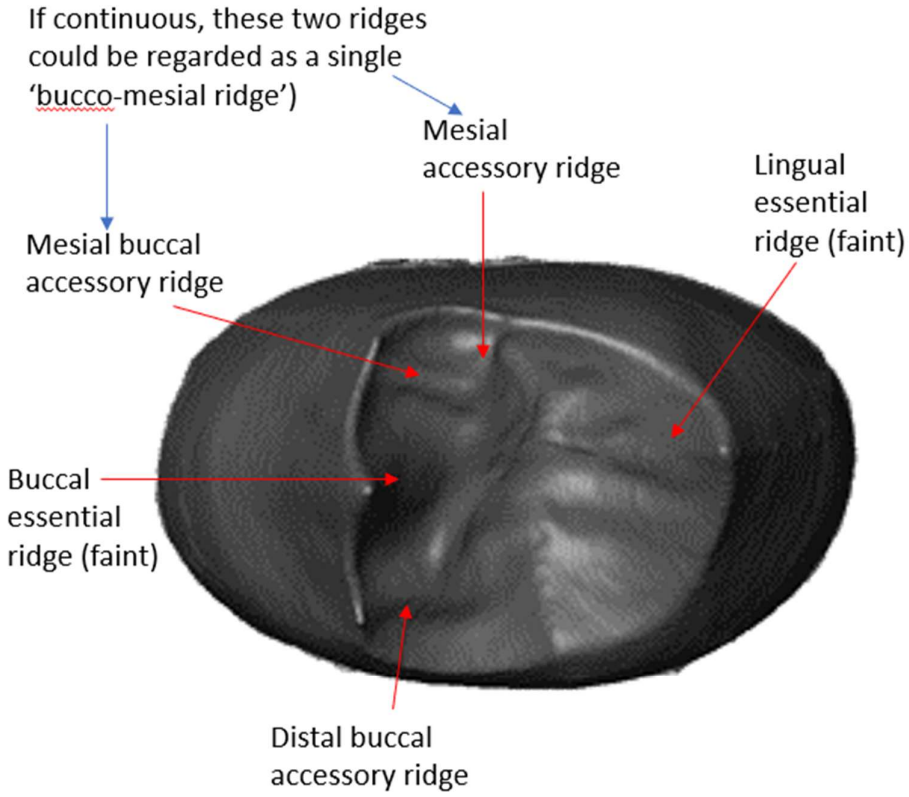

Figure 5.7.6 Ridges of the occlusal surface of the EDJ (Excluding transverse crests).

Distal lingual accessory dentine horn

In some *P. robustus* and *A. africanus* teeth, but not in any species of *Homo* there are features which suggest a trend towards molarisation of the premolar (Fig. 5.7.7). In addition to the presence of a distinct distal buccal accessory dentine horn, widely separated from the main buccal dentine horn, there is also the development of a distal lingual accessory dentine horn. This horn, in a position equivalent to the hypocone in upper molar teeth, lies on a distinctive lingual extension of the disto-lingual part of the EDJ ridge.

Oblique ridge

In some teeth showing signs of molarisation, there is an oblique ridge, which partially separates the distal lingual accessory dentine horn from the rest of the occlusal surface of the EDJ (Fig. 5.7.7). This ridge appears to be a rudimentary version of the oblique ridge which frequently joins the disto-buccal and mesio-lingual cusps of hominin upper molar teeth, forming a boundary between the molar trigon and the hypocone.

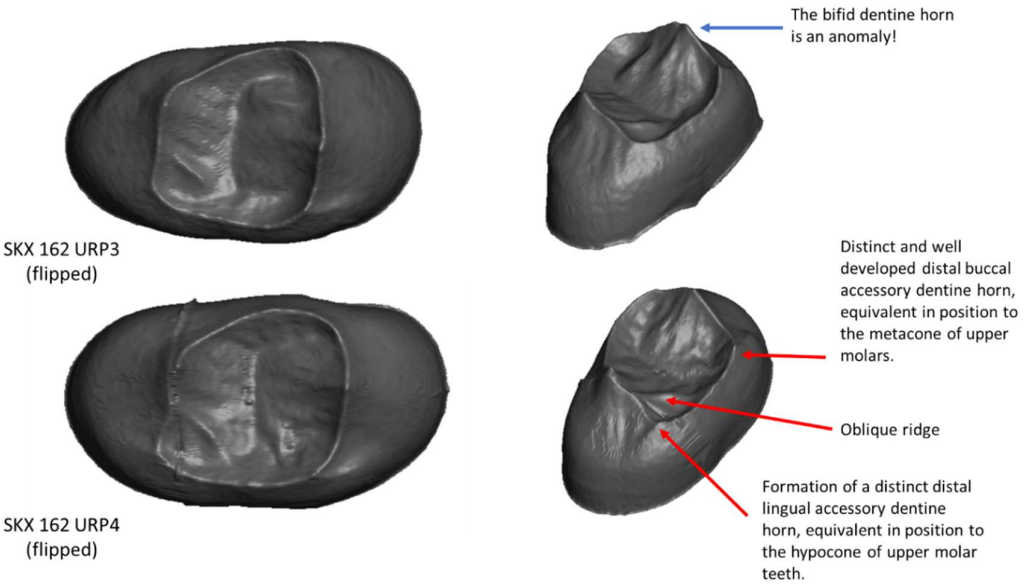

Figure 5.7.7 Features of premolars which suggest a degree of molarisation.

5.7.2 Qualitative morphometrics: Frequencies of the expression of features by species and tooth position

In this section, in order to keep the size of tables to a manageable level, I have grouped the results to focus on different areas of EDJ morphology, such as the features of the EDJ ridge, features associated with the buccal and lingual surfaces of the EDJ and so on.

Table 5.7.1 Counts and percentages of qualitative features of the EDJ ridge (Blank cells are less than 1%).

Species	Tooth	Sample size	MN	MB	DBH	DBS	MBH	MN	MB	DBH	DBS	MBH
Australopithecus africanus	P3	10	0	2	3	0	4		20%	30%		40%
Australopithecus africanus	P4	9	0	0	6	1	5			67%	11%	56%
Homo sapiens (Qafzeh)	P3	3	2	2	0	0	0	67%	67%			
Homo sapiens (Qafzeh)	P4	3	0	0	3	0	1			100%		33%
Homo erectus	P3	2	1	1	1	0	1	50%	50%	50%		50%
Homo erectus	P4	2	0	0	1	1	0			50%	50%	
Homo heidelbergensis	P3	1	1	1	0	0	0	100%	100%			
Homo heidelbergensis	P4	2	0	0	0	2	1				100%	50%
Homo naledi	P3	7	0	5	7	0	4		71%	100%		57%
Homo naledi	P4	6	0	0	6	0	2			100%		33%
Homo neanderthalensis	P3	10	9	6	0	2	0	90%	60%		20%	
Homo neanderthalensis	P4	16	1	0	0	14	0	6%			81%	
Homo sapiens	P3	24	18	13	4	0	2	75%	54%	17%		8%
Homo sapiens	P4	17	0	1	13	2	9		6%	76%	12%	53%
Paranthropus robustus	P3	5	0	0	3	0	2			60%		40%
Paranthropus robustus	P4	4	0	0	4	0	0			100%		

Key

MN	Mesial notch
MB	Mesial bulge
DBH	Distal accesory buccal Horn
DBS	Distal buccal shoulder
MBH	Mesial accesory buccal horn

A distal accessory buccal dentine horn is found in all the fourth upper premolars of *P. robustus*, *H. naledi*, and archaic *H. sapiens* (Qafzeh), in three quarters of modern *H. sapiens* fourth upper premolars and two thirds of *A. africanus* fourth upper premolars (Table 5.7.1). In the fourth upper premolars of *H. neanderthalensis* and *H. heidelbergensis* (including *H. rhodesiensis*) the distal accessory buccal dentine horn is replaced by a distal buccal shoulder. The mesial notch and mesial bulge are found in a half to three quarters of upper third premolars in all *Homo* species except *H. naledi* in which 71% of third upper premolars have a mesial bulge without a mesial notch.

The frequencies of features of the buccal and lingual EDJ surfaces of hominin upper premolars are set out by species and tooth position in table 5.7.2.

Table 5.7.2 Counts and percentages of qualitative features of the buccal and lingual surfaces of the EDJ. (Blank cells are less than 1%).

Species	Tooth	Sample Size	Moderate Ridges	Prominent Ridges	Buccal Bossing	Buccal Cingulum	Lingual Cingulum
Australopithecus africanus	P3	10	1	8	0	9	5
Australopithecus africanus	P4	9	4	3	0	5	5
Homo sapiens (Qafzeh)	P3	3	0	0	1	0	0
Homo sapiens (Qafzeh)	P4	3	0	0	0	0	0
Homo erectus	P3	2	2	0	0	0	0
Homo erectus	P4	2	2	0	0	0	0
Homo heidelbergensis	P3	1	1	0	0	0	0
Homo heidelbergensis	P4	2	1	0	0	0	0
Homo naledi	P3	7	7	0	0	0	0
Homo naledi	P4	6	6	0	0	0	0
Homo neanderthalensis	P3	10	0	0	10	0	0
Homo neanderthalensis	P4	17	0	0	1	0	0
Homo sapiens	P3	24	11	1	0	0	0
Homo sapiens	P4	17	3	0	0	0	0
Paranthropus robustus	P3	5	3	0	0	0	5
Paranthropus robustus	P4	4	3	0	0	0	3
Australopithecus africanus	P3		10%	80%		90%	50%
Australopithecus africanus	P4		44%	33%		56%	56%
Homo sapiens (Qafzeh)	P3				33%		
Homo sapiens (Qafzeh)	P4						
Homo erectus	P3		100%				
Homo erectus	P4		100%				
Homo heidelbergensis	P3		100%				
Homo heidelbergensis	P4		50%				
Homo naledi	P3		100%				
Homo naledi	P4		100%				
Homo neanderthalensis	P3				100%		
Homo neanderthalensis	P4						
Homo sapiens	P3		46%				
Homo sapiens	P4		18%				
Paranthropus robustus	P3		60%				100%
Paranthropus robustus	P4		75%				75%

A. africanus has the most prominent mesial and distal ridges on the buccal surface of the EDJ. 90% of the third upper premolars and 77% of the fourth upper premolars have moderate or prominent ridges. In addition, 90% of *A. africanus* third upper premolars have a buccal cingulum extension. *P. robustus* has less prominent ridges on the buccal surface of the EDJ but 100% of third upper premolars and 75% of fourth upper premolars have a shelf-like lingual cingulum extension. A boss like buccal cingulum is present in all *H. neanderthalensis* third upper premolar and in one third (one tooth) of the Archaic *H. sapiens* (Qafzeh) third upper premolars. *H. neanderthalensis* and the Qafzeh hominins are also distinguished by a lack of ridges on the buccal surface of the EDJ. Modern *H. sapiens* has moderately developed ridges on 46% of third upper premolars and 18% of fourth upper premolars in this sample.

Table 5.7.3 Counts and percentages of the transverse crest of the EDJ. (Blank cells are less than 1%).

Species	Tooth	Sample size	CTC	MTC	BMR	CTC %	MTC %	BMR %	TTC	TTC %
Australopithecus africanus	P3	10	2	4	1	20	40	10	7	70
Australopithecus africanus	P4	9	1	5	0	11	56		6	67
Homo sapiens (Qafzeh)	P3	3	1	0	0	33			1	33
Homo sapiens (Qafzeh)	P4	3	2	1	0	67	33		3	100
Homo erectus	P3	2	2	0	0	100			2	100
Homo erectus	P4	2	2	0	0	100			2	100
Homo heidelbergensis	P3	1	0	1	0		100		1	100
Homo heidelbergensis	P4	2	0	2	0		100		2	100
Homo naledi	P3	7	0	4	3		57	43	7	100
Homo naledi	P4	6	0	6	0		100		6	100
Homo neanderthalensis	P3	10	9	0	0	90			9	90
Homo neanderthalensis	P4	17	17	0	0	100			17	100
Homo sapiens	P3	24	7	3	0	29	13		10	42
Homo sapiens	P4	17	1	1	1	6	6	6	3	18
Paranthropus robustus	P3	5	0	1	0		20		1	20
Paranthropus robustus	P4	4	0	0	0				0	0
Total		122	44	28	5				77	63%

Key

CTC Central transverse crest
MTC Mesial transverse crest
BMR Bucco-mesial ridge
TTC Total transverse crest

The counts and percentages of transverse crests are given in Table 5.7.3. A transverse crest in the EDJ is a common feature in hominins. *H. erectus* and *H. neanderthalensis* have a central transverse crest in all third and fourth upper premolars (there is one *H. neanderthalensis* tooth in the sample, Krapina 48, which has an atypical, anomalous EDJ with an extra cuspule and no clear transverse crest). *H. naledi* has a mesial transverse crest in all fourth upper premolars and either a mesial transverse crest or a bucco-mesial ridge in all third upper premolars. Archaic *H. sapiens* (Qafzeh) have some kind of transverse crest in all fourth upper premolars but in only 33% of third upper premolars. Modern humans have transverse crests in only one fifth of fourth upper premolars and two fifths of third upper premolars. *A. africanus* has a transverse crest in approximately 70% of both third and fourth upper premolars. *P. robustus* seems to have lost the transverse crest, with none in the fourth premolars in this sample and only one out of five third premolars possessing a (mesial) transverse crest.

The results for the main ridges on the EDJ occlusal surface are tabulated in Table 5.7.4. There is a more complex set of relationships in this table than in the other analysis in this qualitative study. The buccal essential ridge is expressed in over 80 % of teeth from most species. The main exceptions to this are *H. erectus*, in which there is no buccal essential ridge in the two third upper premolars in this study, and the archaic *H. sapiens* (Qafzeh), in which the feature appears in two thirds of P4s and one third of P3s. The expression of the lingual essential ridge is more variable and there is no clear pattern across the hominin species. The bucco-mesial ridge is strongly associated with *H. naledi* P3s. The expression of the distal and mesial buccal accessory ridges in most species does not differ much from the mean frequencies in hominins as a whole – 40% for the distal accessory ridge (DAR) and 20% for the mesial accessory ridge (MAR). Both the *H. erectus* fourth upper premolars in this sample had a DAR and one of them also had an MAR. The DAR is associated with *H. naledi* third upper premolars and modern *H. sapiens* fourth upper premolars and has moderately high expression in both tooth positions in *H. neanderthalensis.*

Table 5.7.4 Counts and percentages of the most prominent ridges on the occlusal surface the EDJ. (Blank cells are less than 1%).

Species	Tooth	Sample size	BER	LER	BMR	DAR	MAR	BER	LER	BMR	DAR	MAR
Australopithecus africanus	P3	10	8	5	1	2	5	80%	50%	10%	20%	50%
Australopithecus africanus	P4	9	8	4	0	1	2	89%	44%		11%	22%
Homo sapiens(Qafzeh)	P3	3	1	1	0	1	1	33%	33%		33%	33%
Homo sapiens(Qafzeh)	P4	3	2	1	0	1	0	67%	33%		33%	
Homo erectus	P3	2	0	0	0	0	0					
Homo erectus	P4	2	2	2	0	2	1	100%	100%		100%	50%
Homo heidelbergensis	P3	1	1	1	0	0	0	100%	100%			
Homo heidelbergensis	P4	2	2	2	0	1	0	100%	100%		50%	
Homo naledi	P3	7	7	1	3	5	0	100%	14%	43%	71%	
Homo naledi	P4	6	6	2	0	1	0	100%	33%		17%	
Homo neanderthalensis	P3	10	10	7	0	6	0	100%	70%		60%	
Homo neanderthalensis	P4	17	12	15	0	9	2	71%	88%		53%	12%
Homo sapiens	P3	24	20	8	0	9	4	83%	33%		38%	17%
Homo sapiens	P4	17	15	8	1	12	7	88%	47%	6%	71%	41%
Paranthropus robustus	P3	5	4	2	0	0	2	80%	40%			40%
Paranthropus robustus	P4	4	4	3	0	1	0	100%	75%		25%	
Total		122	102	62	5	51	24	84%	51%	4%	42%	20%

Key

BER Buccal essential ridge
LER Lingual essential ridge
BMR Bucco-mesial ridge
DAR Distal (Buccal) accesory ridge
MAR Mesial (Buccal) accessory ridge

Table 5.7.5 Counts and percentages of features suggesting molarisation of premolars. (Blanks indicate a percentage of less than 1%)

Species	Tooth	Sample Size	Distal acc. Buccal horn	Distal acc. Lingual horn	Oblique ridge	Distal acc. Buccal horn	Distal acc. Lingual horn	Oblique ridge
Australopithecus africanus	P3	10	3	0	0	30%		
Australopithecus africanus	P4	9	6	1	2	67%	11%	22%
Paranthropus robustus	P3	5	3	0	2	60%		40%
Paranthropus robustus	P4	4	4	3	3	100%	75%	75%
Total		28	16	4	7	57%	14%	25%

Table 5.7.5 tabulates the counts and percentages of those traits which suggest incipient molarisation. Perhaps the best single indicator of 'molarisation' is the presence of a distal lingual accessory buccal dentine horn and in *P. robustus* this is seen in 75% of fourth upper premolars. In *A. africanus* it occurs in 11% of fourth upper premolars. These traits are more frequently seen (and more prominent) in fourth upper premolars than in third upper premolars.

5.7.3 Qualitative morphometrics: Multidimensional scaling of group mean percentages of the qualitative features.

All the qualitative traits in this study were combined into a single analysis. The Mahalanobis D^2 distance between the group means (expressed as percentages) was calculated. This was then plotted by using multidimensional scaling to find the directions in the sample space which most accurately reflect these distances. The first dimension accounts for 74% of the total squared distance and the second dimension for a further 12%. In this plot, there is reasonably good separation between species. *H. sapiens* populations (both fossil and modern) lie together near the origin. *H. naledi* is in the bottom right of the plot *and H. neanderthalensis* in the top right. *P. robustus* lies far to the left of the plot. *A. africanus* is separated from the other species in the third dimension of the plot.

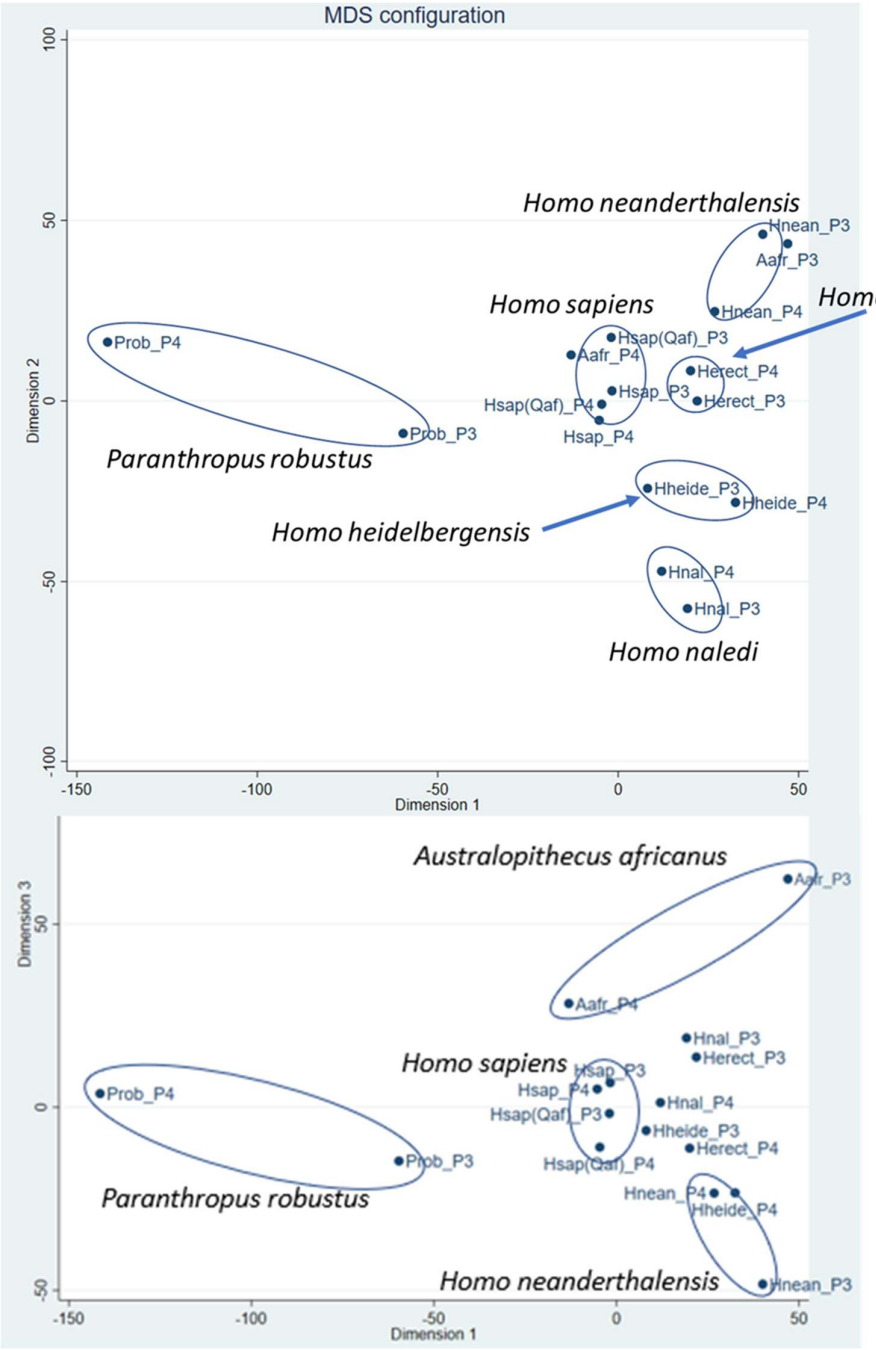

Figure 5.7.8 Multidimensional scaling of the Mahalanobis D^2 distances between group means.

5.7.4 Summary of the qualitative analysis.

Table 5.10.1 summarizes the major associations (generally > 50%) between morphological characteristics and each category of tooth position by species.

Table 5.7.6 Summary of associations between morphological characteristics and tooth category (species combined with tooth position)

Species	Tooth	Associated characteristics.
Australopithecus africanus	P3	Prominent ridges on the buccal surface; extended buccal cingulum; (mesial) transverse crest; buccal essential ridge.
Australopithecus africanus	P4	Moderate to prominent buccal ridges; buccal and lingual cingulum extension; transverse crest; buccal essential ridge.
Homo sapiens (Qafzeh)	P3	Mesial EDJ ridge notch and bulge;
Homo sapiens (Qafzeh)	P4	Distal accessory buccal dentine horn; transverse crest; buccal essential ridge
Homo naledi	P3	Mesial bulge in EDJ ridge; distal accessory buccal dentine horn; moderate ridges on buccal surface; mesial transverse crest OR bucco-mesial ridge; buccal essential ridge
Homo naledi	P4	Distal accessory buccal dentine horn; moderate ridges on buccal surface; mesial transverse crest; buccal essential ridge
Homo neanderthalensis	P3	Notch and bulge on mesial EDJ ridge; boss-shaped bulge on buccal cingulum; (central) transverse crest; distal and buccal essential ridges; distal (buccal) accessory ridge
Homo neanderthalensis	P4	Distal buccal shoulder; (central) transverse crest (100%); distal and buccal essential ridges; distal (buccal) accessory ridge
Homo sapiens	P3	Mesial notch and bulge on mesial EDJ ridge; moderate ridges on buccal surface; buccal essential ridge
Homo sapiens	P4	Distal buccal horn; buccal and lingual essential ridges; distal (buccal) accessory ridge
Paranthropus robustus	P3	Distal accessory buccal horn; lingual cingulum extension; buccal and lingual essential ridges;
Paranthropus robustus	P4	Distal accessory buccal horn (100%); distal accessory lingual horn; oblique crest; lingual cingulum extension; buccal and lingual essential ridges

Some features of the hominin upper premolar EDJ have the potential to distinguish between hominin taxa and tooth positions. For example, in third upper premolars of the genus *Homo* there are associations with a notch and 'bulge' in the mesial EDJ ridge together with a depression or concavity in the mesial surface of the EDJ (except for *H. naledi* where there is a bulge but no notch); fourth upper premolars of all hominin species have a tendency to form a distinct distal accessory buccal dentine horn, except for *H. neanderthalensis*, where there is a distinctive distal buccal shoulder instead; *A. africanus* teeth are associated with prominent ridges on the buccal surface of the

tooth together with extension of the buccal cingulum and lingual cingulum but *P. robustus* is more strongly associated with a shelf-like lingual cingulum; third upper premolars of *H. neanderthalensis* have a distinctive boss-shaped bulge in the buccal cingulum. *P. robustus* and, to a lesser extent *A. africanus*, show a tendency towards molarisation, with an oblique ridge, distal accessory lingual dentine horn and talon extension. A transverse crest is almost universally present in the EDJs of all *Homo* species except for *H. sapiens* (both fossil and modern) and in *H. naledi*, where there is a distinctive bucco-mesial ridge in place of the transverse crest in 43% of third upper premolars.

5.8 Anomalies.

Some anomalies were noted during the examination of the EDJs for the qualitative analysis. In three specimens of *H. naledi*, one *H. sapiens* and one *A. africanus*, the buccal dentine horn was spatulate (spade-like) or bifid (forked) in appearance. (Fig. 5.8.1)

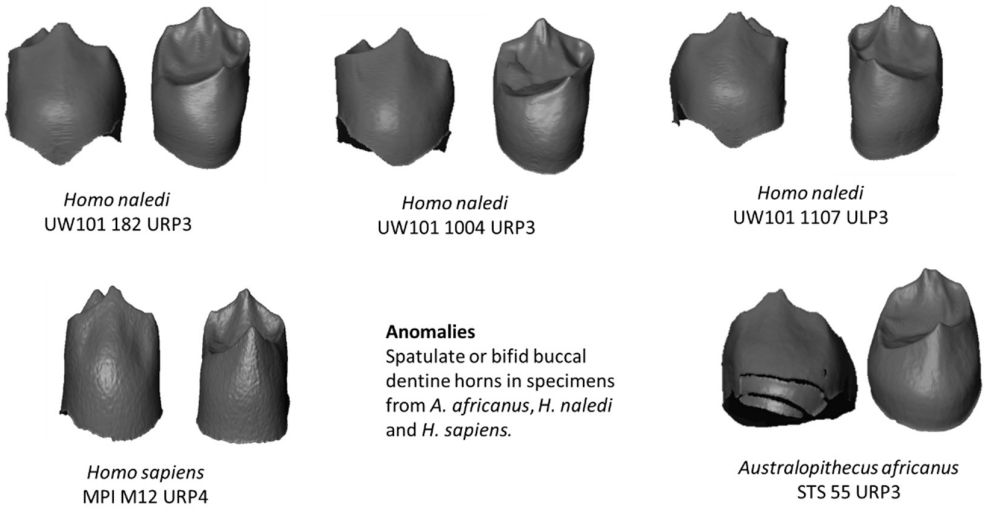

Figure 5.8.1 anomalies of the buccal dentine horn.

The third upper premolar of the *H. neanderthalensis* Krapina 48 maxilla is unusual in two ways. Firstly, it is the only *H. neanderthalensis* specimen in this entire sample which does not possess a continuous transverse crest on the occlusal surface of the EDJ. Secondly, it possesses a large cuspule in the mesio-buccal part of the cingulum. In the EDJ, this forms a distinct structure with its own dentine horn (Fig. 5.8.2)

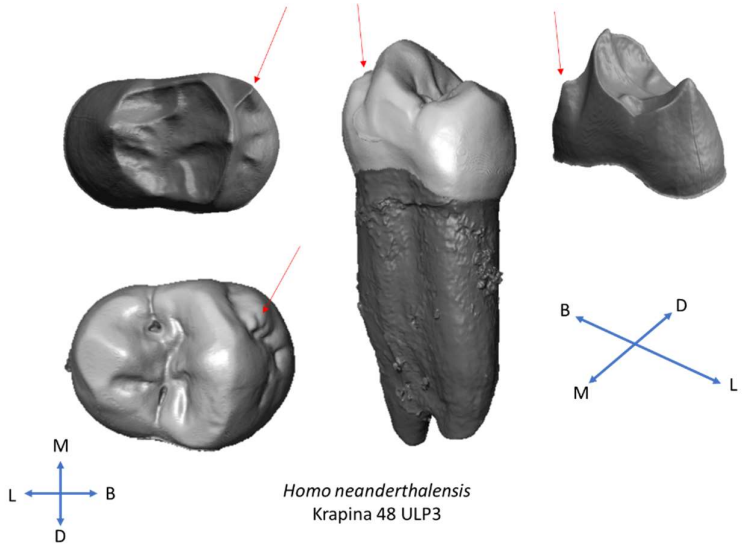

Figure 5.8.2 The Krapina 48 upper left third premolar, showing a cuspule in the mesio-buccal cingulum.

6 DISCUSSION

6.1 Geometric Morphometric trends in hominin upper premolars.

As an initial observation, the simplicity and the similarity in structure of all hominin upper premolars is of benefit for landmark based geometric morphometric analysis. Landmarks can be placed with certainty on corresponding landmarks in each specimen, such as the buccal and lingual dentine horns and morphometric trends can be clearly visualized and interpreted.

The morphometric and allometric trends in EDJ shape reported in this study are consistent with previous morphometric studies of hominin upper premolars. For example, Gómez-Robles *et al.* (2011) performed 2D geometric morphometric analysis of the OES occlusal outline, cusp and fovea positions. They identified "a gradient consisting of an acquisition of a symmetric shape and a reduction of the lingual cusp" (p. 700) from earlier to later hominins. Their 'asymmetric' shape corresponds to what I have described here as a mesially placed buccal dentine horn with disto-lingual expansion of the talon. Their 'symmetric' shape corresponds with a tall buccal dentine horn, centrally placed on the buccal ridge, and a more triangular outline.

In a survey of middle Pleistocene East Asian hominins by Pan *et al.* (2020) using diffeomorphic surface mapping, similar trends are also seen. Although their terminology is different, the findings are like those of the present study. In both third and fourth upper premolars, in their Chinese *H. erectus* sample the EDJ shape was short in height and broad in bucco-lingual width and was separated in the PC plot from the *H. neanderthalensis* and *H. sapiens* sample, where the EDJ was taller and thinner. The *H. erectus* EDJ also had a relatively smaller, more central occlusal basin. *H. neanderthalensis* was slightly broader in mesio-distal width than *H. sapiens* (as is also seen in Figures 5.6.4 and 5.6.5 in this study). They report "a general trend toward a reduction of crown base in relation to occlusal aspects, narrowed lingual aspects, heightened EDJ relief and surface simplification" (p. 8) and these trends are all consistent with the trends reported in this study of a taller, thinner shape and of reduction of the disto-lingual portion of the EDJ in more recent species of *Homo*.

The comparative geometric morphometric study by Détroit *et al.* (2019) of the upper premolars of *Homo luzonensis* used landmarks on just the EDJ ridge. Their principal component analysis (reported in the Supplementary Materials) does show a weak trend from modern humans towards fossil *H. sapiens*, *H. neanderthalensis* and *H. erectus* in a broad general direction, along the diagonals of Détroit *et al.*'s PC plots. The Krapina Neanderthal sample and Qafzeh fossil *H. sapiens* sample used in Détroit *et al.*'s study overlaps extensively with my own sample in which there is a stronger morphometric trend. This may be because the relative distance between the EDJ and the CEJ contributes quite strongly to the morphometric trend in my study and this is not captured by landmarking just the EDJ ridge. *H. luzonensis* and *H. floresiensis* do not lie close to any of the other hominins in Détroit *et al.*'s comparative sample. Looking at the morphology of their EDJs (Figure 2, p. 183; Figure 4, p. 184), *H. luzonensis*, and to a lesser extent *H. floresiensis* have EDJ surfaces which are short and broad, especially in

the bucco-lingual direction, with prominent disto-lingual expansion of the EDJ ridge. That is, they appear to lie towards the *Paranthropus, Australopithecus* and *H. naledi* end of the morphological spectrum reported in my study. It is possible that these EDJs are like the EDJs of more primitive hominins than were included in the original comparative sample.

The morphometric trend that I have described as 'disto-lingual talon expansion', is also consistent with the frequency of expression of the qualitative trait of fourth upper premolar 'lingual crown development'. This is defined by Kaifu *et al.* (2015) as the ratio of the maximum mesio-distal diameter of the lingual part of the tooth to that of the buccal part of the tooth.[8] Kaifu regards the expanded lingual cusp as primitive because it is frequently seen in *Australopithecus, Paranthropus* and *Homo habilis* but is rare in modern *H. sapiens*. He reports (Kaifu *et al.*, 2015) a higher frequency of the trait in *H. habilis*, the Dmanisi population of *Homo* and early Javanese *H. erectus* than in modern *H. sapiens*. In *H. floresiensis* the buccal and lingual parts of the tooth are equal in size. Two thirds of his small sample of East Asian mid to late Pleistocene fossil *Homo* specimens showed the advanced condition of lingual reduction.

6.2 The discriminatory power of geometric morphometrics of the EDJ.

The cross-validated discriminant analysis in the Gómez-Robles *et al*. (2011) 2D geometric morphometric study of the OES correctly identified 78% of modern human and 35% of Neanderthal third upper premolars and 79% of modern human and 46% of Neanderthal fourth upper premolars. The cross-validated correct prediction rate across all species and tooth positions in my study is 84%, suggesting that 3D geometric morphometric analysis of the EDJ may have greater discriminatory power than a 2D analysis of the OES (but the Gómez-Robles *et al.* sample included a higher proportion of *Homo* species, which is where my own study performed most poorly).

In the Davies *et al.* (2019) study of hominoid third lower premolars the overall correct classification rate for a linear discriminant analysis (LDA/CVA) of the combined landmarked EDJ and CEJ was 88% but analysis of the EDJ alone performed almost as well at 87%. The CEJ alone had a correct classification rate of only 69% but this improved to 80% with the addition of a single landmark on the metaconid dentine horn. This study compares well with the results of Davies *et al.* even though the morphological variation in hominin fourth upper premolars appears to casual observation to be much less than the morphological variation in the third lower premolar.

Pan *et al.* (2020) did not report a global correct prediction rate for their diffeomorphic surface matching (DSM) study of upper premolars in *Homo* species but for individual groups their leave-one-out cross-validated rates for between-group PCA (bgPCA) ranged from 80% to 100%. In their study, group separation is wide and correct group

[8] Note that, although Kaifu regards this as a qualitative trait and has turned it into a binary variable, it is a dimensionless ratio between two lengths, which can be regarded as an index of shape!

prediction rates for most species are high. This may be due to the sample not containing intermediate forms or it may be that DSM can pick up features of the EDJ surface which are not captured by landmarking, as suggested by Braga *et al.* (2019). For example, the landmarking of my study does not pick up features on the buccal and lingual surfaces of the EDJ such as marginal ridges and cingulum structures which have been shown in my qualitative analysis to differentiate between species.

6.3 *Homo naledi*

In *H. naledi* the fourth upper premolar is larger than the third upper premolar, as in *A. africanus* and *P. robustus*, but in contrast with other species of *Homo* where the third upper premolar is larger than the fourth upper premolar.

This pattern of relative upper premolar size was noted by Robinson (1956) who observed that the fourth upper premolar was larger than the third in *Paranthropus* and *Australopithecus*, that in *H. erectus* the teeth are similar in size and that in a sample of modern human populations the fourth upper premolar is slightly smaller than the third. He postulated that the larger fourth upper premolar was the primitive condition for the hominins and that the smaller fourth upper premolar is a derived condition in *Homo*.

In the lower premolars, this size ratio has been a subject of interest (de Castro and Nicolás, 1996). The pattern is generally like that in upper premolars. It has been postulated that the size of the fourth lower premolar relative to the third represents differences in size between the anterior teeth and the molars. Essentially, it is claimed that the third lower premolar varies in size with the anterior tooth field and the fourth lower premolar varies with the molar field. In *H. naledi*, however, the third lower premolar is larger than the fourth, as is seen mostly in modern human populations (Davies *et al.* 2020). This contrasts with the size ratio of the *H. naledi* upper premolars found in this study, using the same measure of centroid size.

The other species in this study show a strong allometric trend but *H. naledi* is not on the trend line. In size, *H. naledi* is like fossil species of *Homo* but in shape it resembles more closely the larger teeth of *Australopithecus* and *Paranthropus*. It also has some unique morphological features; the tall distal accessory buccal dentine horn and the short main buccal dentine horn make the EDJ ridge, and hence, the occlusal surface of the EDJ, have a broad and relatively flat appearance when compared with other hominins. In short, *H. naledi* has a unique and highly distinctive shape and form within the hominins.

Not surprisingly, these morphological features match very closely with the features of the *H. naledi* lower premolars (Davies *et al.* 2020), which are in occlusion with the upper premolars. There is a tall, well developed metaconid (lingual dentine horn) in both the third and fourth lower premolar and mesio-distal extension of the occlusal surface in the fourth lower premolar. Both lower premolars have strongly developed mesial marginal ridges. The overall effect is for the occlusal surface of the EDJ to be relatively broad and flat. (By 'flat' I mean that the dentine horns and EDJ ridges are relatively similar in height, compared with other hominins)

Within the genus *Homo*, there has been a trend over time for the upper premolars to become smaller due to lateral compression of EDJ shape, especially in bucco-lingual width. The EDJ has become taller and thinner in overall shape with taller, sharper cusps and ridges at the occlusal surface of the EDJ. The disto-lingual part of the EDJ ridge has diminished, leading to a more triangular outline of the EDJ ridge, especially in third upper premolars. In contrast, *H. naledi* teeth have become smaller whilst largely

retaining their primitive shape. It is feasible that *H. naledi* initially followed the same pattern of size reduction as in other species of *Homo* and then subsequently the teeth became flatter and expanded disto-lingually but this is a less parsimonious and more unlikely explanation.

In addition to these primitive features of the EDJ, *H. naledi* teeth have thick enamel, comparable to *Paranthropus* or to early *Homo* in thickness (Skinner, Lockey *et al.,* 2016) and it has retained multiple roots – whereas in *Homo* as a genus there has been a tendency over time to a reduction in the number of roots to one or two roots for third premolars and one for fourth premolars (Irish *et al.*, 2018). Furthermore, *H. naledi* has a similar body size and brain size to *Australopithecus* species (Garvin *et al.*, 2017) but lacks the large bony attachments, strong skull ridges and wide zygomatic arches which are associated with large, powerful masticatory muscles in those species (Berger *et al*., 2015). Therefore, *H. naledi* was unlikely to have generated strong crushing forces or to have processed large masses of fibrous foods[9].

It does seem likely, in view of the unique morphology of its upper premolars, that *H. naledi* had a different diet to the other members of the genus *Homo*, at least in times of food scarcity, which seems to be the main driver for dental evolution in primates (Ungar, 2017). In general, teeth with flatter occlusal surfaces and thick enamel are associated with the crushing or grinding of hard or fibrous foods whereas taller teeth with sharper, more prominent crests and ridges are associated with the piercing and slicing of tough foods (Ungar, 2017; Lucas, 2007). It may well be that *H. naledi* used its teeth to crush or grind hard foods. One interesting observation by Towle, Irish and De Groot (2017) is that the teeth of *H. naledi* exhibit a high degree of dental chipping in inter-proximal areas and in the posterior teeth and they concluded that a diet containing hard or resistant food, or containing contaminants such as grit, was most likely. Berthaume, Delezene and Kupczik (2018) found that the second lower molar of *H. naledi* was higher crowned and more wear resistant than *Paranthropus* or *Australopithecus*. They hypothesized that these taxa all consumed food with similar fracture properties. Further studies of tooth microwear and stable isotope studies may help to elucidate the dietary adaptations of *H. naledi*.

[9] Although we must remember from basic physics that pressure is the force generated divided by the area over which it is applied, so a smaller muscular force exerted over a smaller occlusal area may still generate a high pressure at the occlusal surface.

6.4 Qualitative morphometrics

Several features of the EDJ surface have been identified in this study which discriminate well between species and tooth position. Some of these were previously described by Sakai *et al.* (1967b) in a modern human Japanese population. They noted that the ridges on the buccal surface of the EDJ, which they called 'marginal ridges' tend to be more prominent in the mesial border of the EDJ and observed rates for moderate to prominent expression of this feature of 58% in third upper premolars and 21 % in fourth upper premolars (46% and 18% in the European population in my study). They observed expression of a moderate or pronounced mesial notch in 43% of third upper premolars and 13% of fourth upper premolars (90% and zero in my study) and they also observed mesial and distal buccal accessory ridges, which had much higher degrees of expression at the OES than at the EDJ – for example, for the distal buccal accessory ridge of the third upper premolar, the rate of expression was 83% at the OES and only 40% at the EDJ (38% at the EDJ in my study)

Of the ASUDAS crown traits (Scott and Irish, 2017), only the premolar accessory ridges (equivalent to my mesial and distal buccal accessory ridges) were observed in the EDJ of any teeth in this study, including the modern human, Western European, sample. These premolar accessory ridges show no clear differences or trends in frequency of expression at the EDJ in fossil hominin species. I did not observe any evidence of accessory cusps on the mesial or distal margins of the EDJ but Irish *et al.* (2018) report accessory cusps in about 15% of *H. naledi* upper premolars at the OES on a sample which overlaps with mine. Sakai *et al.* (1967b) report that the accessory cusps, which they call the 'interstitial tubercles' of the OES are indistinct in the EDJ of modern humans but may correlate with a swelling or protrusion of the EDJ ridge.

The median buccal ridge described by Bailey (Bailey, 2002a; Bailey and Hublin, 2013; Irish *et al.*, 2018)) corresponds to what I have labelled the 'buccal essential ridge', which has high rates of expression (70% - 100%) at the EDJ in nearly all hominins in this study, including modern humans. Rates of expression are also high at the OES, except in modern humans where its frequency of expression may be less than 50% (Irish *et al.,* 2018). This overlaps with Martinón-Torres *et al.'*s (2008, 2012) buccal essential crest trait, which is scored as 'absent', 'present' or 'bifurcated'. (In contrast, Bailey (2002a) scores the prominence of the ridge separately from its bifurcated or non-bifurcated form). This does not seem to correspond well with the EDJ ridges associated with the buccal dentine horn observed in this study. There is often an essential ridge in the EDJ, in all species, and this may have one or more accessory essential ridges (tabulated in Appendix 2). In addition, there may be a transverse crest associated with the buccal dentine horn which is continuous at the EDJ but which is interrupted at the OES. To confound matters further, Martinón-Torres *et al.* (2008, 2012) score the presence of a bifurcated essential crest separately from the transverse crest, but a transverse crest plus a buccal essential ridge at the EDJ often appears as a bifurcated essential crest at the OES. Skinner *et al.* (2008b, 2009b) reported similar discrepancies between the appearance of features at the EDJ and the OES in hominin molars.

The hominin upper premolar transverse crest.

This study found a high prevalence of a continuous transverse crest in the EDJ of both the third and fourth upper premolars of *H. neanderthalensis* and other fossil *Homo* species. The only Neanderthal premolar in the entire sample not to have such a crest is the Krapina 48 maxilla left third upper premolar, which is an abnormal tooth, having a prominent cuspule in the buccal cingulum (Figure 5.8.2). The transverse crest at the EDJ does not correspond with the morphology of the OES, where any potential transverse crest is nearly always interrupted by a sagittal notch or groove. When I inspected the OES of the Neanderthal teeth in this sample, I could only identify a possible transverse crest in two or three specimens, and even in these teeth it was equivocal.

My own observations of the OES in this sample are consistent with low frequencies of expression of an upper premolar transverse crest reported in previous studies. Martinón-Torres *et al.* (2012) reported no transverse crests in third upper premolars and 6% (one individual) in fourth upper premolars in their sample of Neanderthals with frequencies of less than 10% in other *Homo* species. Liao *et al.* (2019) found transverse crests in 7% of upper third premolars and 12% of upper fourth premolars in their Neanderthal sample.

This finding is consistent with the results of Davies *et al.* (2019b). They found that in the lower third premolar of *P. robustus*, *A. africanus* and *H. naledi* a transverse crest was ubiquitous in the EDJ, whereas Irish *et al.* (2018) reported no transverse crest in the OES of any *A. africanus* or *H. naledi* specimens nor in a third of *P. robustus* specimens, in samples which overlapped in the two studies. They concluded that the appearance of this trait differs between the EDJ and the OES and observed that in the OES the transverse crest is often incised by a longitudinal fissure – which runs between the two cusps of the tooth in a mesio-distal direction. They point out that the longitudinal fissure is an OES feature, dependent on such factors as cusp position and enamel thickness, having no EDJ equivalent. They suggest that the lack of dependence of the transverse crest at the EDJ on other crown features is an advantage when scoring crown traits.

The lack of correlation between a transverse crest on the EDJ and the appearance of a crest at the OES in *H. neanderthalensis* upper premolars is in stark contrast to the strong association between EDJ morphology and OES morphology in the mid-trigonid crest in the lower molars of *H. neanderthalensis*. (Skinner *et al.*, 2008b; Bailey *et al.*, 2011; de Pinillos *et al.*, 2014). Bailey *et al.* (2011) graded the mid-trigonid crest on a four-point scale (0 to 3) and found a correlation of 0.91 between the score at the EDJ and at the OES over all groups included in their study, with a correlation of 0.86 in *H. neanderthalensis* and 0.77 in modern *H. sapiens*.

Kaifu et al. (*2015*) report that, in their global sample of *H. sapiens* only 2% have a transverse crest at the OES but that it was relatively common in a sample of early Pleistocene *Homo* species; 35% in third upper premolars and 43% of fourth upper premolars (which included *H. habilis* and Javan *H. erectus*). Both the third and fourth upper premolars of *H. floresiensis* have a transverse crest. They regarded the upper

premolar transverse crest as a primitive trait for the genus *Homo*. My study supports that hypothesis. There are high rates of expression of the trait in the EDJ of early to mid-Pleistocene *Homo* species. The trait seems to have diminished in frequency in modern *H. sapiens* but to have become nearly universal in *H. neanderthalensis*, possibly as a result of genetic drift, as proposed in Hublin's (2009) 'accretion model' for the origin of Neanderthals. Genetic drift is also suggested by Weaver (2007) as a mechanism for differences in Neanderthal and modern human cranial morphology. A transverse crest, possibly mesially placed, also seems likely to have been present in the upper premolars of the last common ancestor of *Australopithecus* and *Paranthropus* but to have been mostly lost in *P. robustus*.

The finding of high frequencies of transverse crests in the EDJs of Neanderthal upper premolars also raises the question of the relationship between these transverse crests, the transverse crest of the fourth lower premolar and the mid-trigonid crests of the lower molars, both of which have high frequencies of expression in *H. neanderthalensis* (Bailey, 2002).

The high rate of expression of a transverse crest in the upper premolar EDJ of *H. neanderthalensis* and other hominins is unexpected. It is important for two reasons. Firstly, it very unusual for such a major feature not to correlate in expression between the EDJ and the OES. It provides a rare example of enamel secretion and accumulation creating morphology (an interruption of the transverse crest) at the OES which is not present at the EDJ. Secondly, it appears to be a primitive hominin trait which has a high degree of expression in early *Homo* and in *H. neanderthalensis* but which is much less frequent in modern *H. sapiens.*

7 FURTHER WORK

This study has shown that geometric morphometrics of the upper premolar EDJ, using landmarks on the EDJ ridge and the CEJ, is effective in identifying hominin species and tooth position within species. This methodology can be extended to explore relationships between the morphology of the upper premolar EDJ in other hominin taxa, especially early to mid-Pleistocene species of *Homo*, which are under-represented in the current sample. This would also enable the creation of a comparative database of landmarked EDJs which would be helpful in identifying and assessing new fossil finds. In short, there is a need to fill in the gaps in the current comparative sample and to extend its geographical and temporal range. The sample could also be extended to cover living and fossil Hominoids with a view to exploring the relationships between living and fossil Hominoids, including the origin of the hominin clade.

The qualitative morphometric study carried out here is an exploratory study, which has identified several morphological features of the EDJ surfaces of upper premolars which have the potential to distinguish between hominin species and between tooth position within species. These need to be defined and described more rigorously, including studies of test-retest and inter-observer reliability. Further studies need to be carried out to identify those traits or characteristics which have the greatest power to discriminate between species.

This study has identified that there is often a continuous transverse crest on the occlusal surface of the EDJ associated with an interrupted transverse crest at the outer enamel surface (OES). A transverse crest at the EDJ may be interpreted as a bifurcated essential ridge at the OES. In addition, there is a difference in taxonomic associations between central transverse crests and mesial transverse crests. Further studies need to be carried out to study the upper premolar transverse crest, including differences in expression of the transverse crest at the EDJ and the OES.

In this study, based on EDJ morphology, some upper premolars seem to have been misidentified as to their tooth position and one maxilla (STS 61) seems to have been misidentified as to species. These specimens need to be re-examined and re-assessed in the context of other dental features and archaeological associations to establish their most likely attribution given these new observations.

8 CONCLUSION

This study has confirmed certain morphological trends in hominin upper premolars which were known from previous studies of the OES and a small number of studies of the EDJ. It has expanded the analysis of the EDJ to a wider range of hominins than previously studied, has systematically described morphological trends in the EDJ and has identified for the first time that there is an allometric trend in hominin upper premolar morphology. It has confirmed that morphometric geometrics of the upper premolar EDJ is able to discriminate well between hominin taxa and between tooth position within taxa.

The findings on the premolar teeth of *H. naledi* have added to the evidence for the uniqueness of this species. It has primitive features of tooth morphology, such as the fourth upper premolar being larger than the third premolar, disto-lingual expansion of the talon and a relatively broad and flat overall shape. The main modern feature of the upper premolars is their small size. They also have some unique features, such as the short main buccal dentine horn and prominent distal accessory buccal dentine horn. These findings are consistent with the hypothesis that *H. naledi* divided from the main line of evolution within the genus *Homo* early, retaining a lot of primitive features, and then survived for a long time alongside other species of *Homo* by successful adaptation to its own specialised ecological niche.

This study has identified several features of the EDJ which discriminate between species and between tooth position within species. Some features are more commonly expressed or more prominent at the OES than they are at the EDJ – for example, an interruption in the transverse crest and the expression of buccal accessory ridges. More commonly, features are expressed more frequently or more clearly at the EDJ than at the OES. Furthermore, features which differ in EDJ morphology may have a common appearance at the OES. This confirms the value of studying the features of the hominin upper premolar EDJ, both in themselves and in comparison with the OES.

9 REFERENCES.

Adams, D.C., Rohlf, F.J. and Slice, D.E., 2004. Geometric morphometrics: ten years of progress following the 'revolution'. *Italian Journal of Zoology*, *71*(1), pp.5-16.

Anemone, R.L., Skinner, M.M. and Dirks, W., 2012. Are there two distinct types of hypocone in Eocene primates? The 'pseudohypocone' of notharctines revisited. *Palaeontologia Electronica*, 15(3), pp.1-13.

Bailey, S.E., 2000. Dental morphological affinities among late Pleistocene and recent humans. *Dental Anthropology* 14, 1-8.

Bailey, S.E., 2002a. *Neandertal dental morphology: implications for modern human origins*. Ph.D. Dissertation, Arizona State University.

Bailey, S.E., 2002b. A closer look at Neanderthal postcanine dental morphology: the mandibular dentition. *The Anatomical Record*, *269*(3), pp.148-156.

Bailey, S.E. and Hublin, J.J., 2013. What does it mean to be dentally "modern"? In: Scott, G.R., Irish, J.D. (Eds.), *Anthropological Perspectives on Tooth Morphology: Genetics, Evolution, Variation*. Cambridge University Press, Cambridge, pp. 222e249.

Bailey, S.E. and Liu, W., 2010. A comparative dental metrical and morphological analysis of a Middle Pleistocene hominin maxilla from Chaoxian (Chaohu), China. *Quaternary international*, *211*(1-2), pp.14-23.

Bailey, S.E. and Wood, B.A., 2007. Trends in postcanine occlusal morphology within the hominin clade: the case of Paranthropus. In *Dental perspectives on human evolution: state of the art research in dental paleoanthropology* (pp. 33-52). Springer, Dordrecht.

Bailey, S.E., Skinner, M.M. and Hublin, J.J., 2011. What lies beneath? An evaluation of lower molar trigonid crest patterns based on both dentine and enamel expression. *American Journal of Physical Anthropology*, 145(4), pp.505-518.

Begun, D. R., 2016. *The Real Planet of the Apes*. Princeton NJ, Princeton University Press.

Begun, D.R., Nargolwalla, M.C. and Kordos, L., 2012. European Miocene hominids and the origin of the African ape and human clade. *Evolutionary Anthropology: Issues, News, and Reviews*, 21(1), pp.10-23.

Benton, M. J., 2015. *Vertebrate Palaeontology* (4th ed.). Chichester, Wiley Blackwell.

Berger, L. R. and Hawkes, J., 2017. *Almost Human*. Washington DC, National Geographic Partners.

Berger, L.R., Hawks, J., de Ruiter, D.J., Churchill, S.E., Schmid, P., Delezene, L.K., Kivell, T.L., Garvin, H.M., Williams, S.A., DeSilva, J.M. and Skinner, M.M., 2015. Homo naledi, a new species of the genus Homo from the Dinaledi Chamber, South Africa. *elife*, *4*, p.e09560.

Berkovitz, B. K. B., Holland, G. R. and Moxham, B. J., 2018. *Oral Anatomy, Histology and Embryology* (5th ed.). London, Elsevier Health Sciences.

Berkovitz, B, and Shellis, P., 2018. *The Teeth of Mammalian Vertebrates*. London, Academic Press.

Berthaume, M.A., Delezene, L.K. and Kupczik, K., 2018. Dental topography and the diet of Homo naledi. *Journal of human evolution*, *118*, pp.14-26.

Bookstein, F.L., 1997. *Morphometric tools for landmark data: geometry and biology*. Cambridge University Press.

Bookstein, F.L., 2018. *A course in morphometrics for biologists: geometry and statistics for studies of organismal form*. Cambridge University Press.

Braga, J., Thackeray, J.F., Subsol, G., Kahn, J.L., Maret, D., Treil, J. and Beck, A., 2010. The enamel–dentine junction in the postcanine dentition of Australopithecus

africanus: intra-individual metameric and antimeric variation. *Journal of Anatomy*, *216*(1), pp.62-79.

Braga, J., Zimmer, V., Dumoncel, J., Samir, C., De Beer, F., Zanolli, C., Pinto, D., Rohlf, F.J. and Grine, F.E., 2019. Efficacy of diffeomorphic surface matching and 3D geometric morphometrics for taxonomic discrimination of Early Pleistocene hominin mandibular molars. *Journal of Human Evolution*, *130*, pp.21-35.

Burnett, S.E., Irish, J.D. and Fong, M.R., 2013. Wear's the problem? Examining the effect of dental wear on studies of crown morphology. In Scott, G.R. and Irish, J.D. eds., *Anthropological perspectives on tooth morphology: genetics, evolution, variation*. Cambridge University Press.

Butler, P.M., 1956. The ontogeny of molar pattern. *Biological Reviews* 31, 30-70.

de Bonis, L. and Koufos, G.D., 1994. Our ancestors' ancestor: Ouranopithecus is a Greek link in human ancestry. *Evolutionary Anthropology: Issues, News, and Reviews*, 3(3), pp.75-83.

Carroll, S.B., Grenier, J.K. and Weatherbee, S.D., 2013. *From DNA to diversity: molecular genetics and the evolution of animal design*. John Wiley & Sons.

de Castro, J.B. and Nicolás, M.E., 1996. Changes in the lower premolar-size sequence during hominid evolution. Physlogenetic implications. *Human evolution*, *11*(3), pp.205-215.

Collard, M. and Wood, B., 2000. How reliable are human phylogenetic hypotheses? *Proceedings of the National Academy of Sciences,* 97(9), pp.5003-5006.

Collard, M. and Wood, B., 2001. Homoplasy and the early hominid masticatory system: inferences from analyses of extant hominoids and papionins. *Journal of Human Evolution*, *41*(3), pp.167-194.

Compton, T., Skinner, M.M., Humphrey, L., Pope, M., Bates, M., Davies, T.W., Parfitt, S.A., Plummer, W.P., Scott, B., Shaw, A. and Stringer, C., 2021. The morphology of the Late Pleistocene hominin remains from the site of La Cotte de St Brelade, Jersey (Channel Islands). *Journal of Human Evolution*, *152*, p.102939.

Corruccini, R.S., 1987. The dentino-enamel junction in primates. *Int. J. Primatol*. 8, 99114.

Corruccini, R.S., 1998. The dentino-enamel junction in primate mandibular molars. In: Lukacs, J.R. (Ed.), *Human Dental Development, Morphology, and Pathology: A Tribute to Albert A. Dahlberg*. Portland, University of Oregon Anthropological Papers. pp. 1-16.

Darwin, C. R., 1845. *The Voyage of the Beagle*.

de Pinillos, M.M., Martinón-Torres, M., Skinner, M.M., Arsuaga, J.L., Gracia-Téllez, A., Martínez, I., Martín-Francés, L. and de Castro, J.M.B., 2014. Trigonid crests expression in Atapuerca-Sima de los Huesos lower molars: Internal and external morphological expression and evolutionary inferences. *Comptes Rendus Palevol*, 13(3), pp.205-221.

Davies, T.W., Delezene, L.K., Gunz, P., Hublin, J.J. and Skinner, M.M., 2019a. Endostructural morphology in hominoid mandibular third premolars: Geometric morphometric analysis of dentine crown shape. *Journal of human evolution*, *133*, pp.198-213.

Davies, T.W., Delezene, L.K., Gunz, P., Hublin, J.J. and Skinner, M.M., 2019b. Endostructural morphology in hominoid mandibular third premolars: Discrete traits at the enamel-dentine junction. *Journal of human evolution*, *136*, p.102670.

Davies, T.W., Delezene, L.K., Gunz, P., Hublin, J.J., Berger, L.R., Gidna, A. and Skinner, M.M., 2020. Distinct mandibular premolar crown morphology in Homo naledi and its implications for the evolution of Homo species in southern Africa. *Scientific reports*, *10*(1), pp.1-13.

Dembo, M., Matzke, N.J., Mooers, A.Ø. and Collard, M., 2015. Bayesian analysis of a morphological supermatrix sheds light on controversial fossil hominin relationships. *Proceedings of the Royal Society B: Biological Sciences*, *282*(1812), p.20150943.

Delezene, Lucas K., Skinner, Matthew M., Bailey, Shara, Brophy, Juliet K., Irish, Joel D., Moggi-Cecchi, Jacopo, Hawks, J., Berger, Lee R., (In preparation). Dental remains of *Homo naledi* from the 2013–2015 excavations of the Dinaledi Chamber, Site U.W. 101, within the Rising Star Cave system, South Africa

Détroit, F., Mijares, A.S., Corny, J., Daver, G., Zanolli, C., Dizon, E., Robles, E., Grün, R. and Piper, P.J., 2019. A new species of Homo from the Late Pleistocene of the Philippines. *Nature*, *568*(7751), pp.181-186.

Diogo, R. and Wood, B., 2011. Soft-tissue anatomy of the primates: phylogenetic analyses based on the muscles of the head, neck, pectoral region and upper limb, with notes on the evolution of these muscles. *Journal of Anatomy*, *219*(3), pp.273-359.

Dirks, P.H., Roberts, E.M., Hilbert-Wolf, H., Kramers, J.D., Hawks, J., Dosseto, A., Duval, M., Elliott, M., Evans, M., Grün, R. and Hellstrom, J., 2017. The age of Homo naledi and associated sediments in the Rising Star Cave, South Africa. *Elife*, *6*, p.e24231.

Dryden, I.L. and Mardia, K.V., 2016. *Statistical shape analysis: with applications in R*. John Wiley & Sons.

Feeney, R.N., 2009. *Microtomographic analysis of sexual dimorphism and dental tissue distribution in human molars* (Doctoral dissertation, The Ohio State University).

Feeney, R., Olejniczak, A.J. and Hublin, J.J., 2010. Three dimensional microtomographic analysis of sexual dimorphism in human molar-crown tissues.

Feuerriegel, E.M., Green, D.J., Walker, C.S., Schmid, P., Hawks, J., Berger, L.R. and Churchill, S.E., 2017. The upper limb of Homo naledi. *Journal of Human Evolution*, *104*, pp.155-173.

Garvin, H.M., Elliott, M.C., Delezene, L.K., Hawks, J., Churchill, S.E., Berger, L.R. and Holliday, T.W., 2017. Body size, brain size, and sexual dimorphism in Homo naledi from the Dinaledi Chamber. *Journal of Human Evolution*, *111*, pp.119-138.

García-Campos, C., Martinón-Torres, M., Martín-Francés, L., Martínez de Pinillos, M., Modesto-Mata, M., Perea-Pérez, B., Zanolli, C., Labajo González, E., Sánchez Sánchez, J.A., Ruiz Mediavilla, E. and Tuniz, C., 2018. Contribution of dental tissues to sex

determination in modern human populations. *American journal of physical anthropology*, *166*(2), pp.459-472.

García-Campos, C., Modesto-Mata, M., Martinón-Torres, M., de Pinillos, M.M., Martín-Francés, L., Arsuaga, J.L. and de Castro, J.M.B., 2020. Sexual dimorphism of the enamel and dentine dimensions of the permanent canines of the Middle Pleistocene hominins from Sima de los Huesos (Burgos, Spain). *Journal of Human Evolution*, *144*, p.102793.

Gómez-Robles, A., Martinón-Torres, M., De Castro, J.B., Margvelashvili, A., Bastir, M., Arsuaga, J.L., Pérez-Pérez, A., Estebaranz, F. and Martínez, L.M., 2007. A geometric morphometric analysis of hominin upper first molar shape. *Journal of Human Evolution*, *53*(3), pp.272-285.

Gomez-Robles, A., Martinon-Torres, M., de Castro, J.M.B., Prado, L., Sarmiento, S. and Arsuaga, J.L., 2008. Geometric morphometric analysis of the crown morphology of the lower first premolar of hominins, with special attention to Pleistocene Homo. *Journal of human evolution*, *55*(4), pp.627-638.

Gomez-Robles A., Martinon-Torres M., Bermudez de Castro J.M., Prado-Simon L., Arsuaga J.L., (2011). A geometric morphometric analysis of hominin upper premolars. Shape variation and morphological integration, *Journal of Human Evolution*, 61 (6), pp. 688-702.

Gómez-Robles, A., de Castro, J.M.B., Martinón-Torres, M., Prado-Simón, L. and Arsuaga, J.L., 2012. A geometric morphometric analysis of hominin upper second and third molars, with particular emphasis on European Pleistocene populations. *Journal of Human Evolution*, *63*(3), pp.512-526.

Gómez-Robles, A., de Castro, J.M.B., Martinón-Torres, M., Prado-Simón, L. and Arsuaga, J.L., 2015. A geometric morphometric analysis of hominin lower molars: Evolutionary implications and overview of postcanine dental variation. *Journal of Human Evolution*, *82*, pp.34-50.

Greenacre, M., 2017. *Correspondence analysis in practice*. CRC press.

Gunz, P., Mitteroecker, P., 2013. Semilandmarks: A method for quantifying curves and surfaces. *It. J. Mammal*. 24, 103–109.

Gunz, P., Mitteroecker, P., Bookstein, F.L., 2005. Semilandmarks in Three Dimensions. In: Slice, D. (Ed.), *Modern Morphometrics in Physical Anthropology.* Kluwer Academic/Plenum Publishers, New York, pp. 73–98.

Guy, F., Lazzari, V., Gilissen, E. and Thiery, G., 2015. To what extent is primate second molar enamel occlusal morphology shaped by the enamel-dentine junction? *PLoS One*, *10*(9), p.e0138802. https://journals.plos.org/plosone/article?id=10.1371/journal.pone.0138802 (18/06/2019)

Häkkinen, T.J., Sova, S.S., Corfe, I.J., Tjäderhane, L., Hannukainen, A. and Jernvall, J., 2019. Modelling enamel matrix secretion in mammalian teeth. *PLoS computational biology*, *15*(5), p.e1007058.

Harcourt-Smith, W.E., Throckmorton, Z., Congdon, K.A., Zipfel, B., Deane, A.S., Drapeau, M.S., Churchill, S.E., Berger, L.R. and DeSilva, J.M., 2015. The foot of Homo naledi. *Nature Communications*, *6*(1), pp.1-8.

Harris, E.F. and Sjøvold, T., 2004. Calculation of Smith's mean measure of divergence for intergroup comparisons using nonmetric data. *Dental Anthropology Journal*, *17*(3), pp.83-93.

Hartwig, W.C. ed., 2002. *The primate fossil record*. Cambridge: Cambridge University Press.

Hawks, J., Elliott, M., Schmid, P., Churchill, S.E., de Ruiter, D.J., Roberts, E.M., Hilbert-Wolf, H., Garvin, H.M., Williams, S.A., Delezene, L.K. and Feuerriegel, E.M., 2017. New fossil remains of Homo naledi from the Lesedi Chamber, South Africa. *Elife*, *6*, p.e24232.

Hennig, W., 1965. Phylogenetic systematics. *Annual review of entomology*, 10(1), pp.97-116.

Hillson, S., 2005. *Teeth* (2nd ed.). Cambridge, Cambridge University Press.

Hillson, S., 2014. *Tooth Development in Human Evolution and Bioarchaeology*. Cambridge, Cambridge University Press.

Hublin, J.J., 2009. The origin of Neandertals. *Proceedings of the National Academy of Sciences*, *106*(38), pp.16022-16027.

Hublin, J.J., 2013. Palaeontology: Free digital scans of human fossils. *Nature*, *497*(7448), p.183.

Hunter, J. and Jernvall, J. 1995. The hypocone as a key innovation in mammalian evolution. *Proceedings of the National Academy of Sciences*, USA, 92:10718-10722.

Irish, J.D., 2010. The mean measure of divergence: Its utility in model-free and model-bound analyses relative to the Mahalanobis D2 distance for nonmetric traits. *American Journal of Human Biology*, *22*(3), pp.378-395.

Irish, J.D., Bailey, S.E., Guatelli-Steinberg, D., Delezene, L.K. and Berger, L.R., 2018. Ancient teeth, phenetic affinities, and African hominins: Another look at where Homo naledi fits in. *Journal of human evolution*, *122*, pp.108-123.

Jernvall, J. and Jung, H.S., 2000. Genotype, phenotype, and developmental biology of molar tooth characters. *American Journal of Physical Anthropology*. 113(S31), pp.171-190.

Jernvall, J. and Thesleff, I., 2000. Reiterative signalling and patterning during mammalian tooth morphogenesis. *Mechanisms of development*, 92(1), pp.19-29.

Kaifu, Y., Kono, R.T., Sutikna, T., Saptomo, E.W. and Due Awe, R., 2015. Unique dental morphology of Homo floresiensis and its evolutionary implications. *PloS one*, *10*(11), p.e0141614. [Last accessed 20/02/2021]

Kendall, D.G., 1977. The diffusion of shape. *Advances in applied probability*, *9*(3), pp.428-430.

Kendall, D.G., 1989. A survey of the statistical theory of shape. *Statistical Science*, pp.87-99.

Kitching, I.J., Forey, P., Humphries, C. and Williams, D., 1998. *Cladistics: the theory and practice of parsimony analysis* (No. 11). Oxford University Press, USA.

Kivell, T.L., Deane, A.S., Tocheri, M.W., Orr, C.M., Schmid, P., Hawks, J., Berger, L.R. and Churchill, S.E., 2015. The hand of Homo naledi. *Nature communications*, *6*(1), pp.1-9.

Kono, R.T., 2004. Molar enamel thickness and distribution patterns in extant great apes and humans: new insights based on a 3-dimensional whole crown perspective. *Anthr. Sci*. 112, 121-146.

Korenhof, C.A.W., 1960. *Morphogenetical aspects of the human upper molar. A comparative study of its enamel and dentine surfaces and their relationship to the crown pattern of fossil and recent primates*. Acad. Proefschrift, Utrecht. Uitg. Mij. Neerl. pp.1-368.

Korenhof, C. A. W., 1978. Remnants of the Trigonid Crests in Medieval Molars of Man of Java. In Butler, J. M. and Joysey, K. A. (Eds.), *Development, Function and Evolution of Teeth*. London, Academic Press.

Korenhof, C. A. W.,1982. Evolutionary trends of the inner enamel anatomy of deciduous molars from Sangiran (Java, Indonesia). In Kurtén, B. ed., 1982. *Teeth--form, Function, and Evolution*. New York, Columbia University Press. (pp. 350-365).

Kraus, B. S., 1952. Morphologic relationship between enamel and dentine surfaces of lower first molar teeth. *J. Dent. Res*. 31, 248 – 256.

Kraus, B.S., Jordan, R., 1965. *The Human Dentition Before Birth*. Philadelphia, Lea and Febiger.

Krzanowski, W.J., 1988. *Principles of Multivariate Analysis*. Oxford, Oxford University Press.

Lack, D., 1947. *Darwin's Finches*. Cambridge, Cambridge University Press.

Le Gros Clark, W. E., 1970. *History of the primates*. London, British Museum (Natural History).

Liao, W., Xing, S., Li, D., Martinón-Torres, M., Wu, X., Soligo, C., de Castro, J.M.B., Wang, W. and Liu, W., 2019. Mosaic dental morphology in a terminal Pleistocene hominin from Dushan Cave in southern China. *Scientific reports*, *9*(1), pp.1-14.

Liu, W., Schepartz, L.A., Xing, S., Miller-Antonio, S., Wu, X., Trinkaus, E. and Martinón-Torres, M., 2013. Late middle pleistocene hominin teeth from Panxian Dadong, South China. *Journal of Human Evolution*, *64*(5), pp.337-355.

Lucas, P., 2007. *Dental Functional Morphology*. Cambridge, Cambridge University Press.

Luo, Z.X., Cifelli, R.L. and Kielan-Jaworowska, Z., 2001. Dual origin of tribosphenic mammals. *Nature,* 409(6816), p.53.

Luo, Z.X., Kielan-Jaworowska, Z. and Cifelli, R.L., 2002. In quest for a phylogeny of Mesozoic mammals. *Acta Palaeontologica Polonica*, 47(1).

Macchiarelli, R., Bondioli, L. and Mazurier, A., 2008. Chapter 18. Virtual dentitions: touching the hidden evidence. In Irish, J. D. and Nelson, G. C (Eds). *Technique and application in dental anthropology*. Cambridge, Cambridge University Press. pp.426 – 440.

Marchi, D., Walker, C.S., Wei, P., Holliday, T.W., Churchill, S.E., Berger, L.R. and DeSilva, J.M., 2017. The thigh and leg of Homo naledi. *Journal of Human Evolution*, *104*, pp.174-204.

Martin, L., 1985. "Significance of enamel thickness in hominoid evolution." *Nature* 314(6008): 260-263.

Martin, R. D., 1990. *Primate Origins and Evolution*. Princeton, NJ, Princeton University Press.

Martinón -Torres, M., Bermúdez de Castro, J., Gómez-Robles, A., Arsuaga, J., Carbonell, E., Lordkipanidze, D., Manzi, G., Margvelashvili, A., 2007. Dental evidence on the hominin dispersals during the Pleistocene. *Proceedings of the National Academy of Sciences* USA 104, 13279e13282.

Martinón -Torres, M., Bermúdez de Castro, J., Gómez-Robles, A., Margvelashvili, A., Prado, L., Lordkipanidze, D., Vekua, A., 2008. Dental remains from Dmanisi (Republic of Georgia): morphological analysis and comparative study. *Journal of Human Evolution* 55, 249e273.

Martinón-Torres, M., de Castro, J.M.B., Gómez-Robles, A., Prado-Simón, L. and Arsuaga, J.L., 2012. Morphological description and comparison of the dental remains from Atapuerca-Sima de los Huesos site (Spain). *Journal of Human Evolution*, *62*(1), pp.7-58.

Martinón -Torres, M., Bermúdez de Castro, J.M., Martín-Frances, L., Gracia-Tellez, A., Martinez, I., Arsuaga, J.L., 2013. Dental morphology of European Middle Pleistocene populations. In: Scott, G.R., Irish, J.D. (Eds.), *Anthropological Perspectives on Tooth Morphology: Genetics, Evolution, Variation*. Cambridge University Press, Cambridge, pp. 201-221

Moggi-Cecchi, J. and Boccone, S., 2007. Maxillary molars cusp morphology of South African australopithecines. In *Dental perspectives on human evolution: state of the art research in dental paleoanthropology* (pp. 53-64). Springer, Dordrecht.

Morita, W., Yano, W., Nagaoka, T., Abe, M., Ohshima, H. and Nakatsukasa, M., 2014. Patterns of morphological variation in enamel–dentin junction and outer enamel surface of human molars. *Journal of anatomy*, *224*(6), pp.669-680.

Morita, W., 2016. Morphological comparison of the enamel–dentine junction and outer enamel surface of molars using a micro-computed tomography technique. *Journal of Oral Biosciences*, *58*(3), pp.95-99.

Nager, G., 1960. Der vergleich zwischen dem räumlichen verhalten des dentin-kronenreliefs und dem schmelzrelief der zahnkrone. *Cells Tissues Organs*, *42*(3), pp.226-250.

Olejniczak, A.J., 2006. *Micro-computed tomography of primate molars*. Ph.D.

Dissertation, Stony Brook University.

Olejniczak, A.J., Gilbert, C.C., Martin, L.B., Smith, T.M., Ulhaas, L., Grine, F.E., 2007. Morphology of the enamel-dentine junction in sections of anthropoid primate maxillary molars. *J. Hum. Evol*. 53 (3), 292-301.

Olejniczak, A.J., Grine, F.E., 2005. High-resolution measurement of Neandertal tooth enamel thickness by micro-focal computed tomography. *S. Afr. J. Sci*. 101, 219-220.

Olejniczak, A.J., Grine, F.E., 2006. Assessment of the accuracy of dental enamel thickness measurements using micro-focal X-ray computed tomography. *Anatomical Record A* 288, 263-275.

Olejniczak, A.J., Martin, L.B., Ulhaas, L., 2004. Quantification of dentine shape in anthropoid primates. Ann. Anat. 186, 479-485.

Ortiz, A., Skinner, M.M., Bailey, S.E. and Hublin, J.J., 2012. Carabelli's trait revisited: An examination of mesiolingual features at the enamel–dentine junction and enamel surface of Pan and Homo sapiens upper molars. *Journal of Human Evolution*, 63(4), pp.586-596.

Ortiz, A., Bailey, S.E., Hublin, J.J. and Skinner, M.M., 2017. Homology, homoplasy and cusp variability at the enamel–dentine junction of hominoid molars. *Journal of anatomy*, *231*(4), pp.585-599.

Pan, L., Dumoncel, J., Mazurier, A. and Zanolli, C., 2019. Structural analysis of premolar roots in Middle Pleistocene hominins from China. *Journal of human evolution*, *136*, p.102669.

Pan, L., Dumoncel, J., Mazurier, A. and Zanolli, C., 2020. Hominin diversity in East Asia during the Middle Pleistocene: A premolar endostructural perspective. *Journal of Human Evolution*, *148*, p.102888.

de Pinillos, M.M., Martinón-Torres, M., Martín-Francés, L., Arsuaga, J.L. and de Castro, J.M.B., 2017. Comparative analysis of the trigonid crests patterns in Homo antecessor molars at the enamel and dentine surfaces. *Quaternary International*, *433*, pp.189-198.

Radovčić, J., Smith, F.H., Trinkhaus, E. and Wolpoff, M.H., 1988. *The Krapina Hominids*. Mladost.

Robert S. Sansom, Matthew Albion Wills, Tamara Williams, Dental Data Perform Relatively Poorly in Reconstructing Mammal Phylogenies: Morphological Partitions Evaluated with Molecular Benchmarks, *Systematic Biology*, Volume 66, Issue 5, September 2017, Pages 813–822, https://doi.org/10.1093/sysbio/syw116

Robinson, J. T., 1956. *The Dentition of the Australopithecinae*. Pretoria, The Transvaal Museum.

Rohlf, F.J. and Marcus, L.F., 1993. A revolution morphometrics. *Trends in ecology & evolution*, *8*(4), pp.129-132.

Sakai, T., Hanamura, H., 1971. A morphology study of enamel-dentin border on the Japanese dentition. Part V. Maxillary molar. *J. Anthropol. Soc. Nippon* 79, 297-322. 175

Sakai, T., Hanamura, H., 1973a. A morphology study of enamel-dentin border on the Japanese dentition. Part VI. Mandibular molar. *J. Anthropol. Soc. Nippon* 81, 25-45.

Sakai, T., Hanamura, H., 1973b. A morphology study of enamel-dentin border on the Japanese dentition. Part VII. General conclusion. *J. Anthropol. Soc. Nippon* 81, 87-102.

Sakai, T., Sasaki, I., Hanamura, H., 1965. A morphology study of enamel-dentin borderon the Japanese dentition. Part I. Maxillary median incisor. *J. Anthropol. Soc. Nippon*

73, 91-109.

Sakai, T., Sasaki, I., Hanamura, H., 1967a. A morphology study of enamel-dentin border on the Japanese dentition. Part II. Maxillary canine. *J. Anthropol. Soc. Nippon* 75,155-172.

Sakai, T., Sasaki, I., Hanamura, H., 1967b. A morphology study of enamel-dentin border on the Japanese dentition. Part III. Maxillary premolar. *J. Anthropol. Soc. Nippon* 75, 207-223.

Sakai, T., Sasaki, I., Hanamura, H., 1969. A morphology study of enamel-dentin border on the Japanese dentition. Part IV. Mandibular premolar. *J. Anthropol. Soc. Nippon* 77, 71-98.

Saunders, S.R., Chan, A.H., Kahlon, B., Kluge, H.F. and FitzGerald, C.M., 2007. Sexual dimorphism of the dental tissues in human permanent mandibular canines and third premolars. *American Journal of Physical Anthropology*, *133*(1), pp.735-740.

Scheid, R. C. and Weiss, G, 2017, *Woelfel's Dental Anatomy*. Philadelphia, PA: Wolters Kluwer.

Schulze, M.A. and Pearce, J.A., 1994, November. A morphology-based filter structure for edge-enhancing smoothing. In *Proceedings of 1st International Conference on Image Processing* (Vol. 2, pp. 530-534). IEEE.

Scott, G.R. and Irish, J.D., 2017. *Human tooth crown and root morphology*. Cambridge University Press.

Scott, G. R., Turner II, C. G., Townsend, G. C. and Martinón-Torres, M., 2018.The *Anthropology of Modern Human Teeth: Dental Morphology and Its Variation in Recent and Fossil Homo sapiens*. (2nd ed.) Cambridge: Cambridge University Press (Cambridge Studies in Biological and Evolutionary Anthropology)

Silvertown, J. (Ed.), 2008. *99% Ape: How Evolution Adds Up*. London, Natural History Museum.

Simons, E., & Ettel, P.,1970. Gigantopithecus. *Scientific American*, 222(1), 76-87. Retrieved from http://www.jstor.org/stable/24964456 (06/06/2019)

Skinner, M.M., 2008. *Enamel-dentine junction morphology of extant hominoid and fossil hominin mandibular molars*. Ph.D. Dissertation, George Washington University

Skinner, M.M., and Gunz, P., 2010. The presence of accessory cusps in chimpanzee lower molars is consistent with a patterning cascade model of development. *J. Anat*. 217, 245-253.

Skinner, M.M., Gunz, P., Wood, B.A., and Hublin, J. 2008a. Enamel-dentine junction (EDJ) morphology distinguishes the lower molars of Australopithecus africanus and Paranthropus robustus*. J. Hum. Evol*. 55, 979-988.

Skinner, M.M., Wood, B.A., Boesch, C., Olejniczak, A.J., Rosas, A., Smith, T.M., and Hublin, J.J., 2008b. Dental trait expression at the enamel-dentine junction of lower molars in extant and fossil hominoids. *J. Hum. Evol*. 54, 173-186.

Skinner, M.M., Gunz, P., Wood, B.A., Boesch, C., and Hublin, J., 2009a. Discrimination of extant Pan species and subspecies using the enamel-dentine junction morphology of lower molars. *Am. J. Phys. Anth*. 140, 234-243.

Skinner, M.M., Wood, B.A. and Hublin, J.J., 2009b. Protostylid expression at the enamel-dentine junction and enamel surface of mandibular molars of Paranthropus robustus and Australopithecus africanus. *J. Hum. Evol*. 56, 76-85.

Skinner, M.M., Gunz, P., Wood, B.A. and Hublin, J.J., 2009c. How many landmarks? Assessing the classification accuracy of Pan lower molars using a geometric morphometric analysis of the occlusal basin as seen at the enamel-dentine junction. In *Comparative Dental Morphology* (Vol. 13, pp. 23-29). Karger Publishers.

Skinner, M.M., Evans, A., Smith, T., Jernvall, J., Tafforeau, P., Kupczik, K., Olejniczak, A.J., Rosas, A., Radovcic, J., Thackeray, J.F., Toussaint, M., and Hublin, J.J., 2010. Brief communication: Contributions of enamel-dentine junction shape and enamel deposition to primate molar crown complexity. *Am. J. Phys. Anth*. 142, 157-163.

Skinner, M.M., Kivell, T.L., Potze, S. and Hublin, J.J., 2013. Microtomographic archive of fossil hominin specimens from Kromdraai B, South Africa. *Journal of human evolution*, *64*(5), pp.434-447.

Skinner, M.M., Alemseged, Z., Gaunitz, C., and Hublin, J., 2015. Enamel thickness trends in Plio-Pleistocene hominin mandibular molars. *J. Hum. Evol*. 85, 35-45.

Skinner, M.M., de Vries, D., Gunz, P., Kupczik, K., Klassen, R.P., Hublin, J., and Roksandic, M., 2016. A dental perspective on the taxonomic affinity of the Balanica mandible (BH-1). *J. Hum. Evol*. 93, 63-81.

Skinner, Matthew, Lockey, Annabelle, Gunz, Philipp, Hawks, John and Delezene, Lucas, 2016. Enamel-dentine junction morphology and enamel thickness of the Dinaledi dental collection. (PDF) Enamel-dentine junction morphology and enamel thickness of the Dinaledi dental collection (researchgate.net) Last accessed 19/02/2021.

Skinner, M. M., Lockey, A. L., Gunz, P., Hawks, J., & Delezene, L. K., 2016. Enamel-dentine junction morphology and enamel thickness of the Dinaledi dental collection. *American Journal of Physical Anthropology*, 159, 293-293.

Smith, T.M., Olejniczak, A.J., Reid, D.J., Ferrell, R.J. and Hublin, J.J., 2006. Modern human molar enamel thickness and enamel–dentine junction shape. *Archives of oral biology*, *51*(11), pp.974-995.

Smith, T.M., Olejniczak, A.J., Zermeno, J.P., Tafforeau, P., Skinner, M.M., Hoffmann, A., Radovčić, J., Toussaint, M., Kruszynski, R., and Menter, C., 2012. Variation in enamel thickness within the genus Homo. *J. Hum. Evol.* 62, 395-411.

Sorenti, M., Martinón-Torres, M., Martín-Francés, L. and Perea-Pérez, B., 2019. Sexual dimorphism of dental tissues in modern human mandibular molars. *American journal of physical anthropology*, *169*(2), pp.332-340.

Szalay, F.S. and Delson, E., 1979. *Evolutionary history of the primates*. London, Academic Press.

Swindler, D.R., 2002. *Primate Dentition: An Introduction to the Teeth of Non-human Primates*. Cambridge, Cambridge University Press.

Thesleff, I., 2014. Current understanding of the process of tooth formation: transfer from the laboratory to the clinic. *Australian dental journal*, 59, pp.48-54.

Towle, I, Irish, J and De Groote, I., 2017. Behavioural inferences from the high levels of dental chipping in Homo naledi. *American Journal of Physical Anthropology*, 164 (1). pp. 184-192. ISSN 1096-8644

Townsend, G., Harris, E.F., Lesot, H., Clauss, F. and Brook, A., 2009. Morphogenetic fields within the human dentition: a new, clinically relevant synthesis of an old concept. *Archives of oral biology*, *54*, pp.S34-S44.

Turner, C.G., 1991. II, Nichol CR, Scott GR: Scoring Procedures for Key Morphological Traits of the Permanent Dentition: The Arizona State University Dental Anthropology System. *Advances in dental anthropology. New York: Wiley-Liss*, pp.13-31.

Ungar, P. S., 2010. *Mammal Teeth: Origin, Evolution and Diversity*. Baltimore, The Johns Hopkins University Press.

Ungar, P. S., 2017. *Evolution's Bite*. Princeton, NJ, Princeton University Press.

Ungar, P.S., Scott, R.S., Scott, J.R. and Teaford, M., 2008. 17 Dental microwear analysis: historical perspectives and new approaches. *Technique and application in dental anthropology*, 53, p.389.

VanSickle, C., Cofran, Z., García-Martínez, D., Williams, S.A., Churchill, S.E., Berger, L.R. and Hawks, J., 2018. Homo naledi pelvic remains from the Dinaledi Chamber, South Africa. *Journal of human evolution*, *125*, pp.122-136.

von Carabelli, G., 1842. *Anatomie des Mundes*. Vienna, Braumüller und Seidel.

Weber, G. W. and Bookstein, F. L., 2011. *Virtual Anthropology. A guide to a new interdisciplinary field*. Wien, Springer Verlag.

Weaver, T.D., Roseman, C.C. and Stringer, C.B., 2007. Were neandertal and modern human cranial differences produced by natural selection or genetic drift?. *Journal of human evolution*, *53*(2), pp.135-145.

Williams, S.A., Garcia-Martinez, D., Bastir, M., Meyer, M.R., Nalla, S., Hawks, J., Schmid, P., Churchill, S.E. and Berger, L.R., 2017. The vertebrae and ribs of Homo naledi. *Journal of Human Evolution*, *104*, pp.136-154.

Wollny, G., Kellman, P., Ledesma-Carbayo, M.J., Skinner, M.M., Hublin, J.J., and Hierl, T., 2013. MIA-A free and open-source software for gray scale medical image analysis. Source code *Biol. Med*. 8, 20.

Wolpoff, M. H., 1979, The Krapina Dental Remains, *American Journal of Physical Anthropology*, 50(1): 67 – 113.

Wood, B.A. and Abbott, S.A., 1983. Analysis of the dental morphology of Plio-pleistocene hominids. I. Mandibular molars: crown area measurements and morphological traits. *Journal of Anatomy*, *136*(Pt 1), p.197.

Wood, B.A., Abbott, S.A. and Graham, S.H., 1983. Analysis of the dental morphology of Plio-Pleistocene hominids. II. Mandibular molars--study of cusp areas, fissure pattern and cross sectional shape of the crown. *Journal of Anatomy*, *137*(Pt 2), p.287.

Wood, B.A. and Uytterschaut, H., 1987. Analysis of the dental morphology of Plio-Pleistocene hominids. III. Mandibular premolar crowns. *Journal of anatomy*, *154*, p.121.

Wood, B.A. and Engleman, C.A., 1988. Analysis of the dental morphology of Plio-Pleistocene hominids. V. Maxillary postcanine tooth morphology. *Journal of Anatomy*, *161*, p.1.

Xing, S., Martinón-Torres, M., de Castro, J.M.B., Zhang, Y., Fan, X., Zheng, L., Huang, W. and Liu, W., 2014. Middle Pleistocene hominin teeth from Longtan Cave, Hexian, China. *PLoS One*, *9*(12), p.e114265.

Xing, S., Martinón-Torres, M., Bermúdez de Castro, J.M., Wu, X. and Liu, W., 2015. Hominin teeth from the early Late Pleistocene site of Xujiayao, Northern China. *American journal of physical anthropology*, *156*(2), pp.224-240.

Xing, S., Sun, C., Martinón-Torres, M., de Castro, J.M.B., Han, F., Zhang, Y. and Liu, W., 2016. Hominin teeth from the Middle Pleistocene site of Yiyuan, eastern China. *Journal of Human Evolution*, *95*, pp.33-54.

Xing, S., Martinón-Torres, M. and de Castro, J.M.B., 2018. The fossil teeth of the Peking Man. *Scientific reports*, *8*(1), pp.1-11.

Xing, S., Martinón-Torres, M. and de Castro, J.M.B., 2019. Late middle Pleistocene hominin teeth from tongzi, southern China. *Journal of human evolution*, *130*, pp.96-108.

Xing, S., Martinón-Torres, M., Deng, C., Shao, Q., Wang, Y., Luo, Y., Zhou, X., Pan, L., Ge, J., de Castro, J.M.B. and Liu, W., 2021. Early Pleistocene hominin teeth from Meipu, southern China. *Journal of Human Evolution*, *151*, p.102924.

Zhang, Y., Jin, C., Kono, R.T., Harrison, T., and Wang, W., 2016. A fourth mandible and associated dental remains of Gigantopithecus blacki from the Early Pleistocene Yanliang Cave, Fusui, Guangxi, South China. *Hist. Biol*. 28, 95-104.

10 APPENDIX 1: Table of specimens included in the sample

Table SM 1. Details of the sample.

Specimen	Side	Tooth type	Taxonomy	Site/Origin	Age (years b.p.)	Current location	Source
UW101 037	R	P3	*Homo naledi*	Rising Star, South Africa	335 - 236 ka	University of the Witwatersrand	Berger et al., 2015
UW101 182	R	P3	*Homo naledi*	Rising Star, South Africa	335 - 236 ka	University of the Witwatersrand	Berger et al., 2015
UW101 277	L	P4	*Homo naledi*	Rising Star, South Africa	335 - 236 ka	University of the Witwatersrand	Berger et al., 2015
UW101 333	L	P4	*Homo naledi*	Rising Star, South Africa	335 - 236 ka	University of the Witwatersrand	Berger et al., 2015
UW101 334	R	P4	*Homo naledi*	Rising Star, South Africa	335 - 236 ka	University of the Witwatersrand	Berger et al., 2015
UW101 455	R	P4	*Homo naledi*	Rising Star, South Africa	335 - 236 ka	University of the Witwatersrand	Berger et al., 2015
UW101 729	R	P3	*Homo naledi*	Rising Star, South Africa	335 - 236 ka	University of the Witwatersrand	Berger et al., 2015
UW101 786	L	P3	*Homo naledi*	Rising Star, South Africa	335 - 236 ka	University of the Witwatersrand	Berger et al., 2015
UW101 808	R	P4	*Homo naledi*	Rising Star, South Africa	335 - 236 ka	University of the Witwatersrand	Berger et al., 2015
UW101 1004	L	P3	*Homo naledi*	Rising Star, South Africa	335 - 236 ka	University of the Witwatersrand	Berger et al., 2015
UW101 1107	L	P3	*Homo naledi*	Rising Star, South Africa	335 - 236 ka	University of the Witwatersrand	Berger et al., 2015
UW101 1277	L	P3	*Homo naledi*	Rising Star, South Africa	335 - 236 ka	University of the Witwatersrand	Berger et al., 2016
UW101 1277	L	P4	*Homo naledi*	Rising Star, South Africa	335 - 236 ka	University of the Witwatersrand	Berger et al., 2017
MPI M4	L	P3	*Homo sapiens*	Anatomical Collection	Modern	Max Planck Institute, Leipzig	MPI records
MPI M12	R	P4	*Homo sapiens*	Anatomical Collection	Modern	Max Planck Institute, Leipzig	MPI records
MPI 07 045	L	P3	*Homo sapiens*	Anatomical Collection	Modern	Max Planck Institute, Leipzig	MPI records
MPI 07 047	L	P3	*Homo sapiens*	Anatomical Collection	Modern	Max Planck Institute, Leipzig	MPI records
MPI 07 078	R	P4	*Homo sapiens*	Anatomical Collection	Modern	Max Planck Institute, Leipzig	MPI records
MPI 07 083	L	P3	*Homo sapiens*	Anatomical Collection	Modern	Max Planck Institute, Leipzig	MPI records
MPI 07 100	L	P3	*Homo sapiens*	Anatomical Collection	Modern	Max Planck Institute, Leipzig	MPI records
MPI 07 114	L	P4	*Homo sapiens*	Anatomical Collection	Modern	Max Planck Institute, Leipzig	MPI records
MPI 07 136	R	P3	*Homo sapiens*	Anatomical Collection	Modern	Max Planck Institute, Leipzig	MPI records
MPI 07 137	L	P3	*Homo sapiens*	Anatomical Collection	Modern	Max Planck Institute, Leipzig	MPI records
MPI 07 232	R	P4	*Homo sapiens*	Anatomical Collection	Modern	Max Planck Institute, Leipzig	MPI records
MPI 07 233	R	P3	*Homo sapiens*	Anatomical Collection	Modern	Max Planck Institute, Leipzig	MPI records
MPI 07 234	L	P3	*Homo sapiens*	Anatomical Collection	Modern	Max Planck Institute, Leipzig	MPI records
MPI 07 256	L	P3	*Homo sapiens*	Anatomical Collection	Modern	Max Planck Institute, Leipzig	MPI records
MPI 07 565	R	P4	*Homo sapiens*	Anatomical Collection	Modern	Max Planck Institute, Leipzig	MPI records
MPI 07 574	R	P3	*Homo sapiens*	Anatomical Collection	Modern	Max Planck Institute, Leipzig	MPI records
MPI 07 602	L	P4	*Homo sapiens*	Anatomical Collection	Modern	Max Planck Institute, Leipzig	MPI records
MPI 07 604	L	P3	*Homo sapiens*	Anatomical Collection	Modern	Max Planck Institute, Leipzig	MPI records
MPI 07 607	L	P3	*Homo sapiens*	Anatomical Collection	Modern	Max Planck Institute, Leipzig	MPI records
MPI 07 613	R	P3	*Homo sapiens*	Anatomical Collection	Modern	Max Planck Institute, Leipzig	MPI records
MPI 07 617	R	P4	*Homo sapiens*	Anatomical Collection	Modern	Max Planck Institute, Leipzig	MPI records
MPI 07 724	L	P4	*Homo sapiens*	Anatomical Collection	Modern	Max Planck Institute, Leipzig	MPI records
MPI T08 046	R	P4	*Homo sapiens*	Anatomical Collection	Modern	Max Planck Institute, Leipzig	MPI records
MPI T08 062	R	P4	*Homo sapiens*	Anatomical Collection	Modern	Max Planck Institute, Leipzig	MPI records
MPI T08 066	L	P3	*Homo sapiens*	Anatomical Collection	Modern	Max Planck Institute, Leipzig	MPI records
MPI T08 069	L	P3	*Homo sapiens*	Anatomical Collection	Modern	Max Planck Institute, Leipzig	MPI records
MPI T08 072	R	P3	*Homo sapiens*	Anatomical Collection	Modern	Max Planck Institute, Leipzig	MPI records
MPI T08 074	R	P3	*Homo sapiens*	Anatomical Collection	Modern	Max Planck Institute, Leipzig	MPI records

Specimen	Side	Tooth type	Taxonomy	Site/Origin	Age (years b.p.)	Current location	Source
MPI T08 076	R	P4	*Homo sapiens*	Anatomical Collection	Modern	Max Planck Institute, Leipzig	MPI records
MPI T08 081	R	P4	*Homo sapiens*	Anatomical Collection	Modern	Max Planck Institute, Leipzig	MPI records
MPI T08 092	L	P3	*Homo sapiens*	Anatomical Collection	Modern	Max Planck Institute, Leipzig	MPI records
MPI T08 094	R	P4	*Homo sapiens*	Anatomical Collection	Modern	Max Planck Institute, Leipzig	MPI records
MPI T08 212	L	P3	*Homo sapiens*	Anatomical Collection	Modern	Max Planck Institute, Leipzig	MPI records
MPI T08 213	R	P3	*Homo sapiens*	Anatomical Collection	Modern	Max Planck Institute, Leipzig	MPI records
MPI T08 224	L	P3	*Homo sapiens*	Anatomical Collection	Modern	Max Planck Institute, Leipzig	MPI records
MPI T08 225	R	P3	*Homo sapiens*	Anatomical Collection	Modern	Max Planck Institute, Leipzig	MPI records
MPI T08 348	R	P3	*Homo sapiens*	Anatomical Collection	Modern	Max Planck Institute, Leipzig	MPI records
MPI T09 112	L	P3	*Homo sapiens*	Anatomical Collection	Modern	Max Planck Institute, Leipzig	MPI records
MPI T09 125	L	P4	*Homo sapiens*	Anatomical Collection	Modern	Max Planck Institute, Leipzig	MPI records
MPI T09 127	R	P4	*Homo sapiens*	Anatomical Collection	Modern	Max Planck Institute, Leipzig	MPI records
MPI T09 129	R	p4	*Homo sapiens*	Anatomical Collection	Modern	Max Planck Institute, Leipzig	MPI records
MPI T09 181	L	P4	*Homo sapiens*	Anatomical Collection	Modern	Max Planck Institute, Leipzig	MPI records
MPI T09 311	R	P4	*Homo sapiens*	Anatomical Collection	Modern	Max Planck Institute, Leipzig	MPI records
KRP 46	L	P3	*Homo neanderthalensis*	Krapina, Croatia	130 ka (OIS 5e)	Croatian Museum of Natural HIstory	Radovčić et al., 1988
KRP 46	L	P4	*Homo neanderthalensis*	Krapina, Croatia	130 ka (OIS 5e)	Croatian Museum of Natural HIstory	Radovčić et al., 1988
KRP 47	L	P4	*Homo neanderthalensis*	Krapina, Croatia	130 ka (OIS 5e)	Croatian Museum of Natural HIstory	Radovčić et al., 1988
KRP 48	L	P3	*Homo neanderthalensis*	Krapina, Croatia	130 ka (OIS 5e)	Croatian Museum of Natural HIstory	Radovčić et al., 1988
KRP 48	L	P4	*Homo neanderthalensis*	Krapina, Croatia	130 ka (OIS 5e)	Croatian Museum of Natural HIstory	Radovčić et al., 1988
KRP 49	L	P3	*Homo neanderthalensis*	Krapina, Croatia	130 ka (OIS 5e)	Croatian Museum of Natural HIstory	Radovčić et al., 1988
KRP 49	L	P4	*Homo neanderthalensis*	Krapina, Croatia	130 ka (OIS 5e)	Croatian Museum of Natural HIstory	Radovčić et al., 1988
KRP D38	L	P3	*Homo neanderthalensis*	Krapina, Croatia	130 ka (OIS 5e)	Croatian Museum of Natural HIstory	Radovčić et al., 1988
KRP D39	R	P3	*Homo neanderthalensis*	Krapina, Croatia	130 ka (OIS 5e)	Croatian Museum of Natural HIstory	Radovčić et al., 1988
KRP D41	L	P4	*Homo neanderthalensis*	Krapina, Croatia	130 ka (OIS 5e)	Croatian Museum of Natural HIstory	Radovčić et al., 1988
KRP D42	R	P4	*Homo neanderthalensis*	Krapina, Croatia	130 ka (OIS 5e)	Croatian Museum of Natural HIstory	Radovčić et al., 1988
KRP D43	L	P3	*Homo neanderthalensis*	Krapina, Croatia	130 ka (OIS 5e)	Croatian Museum of Natural HIstory	Radovčić et al., 1988
KRP D44	R	P4	*Homo neanderthalensis*	Krapina, Croatia	130 ka (OIS 5e)	Croatian Museum of Natural HIstory	Radovčić et al., 1988
KRP D45	L	P3	*Homo neanderthalensis*	Krapina, Croatia	130 ka (OIS 5e)	Croatian Museum of Natural HIstory	Radovčić et al., 1988
KRP D49	L	P4	*Homo neanderthalensis*	Krapina, Croatia	130 ka (OIS 5e)	Croatian Museum of Natural HIstory	Radovčić et al., 1988
KRP D52	L	P3	*Homo neanderthalensis*	Krapina, Croatia	130 ka (OIS 5e)	Croatian Museum of Natural HIstory	Radovčić et al., 1988
KRP D53	R	P3	*Homo neanderthalensis*	Krapina, Croatia	130 ka (OIS 5e)	Croatian Museum of Natural HIstory	Radovčić et al., 1988
KRP D110	R	P3	*Homo neanderthalensis*	Krapina, Croatia	130 ka (OIS 5e)	Croatian Museum of Natural HIstory	Radovčić et al., 1988
KRP D112	R	P3	*Homo neanderthalensis*	Krapina, Croatia	130 ka (OIS 5e)	Croatian Museum of Natural HIstory	Radovčić et al., 1988
KRP D115	R	P4	*Homo neanderthalensis*	Krapina, Croatia	130 ka (OIS 5e)	Croatian Museum of Natural HIstory	Radovčić et al., 1988
SCLA 4A 2	R	P4	*Homo neanderthalensis*	Scladina, Belgium	100 ka	Croatian Museum of Natural HIstory	Toussaint et al., 1998
Le Moustier 1	L	P3	*Homo neanderthalensis*	Le Moustier, France	40 ka	Staatlicher Museen, Berlin	Weinert, 1925
Le Moustier 1	L	P4	*Homo neanderthalensis*	Le Moustier, France	40 ka	Staatlicher Museen, Berlin	Weinert, 1925
SD 50	R	P4	*Homo neanderthalensis*	El Sidron, Spain	49 - 39 ka		Rosas et al., 2006
SD 411	L	P4	*Homo neanderthalensis*	El Sidron, Spain	49 - 39 ka		Rosas et al., 2006
SD 566	R	P3	*Homo neanderthalensis*	El Sidron, Spain	49 - 39 ka		Rosas et al., 2006
SD 1106	R	P4	*Homo neanderthalensis*	El Sidron, Spain	49 - 39 ka		Rosas et al., 2006

Specimen	Side	Tooth type	Taxonomy	Site/Origin	Age (years b.p.)	Current location	Source
Qafzeh 9	L	P3	*Homo sapiens*	Qafzeh, Israel	100 - 80 ka	Tel Aviv University	Vandermeersch, 1981
Qafzeh 9	L	P4	*Homo sapiens*	Qafzeh, Israel	100 - 80 ka	Tel Aviv University	Vandermeersch, 1981
Qafzeh 10	L	P3	*Homo sapiens*	Qafzeh, Israel	100 - 80 ka	Tel Aviv University	Vandermeersch, 1981
Qafzeh 10	L	P4	*Homo sapiens*	Qafzeh, Israel	100 - 80 ka	Tel Aviv University	Vandermeersch, 1981
Qafzeh 11	R	P4	*Homo sapiens*	Qafzeh, Israel	100 - 80 ka	Tel Aviv University	Vandermeersch, 1981
Qafzeh 12	R	P3	*Homo sapiens*	Qafzeh, Israel	100 - 80 ka	Tel Aviv University	Vandermeersch, 1981
Qafzeh 15		P3	*Homo sapiens*	Qafzeh, Israel	100 - 80 ka	Tel Aviv University	Vandermeersch, 1981
Qafzeh 15		P4	*Homo sapiens*	Qafzeh, Israel	100 - 80 ka	Tel Aviv University	Vandermeersch, 1981
Thomas 3	R	P3	*Homo rhodesiensis*	Thomas Quarry, Morocco	470 - 360 ka		Raynal *et al.,*2010
Thomas 3	R	P4	*Homo rhodesiensis*	Thomas Quarry, Morocco	100 - 80 ka		Raynal *et al.,*2010
Steinheim 17230	R	P4	*Homo heidelbergensis*	Steinheim, Germany	243 -191 ka (OIS 7)	Staatliches Museen, Stuttgart	Howell, 1960
KNM-ER 3733	L	P3	*Homo aff. H.erectus*	Koobi Fora	1.63 Ma	Kenya National Museum	Wood, 1991, Koobi Fora v4
KNM-ER 3733	R	P4	*Homo aff. H.erectus*	Koobi Fora	1.63 Ma	Kenya National Museum	Wood, 1991, Koobi Fora v4
Sangiran 4	L	P3	*Homo erectus*	Sangiran, Java	1.6 Ma	Senckenberg Museum, Frankfurt	Weidenreich, 1945
Sangiran 4	L	P4	*Homo erectus*	Sangiran, Java	1.6 Ma	Senckenberg Museum, Frankfurt	Weidenreich, 1945
Sangiran 16	L	P3	*Homo erectus*	Sangiran, Java	1.6 Ma	GRCD*, Bandung, Indonesia	Jacob, 1973
MLD 6	R	P4	*Australopithecus africanus*	Makapansgat, South Africa	2.85 - 2.58 Ma	University of the Witwatersrand	Witwatersrand records
MLD 11 30	R	P3	*Australopithecus africanus*	Makapansgat, South Africa	2.85 - 2.58 Ma	University of the Witwatersrand	Witwatersrand records
MLD 23	L	P3	*Australopithecus africanus*	Makapansgat, South Africa	2.85 - 2.58 Ma	University of the Witwatersrand	Witwatersrand records
MLD 45	R	P4	*Australopithecus africanus*	Makapansgat, South Africa	2.85 - 2.58 Ma	University of the Witwatersrand	Witwatersrand records
Sts 1	L	P3	*Australopithecus africanus*	Sterkfontein, South Africa	2.6 - 2.0 Ma	Ditsong National Museum (Nat. Hist.)	Brain, 1981
Sts 52a	R	P3	*Australopithecus africanus*	Sterkfontein, South Africa	2.6 - 2.0 Ma	Ditsong National Museum (Nat. Hist.)	Robinson, 1956
Sts 52a	L	P4	*Australopithecus africanus*	Sterkfontein, South Africa	2.6 - 2.0 Ma	Ditsong National Museum (Nat. Hist.)	Robinson, 1956
Sts 55a	R	P3	*Australopithecus africanus*	Sterkfontein, South Africa	2.6 - 2.0 Ma	Ditsong National Museum (Nat. Hist.)	Brain, 1981
Sts 57	L	P4	*Australopithecus africanus*	Sterkfontein, South Africa	2.6 - 2.0 Ma	Ditsong National Museum (Nat. Hist.)	Brain, 1981
Sts 61	R	P3	*Australopithecus africanus*	Sterkfontein, South Africa	2.6 - 2.0 Ma	Ditsong National Museum (Nat. Hist.)	Brain, 1981
Sts 61	R	P4	*Australopithecus africanus*	Sterkfontein, South Africa	2.6 - 2.0 Ma	Ditsong National Museum (Nat. Hist.)	Brain, 1981
Stw 73	L	P3	*Australopithecus africanus*	Sterkfontein, South Africa	2.6 - 2.0 Ma	University of the Witwatersrand	Moggi-Cecchii et al., 2006
Stw 73	L	P4	*Australopithecus africanus*	Sterkfontein, South Africa	2.6 - 2.0 Ma	University of the Witwatersrand	Moggi-Cecchii et al., 2006
Stw 192a	L	P3	*Australopithecus africanus*	Sterkfontein, South Africa	2.6 - 2.0 Ma	University of the Witwatersrand	Moggi-Cecchii et al., 2006
Stw 252	R	P3	*Australopithecus africanus*	Sterkfontein, South Africa	2.6 - 2.0 Ma	University of the Witwatersrand	Moggi-Cecchii et al., 2006
Stw 252	L	P4	*Australopithecus africanus*	Sterkfontein, South Africa	2.6 - 2.0 Ma	University of the Witwatersrand	Moggi-Cecchii et al., 2006
Stw 280	R	P3	*Australopithecus africanus*	Sterkfontein, South Africa	2.6 - 2.0 Ma	University of the Witwatersrand	Moggi-Cecchii et al., 2006
Stw 280	R	P4	*Australopithecus africanus*	Sterkfontein, South Africa	2.6 - 2.0 Ma	University of the Witwatersrand	Moggi-Cecchii et al., 2006
SK 24	L	P3	*Paranthropus robustus*	Swartkrans, South Africa	2.25 - 1.8 Ma	Ditsong National Museum (Nat. Hist.)	Ditsong Museum Records
SK 28	L	P4	*Paranthropus robustus*	Swartkrans, South Africa	2.25 - 1.8 Ma	Ditsong National Museum (Nat. Hist.)	Ditsong Museum Records
SK 52	L	P3	*Paranthropus robustus*	Swartkrans, South Africa	2.25 - 1.8 Ma	Ditsong National Museum (Nat. Hist.)	Brain, 1981
SK 74c	R	P3	*Paranthropus robustus*	Swartkrans, South Africa	2.25 - 1.8 Ma	Ditsong National Museum (Nat. Hist.)	Ditsong Museum Records
SKX 162	R	P3	*Paranthropus robustus*	Swartkrans, South Africa	2.25 - 1.8 Ma	Ditsong National Museum (Nat. Hist.)	Ditsong Museum Records
SKX 162	R	P4	*Paranthropus robustus*	Swartkrans, South Africa	2.25 - 1.8 Ma	Ditsong National Museum (Nat. Hist.)	Ditsong Museum Records
SKX 26625	L	P4	*Paranthropus robustus*	Swartkrans, South Africa	2.25 - 1.8 Ma	Ditsong National Museum (Nat. Hist.)	Grine, 1989

Table SM 1 (contd.) Tooth position in the sample.

Specimen	Side	Tooth type	Taxonomy	Position basis	Position source
UW101 037	R	P3	*Homo naledi*	3	Lucas Delezene (Personal communication)
UW101 182	R	P3	*Homo naledi*	3	Lucas Delezene (Personal communication)
UW101 277	L	P4	*Homo naledi*	3	Lucas Delezene (Personal communication)
UW101 333	L	P4	*Homo naledi*	3	Lucas Delezene (Personal communication)
UW101 334	R	P4	*Homo naledi*	3	Lucas Delezene (Personal communication)
UW101 455	R	P4	*Homo naledi*	3	Lucas Delezene (Personal communication)
UW101 729	R	P3	*Homo naledi*	3	Lucas Delezene (Personal communication)
UW101 786	L	P3	*Homo naledi*	3	Lucas Delezene (Personal communication)
UW101 808	R	P4	*Homo naledi*	3	Lucas Delezene (Personal communication)
UW101 1004	L	P3	*Homo naledi*	3	Lucas Delezene (Personal communication)
UW101 1107	L	P3	*Homo naledi*	3	Lucas Delezene (Personal communication)
UW101 1277	L	P3	*Homo naledi*	1	Lucas Delezene (Personal communication)
UW101 1277	L	P4	*Homo naledi*	1	Lucas Delezene (Personal communication)
MPI M4	L	P3	*Homo sapiens*	1	Tooth extraction
MPI M12	R	P4	*Homo sapiens*	1	Tooth extraction
MPI 07 045	L	P3	*Homo sapiens*	1	Tooth extraction
MPI 07 047	L	P3	*Homo sapiens*	1	Tooth extraction
MPI 07 078	R	P4	*Homo sapiens*	1	Tooth extraction
MPI 07 083	L	P3	*Homo sapiens*	1	Tooth extraction
MPI 07 100	L	P3	*Homo sapiens*	1	Tooth extraction
MPI 07 114	L	P4	*Homo sapiens*	1	Tooth extraction
MPI 07 136	R	P3	*Homo sapiens*	1	Tooth extraction
MPI 07 137	L	P3	*Homo sapiens*	1	Tooth extraction
MPI 07 232	R	P4	*Homo sapiens*	1	Tooth extraction
MPI 07 233	R	P3	*Homo sapiens*	1	Tooth extraction
MPI 07 234	L	P3	*Homo sapiens*	1	Tooth extraction
MPI 07 256	L	P3	*Homo sapiens*	1	Tooth extraction
MPI 07 565	R	P4	*Homo sapiens*	1	Tooth extraction

MPI 07 574	R	P3	*Homo sapiens*	1	Tooth extraction
MPI 07 602	L	P4	*Homo sapiens*	1	Tooth extraction
MPI 07 604	L	P3	*Homo sapiens*	1	Tooth extraction
MPI 07 607	L	P3	*Homo sapiens*	1	Tooth extraction
MPI 07 613	R	P3	*Homo sapiens*	1	Tooth extraction
MPI 07 617	R	P4	*Homo sapiens*	1	Tooth extraction
MPI 07 724	L	P4	*Homo sapiens*	1	Tooth extraction
MPI T08 046	R	P4	*Homo sapiens*	1	Tooth extraction
MPI T08 062	R	P4	*Homo sapiens*	1	Tooth extraction
MPI T08 066	L	P3	*Homo sapiens*	1	Tooth extraction
MPI T08 069	L	P3	*Homo sapiens*	1	Tooth extraction
MPI T08 072	R	P3	*Homo sapiens*	1	Tooth extraction
MPI T08 074	R	P3	*Homo sapiens*	1	Tooth extraction
MPI T08 076	R	P4	*Homo sapiens*	1	Tooth extraction
MPI T08 081	R	P4	*Homo sapiens*	1	Tooth extraction
MPI T08 092	L	P3	*Homo sapiens*	1	Tooth extraction
MPI T08 094	R	P4	*Homo sapiens*	1	Tooth extraction
MPI T08 212	L	P3	*Homo sapiens*	1	Tooth extraction
MPI T08 213	R	P3	*Homo sapiens*	1	Tooth extraction
MPI T08 224	L	P3	*Homo sapiens*	1	Tooth extraction
MPI T08 225	R	P3	*Homo sapiens*	1	Tooth extraction
MPI T08 348	R	P3	*Homo sapiens*	1	Tooth extraction
MPI T09 112	L	P3	*Homo sapiens*	1	Tooth extraction
MPI T09 125	L	P4	*Homo sapiens*	1	Tooth extraction
MPI T09 127	R	P4	*Homo sapiens*	1	Tooth extraction
MPI T09 129	R	p4	*Homo sapiens*	1	Tooth extraction
MPI T09 181	L	P4	*Homo sapiens*	1	Tooth extraction
MPI T09 311	R	P4	*Homo sapiens*	1	Tooth extraction
KRP 46	L	P3	*Homo neanderthalensisis*	1	In jaw KDP 2 (Radovčić et al., 1988)
KRP 46	L	P4	*Homo neanderthalensis*	1	In jaw KDP 2 (Radovčić et al., 1988)
KRP 47	L	P4	*Homo neanderthalensis*	1	In jaw KDP 3 (Radovčić et al., 1988)

KRP 48	L	P3	*Homo neanderthalensis*	1	In jaw KDP 4 (Radovčić et al., 1988)
KRP 48	L	P4	*Homo neanderthalensis*	1	In jaw KDP 4 (Radovčić et al., 1988)
KRP 49	L	P3	*Homo neanderthalensis*	1	In jaw KDP 5 (Radovčić et al., 1988)
KRP 49	L	P4	*Homo neanderthalensis*	1	In jaw KDP 5 (Radovčić et al., 1988)
KRP D38	L	P3	*Homo neanderthalensis*	2	Association KDP 18 (Radovčić et al., 1988)
KRP D39	R	P3	*Homo neanderthalensis*	3	Radovčić et al., 1988
KRP D41	L	P4	*Homo neanderthalensis*	2	Association KDP 23 (Radovčić et al., 1988)
KRP D42	R	P4	*Homo neanderthalensis*	3	Radovčić et al., 1988
KRP D43	L	P3	*Homo neanderthalensis*	3	Radovčić et al., 1988
KRP D44	R	P4	*Homo neanderthalensis*	3	Radovčić et al., 1988
KRP D45	L	P3	*Homo neanderthalensis*	2	Association KDP 6 (Radovčić et al., 1988)
KRP D49	L	P4	*Homo neanderthalensis*		Association KDP 6 (Radovčić et al., 1988)
KRP D52	L	P3	*Homo neanderthalensis*	2	Association KDP 23 (Radovčić et al., 1988)
KRP D53	R	P3	*Homo neanderthalensis*	2	Association KDP 3 (Radovčić et al., 1988)
KRP D110	R	P3	*Homo neanderthalensis*	2	Association KDP 2 (Radovčić et al., 1988)
KRP D112	R	P3	*Homo neanderthalensis*	2	Association KDP 1 (Radovčić et al., 1988)
KRP D115	R	P4	*Homo neanderthalensis*	2	Association KDP 1 (Radovčić et al., 1988)
SCLA 4A 2	R	P4	*Homo neanderthalensis*	1	In jaw
Le Moustier 1	L	P3	*Homo neanderthalensis*	1	In jaw
Le Moustier 1	L	P4	*Homo neanderthalensis*	1	In jaw
SD 50	R	P4	*Homo neanderthalensis*	2	Associated dentition (Antonio_Rosas, 2009 (pers comm))
SD 411	L	P4	*Homo neanderthalensis*	2	Associated dentition (Antonio_Rosas, 2009 (pers comm))
SD 566	R	P3	*Homo neanderthalensis*	2	Associated dentition (Antonio_Rosas, 2009 (pers comm))
SD 1106	R	P4	*Homo neanderthalensis*	2	Associated dentition (Antonio_Rosas, 2009 (pers comm))
Qafzeh 9	L	P3	*Homo sapiens* (Qafzeh)	1	In jaw
Qafzeh 9	L	P4	*Homo sapiens* (Qafzeh)	1	In jaw
Qafzeh 10	L	P3	*Homo sapiens* (Qafzeh)	1	In jaw
Qafzeh 10	L	P4	*Homo sapiens* (Qafzeh)	1	In jaw
Qafzeh 11	R	P4	*Homo sapiens* (Qafzeh)	1	In jaw
Qafzeh 12	R	P3	*Homo sapiens* (Qafzeh)	3	Vandermeersch, 1981
Qafzeh 15		P3	*Homo sapiens* (Qafzeh)	1	In jaw

Qafzeh 15		P4	*Homo sapiens* (Qafzeh)	1	In jaw
Thomas 3	R	P3	*Homo rhodesiensis*	1	Associated dentition
Thomas 3	R	P4	*Homo rhodesiensis*	1	Associated dentition
Steinheim 17230	R	P4	*Homo heidelbergensis*	1	In jaw
KNM-ER 3733	L	P3	*Homo aff. H.erectus*	1	In jaw
KNM-ER 3733	R	P4	*Homo aff. H.erectus*	1	In jaw
Sangiran 4	L	P3	*Homo erectus*	1	In jaw
Sangiran 4	L	P4	*Homo erectus*	1	In jaw
Sangiran 16	L	P3	*Homo erectus*	3	Jacob, 1975
MLD 6	R	P4	*Australopithecus africanus*	1	In jaw
MLD 11 30	R	P3	*Australopithecus africanus*	3	
MLD 23	L	P3	*Australopithecus africanus*	1	In jaw
MLD 45	R	P4	*Australopithecus africanus*	1	In jaw
Sts 1	L	P3	*Australopithecus africanus*	1	In jaw
Sts 52a	R	P3	*Australopithecus africanus*	1	In jaw
Sts 52a	L	P4	*Australopithecus africanus*	1	In jaw
Sts 55a	R	P3	*Australopithecus africanus*	1	In jaw
Sts 57	L	P4	*Australopithecus africanus*	1	In jaw
Sts 61	R	P3	*Australopithecus africanus*	1	In jaw
Sts 61	R	P4	*Australopithecus africanus*	1	In jaw
Stw 73	L	P3	*Australopithecus africanus*	1	In jaw
Stw 73	L	P4	*Australopithecus africanus*	1	In jaw
Stw 192a	L	P3	*Australopithecus africanus*	3	Moggi-Cecchii et al., 2006
Stw 252	R	P3	*Australopithecus africanus*	2	Associated, Moggi-Cecchii et al., 2006
Stw 252	L	P4	*Australopithecus africanus*	2	Associated, Moggi-Cecchii et al., 2006
Stw 280	R	P3	*Australopithecus africanus*	2	Associated, Moggi-Cecchii et al., 2006
Stw 280	R	P4	*Australopithecus africanus*	1	Associated, Moggi-Cecchii et al., 2006
SK 24	L	P3	*Paranthropus robustus*	2	Robinson, 1956
SK 28	L	P4	*Paranthropus robustus*	2	Robinson, 1956
SK 52	L	P3	*Paranthropus robustus*	1	In jaw
SK 74c	R	P3	*Paranthropus robustus*	2	Ditsong Museum Records

SKX 162	R	P3	*Paranthropus robustus*	2	Ditsong Museum Records
SKX 162	R	P4	*Paranthropus robustus*	2	Ditsong Museum Records
SKX 26625	L	P4	*Paranthropus robustus*	2	Grine, 1989

References

Adam, K.D., 1954. Die zeitliche Stellung der Urmenschen-Fundschicht von Steinheim an der Murr innerhalb des Pleistozäns. *E&G Quaternary Science Journal*, *4*(1), pp.18-21.

Berger, L.R., Hawks, J., de Ruiter, D.J., Churchill, S.E., Schmid, P., Delezene, L.K., Kivell, T.L., Garvin, H.M., Williams, S.A., DeSilva, J.M. and Skinner, M.M., 2015. Homo naledi, a new species of the genus Homo from the Dinaledi Chamber, South Africa. *elife*, *4*, p.e09560.

Brain, C.K., 1981. *The hunters or the hunted?: an introduction to African cave taphonomy*. University of Chicago Press.

Grine, F.E., 1989. New hominid fossils from the Swartkrans Formation (1979–1986 excavations): craniodental specimens. *American Journal of Physical Anthropology*, *79*(4), pp.409-449.

Howell, F.C., 1960. European and northwest African middle Pleistocene hominids. *Current Anthropology*, *1*(3), pp.195-232.

Jacob, T., 1973. Palaeoanthropological discoveries in Indonesia with special reference to the finds of the last two decades. *Journal of Human Evolution*, *2*(6), pp.473-485.

Moggi-Cecchi, Jacopo, Frederick E. Grine, and Phillip V. Tobias. "Early hominid dental remains from Members 4 and 5 of the Sterkfontein Formation (1966–1996 excavations): catalogue, individual associations, morphological descriptions and initial metrical analysis." *Journal of Human Evolution* 50, no. 3 (2006): 239-328.

Radovčić, J., Smith, F.H., Trinkhaus, E. and Wolpoff, M.H., 1988. *The Krapina Hominids*. Mladost.

Raynal, J.P., Sbihi-Alaoui, F.Z., Mohib, A., El Graoui, M., Lefèvre, D., Texier, J.P., Geraads, D., Hublin, J.J., Smith, T., Tafforeau, P. and Zouak, M., 2010. Hominid Cave at Thomas Quarry I (Casablanca, Morocco): recent findings and their context. *Quaternary International*, *223*, pp.369-382.

Robinson, J. T., 1956. *The Dentition of the Australopithecinae*. Pretoria, The Transvaal Museum.

Rosas, A., Martínez-Maza, C., Bastir, M., García-Tabernero, A., Lalueza-Fox, C., Huguet, R., Ortiz, J.E., Julià, R., Soler, V., de Torres, T. and Martínez, E., 2006. Paleobiology and comparative morphology of a late Neandertal sample from El Sidrón, Asturias, Spain. *Proceedings of the National Academy of Sciences*, *103*(51), pp.19266-19271.

Toussaint, M., Otte, M., Bonjean, D., Bocherens, H., Falguères, C. and Yokoyama, Y., 1998. Les restes humains néandertaliens immatures de la couche 4A de la grotte Scladina (Andenne, Belgique). *Comptes Rendus de l'Académie des Sciences-Series IIA-Earth and Planetary Science*, *326*(10), pp.737-742.

Vandermeersch, B., 1981. Les Hommes fossiles de Qafzeh (Israël). Éditions du CNRS. *Cahiers de paléontologie (Paléoanthropologie), Paris*.

Weidenreich, F., 1944. Giant early man from Java and South China. *Science*, *99*(2581), pp.479-482.

Weinert, H., 1925. *Der Schädel des eiszeitlichen Menschen von Le Moustier in neuer Zusammensetzung*. J. Springer.

Wood, B., 1991. *Koobi Fora research project: researches into geology, palaeontology, and human origins. 4. Hominid cranial remains*. Clarendon Press.

11 APPENDIX 2: Table of EDJ qualitative morphological features

Key	
CTC	Transverse crest (Central)
MTC	Transverse crest (Mesial)
MBR	Moderate buccal ridges
PBR	Prominent buccal ridges
MN	Notch in mesial EDJ ridge
DBH	Distal accesory buccal dentine horn
DBS	Distal buccal shoulder
MBH	Mesial accessory buccal dentine horn
BER	Buccal essential ridge
LER	Lingual essential ridge
BMR	Bucco-mesial ridge
MB	Mesial bulge in mesial EDJ ridge
DB	Bulge in distal EDJ ridge
DAR	Distal accesory (buccal) ridge
MAR	Mesial accessory (buccal) ridge
dacr	Distal accesory essential (central buccal) ridge
macr	Mesial accesory essential (central buccal) ridge
boss	Boss shaped cingulum extension
bucc_cing	Shelf-like buccal cingulum
ling_cing	Shelf-like lingual cingulum
ObIR	Oblique ridge
DLH	Distal accesory lingual dentine horn

Table SM 2. EDJ surfaces scored for the presence of qualitative morphological features.

Specimen	Tooth type	Taxonomy	CTC	MTC	MBR	PBR	MN	DBH	DBS	MBH	BER	LER	BMR	MB	DB	DAR	MAR	dacr	macr	boss
MLD 11 30	P3	*A. africanus*	0	1	0	1	0	0	0	0	1	1	0	0	0	0	0	0	0	0
MLD 23	P3	*A. africanus*	0	1	0	1	0	0	0	0	1	1	0	0	0	0	0	0	0	0
MLD 45	P3	*A. africanus*	0	0	0	1	0	0	0	1	1	1	0	0	0	0	1	0	0	0
Sts 1	P3	*A. africanus*	1	0	0	1	0	1	0	1	0	0	0	0	0	1	1	0	0	0
Sts 52a	P3	*A. africanus*	0	0	0	1	0	1	0	1	1	0	0	0	0	0	1	0	0	0
Sts 55	P3	*A. africanus*	0	0	1	0	0	1	0	0	1	0	0	0	0	0	1	0	0	0
Sts 61	P3	*A. africanus*	1	0	0	1	0	0	0	0	0	0	0	0	0	1	1	0	0	0
Stw 73	P3	*A. africanus*	0	1	0	1	0	0	0	0	1	1	0	1	0	0	0	0	0	0
Stw 252	P3	*A. africanus*	0	1	0	1	0	0	0	0	1	0	0	0	0	0	0	0	0	0
Stw 280	P3	*A. africanus*	0	0	0	0	0	0	0	1	1	1	1	1	0	0	0	0	0	0
MLD 6	P4	*A. africanus*	0	1	0	1	0	1	0	0	1	0	0	0	0	0	0	0	0	0
Sts 52a	P4	*A. africanus*	0	1	0	1	0	1	0	1	1	0	0	0	0	0	0	0	0	0
Sts 55	P4	*A. africanus*	0	0	0	0	0	0	0	0	0	0	0	0	0	0	0	0	0	0
Sts 57	P4	*A. africanus*	0	0	1	0	0	0	0	0	1	1	0	0	0	1	1	1	0	0
Sts 61	P4	*A. africanus*	1	0	1	0	0	0	1	1	1	0	0	0	0	0	0	0	1	0
Stw 73	P4	*A. africanus*	0	1	0	0	0	1	0	0	1	1	0	0	0	0	0	0	0	0
Stw 192a	P4	*A. africanus*	0	1	0	1	0	1	0	1	1	0	0	0	0	0	0	0	0	0
Stw 252	P4	*A. africanus*	0	1	1	0	0	1	0	1	1	1	0	0	0	0	0	0	0	0
Stw 280	P4	*A. africanus*	0	0	1	0	0	1	0	1	1	1	0	0	0	0	1	0	0	0
KNM-ER 3733	P3	*H. erectus*	1	0	1	0	0	1	0	1	0	0	0	0	1	0	0	0	0	0
Sangiran 4	P3	*H. erectus*	1	0	1	0	1	0	0	0	0	0	0	1	0	0	0	0	0	0
KNM-ER 3733	P4	*H. erectus*	1	0	1	0	0	0	1	0	1	1	0	0	0	1	1	0	0	0
Sangiran 4	P4	*H. erectus*	1	0	1	0	0	1	0	0	1	1	0	0	0	1	0	0	0	0
Thomas 3	P3	*H. heidelbergensis*	0	1	1	0	1	0	0	0	1	1	0	1	0	0	0	1	0	0
Thomas 3	P4	*H. heidelbergensis*	0	1	1	0	0	0	1	1	1	1	0	0	0	1	0	1	0	0
Steinheim 17230	P4	*H. heidelbergensis*	0	1	0	0	0	0	1	0	1	1	0	0	0	0	0	0	0	0
UW101 037	P3	*H. naledi*	0	1	1	0	0	1	0	1	1	0	0	1	0	0	0	0	0	0
UW101 182	P3	*H. naledi*	0	1	1	0	0	1	0	1	1	0	0	0	0	1	0	0	0	0
UW101 729	P3	*H. naledi*	0	1	1	0	0	1	0	1	1	0	0	0	0	1	0	0	0	0
UW101 786	P3	*H. naledi*	0	0	1	0	0	1	0	1	1	1	1	1	0	1	0	0	0	0
UW101 1004	P3	*H. naledi*	0	0	1	0	0	1	0	0	1	0	1	1	0	1	0	0	0	0
UW101 1107	P3	*H. naledi*	0	0	1	0	0	1	0	0	1	0	1	1	0	0	0	0	0	0
UW101 1277	P3	*H. naledi*	0	1	1	0	0	1	0	0	1	0	0	1	0	1	0	0	0	0
UW101 277	P4	*H. naledi*	0	1	1	0	0	1	0	1	1	0	0	0	0	1	0	0	0	0
UW101 333	P4	*H. naledi*	0	1	1	0	0	1	0	0	1	1	0	0	0	0	0	0	0	0
UW101 334	P4	*H. naledi*	0	1	1	0	0	1	0	0	1	0	0	0	0	0	0	0	0	0

Specimen	Tooth type	Taxonomy	CTC	MTC	MBR	PBR	MN	DBH	DBS	MBH	BER	LER	BMR	MB	DB	DAR	MAR	dacr	macr	boss
UW101 455	P4	*H. naledi*	0	1	1	0	0	1	0	0	1	0	0	0	0	0	0	0	0	0
UW101 808	P4	*H. naledi*	0	1	1	0	0	1	0	0	1	1	0	0	0	0	0	0	0	0
UW101 1277	P4	*H. naledi*	0	1	1	0	0	1	0	1	1	0	0	0	0	0	0	0	0	0
KRP 46	P3	*H. neanderthalensis*	1	0	0	0	1	0	0	0	1	0	0	1	0	1	0	0	0	1
KRP 48	P3	*H. neanderthalensis*	0	0	0	0	1	0	1	0	1	1	0	0	0	0	0	0	0	1
KRP 49	P3	*H. neanderthalensis*	1	0	0	0	1	0	0	0	1	0	0	0	0	1	0	0	0	1
KRP D38	P3	*H. neanderthalensis*	1	0	0	0	1	0	1	0	1	0	0	1	0	0	0	0	0	1
KRP D45	P3	*H. neanderthalensis*	1	0	0	0	0	0	0	0	1	1	0	1	0	1	0	0	0	1
KRP D53	P3	*H. neanderthalensis*	1	0	0	0	1	0	0	0	1	1	0	1	0	1	0	0	0	1
KRP D110	P3	*H. neanderthalensis*	1	0	0	0	1	0	0	0	1	1	0	1	0	1	0	0	0	1
KRP D112	P3	*H. neanderthalensis*	1	0	0	0	1	0	0	0	1	1	0	1	0	0	0	0	0	1
Le Moustier 1	P3	*H. neanderthalensis*	1	0	0	0	1	0	0	0	1	1	0	0	0	1	0	0	0	1
SD 566	P3	*H. neanderthalensis*	1	0	0	0	1	0	0	0	1	1	0	0	0	0	0	0	0	1
KRP 46	P4	*H. neanderthalensis*	1	0	0	0	0	0	1	0	1	1	0	0	0	1	0	0	0	0
KRP 47	P4	*H. neanderthalensis*	1	0	0	0	0	0	1	0	1	1	0	0	0	1	0	0	0	0
KRP 48	P4	*H. neanderthalensis*	1	0	0	0	0	0	0	0	0	1	0	0	0	0	0	0	0	0
KRP 49	P4	*H. neanderthalensis*	1	0	0	0	0	0	0	0	0	1	0	0	0	0	0	0	0	0
KRP D39	P4	*H. neanderthalensis*	1	0	0	0	0	0	1	0	1	1	0	0	0	0	0	0	0	0
KRP D41	P4	*H. neanderthalensis*	1	0	0	0	0	0	1	0	1	0	0	0	0	1	0	0	0	0
KRP D42	P4	*H. neanderthalensis*	1	0	0	0	0	0	1	0	0	1	0	0	0	1	0	0	0	0
KRP D43	P4	*H. neanderthalensis*	1	0	0	0	0	0	1	0	1	1	0	0	0	1	1	0	0	0
KRP D44	P4	*H. neanderthalensis*	1	0	0	0	0	0	1	0	1	1	0	0	0	1	1	0	0	0
KRP D49	P4	*H. neanderthalensis*	1	0	0	0	1	0	1	0	1	1	0	0	0	1	0	0	0	0
KRP D52	P4	*H. neanderthalensis*	1	0	0	0	0	0	0	0	1	1	0	0	0	0	0	0	0	0
KRP D115	P4	*H. neanderthalensis*	1	0	0	0	0	0	1	0	1	1	0	0	0	1	0	0	0	0
SCLA 4A 2	P4	*H. neanderthalensis*	1	0	0	0	0	0	1	0	1	1	0	0	0	1	1	0	0	0
Le Moustier 1	P4	*H. neanderthalensis*	1	0	0	0	0	0	1	0	1	1	0	0	0	0	0	0	0	0
SD 50	P4	*H. neanderthalensis*	1	0	0	0	0	0	1	0	1	1	0	0	0	0	0	0	0	0
SD 411	P4	*H. neanderthalensis*	1	0	0	0	0	0	1	0	1	1	0	0	0	1	0	0	0	0
SD 1106	P4	*H. neanderthalensis*	1	0	0	0	0	0	1	0	0	1	0	0	0	0	0	0	0	1
MPI 07 045	P3	*H. sapiens*	1	0	1	0	1	0	0	0	0	0	0	1	0	1	0	0	0	0
MPI 07 047	P3	*H. sapiens*	0	0	0	0	1	0	0	0	0	0	0	1	0	0	1	1	0	0
MPI 07 083	P3	*H. sapiens*	0	0	2	0	1	0	0	0	1	0	0	1	0	1	0	0	0	0
MPI 07 100	P3	*H. sapiens*	0	1	1	0	1	0	0	0	1	1	0	0	0	0	0	0	0	0
MPI 07 136	P3	*H. sapiens*	0	0	0	0	1	0	0	0	1	0	0	1	0	0	0	0	0	0
MPI 07 137	P3	*H. sapiens*	1	0	0	0	0	1	0	1	1	0	0	0	0	0	0	0	0	0
MPI 07 233	P3	*H. sapiens*	1	0	0	0	1	1	0	0	1	0	0	1	0	1	0	0	0	0
MPI 07 234	P3	*H. sapiens*	0	1	0	0	1	0	0	0	1	1	0	1	0	1	0	0	0	0

Specimen	Tooth type	Taxonomy	CTC	MTC	MBR	PBR	MN	DBH	DBS	MBH	BER	LER	BMR	MB	DB	DAR	MAR	dacr	macr	boss
MPI 07 256	P3	*H. sapiens*	0	0	1	0	1	0	0	0	1	0	0	1	0	1	0	0	0	0
MPI 07 574	P3	*H. sapiens*	0	0	0	0	1	0	0	0	1	1	0	0	0	0	0	0	0	0
MPI 07 604	P3	*H. sapiens*	1	0	1	0	0	0	0	0	0	0	0	0	0	0	0	0	0	0
MPI 07 607	P3	*H. sapiens*	0	0	0	1	0	0	0	0	1	1	0	0	0	0	0	0	0	0
MPI 07 613	P3	*H. sapiens*	1	0	0	0	1	0	0	0	0	0	0	1	0	0	0	0	0	0
MPI T08 066	P3	*H. sapiens*	0	0	0	0	1	0	0	0	1	0	0	1	0	0	0	0	0	0
MPI T08 069	P3	*H. sapiens*	1	0	1	0	1	0	0	0	1	0	0	1	0	0	0	0	0	0
MPI T08 072	P3	*H. sapiens*	1	0	1	0	1	0	0	0	1	0	0	`	0	1	1	0	0	0
MPI T08 074	P3	*H. sapiens*	0	0	1	0	0	1	0	0	1	1	0	0	0	0	0	0	0	0
MPI T08 092	P3	*H. sapiens*	0	0	1	0	1	0	0	0	1	1	0	1	0	1	1	0	0	0
MPI T08 212	P3	*H. sapiens*	0	0	0	0	0	1	0	0	1	0	0	0	0	1	0	0	0	0
MPI T08 213	P3	*H. sapiens*	0	0	0	0	0	0	0	0	1	0	0	0	0	1	0	0	0	0
MPI T08 224	P3	*H. sapiens*	0	0	0	0	1	0	0	0	1	0	0	0	0	0	1	0	0	0
MPI T08 225	P3	*H. sapiens*	0	0	0	0	1	0	0	0	1	0	0	0	0	0	0	0	0	0
MPI T09 112	P3	*H. sapiens*	0	1	1	0	1	0	0	0	1	1	0	1	1	0	0	0	0	0
MPI T09 181	P3	*H. sapiens*	0	0	0	0	1	0	0	1	1	1	0	1	0	0	0	0	0	0
MPI 07 078	P4	*H. sapiens*	0	0	1	0	0	1	0	0	1	0	0	1	0	1	1	0	0	0
MPI 07 114	P4	*H. sapiens*	0	0	0	0	0	1	0	1	1	1	0	0	0	1	0	0	0	0
MPI 07 232	P4	*H. sapiens*	0	0	0	0	0	1	0	0	1	1	0	0	0	0	0	0	0	0
MPI 07 565	P4	*H. sapiens*	0	0	0	0	0	1	0	0	1	1	0	0	0	1	0	0	0	0
MPI 07 602	P4	*H. sapiens*	0	0	0	0	0	0	1	0	0	0	0	0	0	0	0	0	0	0
MPI 07 617	P4	*H. sapiens*	0	0	1	0	0	1	0	1	1	1	0	0	0	1	1	0	0	0
MPI 07 724	P4	*H. sapiens*	0	0	0	0	0	1	0	0	1	0	0	0	0	1	1	0	0	0
MPI T08 046	P4	*H. sapiens*	0	0	0	0	0	1	0	1	1	1	1	0	0	1	0	0	0	0
MPI T08 062	P4	*H. sapiens*	1	0	0	0	0	1	0	1	0	0	0	0	0	1	1	0	0	0
MPI T08 076	P4	*H. sapiens*	0	0	0	0	0	0	0	0	1	0	0	0	0	1	0	0	0	0
MPI T08 081	P4	*H. sapiens*	0	1	1	0	0	1	0	1	1	1	0	0	0	1	1	0	0	0
MPI T08 094	P4	*H. sapiens*	0	0	0	0	0	0	1	0	1	0	0	0	0	0	1	0	0	0
MPI T08 348	P4	*H. sapiens*	0	0	0	0	0	0	0	0	1	0	0	0	0	1	1	0	0	0
MPI T09 125	P4	*H. sapiens*	0	0	0	0	0	1	0	1	1	1	0	0	0	1	0	0	0	0
MPI T09 127	P4	*H. sapiens*	0	0	0	0	0	1	0	1	1	1	0	0	0	1	0	1	0	0
MPI T09 129	P4	*H. sapiens*	0	0	0	0	0	1	0	1	1	0	0	0	0	0	0	0	0	0
MPI T09 311	P4	*H. sapiens*	0	0	0	0	0	1	0	1	1	0	0	0	0	0	0	0	0	0
Qafzeh 10	P3	*H. sapiens (Qaf.)*	0	0	0	0	1	0	0	0	1	1	0	1	0	1	1	0	0	1
Qafzeh 11	P3	*H. sapiens (Qaf.)*	0	0	0	0	0	0	0	0	0	0	0	0	0	0	0	1	0	0
Qafzeh 15	P3	*H. sapiens (Qaf.)*	1	0	0	0	1	0	0	0	0	0	0	1	0	0	0	0	0	0
Qafzeh 10	P4	*H. sapiens (Qaf.)*	0	1	0	0	0	1	0	0	1	1	0	0	0	0	0	1	0	0
Qafzeh 11	P4	*H. sapiens (Qaf.)*	1	0	0	0	0	1	0	1	1	0	0	0	0	0	0	1	0	0

Specimen	Tooth type	Taxonomy	CTC	MTC	MBR	PBR	MN	DBH	DBS	MBH	BER	LER	BMR	MB	DB	DAR	MAR	dacr	macr	boss
Qafzeh 15	P4	*H. sapiens (Qaf.)*	1	0	0	0	0	1	0	0	0	0	0	0	0	1	0	0	0	0
SK_24	P3	*P. robustus*	0	0	1	0	0	0	0	0	1	0	0	0	0	0	0	1	0	0
SK_28	P3	*P. robustus*	0	0	0	0	0	0	0	0	1	0	0	0	0	0	0	1	0	0
SK_52	P3	*P. robustus*	0	0	0	0	0	1	0	1	0	0	0	0	0	0	1	1	0	0
SK_74c	P3	*P. robustus*	0	1	1	0	0	1	0	1	1	1	0	0	0	0	0	1	1	0
SKX_162	P3	*P. robustus*	0	0	1	0	0	1	0	0	1	1	0	0	0	0	1	1	0	0
SK_52	P4	*P. robustus*	0	0	1	0	0	1	0	0	1	0	0	0	0	0	0	1	1	0
SK_99	P4	*P. robustus*	0	0	0	0	0	1	0	0	1	1	0	0	0	1	0	0	0	0
SKX_162	P4	*P. robustus*	0	0	1	0	0	1	0	0	1	1	0	0	0	0	0	1	0	0
SKX_26625	P4	*P. robustus*	0	0	1	0	0	1	0	0	1	1	0	0	0	0	0	1	0	0

Table SM 2. (Contd.) EDJ surfaces scored for the presence of qualitative morphological features.

Specimen	Tooth type	Taxonomy	bucc_cing	ling_cing	OblR	DLH
MLD 11 30	P3	*A. africanus*	1	0	0	0
MLD 23	P3	*A. africanus*	1	0	0	0
MLD 45	P3	*A. africanus*	1	0	0	0
Sts 1	P3	*A. africanus*	1	1	0	0
Sts 52a	P3	*A. africanus*	1	1	0	0
Sts 55	P3	*A. africanus*	1	0	0	0
Sts 61	P3	*A. africanus*	0	0	0	0
Stw 73	P3	*A. africanus*	1	1	0	0
Stw 252	P3	*A. africanus*	1	1	0	0
Stw 280	P3	*A. africanus*	1	1	0	0
MLD 6	P4	*A. africanus*	0	0	0	0
Sts 52a	P4	*A. africanus*	1	1	0	0
Sts 55	P4	*A. africanus*	0	0	0	0
Sts 57	P4	*A. africanus*	0	0	0	0
Sts 61	P4	*A. africanus*	0	0	0	0
Stw 73	P4	*A. africanus*	1	1	0	0
Stw 192a	P4	*A. africanus*	1	1	1	0
Stw 252	P4	*A. africanus*	1	1	1	1
Stw 280	P4	*A. africanus*	1	1	0	0
KNM-ER 3733	P3	*H. erectus*	0	0	0	0
Sangiran 4	P3	*H. erectus*	0	0	0	0
KNM-ER 3733	P4	*H. erectus*	0	0	0	0
Sangiran 4	P4	*H. erectus*	0	0	0	0
Thomas 3	P3	*H. heidelbergensis*	0	0	0	0
Thomas 3	P4	*H. heidelbergensis*	0	0	0	0
Steinheim 17230	P4	*H. heidelbergensis*	0	0	0	0
UW101 037	P3	*H. naledi*	0	0	0	0
UW101 182	P3	*H. naledi*	0	0	0	0
UW101 729	P3	*H. naledi*	0	0	0	0
UW101 786	P3	*H. naledi*	0	0	0	0
UW101 1004	P3	*H. naledi*	0	0	0	0
UW101 1107	P3	*H. naledi*	0	0	0	0
UW101 1277	P3	*H. naledi*	0	0	0	0
UW101 277	P4	*H. naledi*	0	0	0	0

Specimen	Tooth type	Taxonomy	bucc_cing	ling_cing	OblR	DLH
UW101 333	P4	*H. naledi*	0	0	0	0
UW101 334	P4	*H. naledi*	0	0	0	0
UW101 455	P4	*H. naledi*	0	0	0	0
UW101 808	P4	*H. naledi*	0	0	0	0
UW101 1277	P4	*H. naledi*	0	0	0	0
KRP 46	P3	*H. neanderthalensis*	0	0	0	0
KRP 48	P3	*H. neanderthalensis*	0	0	0	0
KRP 49	P3	*H. neanderthalensis*	0	0	0	0
KRP D38	P3	*H. neanderthalensis*	0	0	0	0
KRP D45	P3	*H. neanderthalensis*	0	0	0	0
KRP D53	P3	*H. neanderthalensis*	0	0	0	0
KRP D110	P3	*H. neanderthalensis*	0	0	0	0
KRP D112	P3	*H. neanderthalensis*	0	0	0	0
Le Moustier 1	P3	*H. neanderthalensis*	0	0	0	0
SD 566	P3	*H. neanderthalensis*	0	0	0	0
KRP 46	P4	*H. neanderthalensis*	0	0	0	0
KRP 47	P4	*H. neanderthalensis*	0	0	0	0
KRP 48	P4	*H. neanderthalensis*	0	0	0	0
KRP 49	P4	*H. neanderthalensis*	0	0	0	0
KRP D39	P4	*H. neanderthalensis*	0	0	0	0
KRP D41	P4	*H. neanderthalensis*	0	0	0	0
KRP D42	P4	*H. neanderthalensis*	0	0	0	0
KRP D43	P4	*H. neanderthalensis*	0	0	0	0
KRP D44	P4	*H. neanderthalensis*	0	0	0	0
KRP D49	P4	*H. neanderthalensis*	0	0	0	0
KRP D52	P4	*H. neanderthalensis*	0	0	0	0
KRP D115	P4	*H. neanderthalensis*	0	0	0	0
SCLA 4A 2	P4	*H. neanderthalensis*	0	0	0	0
Le Moustier 1	P4	*H. neanderthalensis*	0	0	0	0
SD 50	P4	*H. neanderthalensis*	0	0	0	0
SD 411	P4	*H. neanderthalensis*	0	0	0	0
SD 1106	P4	*H. neanderthalensis*	0	0	0	0
MPI 07 045	P3	*H. sapiens*	0	0	0	0
MPI 07 047	P3	*H. sapiens*	0	0	0	0
MPI 07 083	P3	*H. sapiens*	0	0	0	0
MPI 07 100	P3	*H. sapiens*	0	0	0	0
MPI 07 136	P3	*H. sapiens*	0	0	0	0
MPI 07 137	P3	*H. sapiens*	0	0	0	0

Specimen	Tooth type	Taxonomy	bucc_cing	ling_cing	OblR	DLH
MPI 07 233	P3	*H. sapiens*	0	0	0	0
MPI 07 234	P3	*H. sapiens*	0	0	0	0
MPI 07 256	P3	*H. sapiens*	0	0	0	0
MPI 07 574	P3	*H. sapiens*	0	0	0	0
MPI 07 604	P3	*H. sapiens*	0	0	0	0
MPI 07 607	P3	*H. sapiens*	0	0	0	0
MPI 07 613	P3	*H. sapiens*	0	0	0	0
MPI T08 066	P3	*H. sapiens*	0	0	0	0
MPI T08 069	P3	*H. sapiens*	0	0	0	0
MPI T08 072	P3	*H. sapiens*	0	0	0	0
MPI T08 074	P3	*H. sapiens*	0	0	0	0
MPI T08 092	P3	*H. sapiens*	0	0	0	0
MPI T08 212	P3	*H. sapiens*	0	0	0	0
MPI T08 213	P3	*H. sapiens*	0	0	0	0
MPI T08 224	P3	*H. sapiens*	0	0	0	0
MPI T08 225	P3	*H. sapiens*	0	0	0	0
MPI T09 112	P3	*H. sapiens*	0	0	0	0
MPI T09 181	P3	*H. sapiens*	0	0	0	0
MPI 07 078	P4	*H. sapiens*	0	0	0	0
MPI 07 114	P4	*H. sapiens*	0	0	0	0
MPI 07 232	P4	*H. sapiens*	0	0	0	0
MPI 07 565	P4	*H. sapiens*	0	0	0	0
MPI 07 602	P4	*H. sapiens*	0	0	0	0
MPI 07 617	P4	*H. sapiens*	0	0	0	0
MPI 07 724	P4	*H. sapiens*	0	0	0	0
MPI T08 046	P4	*H. sapiens*	0	0	0	0
MPI T08 062	P4	*H. sapiens*	0	0	0	0
MPI T08 076	P4	*H. sapiens*	0	0	0	0
MPI T08 081	P4	*H. sapiens*	0	0	0	0
MPI T08 094	P4	*H. sapiens*	0	0	0	0
MPI T08 348	P4	*H. sapiens*	0	0	0	0
MPI T09 125	P4	*H. sapiens*	0	0	0	0
MPI T09 127	P4	*H. sapiens*	0	0	0	0
MPI T09 129	P4	*H. sapiens*	0	0	0	0
MPI T09 311	P4	*H. sapiens*	0	0	0	0
Qafzeh 10	P3	*H. sapiens (Qaf.)*	0	0	0	0
Qafzeh 11	P3	*H. sapiens (Qaf.)*	0	0	0	0
Qafzeh 15	P3	*H. sapiens (Qaf.)*	0	0	0	0

Specimen	Tooth type	Taxonomy	bucc_cing	ling_cing	OblR	DLH
Qafzeh 10	P4	*H. sapiens (Qaf.)*	0	0	0	0
Qafzeh 11	P4	*H. sapiens (Qaf.)*	0	0	0	0
Qafzeh 15	P4	*H. sapiens (Qaf.)*	0	0	0	0
SK_24	P3	*P. robustus*	0	1	0	0
SK_28	P3	*P. robustus*	0	1	1	0
SK_52	P3	*P. robustus*	0	1	0	0
SK_74c	P3	*P. robustus*	0	1	0	0
SKX_162	P3	*P. robustus*	0	1	1	0
SK_52	P4	*P. robustus*	0	1	1	0
SK_99	P4	*P. robustus*	0	0	0	1
SKX_162	P4	*P. robustus*	0	1	1	1
SKX_26625	P4	*P. robustus*	0	1	1	1